Universidade de Lisboa

Faculdade de Farmácia

Departamento de Química Farmacêutica e Terapêutica

Boronic acids as partners in Multicomponent reactions

Francesco Montalbano

Doutoramento em

Química Farmacêutica e Terapêutica

Orientadores:

Doutor Pedro Miguel Pimenta Góis (FF, UL)

Professor Doutor Rui Ferreira Alves Moreira (FF, UL)

2014

Summary

Index of figures

Abreviation and nomenclature

2OG…2-Oxoglutarate

α1-PI…α1-Proteinase inhibitor

ALI…Acute lung injury

ARS…Acute respiratory distress syndrome

BH4…Tetrahydrobiopterin

CAD…Coronary artery disease

cAMP…Cyclic adenosine monophosphate

CBAs…Carbohydrate-binding agents

COPD…Chronic obstructive pulmonary disease

DCM…Diclhoromethane

DCMS…Dynamic-combinatorial mass spectrometry

DFT…Density functional theory

DMSO…Dimethyl sulfoxide

DPPIV…Dipeptidyl peptidase IV

EL…Endothelial lipase

ENR…Enoyl-acyl carrier protein reductase

ERs…Estrogen receptors

FAS…Fatty acid synthase

GLA…Glutaminase

Glu-AdT…Glutatamyl amidotransferase

Gly…Glycine

GT…Glycotransferase

HDL…High density lipoprotein

HepG2…Human hepatocellular carcinoma.

His…Histidine

HIV…Human Immunodeficiency Virus

HNE…Humans neutrophil elastase

LC ESI-MS…Liquid chromatography-electrospray ionization mass

LPL…Lipoprotein lipase

MCR…Multi-component reaction

MDM2…Murine double minute 2

mRNA…Messenger ribonucleic acid

MIDA…Methyliminodiacetic acid

$NADP^+$ …Nicotinamide adenine dinucleotide phosphate

PAH…Phenylalanine hydroxylase

PBPs…Penicillin binding proteins

PHD2…Prolyl hydroxylase domain 2

PPE…Porcine pancreatic elastase

PLA2…Phospholipase A2

PR3…Proteinase 3

RNA…Ribonucleic acid

Ser…Serine

SLPI…Secretory leukocyte protease inhibitor

THF…Tetrahydrofuran

TP…Transpeptidation

TRA…Transferase

VLDL…Very Low Density Lipoprotein

Palavras-Chave

Reação Multicomponente

Heterocíclos boratos

Diazoborina

Elastase neutrofilica humana

Fenilalanina hidroxilase

Keywords

Multi-component reaction

Boronate heterocycles

Diazoborine

Humans neutrophil elastase

Phenylalanine hydroxylase

Index Of Structures

Fused tricycle-boronate heterocycles

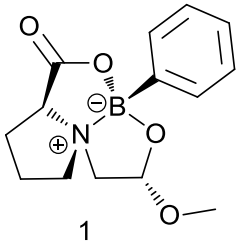

1
pag 23, 115

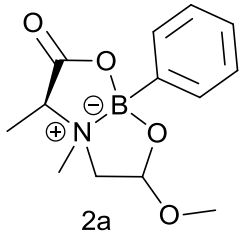

2a
pag 27, 117

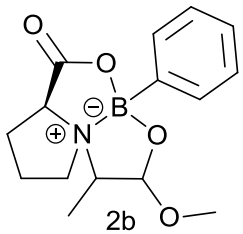

2b
pag 27, 118

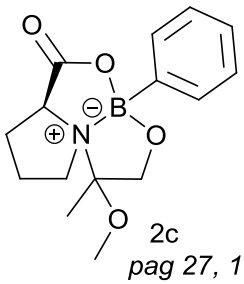

2c
pag 27, 118

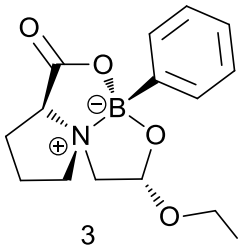

3
pag 29, 119

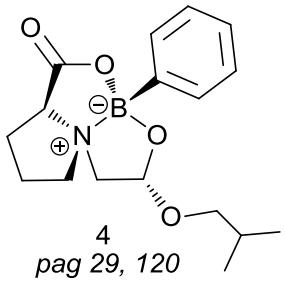

4
pag 29, 120

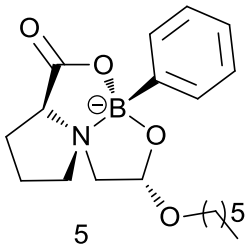

5
pag 29, 121

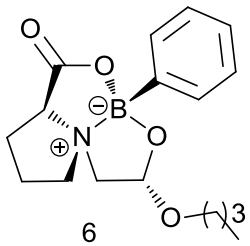

6
pag 29, 122

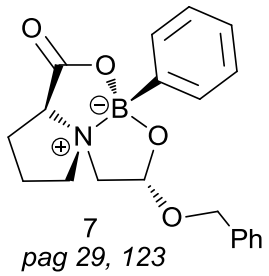

7
pag 29, 123

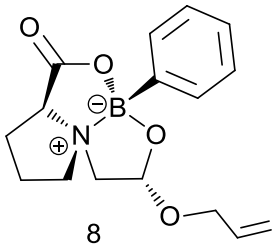

8
pag 29, 124

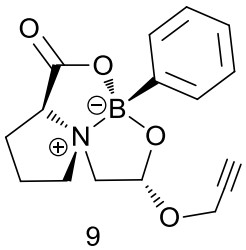

9
pag 29, 125

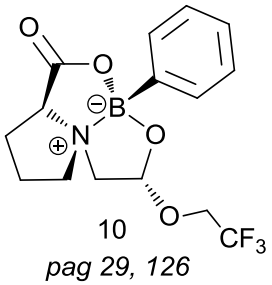

10
pag 29, 126

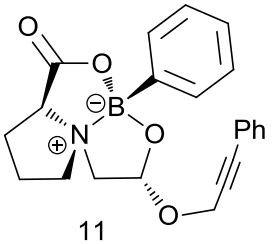

11
pag 29, 127

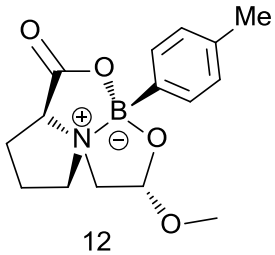

12
pag 30, 128

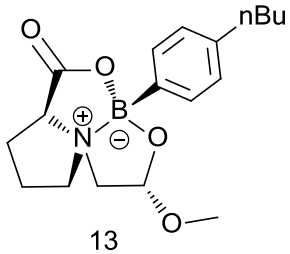

13
pag 30, 129

Fused tricycle-boronate heterocycles

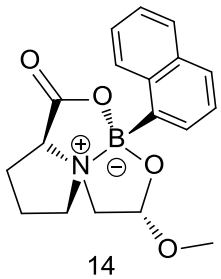

14
pag 30, 130

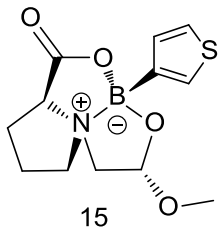

15
pag 30, 131

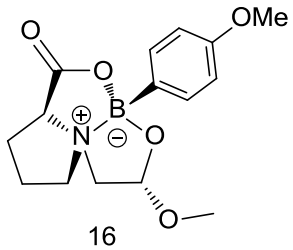

16
pag 30, 132

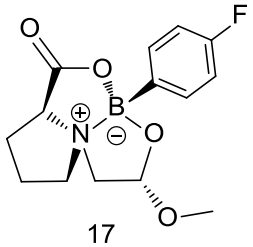

17
pag 30, 133

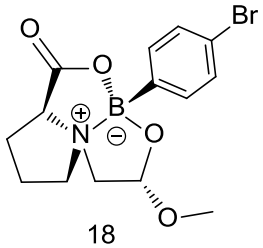

18
pag 30, 134

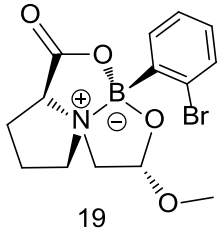

19
pag 30, 135

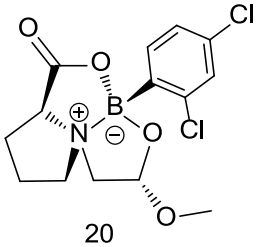

20
pag 30, 136

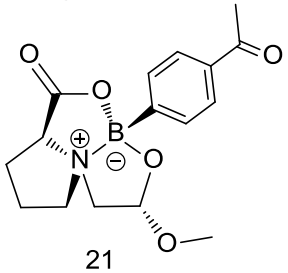

21
pag 30, 137

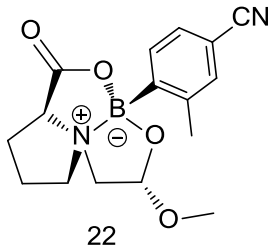

22
pag 30, 138

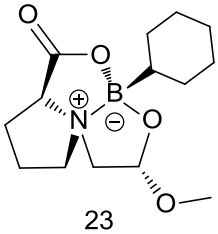

23
pag 30, 139

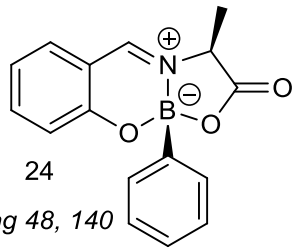

pag 48, 140

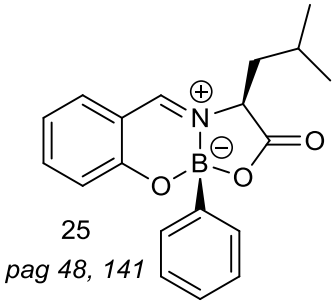

pag 48, 141

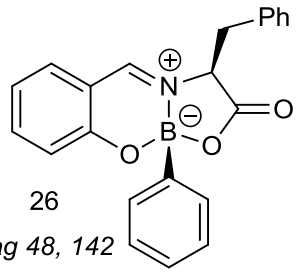

pag 48, 142

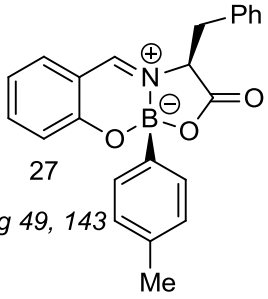

pag 49, 143

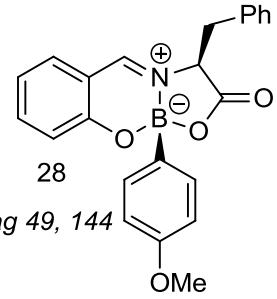

pag 49, 144

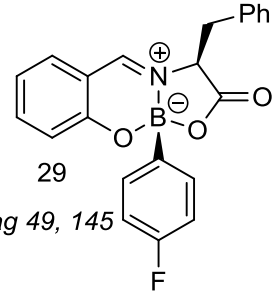

pag 49, 145

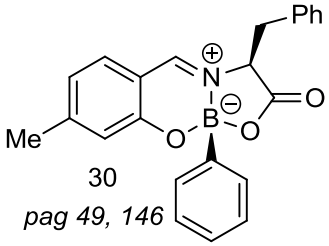

pag 49, 146

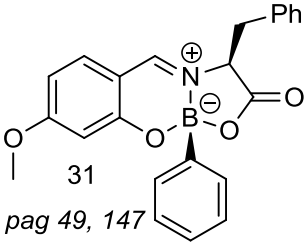

pag 49, 147

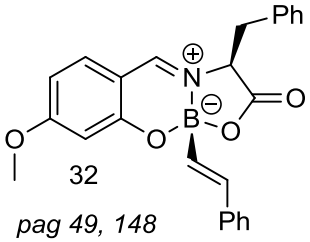

pag 49, 148

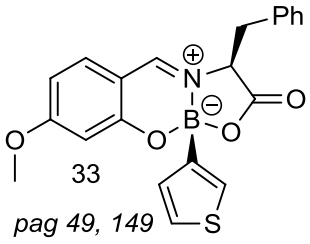

pag 49, 149

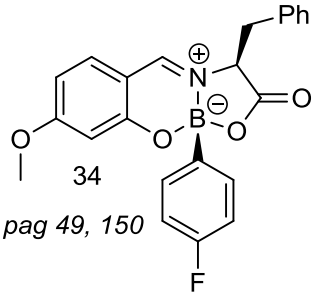

pag 49, 150

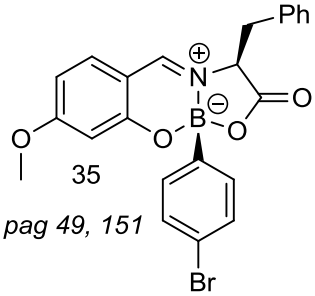

pag 49, 151

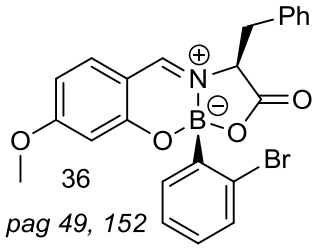

36

pag 49, 152

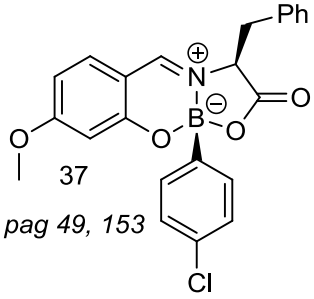

37

pag 49, 153

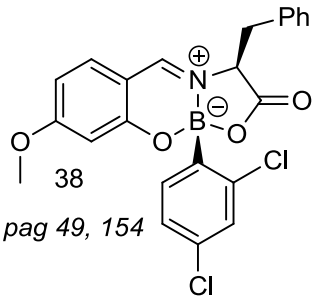

38

pag 49, 154

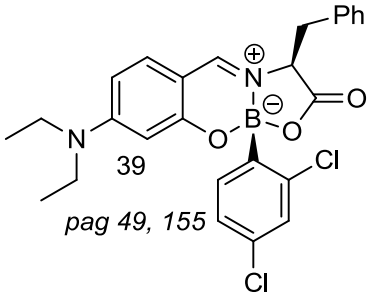

39

pag 49, 155

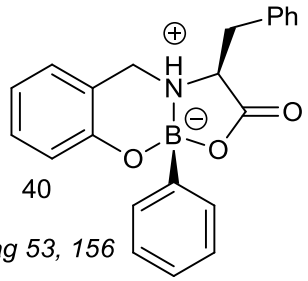

40

pag 53, 156

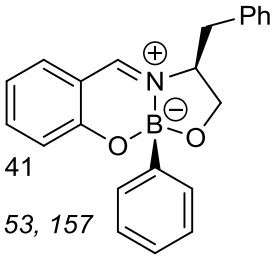

41

pag 53, 157

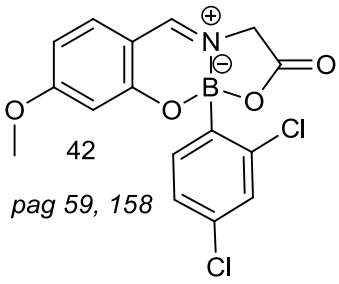

42

pag 59, 158

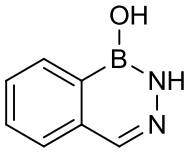

43

pag 78, 159

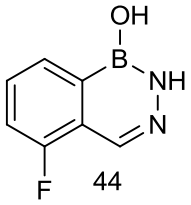

44

pag 78, 160

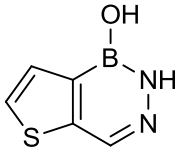

45

pag 78, 161

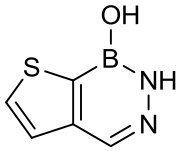

46

pag 78, 162

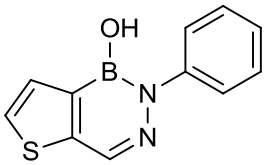

47

pag 79, 163

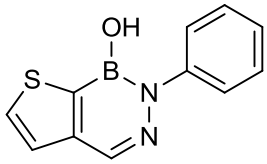

48

pag 79, 164

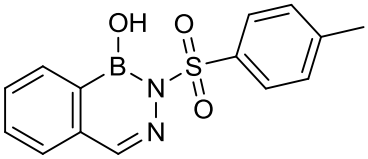

49

pag 80, 165

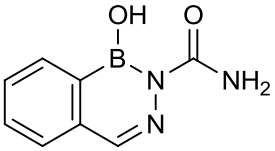

50

pag 80, 166

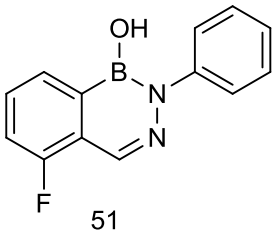

51

pag 80, 167

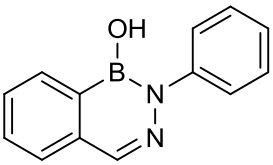

52

pag 80, 168

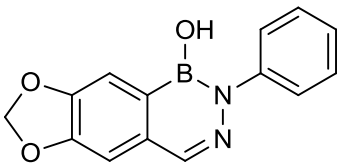

53

pag 80, 169

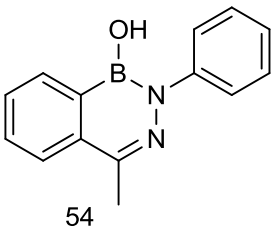

54

pag 81, 170

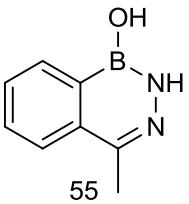

55

pag 81, 171

Acknowledgments:

I wish to thank Dr. Pedro Gois, supervisor of this thesis, for his continuous support and scientific guidance which made possible to achieve the result disclose in this thesis. I do thank him sincerely for the opportunity to do investigation in medicinal chemistry.
A warm thank to Professor Rui Moreira which his co-supervisor role made possible to realize this work.

I also want to thank, Dr. Lidia Goncalves for her collaboration in the enzymatic studies with HNE that were of pivotal importance in the development of this thesis project. Professor Luis Vireos at the Instituto Superior Técnico de Lisboa, for the studies related with the complex world of computational chemistry. I thank, Dr Susana Lucas for her contribution with the molecular modeling of our molecules against HNE. These studies played an important role in the comprehension of the mechanisms of HNE inhibition. I thank, Dr Raquel Frade, for giving me the opportunity to learn how to perform cellular essays. To Dr. Joao Vicente and Dr Joao Leandro I thank for the guidance on the work related with the enzyme PHA.

I want to express my sincere gratitude to Dr. Joao Rose and all my laboratory colleagues, master and project students and the technical staff that worked with me throughout these four years.

Special thank goes to my love Michaela, my family and friend that supported me and made all this possible.

Abstract

In the last three decades, the boronic acid notoriety and usefulness changed from almost neglected to a highly used class of synthetic reactant. The mild Lewis acidity, together with their stability, easy handling and environmental friendly impact attracted the attention of the synthetic community towards these peculiar compounds. They found use in classical organic chemistry as synthetic reagents as well as in the medicinal chemistry as potent inhibitors. The purpose of this work was to explore a relatively new field of application, in which the boronic acid functionality acts as a template to promote the assembly of simple building blocks into more complex molecules, and explore this strategy as a tool to easily synthesize small collections of active compounds. The biological activity of such collections was tested against eligible targets (HNE; PHA) in order to select the most promising compounds and use them as a new benchmark for a new round of interactive optimization aiming to amplify the percentage of success in the discovery of new lead compounds. reaction design to mimic the natural architecture using boronic acids as tethers for building blocks:

- ***Synthesis of the fused tricycle-boronate heterocycles****.*

  The B ability to act as a tether was used to simply assemble heterocycles through covalent bond formation with two oxygen and a dative bond with the N. A highly efficient one-pot four component reaction is the protocol exploited to assemble 23 tricycle boronated heterocycles in yields and diastereoselectivities up to 95% and 97% respectively. DFT calculation were performed to clarify the reaction mechanism.

- ***Synthesis of fused bicycle-boronate heterocycles and their enzymatic evaluation as new human neutrophil elastase (HNE)inhibitors.***

  Herein we demonstrate that boron tether strategy may synthetize collection of molecules to discover new hit compounds. Through a one pot three components

reaction 17 new compounds were synthesize in excellent yields up to 98%, high diastereoselectivities up to de100%. The compounds were tested as novel enzyme inhibitors for HNE and reaching the IC_{50} up to 1.10 μM. Docking studies were performed to enlighten the enzymatic interaction between the molecules and the active site of the HNE. .

Design of phenylalanine hydroxylase (PAH) inhibitors based on fused bicycle-boronate heterocycles

The bicycle boronate heterocycles were also tested against the wild type PHA compound 27 seems able to stabilize the protein affording a new scaffold for further optimization.

- ***Synthesis of diazaborines and their enzymatic evaluation as new HNE inhibitors***

  Herein we disclose the value of the diazaborines as inhibitor of the HNE. The collection was synthetize through optimization of the Dewar's procedure that enabled the synthesis of the diazaborine in yield up to 89%. and IC_{50} 2.5μM potency against HNE.

Resumo

No decorrer das últimas 3 décadas, os ácidos borónicos evoluíram de quase curiosidades químicas até ao reconhecimento como reagentes de grande utilidade preparativa. A acidez de Lewis moderada, acompanhada de uma boa estabilidade, facilidade de manuseamento e baixo impacto ambiental, chamaram a atenção da comunidade sintética para estes compostos peculiares. Encontraram aplicação em química orgânica clássica como reagentes sintéticos, bem como em química medicinal como poderosos inibidores enzimáticos. O objecto deste trabalho foi explorar um campo de aplicação emergente, no qual o grupo funcional ácido borónico actua como molde para promover a associação de blocos constitutivos simples em moléculas mais complexas, e aplicar esta estratégia como ferramenta para a síntese de pequenas bibliotecas de compostos activos. A eficácia destas bibliotecas foi ensaiada em alvos selecionados (HNE; PHA) por forma a eleger os compostos mais promissores, por sua vez utilizados como padrões para um novo ciclo de optimização estrutural. Procurou-se assim maximizar a percentagem de sucesso no processo de descoberta de novas moléculas promissoras. Ensaiaram-se os seguintes conceitos estruturais por forma a mimetizar arquitecturas encontradas em produtos naturais:

Síntese de arquiteturas bora-tricíclicas fundidas:
A capacidade do boro para actuar como elo de ligação foi aproveitada para a construção de estruturas heterocíclicas via ligação covalente com dois átomos de oxigénio e uma ligação dativa com um átomo de azoto. Através de uma reacção de uma só etapa envolvendo quatro componentes, construíram-se 23 espécies tricíclicas boradas em rendimentos e diastereoselectividades de até, respectivamente, 95 e 97%. Cálculos de DFT permitiram obter informação sobre o mecanismo da reacção.

Síntese de arquiteturas bora-bicíclicas fundidas e respectiva avaliação como inibidores da elastase neutrofílica humana (HNE):
Demonstrou-se que a estratégia de utilizar o boro como elo permite a síntese rápida de um conjunto de moléculas, acelerando a descoberta de novas moléculas activas. A reacção de três componentes numa só etapa permitiu a síntese de 17 novos compostos em excelentes rendimentos de até 98%, e diastereoselectividades de até 100%. O ensaio

dos compostos como inibidores enzimáticos da HNE evidenciou IC50's de até 1,10 μM. Efectuaram-se estudos de docking no sentido de elucidar a interacção entre as moléculas e o centro activo da HNE.

Desenvolvimento de inibidores da fenilalanina hidroxilase (PAH) baseados na arquitetura bora-bicíclica fundida:

Os referidos bora-bicíclicos foram também ensaiados perante a PAH de tipo selvagem. O composto **27** aparenta ser capaz de estabilizar a proteína, servindo de ponto de partida para posterior optimização.

Síntese de diazaborinas e respectiva avaliação como novos inibidores da HNE:

Demonstrou-se o valor de certas diazaborinas como inibidores da HNE. Esta biblioteca foi sintetizada por meio da optimização do procedimento de Dewar, tendo-se obtido os compostos pretendidos com rendimentos de até 89%, os quais evidenciaram IC_{50}'s de até 2,5μm contra a HNE.

1. General introduction

1.1 Overview

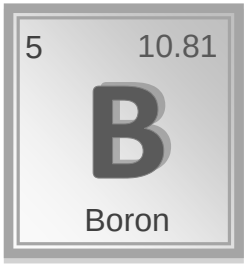

Boron is a very curious element, with an uncommon history, starting from its primordial creation into the universe, passing through the chemists bench, ending inside a living organism playing the pivotal role of pharmacophore. The creation process of the boron atom was different from most of the heavier elements present the solar system; [1,2,] Indeed, while nuclear fusion (two atoms colliding to generate a third new one) is the responsible for the genesis of all atoms up to iron and nickel, cosmic ray spallation (alpha particles, electron, protons, and heavier nuclei, impacting against an object)[3] is the process that is believed to have generated boron, beryllium and lithium elements. Boron is one of the members of the 13th group of the periodic table. This group is characterized by only three electrons in the valence shell which confers the ability to yield molecules with only three-sigma bonds. Boric, boronic and borinic acids are only some possible example of the ability of boron to form stable compounds without completing the octet. Such molecules possess a planar sp^2 geometry around the central atom (B) which bears an empty *p* orbital and, despite the octet rule resulting unsatisfied, these molecules are enough stable to be stored and manipulated in ordinary laboratory activities. The empty *p* orbital plays an important role to determine the characteristic chemistry of such molecules. Indeed the boron atom, when arranged in the sp^2 geometry, is able to receive two extra electrons from a donor that allows the boron to achieve the full octet, forming a stable complex. The formation of this dative bond also determines a couple of changes in the molecule that are noteworthy: a negative charge is formally placed onto the boron and it rearranges from sp^2 to sp^3.

1.2 Boronic acid compounds as synthetic reagents

Among the boron containing molecules the boronic acids gathered the attention of organic chemists for their versatility easy handling. Some examples of reaction in which boronic acids found an employment are: aminations, halogenations, allylations or cross-coupling reactions. Since this constitutes an immense research field, in this report only some examples of the most relevant and useful transformations will be discussed in more detailed namely: the Suzuki Miyaura cross coupling reaction, the rhodium-catalyzed additions to π-bonds, multicomponent reaction (MCR) and the preparation of tridentate boronate-complexes.

Suzuki Miyaura cross coupling reaction

The Suzuki-Miyaura cross coupling reaction is one of the most famous and useful reactions to form C-C bonds and was disclosed in 1979 by Suzuki and Miyaura. It is a Pd (0)-catalyzed coupling between boron compounds and organohalides in the presence of a base. This reaction affords a new C-C bond formed between the two organo-substituents of the starting materials, in many cases with very high yields.[4] (Figure 1)

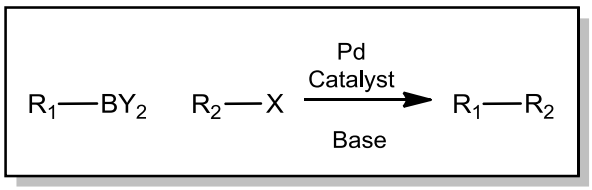

Figure 1- General scheme of Suzuki-Miyaura cross coupling reaction.

The generally accepted mechanism for this process involves the Pd (0) oxidative addition to the halide to give a Pd (II) intermediate, followed by a transmetallation step and the final reductive elimination that affords the product and regenerates the catalyst.[4] The transmetallation is thought to be facilitated by the base-mediated formation of a tetra coordinate boronate anion. (Figure 2)

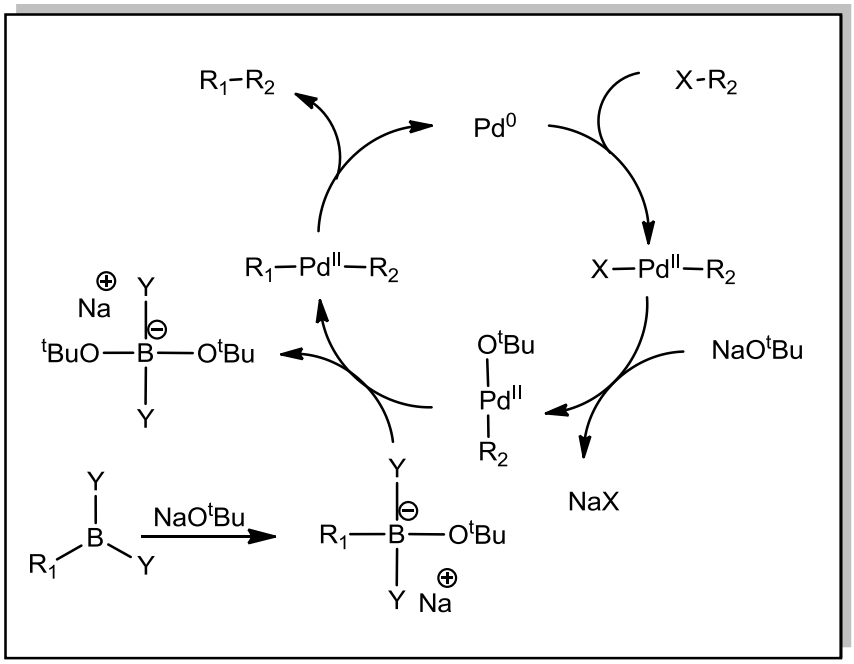

Figure 2- Suzuki-Miyaura cross coupling general mechanism.

Rhodium-catalyzed addition to π systems

The rhodium-catalyzed addition of boronic acids to electron-deficient olefins and carbonyl compounds is another method that exploits boronic acids exquisite reactivity. Such carbon-carbon bond formation is a very efficient reaction in terms of yields and selectivity. Depending on the ligand used, the rhodium-catalyzed addition of boronic acids may also proceed with high levels of asymmetry, this is particularly true for 1,4 additions to conjugated ketones. The mechanism features the transmetallation of a phenyl group from boron to the hydroxorhodium, giving a phenyl rhodium species. The insertion of the α-ß unsaturated carbonyl compound into the phenyl-rhodium generates the oxa-π-allylrhodium intermediate which upon hydrolysis affords the conjugate addition product regenerating the hydroxorhodium active catalyst.[5] (Figure 3)

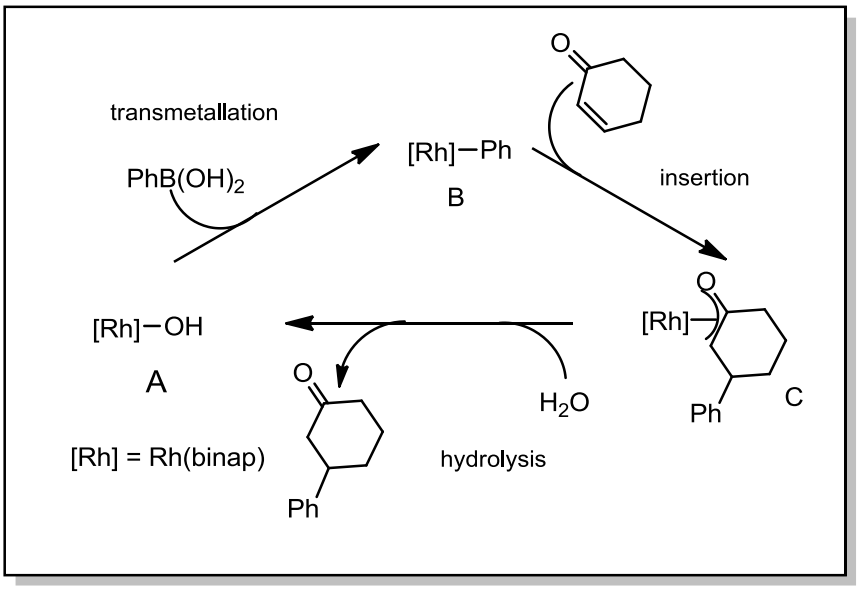

Figure 3- General mechanism for the Rh-catalyzed additions of boronic acids to conjugate ketones.

Multi-component reactions

The chemical properties of boron makes the boronic acid a “dynamic functional group”, which is able to respond to the “context”, interconverting and rearranging to give the most stable molecule or configuration. A clear example of this is the reaction between boronic acid and vicinal nucleophiles like diols, to yield boronic esters, a reaction that is reversible in aqueous solution and dependent on the *pH* used.[6] This ability makes the boronic acid an ideal partner for multicomponent reactions (MCR), a protocol based on one-pot reaction of more than two compounds that afford the product often in high yields. Ideally, the molecules involved in a MCR process, are able to afford many different products depending on the structural diversity of the reactants used and for that reason are ideal to generate libraries of structurally diverse compounds for biological evaluation.

Generally, MCRs involve a series of reversible and irreversible steps, and can be ranked in 3 main categories:

TYPE1: when only chemical equilibriums are involved in the transformation of the starting materials up to the final product.

TYPE2: when the process involves several reversible reactions and one final irreversible step leading to the product formation.

TYPE3: were a sequence of irreversible elementary reactions affords the product.

For MCR of TYPE1 and 2 the reagents can flow towards the most favorable product, which depends on the reaction conditions. Under this light, the success of a MCR depends on the efficient interconversion among the reactive intermediates, in other words, the careful selection of the reactants and reaction condition are of pivotal importance. For MCR of TYPE3, the order of addition dramatically influences the outcome of the reaction, since the reaction proceeds through irreversible steps.

The Petasis MCR (1993) is an effective example of the use of boronic acids in MCR. This reaction involves the simultaneous mixing of a primary or secondary amine, an aldehyde and a boronic acid, yielding a secondary or tertiary amine and a new C-C bond, under mild conditions. The Petasis reaction mechanism [7] involves the iminium or imine formation between the amine and the aldehyde and the subsequent reaction of this species with boronic acids, via an ATE-complex. The irreversible nucleophilic addition of the alkyl or aryl boron substituent yields the product. The fundamental functionality for the process is the presence of a hydroxyl group that reacts with the boronic acid generating a more nucleophilic tetrahedral boronate species.(Figure 4)

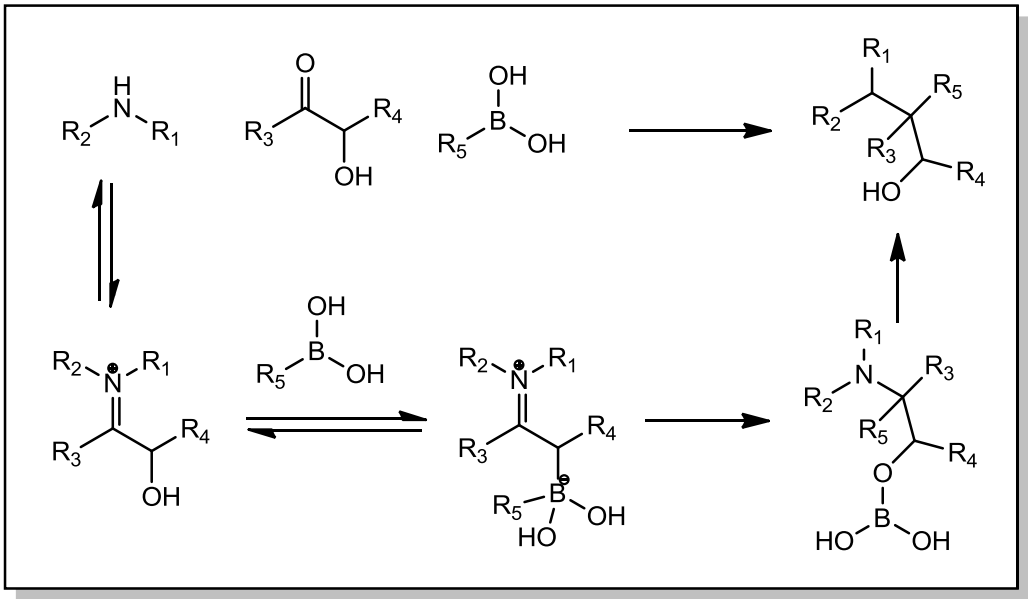

Figure 4 - General mechanism for the Petasis MCR.

Boronate heterocycles formed with tridentate ligands

Boronic acids can easily afford stable boronate-complexes when involved in reactions with di or tri-dentate ligands. A clear example of this, are the complexes obtained when boronic acid reacts with oxygenated or nitrogenated compounds, as for instance N-methyl-diiminodiacetic acid (MIDA) (Figure 5), affording a range of complexes in which MIDA maybe successfully employed as the boron protecting group to mitigate transmetallation in the Suzuki-Miyaura reaction,[8]enabling an iterative cross coupling reaction in presence of unprotected boronic acid. (Figure 5). More sophisticated complexes were prepared by Farfan et al.(Figure 6) This group reported the selective preparation of a boronate complex, by reacting the 2-[[(2-hydroxyphenyl)amino]methyl]-phenols with an equimolecular amount of boronic acids, salicylaldehyde and 3,5-di-tert-butyl-2-hydroxybenzaldehyde to afford the bicycle-boronate heterocycle. The resulting tridentate complex was obtained in yields ranging from 59% to 91%. [9] (Figure 6)

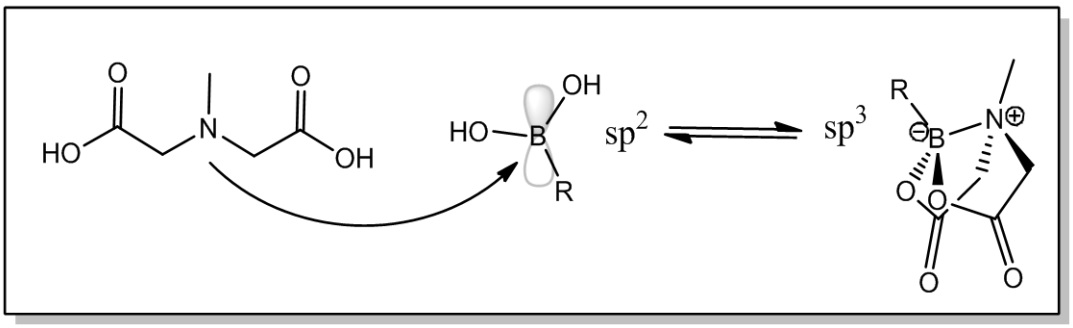

Figure 5 - Tridentate ligand (MIDA) that maybe used as a boron protecting group.

Grimme et al disclosed for the first time, the determination of the absolute configuration at a stereogenic boron by CD spectroscopy. In this communication, boronate complexes were obtained from 2-amino-1,2,2-triphenylethanol (chosen example) and 2-amino-2,2-diphenylethanol and were isolated as pure diastereoisomers and/or enantiomers. From the crystal structure analyses, the distance between the nitrogen and the boron atom (1.588 to 1.607 Å), clearly indicates the existence of a B-N dative bond. In addition to this, the configuration at the boron atom was determined to be *R,* and more importantly epimerization at the boron center was never observed.[10] (Figure 7).

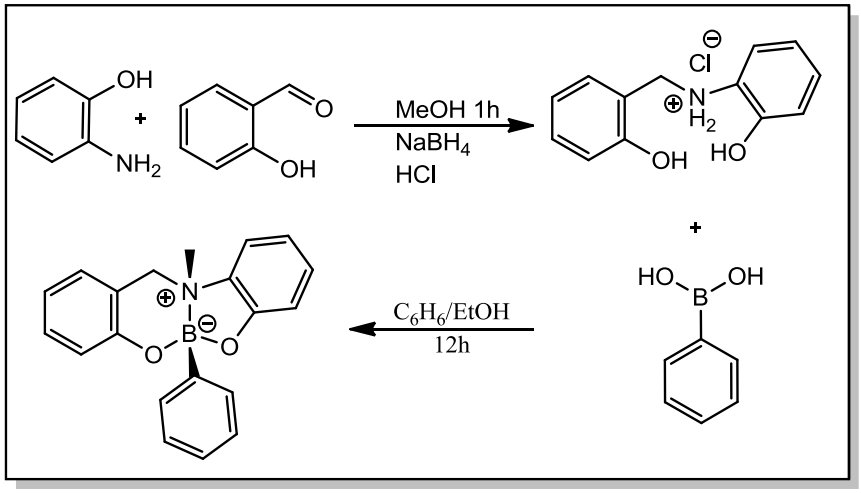

Figure 6 - Stable boronate complexes prepared by Farfan et al.

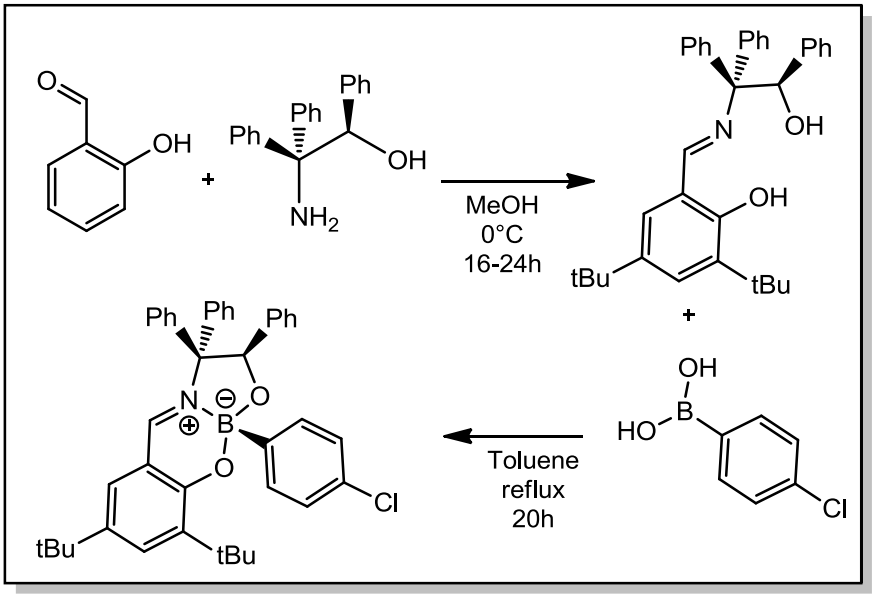

Figure 7 - Stable boronate complex prepared by Grimme et al.

In the same line, Hutton et al developed a stereoselective asymmetric synthesis of a chiral boron complex. Their results demonstrate that the formation of the complexes occurs in a highly enantioselective manner by using the Betti base as the chiral o-hydroxybenzylamine derivative. By mixing the Betti base, glyoxylic acid, and phenylboronic acid in DMF at 50 °C for 24 h the boronate complex depicted in Figure 8 was directly obtained in 97% yield. According to Hutton the formation of the tridentate ligand must involve three important steps: condensation of the amine with the aldehyde to give the corresponding imine,

complexation of phenylboronic acid, and isomerization of the aldimine to the corresponding ketimine with concomitant loss of the carbon stereocenter.[11] (Figure 8)

Severin et al reported a new synthetic strategy for the construction of boron-based macrocycles and dendrimers. Condensation of aryl- and alkylboronic acids with 3,4-dihydroxypyridine and a primary amine R-NH_2 was shown to give pentameric macrocycles in a highly diastereoselective self-assembly process, in which five boronate esters are connected by dative B-N bonds. [12] (Figure 9)

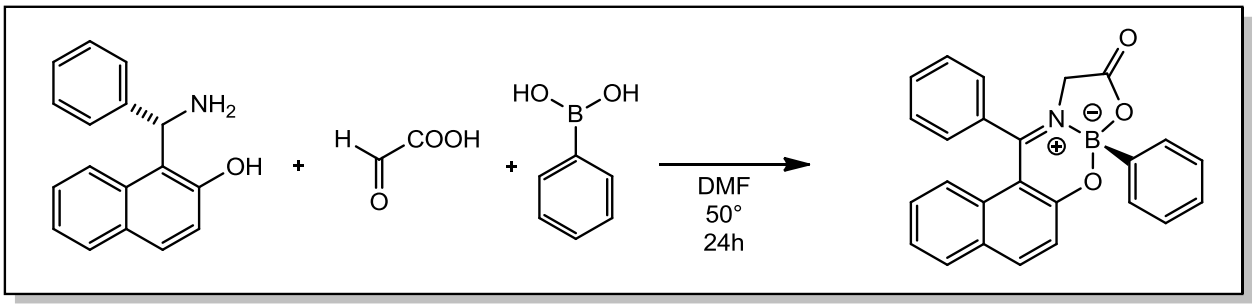

Figure 8 - Stable boronate complex prepared by Hutton.

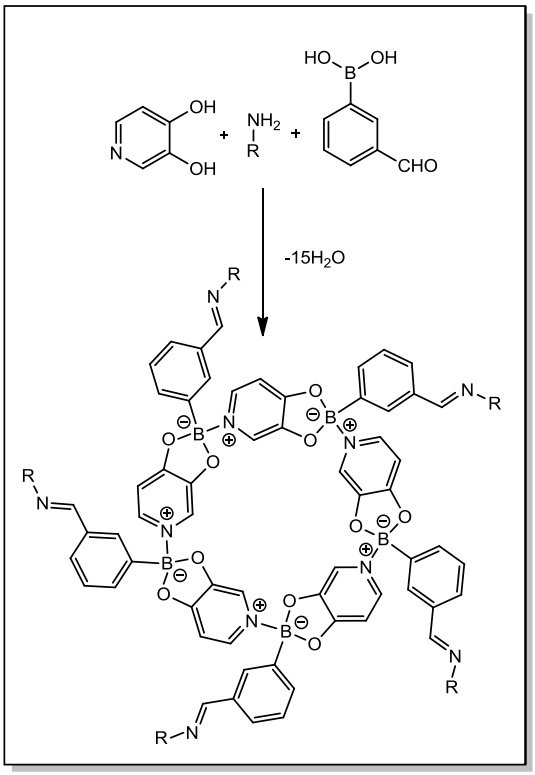

Figure 9 - Boron-based macrocycles prepared by Severin.

1.3 Boron-containing natural products

Despite the relative abundance of boron in the earth crust there are very few natural products that contain this element. The most well known boron-containing natural products are: boromycin, aplasmomycin, tartrolons and borophycin. All this compounds belong to a macrolide type family of complex molecules that exhibit a polyhydroxy framework, that act as tetradentate ligand for a central boron atom.

The first compound of this family to be discovered was boromycin[13] (Figure 10), which displays antibiotic properties and was isolated from the Streptomyces antibioticus, a bacteria found in Ivory coast soil. The macrolide aforementioned, was shown to be active mainly against Gram-positive bacteria, plasmodie and babesie protozoa.[14] In 1996 was also found to be strongly active against the replication of HIV-1.[15] A similar profile, in terms of antibiotic activity is exhibited by the Aplasmocyn natural product (Figure 10), isolated from Streptomyces griseus. This compound was shown active against Gram-positive bacteria and was reported as a potential adjuvant in ruminant animal breeding as enhancer of growth through metabolic changes, by increasing the proportion of proprionate and butyrate, decreasing at the same time the concentration of methane and acetate.[16]

The tartrolon natural product (Figure 10) is the third of the boron containing natural products depicted in Figure 10. This molecule was extracted from Sorangium cellulosum and Streptomyces family, and like the two macrolides aforementioned, exhibits a similar biological profile like the antibiotic activity against Gram-positive bacteria. In addition to this, it also presents a certain larvicide activity on the beet army worm and tobacco bud worm.[17,18]

Finally Borophycin (Figure 10), was isolated from the blue-green alga Nostoc linckia and is made of two identical halves with an overall structure reminiscent of other boron-containingantibiotics.[19]

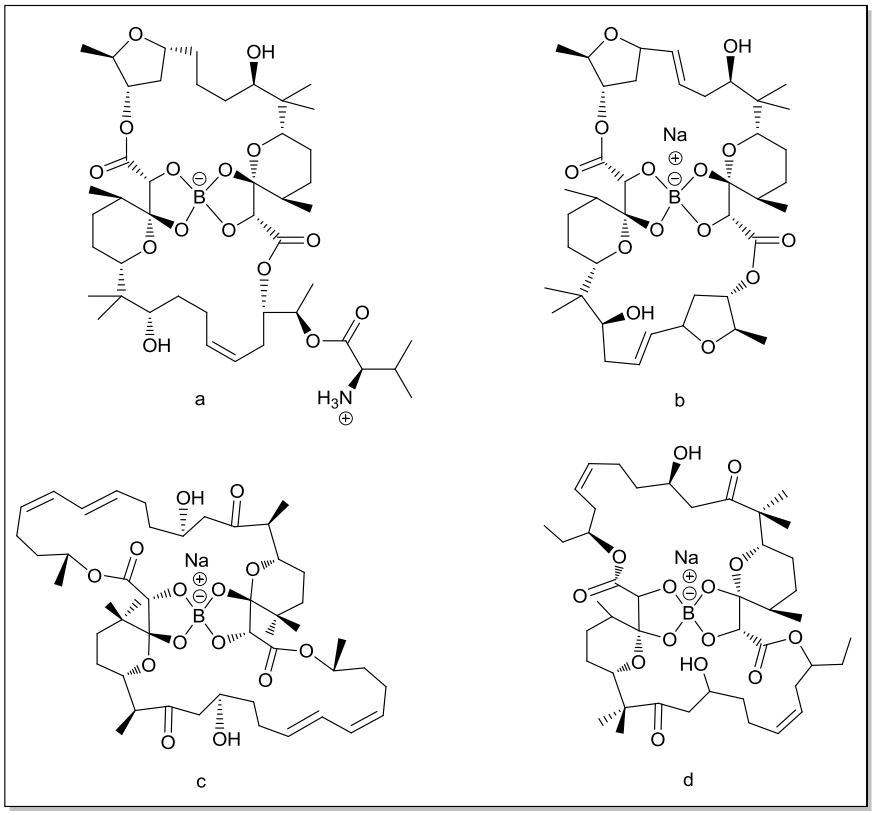

Figure 10 - Boron-containing natural products are: a) boromycin, b) aplasmomycin, c) tartrolons, d) borophycin.

1.3 Biological activity of boron containing compounds

Compounds containing boron have been investigated in many different fields for the peculiar properties of this element in particular they have been extensively explored for their unique biological activity profile. The biological uses of boron containing compounds is an immense field, therefore, is not the purpose of this work to make a comprehensive discussion of all biological uses of boron containing compounds. Nevertheless, in the hope to give an idea of the potential of this class of compounds as drugs herein is presented a brief description of several examples related with the use of boronic compounds in the fight against the major diseases that nowadays affect western societies: cancer, heart and coronary artery disease, diabetes, HIV and bacterial infections.

Overview

Generally the biological activity of boron containing compounds can be traced back to three basic principles related with boron chemistry:

- *The ready sp^2 -sp^3 rearrangement, of boron centers*
- *The formation of stable anions, centred on boron*
- *Boron's strong affinity for oxygen nucleophiles*

These three distinctive properties afford a solid base to comprehend the basic mechanisms that mostly regulate the biological activity of boron compounds. A valid example of the influence of the first two factors mentioned above (Figure 11), came from the comparison between the biological activities, against the same target, of the boronic acid and the carboxylic group as they are classically considered as isosters and both are able to receive a lone pair of electrons and as a consequence both groups form a negative ion changing their configuration from sp^2 to sp^3.

Nakamura et al [20] in 2006, showed that the *cis*-stilbene substituted with carboxylic acid inhibited the cell growth 10,000 folds less than its boronic acid isoster (Figure 12).This observation was related to a higher Lewis acidic character of the boronic acid.[21]

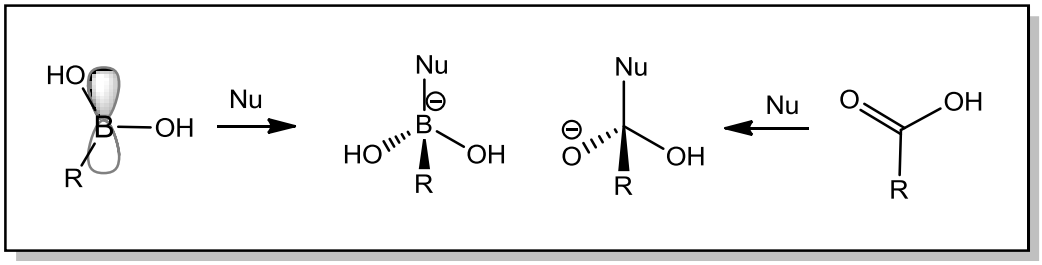

Figure 11- Boron sp^2 -sp^3 rearrangement.

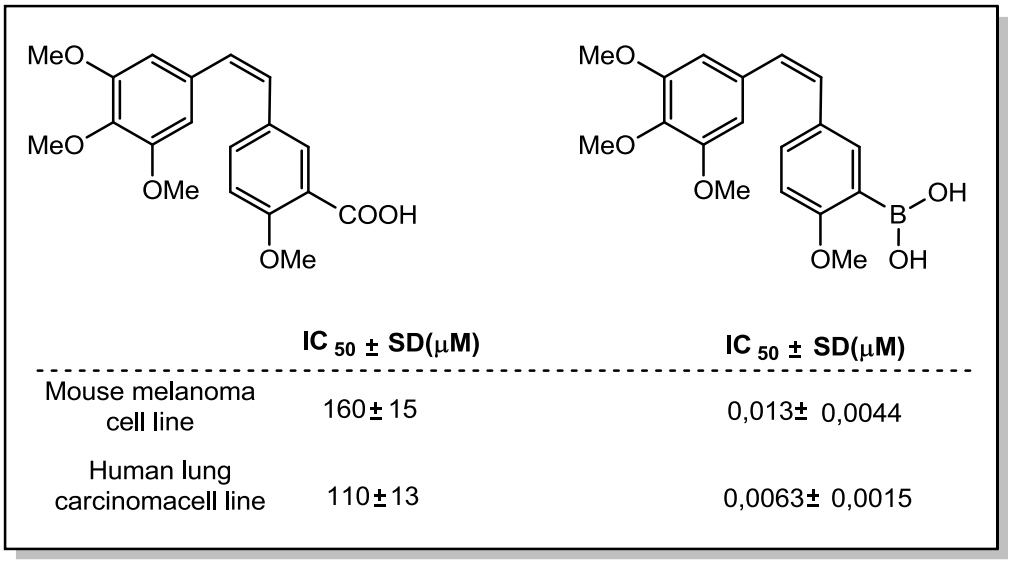

	$IC_{50} \pm SD(\mu M)$	$IC_{50} \pm SD(\mu M)$
Mouse melanoma cell line	160± 15	0,013± 0,0044
Human lung carcinomacell line	110± 13	0,0063± 0,0015

Figure 12 - Comparison between the biologic activity of cis stilbene boronic acid and its carboxylic isoster against Mouse melanoma cell line and human lung carcinoma.

In the same line Kumar et al. while investigating the complex p53/MDM2, synthesized a number of boronic-chalcone derivatives (Figure 13).[22] Murine double minute 2 (MDM2) is an oncogenes responsible of the inactivation of the tumor suppressor p53. This group speculated that, if the *p*H is neutral the substitution of the carboxylic acid moiety by a boronic acid could result in a stronger salt bridge formation: "*due to the electron deficient nature* (higher performance as Lewis acid) *of the boronic acid functionality and the electron donating nature of the amino group"*. [21]

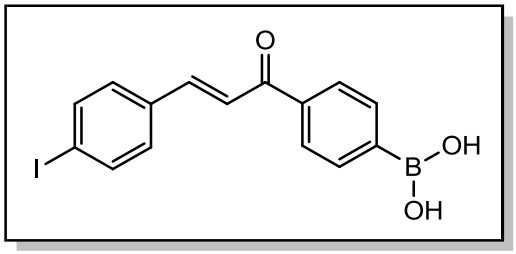

Figure 13 - Boronic-chalcone analogues synthesized to target breast cancer.

The ability of boron to replace a carbonyl group goes beyond the isosteric correspondence between boronic acids and carboxylic acids. Indeed the boron of a boronic acid is able to substitute efficiently the carbonyl functionality of a *β*-lactam. Between this two functional groups, there is no isosteric identity, for this reason the success of the replacement is most likely due to a stronger electrophile character of the boron centre.[21] In this line, Nakamura et al synthesized a series of belactosin C analogs, with the *β*-lactam moiety substituted by a boronic acid functionality. The Nakamura's boronic acid analog of belactosin C displayed a significant cell growth inhibition (IC_{50} 1⁄4 0.35 μM), clearly demonstrating the utility of replacing the *β*-lactam ring by a boronic acid moiety (Figure 14).[23] Latter Shoichet et al synthesized a series of boronic acid *β*-lactamase inhibitors, mimicking the structure of cephalotin (Figure 15). They found that the maintenance of the original framework of the natural substrate was important to maintain the activity levels; indeed the more similar the boron analogue was the greater observed inhibitory activity. [24] The third factor that influences dramatically boron biological activity is the affinity of oxygen towards boron. In this field, Adams et al traced back the potent antitumoral activity of bortezomib which is a 26S proteasome inhibitor, to the formation of a more stable B-O bond then the one formed by parent aldehyde functionality. Bortezomib, became the first FDA approved boron containing compound (Figure 16).[25]

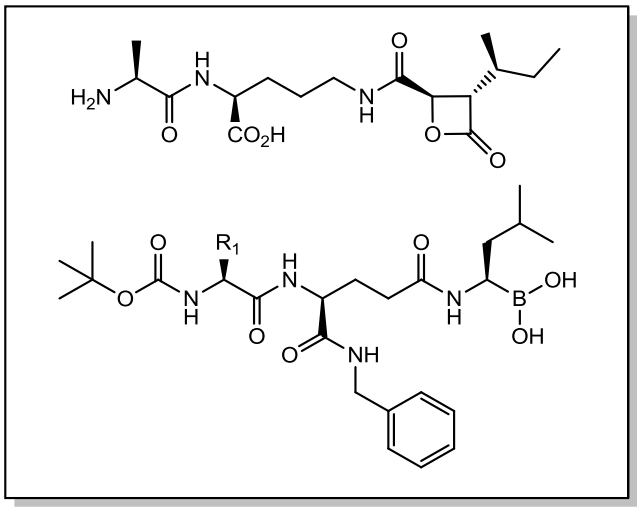

Figure 14 - Belactosin C and boronic acid derivatives developed by Nakamura et al.

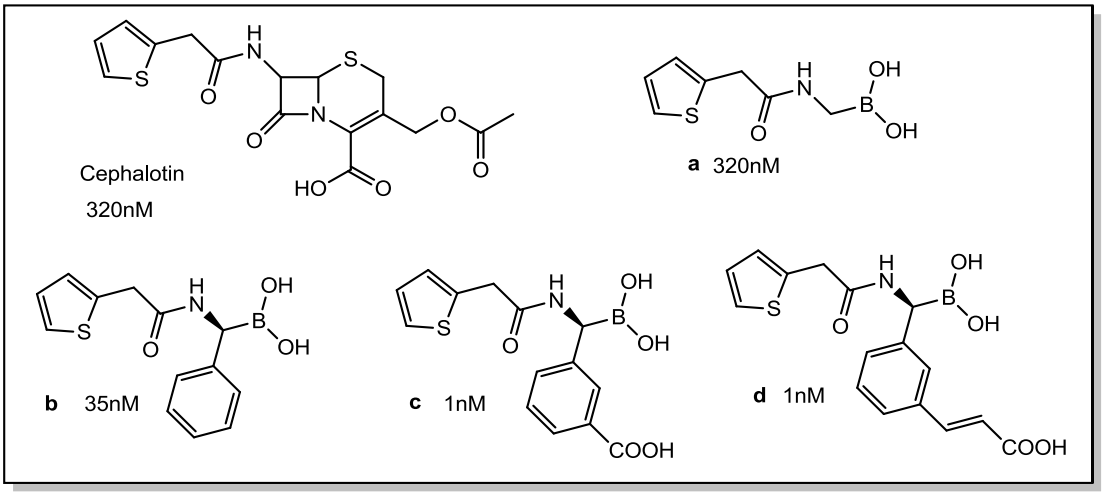

Figure 15 - K_i values against AmpC *β*-lactamase for boronic acid inhibitors developed by Shoichet et al.

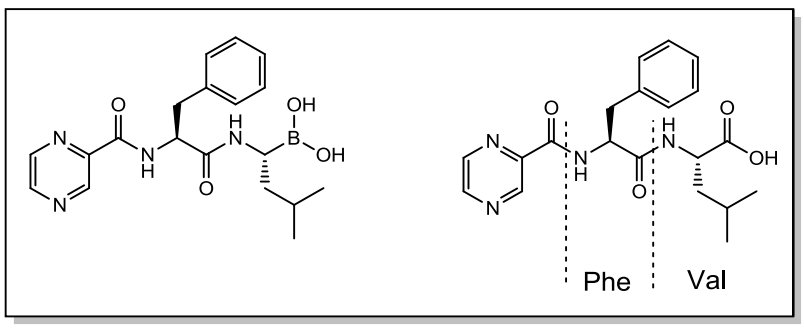

Figure 16 - Bortezomib and the corresponding amino acid dipeptid

Anticancer activity

Bortezomib® is a 26S proteasome inhibitor which binds to a threonine OH residue through a B–O covalent linkage, generating an sp^3 hybridized tetrahedral complex. The ubiquitine-proteasome pathway is an important mechanism for the degradation of abnormal and misfolded proteins with an high rate of specificity to target, time and space.[26] Due to the importance of this class of proteins play, over homeostasis and regulation, the proteasome enzymes are deeply involved in a series of cellular processes such as: cell differentiation, cell cycle, antigen processing and hormone metabolism.[27,28] Among the several components of the proteasome family, the 26S is the main player, its structure is based on three sub units, one 20S responsible to the actual proteolysis , and two regulatory cup subunits 19S, which are placed at each end of the 20S subunit. The 19S controls the recognition, the misfolding and the transfer of the processed protein into the lumen of the 20S unit.[29]

Bortezomib is derived from a series of previously reported dipeptide aldehydes,[30] that were non-specific proteasome inhibitors. The substitution of the aldehyde by the boronic acid, produces a highly potent and selective inhibitor of the 26S proteasome (Figure 16).[31] The Bortezomib® not only demonstrated the potential of boron in drug discovery, but also proved that the 26S proteasome is a suitable target for the treatment of cancer. Despite the success, Bortezomib exhibits important adverse effects while used in the treatment of solid tumours; among these, peripheral neuropathy (PN) is perhaps the most important. The severe impact of PN is a limiting factor of the administrable dose and therefore the efficacy,[32] often leading the patients to leave the therapy. Despite the efficacy of Bortezomib, its strong side effects prompt several groups to search for inhibitors with higher or comparable efficacy though with a considerable lower toxic profile.

The efforts of these investigation have indeed produced a second generation of inhibitors as shown in Figure 18.[33] Among these new compounds, MLN9708 was shown to be one of the most interesting, since it is a low affinity inhibitor that still shows IC_{50} values in the same range of Bortezomib, which is a high affinity inhibitor. It was suggested that to achieve therapeutic efficacy against solid tumor, the pharmacokinetics profile of a compound is more relevant than its pharmacodynamics, the fast off-rate of MLN9708 has to result in a greater distribution of the drug into the tissues and thereby into the tumor. The adverse effects observed for Bortezomib and other proteasome inhibitors are quite likely to arise from “on-target” inhibition in “off-target tissues” (which means to hit the

proper enzyme in a non-carcinogen tissue), rather than off-target inhibition of non-proteasomal enzymes. For example neuropathic pain occurs to some degree with each of the above inhibitors, has been linked to the accumulation of ubiquitinated proteins in cells of the peripheral nervous system.[34] Bearing in mind, Bachovchin et *al* in 2011 envisioned that would be possible to achieve higher efficacy against solid tumors with a proteasome inhibitor with improved inhibitory selectivity for tumor tissues, rather than by developing molecules with improved inhibitory potency or specificity for the proteasome.[35] To achieve an improved tissue selectivity and decrease the "on-target" inhibition in "off-target tissues", they used a double strategy. They developed a tumor-activated prodrug that could provide such tissue specificity, using a tumor-specific protease as trigger whose action releases a shorter peptide of boro-leucine from a longer and in active prodrug (Figure 19). This shorter boro-leucine peptide is the actual proteasome inhibitor, and is expected to undergo a *p*H-dependent cyclization that could significantly attenuate their inhibitor potency at physiological *p*H, which would help to attenuate systemic effects as excess inhibitor diffuses from the tumor site (Figure 17). Such defined and programmed loss of pharmacological activity with time is characteristic of the action of agents termed "soft drugs". Typically soft drugs need to be applied directly to the intended site of action (Figure 19).[36]

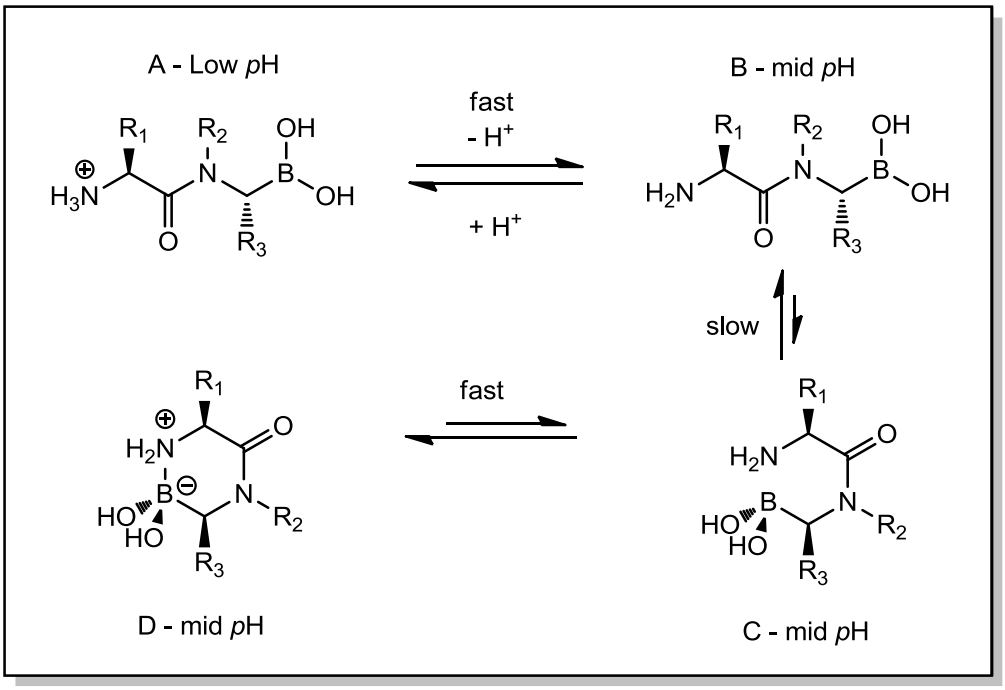

Figure 17 - pH-Dependent cyclization that attenuate systemic side effects.

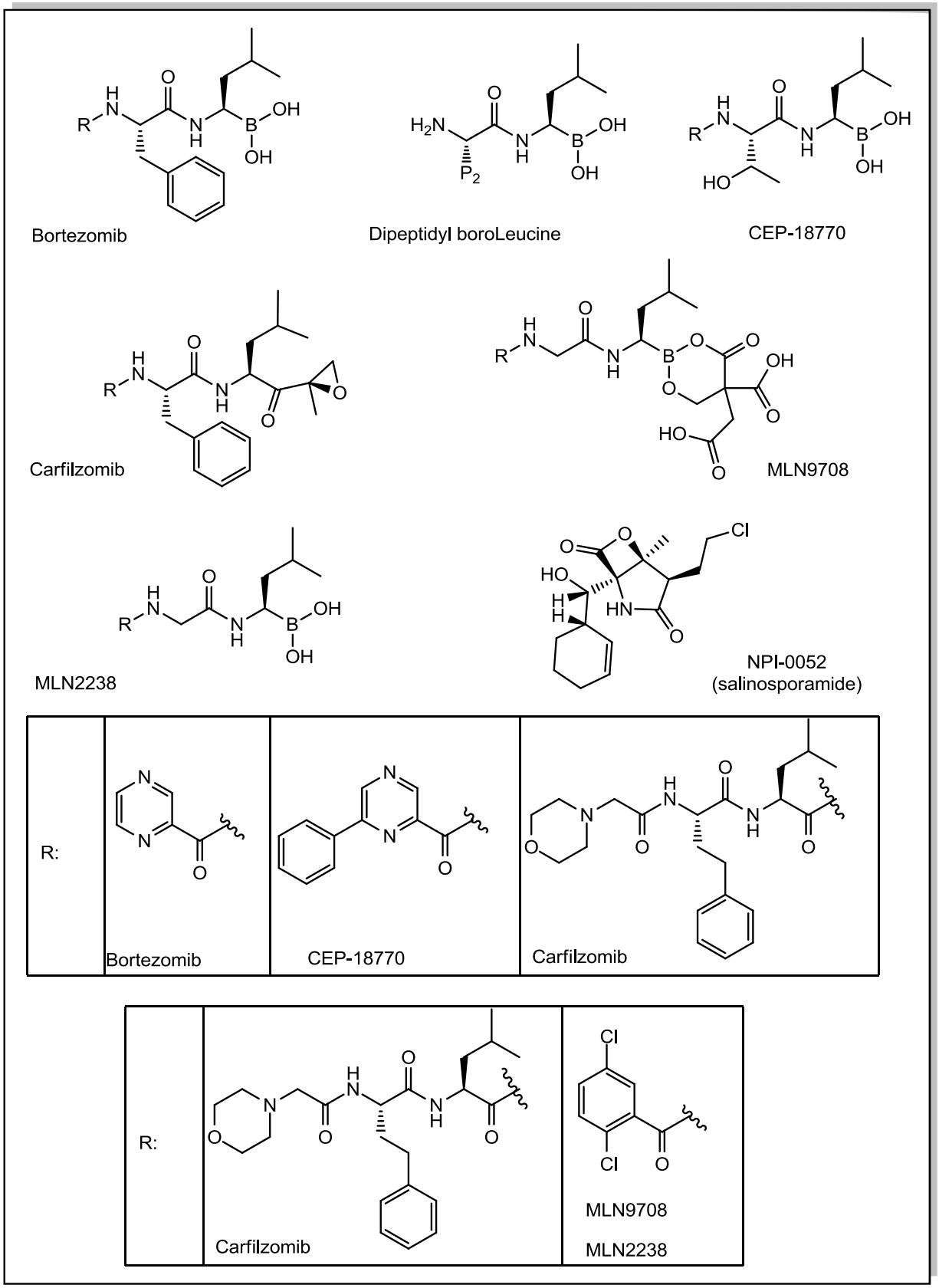

Figure 18 - Second generation of inhibitors to the 26S proteasome.

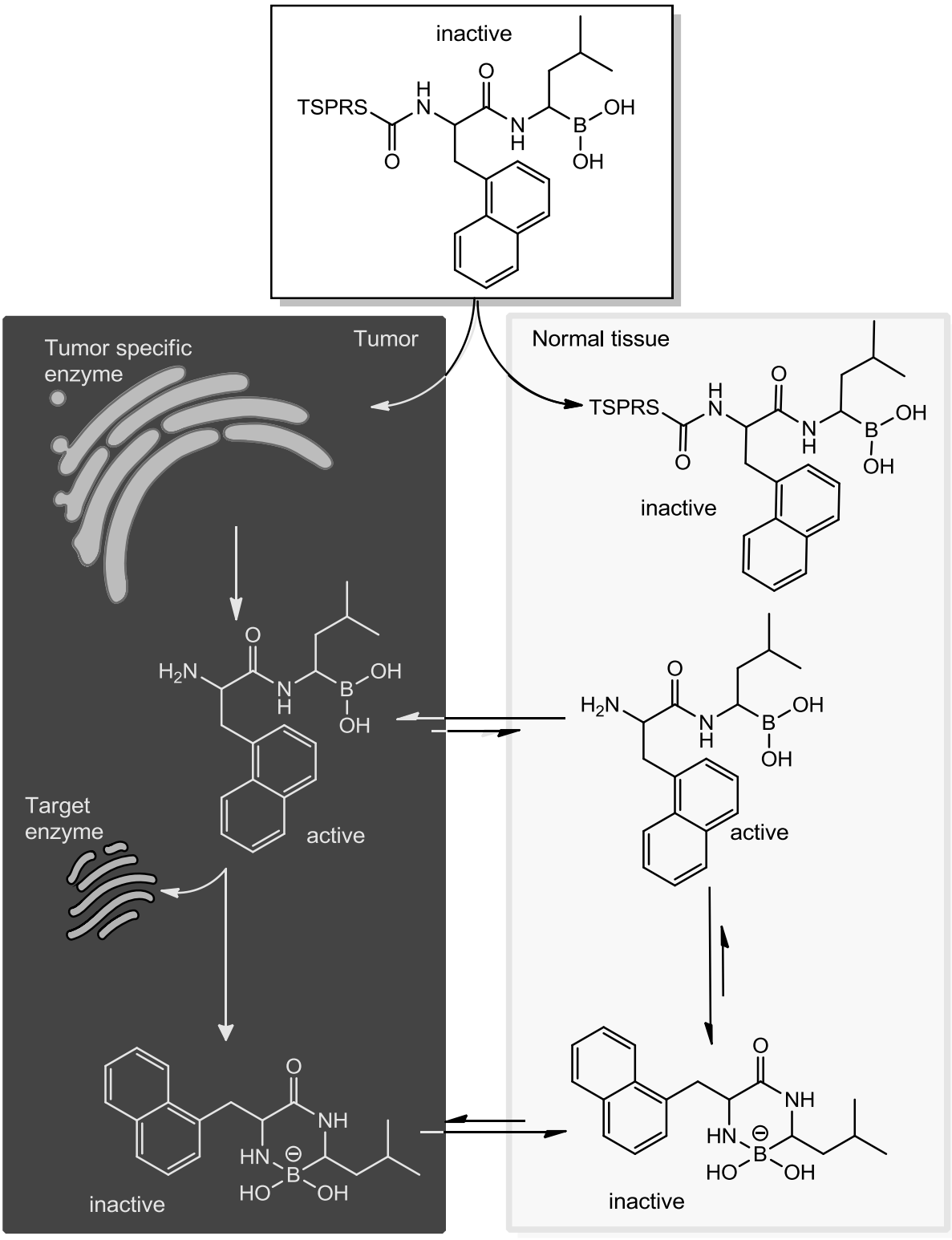

Figure 19 - Pro-soft-drug selectivity to avoid "on-target" inhibition in "off-target tissues".

Heart disease and coronary artery disease

Heart disease is the number one cause of death in the United States, and hyperlipidemia can greatly increase the risk incidence of such traumatic events.[36] In the contest of coronary artery disease (CAD), serum concentrations of high density lipoprotein (HDL) cholesterol are inversely correlated with the risk for developing CAD. Lipoprotein lipase (LPL) is a member of the lipase family, involved in the metabolism of VLDL and chylomicrons, promoting the mobilization of fatty acids from the hematic stream to the muscles, where it can be used as energy source, or to the adipose tissues, for storage, reducing the risk of CAD. There is a positive correlation between HDL-C levels and LPL activity.[37] Differently the endothelial lipase (EL), which is a triglyceride lipase, preferentially explain its hydrolytic activity towards HDL over other lipoproteins. Moreover, HDL is modulated by EL more than by any other lipase.[38] The inhibition of EL over LPL would be crucial to achieve the goal of decreasing the risks of CAD, by means of increasing the levels of HDL-C. In this context, Bachovchin et *al* reported the synthesis of alkyl, aryl, or acyl-substituted phenylboronic acids that inhibit preferentially EL over LPL. They showed that a modification with an alkylic chain at the *para*-position of a phenyl boronic acid, provide such selectivity, achieving the acumen of discrimination with the nonyl alkylic chain (Figure 20) An approach to control the levels of lipids into the blood could be achieved by transcriptional control of lipogenic and cholesterogenic enzymes, since they are involved in the regulation of lipidic metabolism [39]. In 2011 Fajun Yang et all synthesized and tested a small library of boron-containing stilbene derivatives (Figure 21), this library was further tested for its biological effects as lipogenic inhibitors. In this study the mRNA level of fatty acid synthase (FAS) was used as the readout.[40] Treatment of HepG2, a line of human hepatoma cells, with the compounds of the library at 30 μM resulted in a significant decrease of FAS expression. Also the hepatocytes cell line when treated with BF102 resulted in a significant decrease of mRNA levels of both fatty acids and cholesterol.

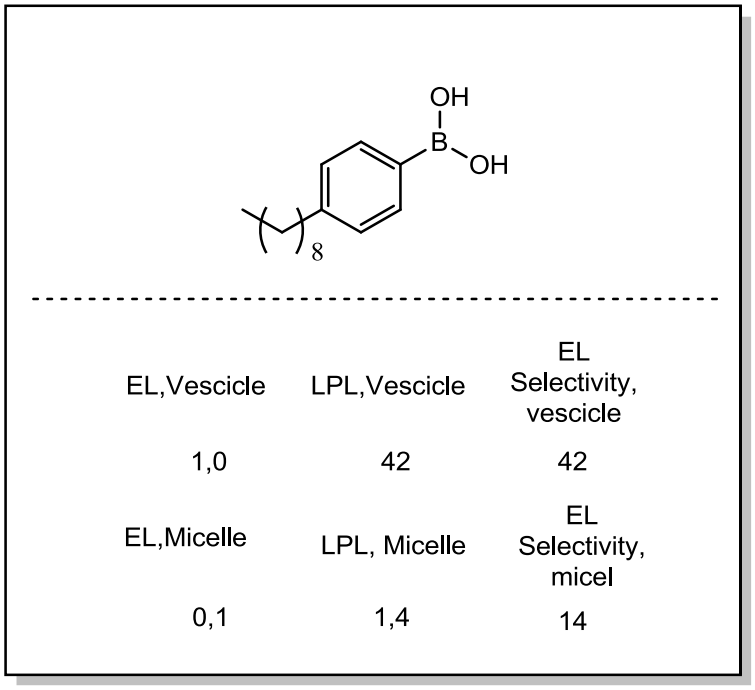

Figure 20– IC_{50} express in µM of the alkyl chain in the *para* position on the phenyl boronic acid tested by Bachovchin et al.

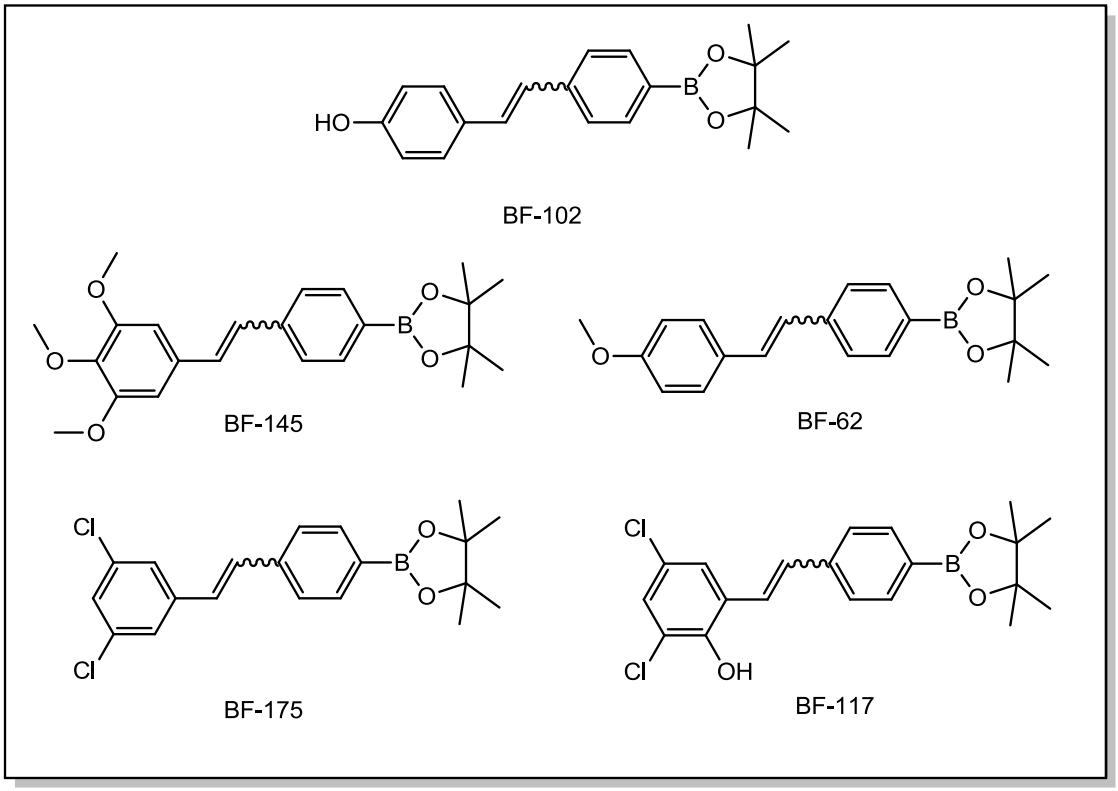

Figure 21 - Boron-containing stilbene derivatives tested as lipogenic inhibitors.

Diabetes

Val-boroPro (Figure 22 a), also known as PT-1001 or talabostat and its closely related dipeptide boronic acid Ala-boroPro (Figure 22 b), were firstly synthesized as inhibitors of dipeptidyl peptidase IV (DPPIV). DPPIV is a member of the prolyl oligopeptidase subfamily,[41,42,43] and a valid target for the treatment of type 2 diabetes.[44, 45]

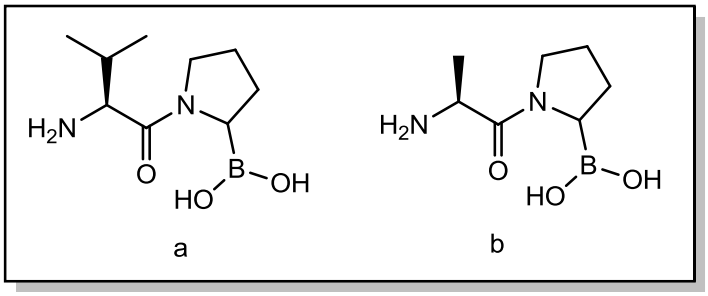

Figure 22 - Val-boroPro and Ala-boroPro inhibitors of dipeptidyl peptidase IV.

The mechanism whereby DPPIV decreases the blood levels of insuline, involves the degradation of gastrointestinal hormones incretins, which promotes the secretion of insuline.[46] The compound **a** depicted in Figure 22, was never considered as a clinical candidate, for diabetes, due to its toxicity. The other members of the prolyl oligopeptidase sub family are reported to be inhibited as potently as DPPIV [41,42,43] and they could be involved in the toxic profile of this molecule. The presence of boron in compound **a** confers the interesting characteristic to undergoes cyclization in water according to the *p*H (Figure 23). The cyclization reaction is a slow process ($T_{1/2}$=30'), and at physiological *p*H the equilibrium is shifted towards the cyclic structure,[44,45,47] which in turn makes the molecule inactive against its target.

Such features were beautifully exploited by Bachovchin et al to mitigate the toxicity of these molecules. This group reported the synthesis of a pro-soft-drug (Figure 24)that was designed to deactivate in a predictable and controlled manner to prevent unwanted systemic effects after exerting their therapeutic action.[48] The author showed that the compound depicted in Figure 24, either in vitro and in vivo (Chg-Pro-Val-boroPro), acts as a prodrug of **a** in Figure 22, which is activated and targeted to the same enzyme dipeptidyl peptidase IV. DPPIV first activates the pro-soft-drug of **a** in Figure 22, the compound

released is still in the open chain structure which enable it to exert its pharmaceutical activity, the molecules which escape from the “target tissue” will be inactivated through the cyclization process above discussed (Figure 24).

This approach enables the molecule to preserve its biological activity against DPPIV but decreases the toxics effects, resulting from inhibition of other prolyl oligopeptidases.

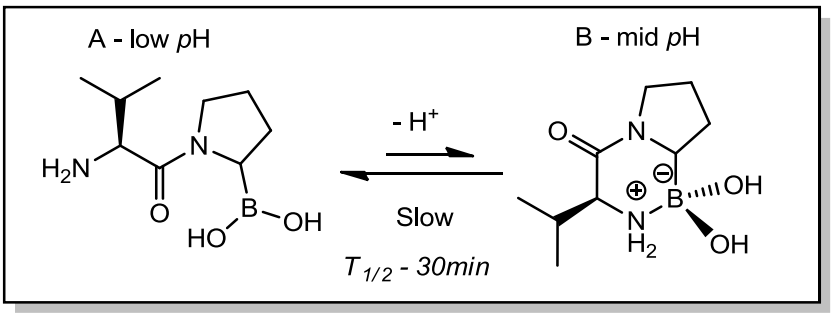

Figure 23 - pH Dependent cyclization.

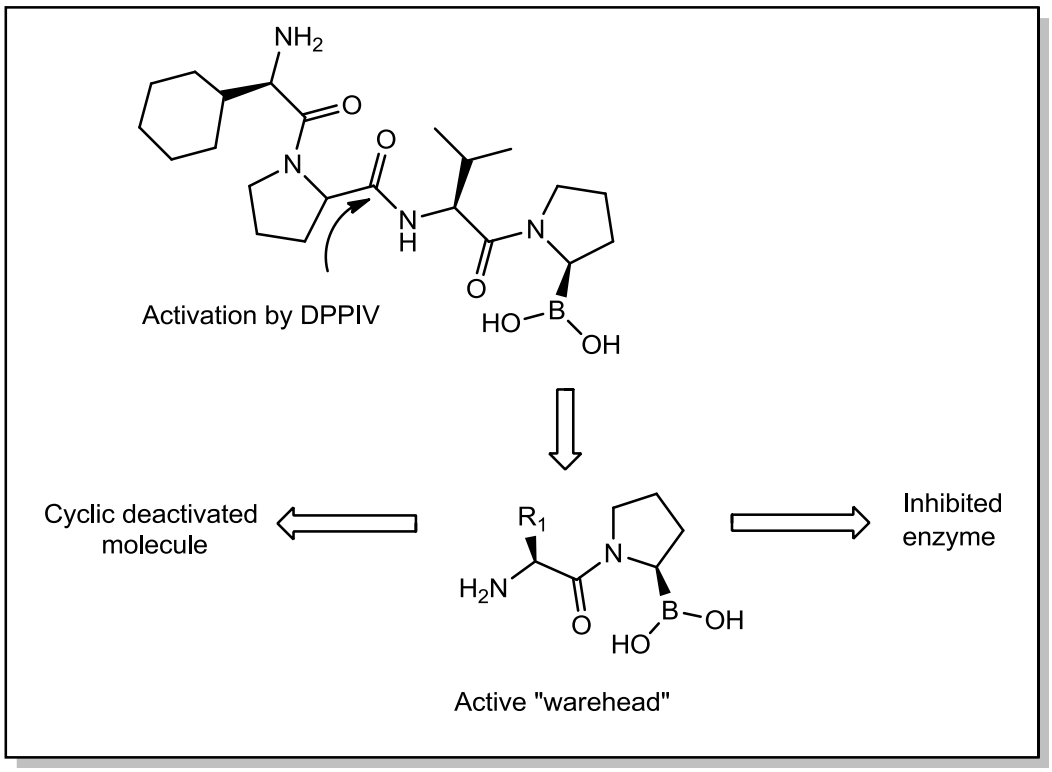

Figure 24 - Pro-soft-drug that is activated in situ, yielding the active molecule, which will cyclise in a predictable and controlled manner losing its biological activity.

Anti HIV viral entry

Balzarini et al in 2007, [49] hypothesized that carbohydrate-binding agent (CBAs), could be able to bind the glycan moiety of the Envelope glycoprotein GP120 (gp120) of HIV-1. The CBAs could have a double mechanism interfering with the binding between the membrane of CD4+ T-lymphocytes and gp120, disabling the mutation process, which guarantees the virus escape from the drug activity. Based on this idea Jay et al[50] developed a novel microbicide based on the boronic acid ability as CBAs and the protein lectins. This approach has the drawback of using expensive components like the protein lectins, making it a unsustainable cure for patients of undeveloped countries, which represent the most part of worldwide patients. Barbue et *al* [51] overcame this problem, synthesizing and testing a water-soluble polymer, which is polyfunctionalized with benzoboroxol alongside with the polymer chain (Figure 25). The polymer was prepared with 25, 50, 75 mol % of benzoboroxol, and the latter showed a 11nM activity in reducing HIV viral entry in an in vivo test.

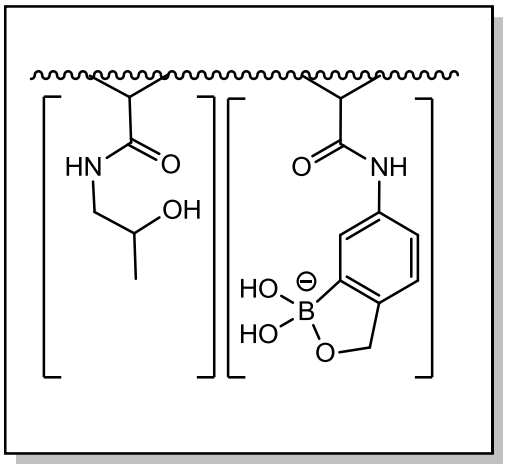

Figure 25 - Water-soluble polymer based on benzoboroxol.

Boron based antibiotics

Bacterial infections have always been one of the main issues of worldwide health care. Bacterias and their hosts have influenced the evolution of each other through a process of exposition-and-selection, between the pathogen agent which selected the more resistant host,whicht in turns with its adapted immune system selected differently virulent pathogens, in a never ending dance. The discovery of penicillin and invention of β-lactamic antibiotics, have introduced a new efficient way to address this problem. Unfortunately the bacteria quickly responded with the synthesis of β-lactamases. Thus the strategies used by the pathogen to overcome the use of antibiotics can be resumed in three mechanisms [52].

- *β-Lactamases*
- *Low affinity Penicillin Binding Proteins (PBPs) for β-lactams*
- *Over expression of resistant PBPs*

The PBPs family, which is the main target for the therapy against the bacterial infections, can be divided in three classes.[53,54] Classes A and B, ranked as high-molecular mass PBPs which contain two catalytic domains (glycotransfer (GT) and the transpeptidation (TP)). Finally, class C is composed by low-molecular mass PBPs, named CPBPs [54,55] with a TP activity. The TP domains mostly catalyze the cross-linking of stem peptides via an acyl-enzyme intermediate formed by nucleophilic attack of a serine residue. Zervosen et *al*. have shown that boronic acids are potent β-lactamase inhibitors, bearing in mind the already reported ability of the boronic acid to form reversible covalent adducts with OH groups, which mimic the tetrahedral intermediates in the PBP-catalyzed acylation reactions.[52]

Zervosen group, in 2012 synthesized and studied the potential of a number of acylaminomethylboronic acids as inhibitors of PBPs. Several derivatives inhibited PBPs of classes A, B and C from penicillin sensitive strains (Figure 26).

In 2011 Trivedi et *al* described the preparation of chiral aryl boronate esters of 1,2-o-isopropylidene-α-D-xylofuranose to screen their activity as a new class of antimicrobial agent (Figure 27a).They elected the protected pentose sugar, 1,2-O-isopropylidene-a-D-

xylofuranose[56] as a precursor because of its known utility as a key intermediate in the synthesis of many drugs among them: anti-HIV agents,[57] nucleosides,[58] antibiotics.[59]

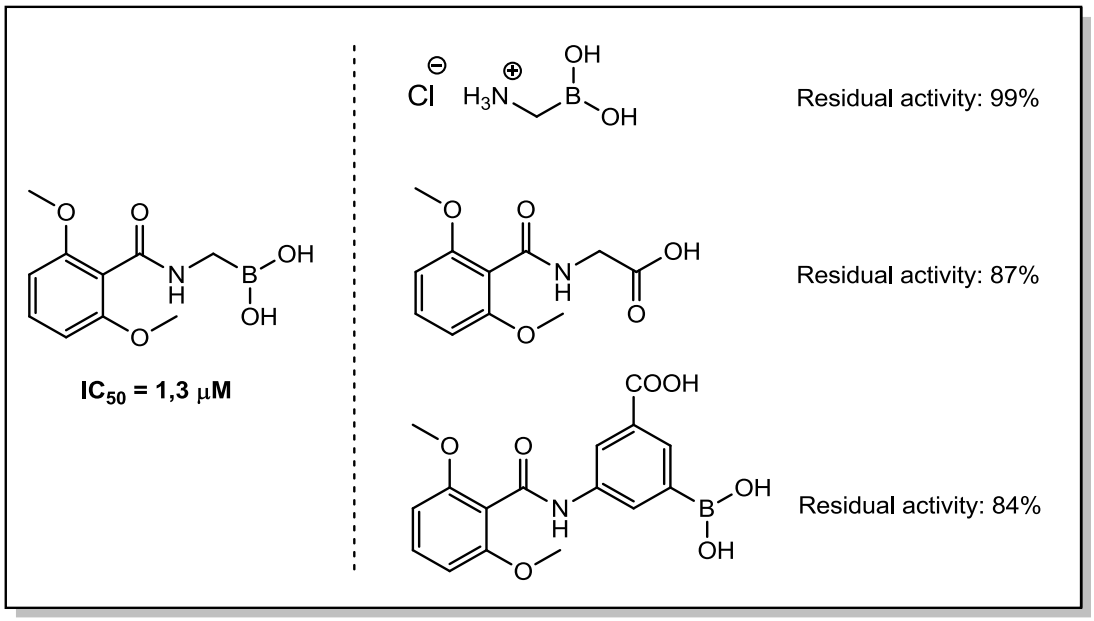

Figure 26 - Acylaminomethylboronic acids developed by as inhibitors of PBPs.

This synthetic approach led them to an efficient and easy way to prepare a wide range of boronate esters in a single step. The reaction proceeds in Et_2O as solvent at room temperature affording the final product in 92% yield for the basic compound **a**(Figure 27)used as benchmark. They synthesized several compounds using different boronic acids. The evaluation of these compounds revealed that their activity is modulated by structural modifications in the aryl group attached to the boron atom. Of all compounds tested **b** and the **c** depicted in Figure 27 showed an interesting activity as anti-bacterial and anti-fungal agents.[56]

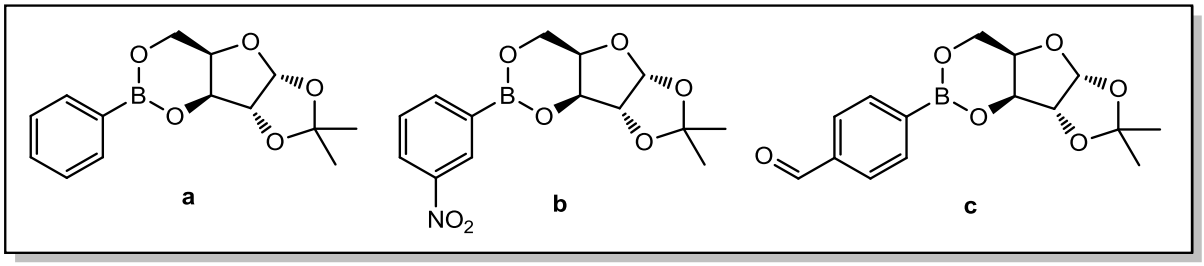

Figure 27 - Chiral aryl boronate esters of 1,2-o-isopropylidene-a-D-xylofuranose developed as new antimicrobical agent.

Typically, chemotherapic agents that aim to minimize the adverse sides effects, should point to a target that is present in the cells of the pathogen but absent in the cells of the host. The bacterial amidotransferase (Glu-AdT), is an essential enzyme to synthesize Glu-tRNA (Gln), that satisfies this characteristic.[60] Boronate ester were successfully designed to inhibit Glu-Adt, through a putative serine trap mechanism. Decicco [61] in his study suggested that the presence of a serine hydroxyl functionality is essential for the activity of the enzyme Glu-AdT. Thus many serine trap inhibitors were tested against this enzyme. In general, a serine trap embodies in its structure an electrophilic center capable of accept in a lone pair of electrons from a nucleophile. Ketones with alpha electron withdrawing groups (esters, amides, halogen, phosphonates, β-lactams) have been studied as inhibitors of the Glu-AdT.[62]

Decicco et al synthesized Glu-γ-B(O_2R) a compound that displayed IC_{50} values of 1.6μM and 100nM, respectively, against the glutaminase (GLA into the Figure 28) and the transferase (TRA into the Figure 28) activity of Glu-AdT (Figure 28).

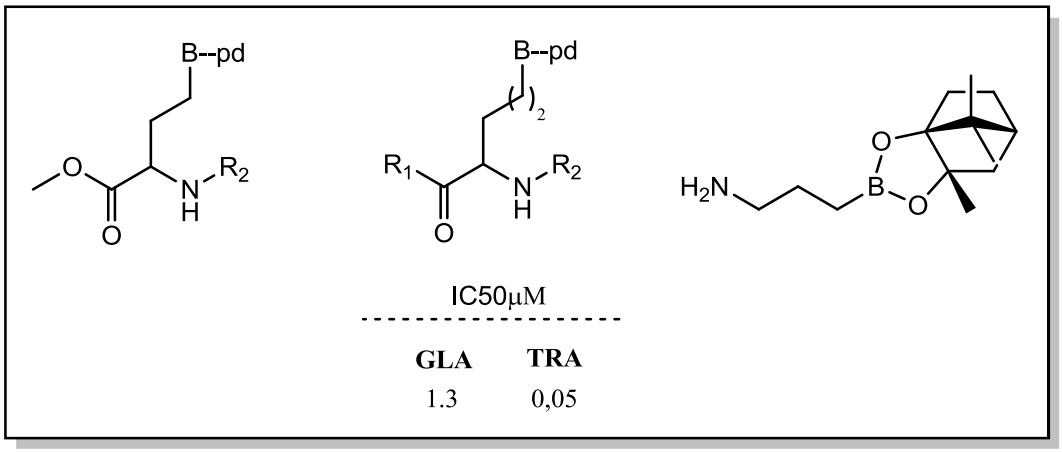

Figure 28 - Decicco's Glu-γ-B(O_2R) compounds active against the glutaminase and transferase activities of Glu-AdT (values in μg/ml).

The DD-peptidase is the enzyme responsible for the final step of the bacterial cell wall synthesis, through the incorporation of the monomers in the already formed structure of the peptidoglycan.[63] Pratt et al describe the synthesis of (D-R-aminopimelylamino)-D-1-ethylboronic acid (Figure 29) for the R39 DD-peptidase inhibition a low molecular weight class of the sub group C penicillin-binding protein. Their study suggested that boronates could indeed be a very powerful class of molecules as DD-peptidase inhibitors, as mentioned boronate inhibited the peptidase with a Ki value of 32±6 nM.

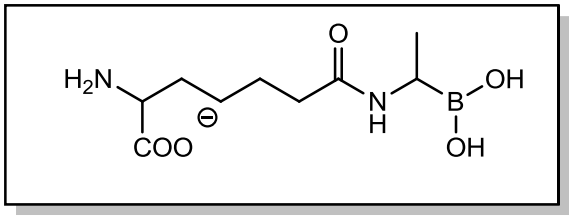

Figure 29 - (D-R-aminopimelylamino)-D-1- ethylboronic acid.

To understand the possible mechanism of inhibition of D-R-aminopimelylamino)-D-1-ethylboronic acid, they performed a crystallography analysis, which suggested that the compound could explicit its activity through a transition state fashion mechanism resulting in a inhibition of the R39 DD- peptidase as shown in Figure 30.

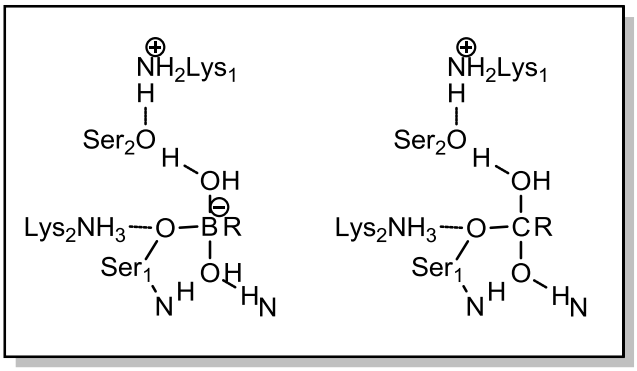

Figure 30 - Crystallography analysis of (D-R-aminopimelylamino)-D-1- and R39 DD-peptidase.

1.4 Boronic acids as templates to promote the assemblage of simple building blocks

When considering the structure of a biologically active molecule, it can be ideally divided in:

- *Active functionalities: the elements of interaction with the host, while performing the biological activity (pharmacophores, groups which take part in the interaction with the biological target)*
- *Inert framework that supplies support to the active functionalities appended on it.*

At a first sight, it seems that the biological activity is influenced more pronouncedly by the active functionality rather than the inert frame work. Despite the framework lack of direct contact with the reactive residues of the protein, it is responsible for the proper geometric orientation of the active functionalities. Under this light the biological activity of a molecule depends on the “inert” framework as much as the active functionalities. Ideally the active functionalities can be pictured as heteroatoms, functional groups of different π-systems, while the framework as an all-carbon structure.

In this context, it is possible to exploit the ability of boron to readily react and establish dative bonds with oxygen and nitrogen nucleophiles, to create complex structures that may serve as a framework embodying the required geometrical features to maximize the pharmacophore enzyme interaction.

Synthetic utility of oxygen and nitrogen ligation to boron

The classical synthetic approach, made of multistep synthesis interspaced by various separation techniques is a time and resource consuming process. Even more when applied to the synthesis of compound libraries, where the magnitude of this "complexity" has to be multiplied by the number of the library components.

The propensity of boron to easily promote the assembly of simple building blocks containing oxygen and nitrogen nucleophiles, may contribute to reduce the efforts of multistep synthesis of complex molecules. In his context, it is expected that by using simple buildings blocks, rationally functionalized with oxygen and nitrogen atoms, it may be possible to create structures with the required "active functionalities" and geometry, via an assembly reaction promoted by a a boron tether. The implementation of this innovative strategy would enable the straightforward generation of discrete molecular surfaces with distinct pharmacophore that may be readily tuned for optimal interaction with the biological target.

Based on this idea several approaches have been made to achieve the efficient synthesis of small molecules using born tethers. In particular, three of these strategies have been well succeeded, and will be discussed in the next few pages:

- *Using the B-N bond as a surrogate of the C=C bond.*
- *Exploiting the B-O coordination to construct all-carbon analogues.*
- *Using boronic acids as templates for multi component assemblies.*

Using the B=N bond as a surrogate for the C=C bond

The relationship between the single bond B-N and the double C=C bond is well known across many fields of chemistry (organic, inorganic, materials etc.), since the similarity has been disclosed, by the seminal work of Dewars et al.[64,65,66,67]

The analogy triggered the imagination of many scientists, lured by the possibility of replacing a difficult task of synthesizing a new bond between two carbon atoms, with a much easier strategy, which involves the creation of a link between boron and nitrogen atoms. The correlation between the two systems, starts from the position of the boron, carbon and nitrogen in the periodic table. The order in which they appear into the second period is: B, C, N, in other words boron has one less electron than carbon whereas nitrogen has one more electron. Thus, when compared, the B-N and the C=C bonds, share the same number of electrons, and in 20% of the cases they also have the same numbers of protons and neutrons (natural abundance of B^{10}). Despite these common characteristics, these compounds are still not sufficiently similar to consider the B-N as a perfect surrogate of the C=C bond. The difference of electronegativity between boron and nitrogen is responsible for a sensible polarization of the σ-bond, giving it a considerable ionic character, which can alter the global electronic profile of the molecule (ionic against the apolar character of the C=C).[68] Moreover the B-N single bond is susceptible to rotate around its axis, characteristic that does not afford the structural rigidity idiosyncratic to the C=C bond.

The difference of polarization between B-N and C=C dramatically affects the macroscopic property of the molecules or materials in which is present. An example of this difference is the case of graphite that is a carbon allotrope, which is black, has a metallic structure and high conductivity property, while the B-N analogue of graphite, is white with insulating properties.[69]

A possible solution to increase the homology between molecules and materials featuring the two different bond systems, is the presence of an additional dative bond between B-N. This dative bond indeed benefits the correspondence between C=C an B-N bond by reducing the polarization of the σ bond. In fact, while the direction of the dipole is from boron to nitrogen (B-N) in the sigma bond due to the difference of electronegativity, in the dative bond, the current is reversed (Figure 31). [70,71,72] In addition to this, the partial π-interaction determines a geometrical rigidity along the B-N bond.

Based on the aforementioned, one must conclude that for a proficient C=C/B-N replacement strategy, the components should comprise a nitrogen moiety with an available lone pair of electrons and a vacant *p*-orbital centered in the boron atom.

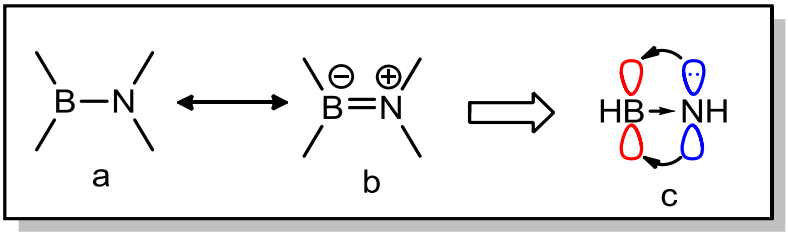

Figure 31 - Polarization of the σ and π B-N bonds.

The molecules with a C=C/B-N isosterism, which satisfy these conditions, can be defined as isoelectronic and both are arranged in sp^2 hibridization. The only difference between the two systems is that in the C=C, bond each carbon contribute in equal manner to the bond, while in the B-N π-bond the two electrons are provided by the nitrogen.[73]

In 2011 Katzenellenbogen et al exploited the possibility of replacingthe C=C bond with the B-N bond to synthesize a novel compound active against estrogen receptors (ERs). While investigating the design active compounds against this target, they observed that despite the structural differences of the molecules tested, they still shared some repetitive substructure motifs (active functionalities) which was vital for the biological response.[74] They postulated that these “repetitive motifs” were embodied in a core that had essentially no contact with the protein. Thus, following on this observation, they proposed that the “inert core” could be readily assembled based on the simple condensation of reactants exploring the B-N bond. The advantage of this strategy lies in the possibility of producing libraries of compounds in a modular fashion. So while the focus of their work, was the synthesis of ER active molecules, the climax was achieved through the idea of designing a generic and synthetically accessible core, where to attach multiple “active components”.

The functionality identified as “repetitive active motif” was: a phenol in a homodibenzyl motif (Figure 32).

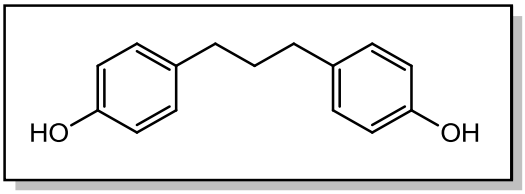

Figure 32 - Repetitive homodibenzyl motif ERs.

In addiction they also found that the C=C double bonds were also present in the core of a number of nonsteroidal ER ligands, manly those belonging to the cyclophenil and triarylethylene class (respectively structures **a** and **b**, in Figure 33).

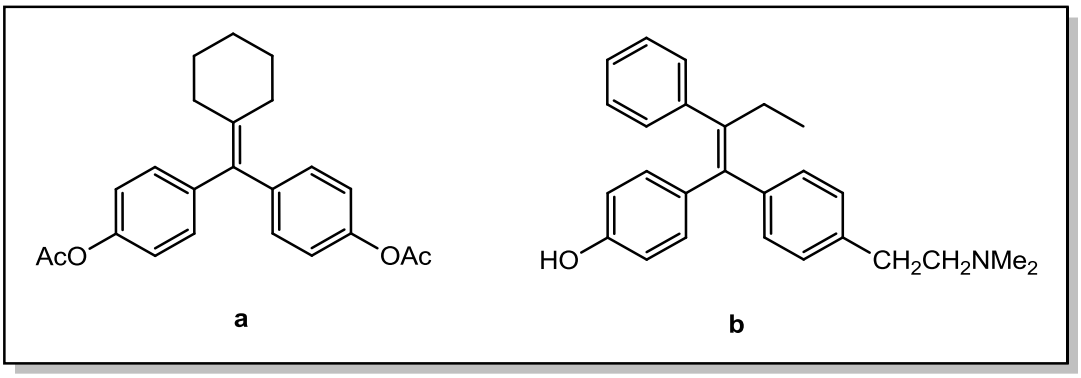

Figure 33 - Cyclophenil and triarylethylene.

Based on these two observations, Katzenellenbogen et al designed and syntesized a series of anilino dimesitylboranes in order to reproduce the structure of the triarylethylene ER ligand, replacing the C=C double bond by a B-N bond (Figure 34). These B-N analogues showed not only a remarkable stability and affinity for the ERα, but they were also much easier to prepare. The synthetic simplicity suggested and biological activity uncovered in this study clearly suggested that B-N for C=C substitution could be widely used for the preparation of analogues of drug candidates.

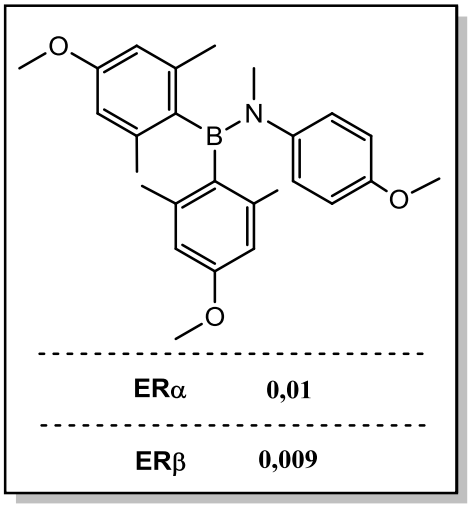

Figure 34–Anilino dimesiylboranes that replace a double bond C=C with a B-N and its ER relative binding affinity.

Exploiting the B-O coordination to construct a all-carbon analogues

A clear example of this second strategy, was recently disclosed by the work of Woon and Schofield that assembled several boronate esters in presence of prolyl hydroxylase domain isoform 2 (PHD2), a Fe^{II} and 2-oxoglutarate (2OG) oxygenase that regulates the human hypoxic response,[75] using the dynamic-combinatorial mass spectrometry (DCMS) to detect labile complexes derived from mixtures of boronate formed in situ and the enzyme.

The motif that served as the structural guide for the design of the boronated analogues was the 2-(picolinamido)-acetic acid scaffold. Because, based on crystal structures of PHD2,[76] was determined that this scaffold chelates with Fe^{II} at the active site. Therefore, the experiments proceed through the incorporation of a boronic acid moiety, into the 2-(picolinamido)-acetic acid scaffold as shown in Figure 35. Several diols were let to react with the new scaffold, in order to form the cognate boronate esters.

The diols 2,4-Dihydroxybenzoic acid and cathecol depicted in Figure 35, demonstrated to generate the most active compounds against the targeted enzyme. Therefore to validate this approach and the potential of this strategy to discover new lead compounds, the authors synthesized two stable all-carbons analogues (Figure 35) using the benzofuran- and naphthalene-moiety to mimic the structure of the boronate derived from the assembly of boronic acid with the diols depicted in the Figure 35. The binding constants of the all

carbons analogues were in the same range suggesting that the replacement of the boronate with the two rings system was indeed a very effective strategy to discover new compounds with biological activity against this strategy.

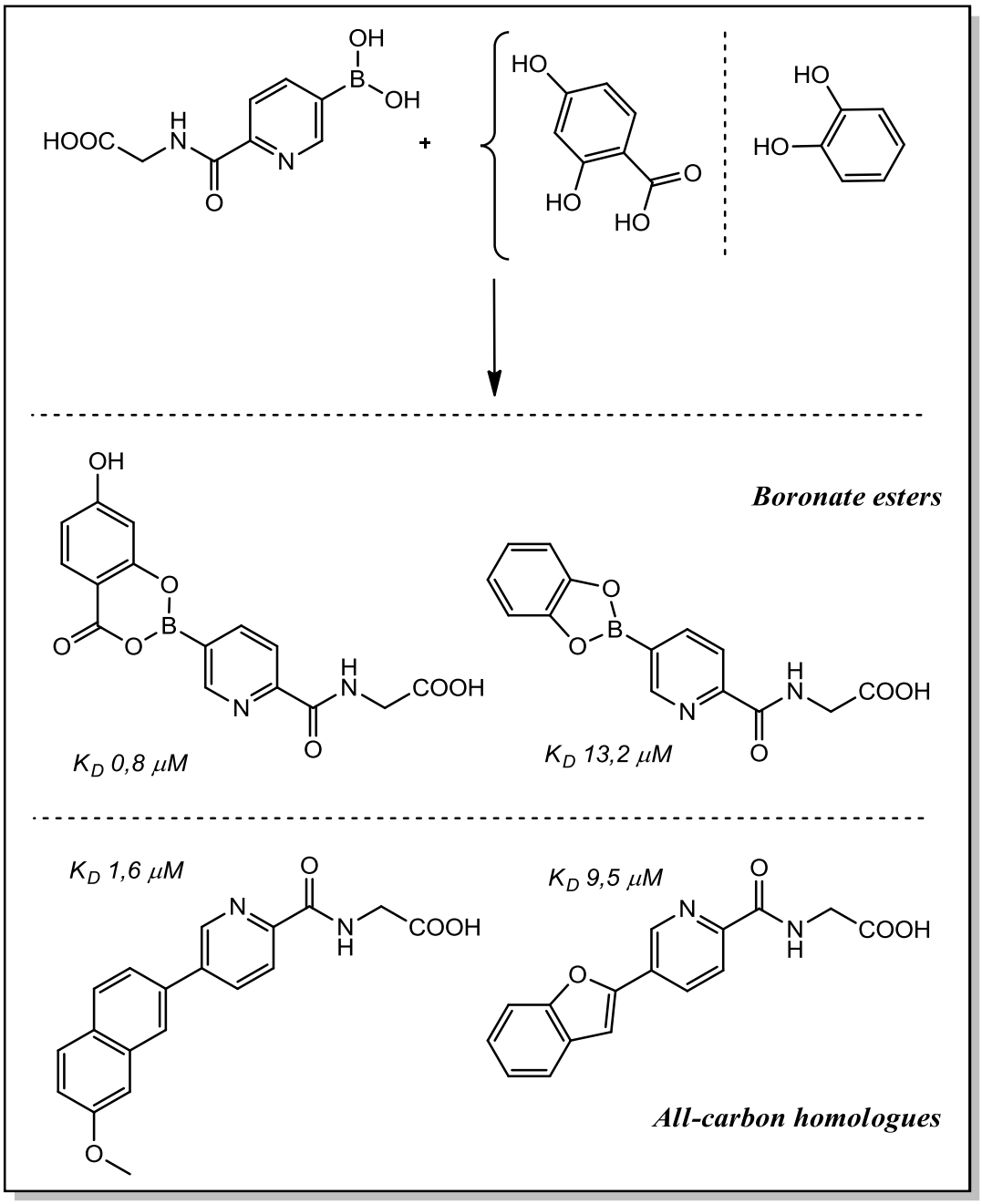

Figure 35 - 2-(Picolinamido)-boronic acetic acid derivatives and their all carbon analogues.

Using boronic acids as templates for multi-component assemblies

The ability of boronic acid functionality to act as an internal tether for oxygenated and or nitrogenated compounds and their ability to engaged in MCR, makes this versatile functionality very useful to create collections of complex compounds with a framework designed to correctly present the pharmacophore sat the enzyme active site, and this constitutes the realm of this thesis.

If successful, this approach (which will be named *boron tether strategy*) affords a direct synthesis of complex active molecules *via* the assemblage of distinct building blocks, that may be rationally tuned to improve the uncovered biological activity. In addition to this and from a synthetic point of view, this approach, based on a one–pot multicomponent reaction, contributes to reduce the long plethora of complex methodologies frequently used in a multi-step sequence, which often yield the target compounds in low yields determining the need for extensive purification steps (Figure 36).

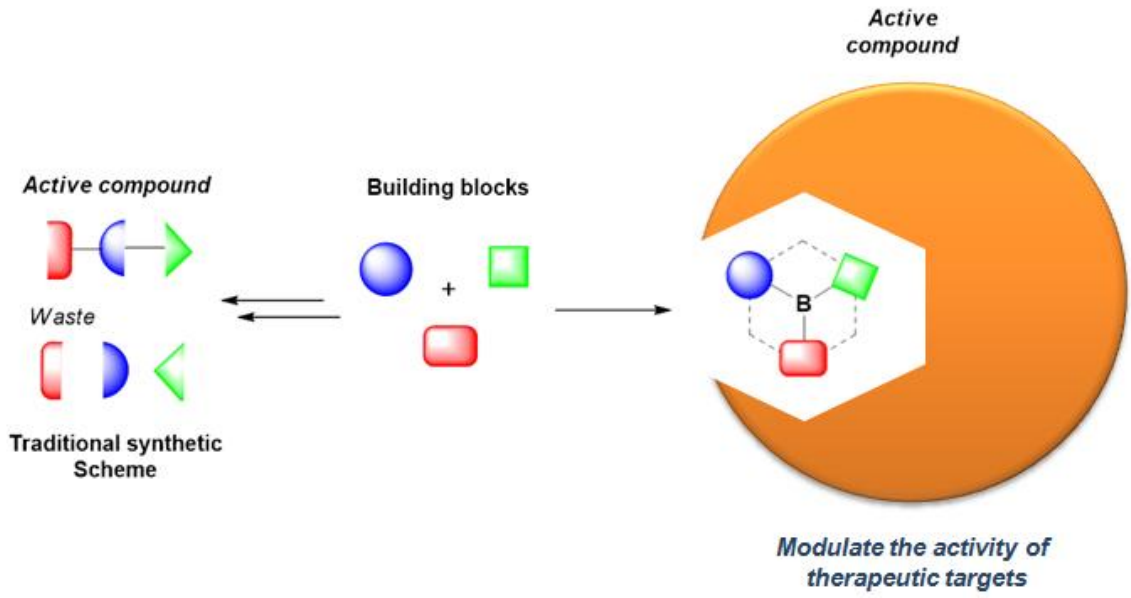

Figure 36– Boron tether strategy Vs classical chemical approach.

2. Fused tricyclo-boronate heterocycle

2.1 Overview

The chemical modification of natural products is an extensively used procedure in medicinal chemistry. Such an approach aims to produce natural-product like compounds with an improved biological profile. The pursuit of such goal, often requires the discovery of new and complex synthetic routes. Therefore, we envisioned that the boron tether strategy could offer the possibility to perform the synthesis of natural-product like compounds, overcoming the cost and time demanding problems of classical chemical modification of natural compounds and uncover new hit compounds.

To demonstrate this concept, we looked at Nature seeking for inspiration to select a chemical structure combining a certain degree of geometrical complexity and an interesting biological profile, which may serve as the base for the design of boronated analogues via the assembly of simple building blocks.

Bearing these requirements in mind, we focused our attention in the family of spongiane diterpenoids that display very interesting structural features and a wide range of biological properties, that includes: antifungal, antimicrobial, antiviral, antitumor, antihypertensive, anti-inflammatory activity.

2.2 The spongiane diterpenoids

Sponges are classified as sessile animals, which means that they are permanently attached to a solid substrate. The impossibility to escape from predator attacks, forced them to focus all their defensive strategies on a chemical arsenal mainly composed of a wide range of terpenoids. Despite this family of molecules been largely shared by all the marine phyla, the spongiane diterpenoids are exclusively present in two families of animals: the sponges, which use them as defensive chemical weapons, and the nudibranchs. The latter are shell-less mollusks, which feed on sponges, and are able to store the spongiane-derived metabolites and even to use them as own self-defense strategy.[77] The first compound of this family to be discovered was the isoagatholactone (Figure 37), isolated by Minale et al.[78] in 1974 from *Spongia officinalis.*

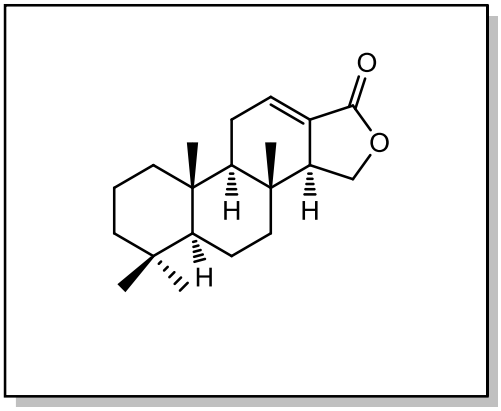

Figure 37 – Isoagatholactone.

The terpenic structure of the spongianes is quite heterogeneous and may present very important differences among several structures. Gonzàles in a recent review, tried to organize the spongiane terpenoids taking as model the general skeleton of isoagatholactone highlighted in Figure 37.

In this review,[78] Gonzàles ranked the nearly 200 compounds (known at the moment of writing), keeping in mind the massive number of modifications that can occur on the model skeleton (Figure 37), namely the degree of oxidation as well as the rearrangement of the 6,6,6,5 carbocyclyc system of the model structure aforementioned. According to these elements, Gonzàles divided the entire number of compounds in two main subgroups:

- *Compounds having the intact spongiane skeleton*
- *Compounds with an incomplete spongiane skeleton*

The molecules belonging to the first subgroup are characterized by a large number of different functionalizations, which taken together produce a very high number of variations of the intact spongiane skeleton.

Among the different structural motifs, the oxofuro[2,3-b]furan unit (Figure 38) is an intriguing and prevalant highly oxygenated double ring moiety. Schmitz suggested that such highly oxygenated bicycle unit could complex cations when interacting with some biological target.[77] The mentioned sub-structure is present in the skeletons of the aplyroseol-1 a mildly cytotoxic agent in lymphocytic leukemia PS cells, which also possesses inhibitor activity against the phospholipase A2 (PLA2), an enzyme involved in

inflammatory processes, sharing this activity with aplyroseol-5 and aplyroseol-6.[78] Also dendrillol-1 has proved to have cytotoxic activity on tumor cells (Figure 38).[79]

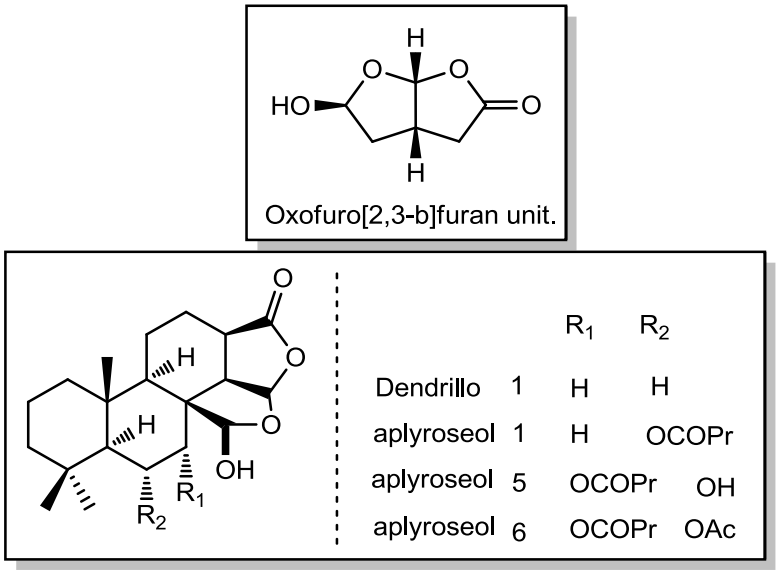

Figure 38 - Oxofuro[2,3-b]furan unit and some compound having the intact spongiane skeleton .

The oxofuro[2,3-b]furan unit depicted in Figure 38, is also a recurrent motif in some of the compounds belonging to the second subgroup described by Gonzàles, where it is even more prevalent. The first compound belonging to this family is norrisolide (Figure 39). Isolated by Faulkner and Clardy from *Chromodoris norrisi* [78].

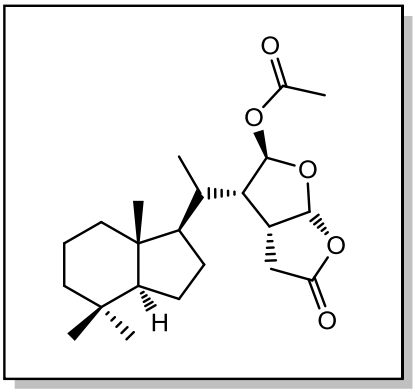

Figure 39 - Norrisolide, molecule that belongs to the second subgroup (compounds with an incomplete skeleton), that embodies a oxofuro[2,3-b]furan unit.

Other examples are the structures of omriolide A (Figure 40a), isolated from the *Dictyodendrilla aff. Retiara,*[80] which possesses an interesting trioxatricyclodecane ring system and chromodorolides A (Figure 40**b**) and B (Figure 40**c**)**,** both extracted from *Chromodoris cavae.* Interestingly, compound **c** showed both cytotoxic and an antimicrobial activities.[81][82]

A classical approach to synthesize the oxofuro[2,3-b]furan unit (Figure 38) was developed by Reiser *et al*, involving a long processes made of seven steps, characterized by the use of organometallic reagents and harsh conditions.[83]

As aforementioned, a main goal of this doctoral project was to develop the synthesis of natural-product like compounds *via* the assembly of building blocks based on the boronic acid functionality. As shown in Figure 40, we envisioned that boronate analogues of the oxofuro[2,3-b]furan unit, could be prepared substituting the C-C bond between the fused cycles by a isoeletronic N-B bond.[98]

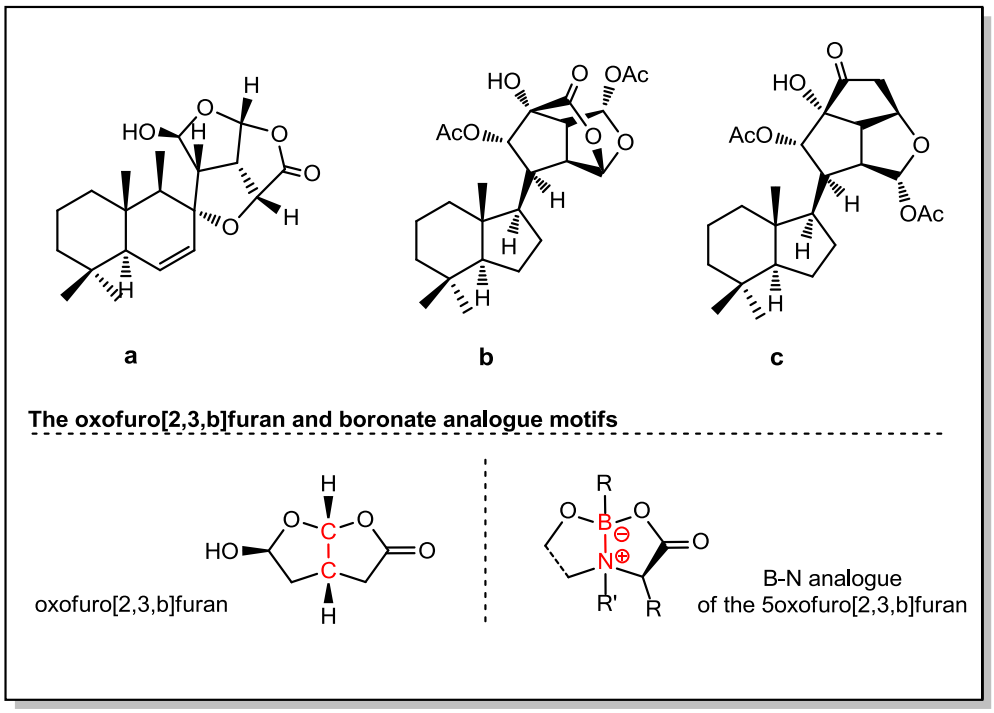

Figure 40 - Others possible examples of structures that embody the oxofuro[2,3-b]furan unit.

Implementing a boron tether strategy to design the oxofuro[2,3-b]furan motif

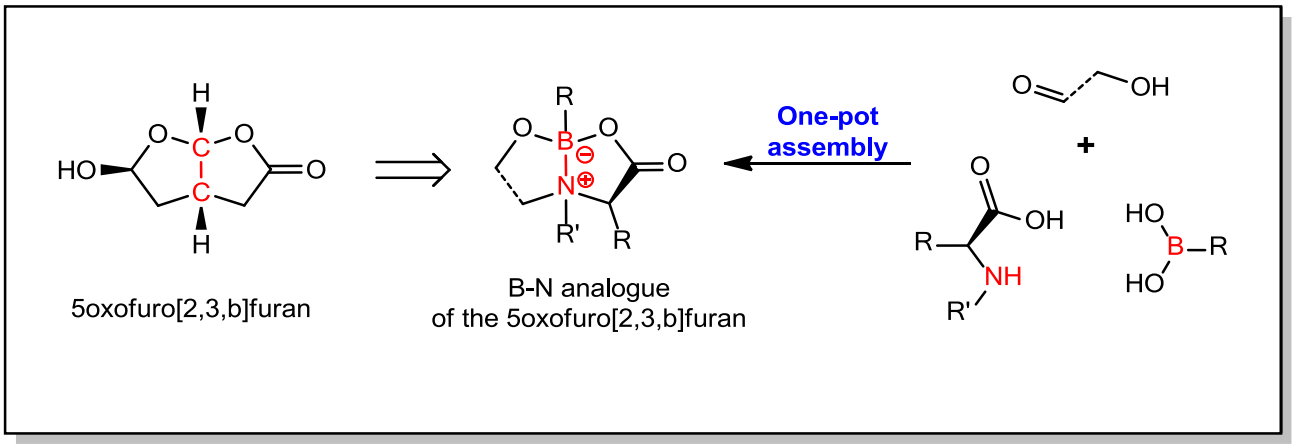

Figure 41– Boron tether strategy to achieve the 5 oxofuro[2,3-b]furan motif.

To design an assembly reaction that could yield the 5-oxofuro[2,3,b]furan analogue depicted in Figure 41, we envisioned that an α-amino acid could complex with the boronic acid affording a five member ring featuring the key B-N bond isosteric to the C-C bond present in the natural product motif. To append the second ring system, we conceived that the candidate building block should comprise an electrophilic center to react with the nitrogen, and an α-alcohol to chelate the boron yielding the bicyclo heteroatom analogue of the 5-oxofuro[2,3,b]furan unit.

Based on the aforementioned, apart from the boronic acid, we selected as starting components for this assembly reaction, proline as it is a conformational constrained nucleophilic amino acid and glycolaldehyde that exhibits an electrophilic aldehyde and OH group (Figure 41).

2.3Synthesis of 5 oxofuro[2,3-b]furan motif analogue

Bearing in mind the rational design aforementioned, we initiated our study by reacting L-proline with phenyl boronic acid and glycolaldehyde dimer (Figure 42), using several solvents (THF, DCM, H_2O, CH_3CN), different equivalent ratios, temperatures and reaction

times. Very gratifyingly, using methanol as solvent after 1 h of reaction at 60°C and using 2 equivalents of the amino acid, 1,5 equivalent of the glycolaldehyde dimer afforded the heterocycle **1** which structure was determined by X-ray analysis (see below) in 95% yield and 94% diastereoselectivity (Figure 43)

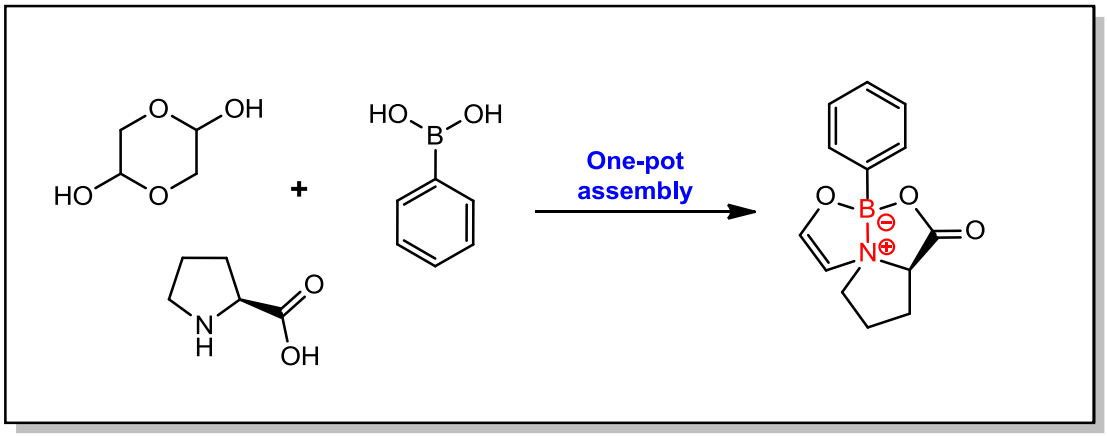

Figure 42 – Reaction design of the first B-N compound analogue of the oxofuro[2,3-b]furan unit.

The diasteroselectivity of the reaction was determined by comparison of the integration values of the signals relatives to the protons derived from the α-carbon of the amino acid employed in the reaction.

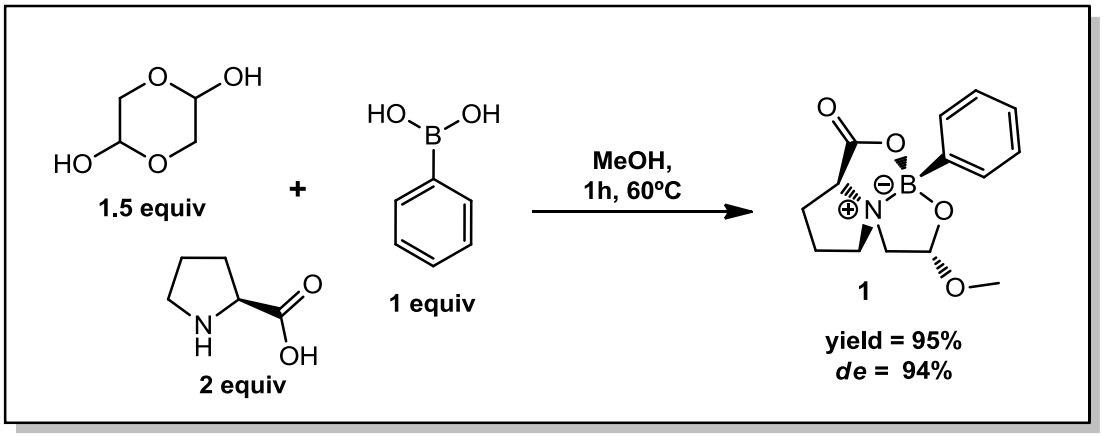

Figure 43 - Synthesis of boronate tricycle-heteroatom architecture using MeOH as solvent.

Very surprisingly, the X-ray crystallography analysis of the crystal obtained for heterocycles **1**, revealed that what in the NMR spectra of the compound **1** appeared to be

a residual impurity coming from the MeOH used as the reaction solvent was instead an unexpected functionality of the molecule. Indeed instead of a three-component assembly, the tricyclic heterocycle **1** was obtained *via* a one-pot four-component condensation in which methanol entered at the concave face of the lactone-acetal bicyclic system, (Figure 44). This rather unexpected result increased considerably the homology of the boronate complex with the natural-product motif.

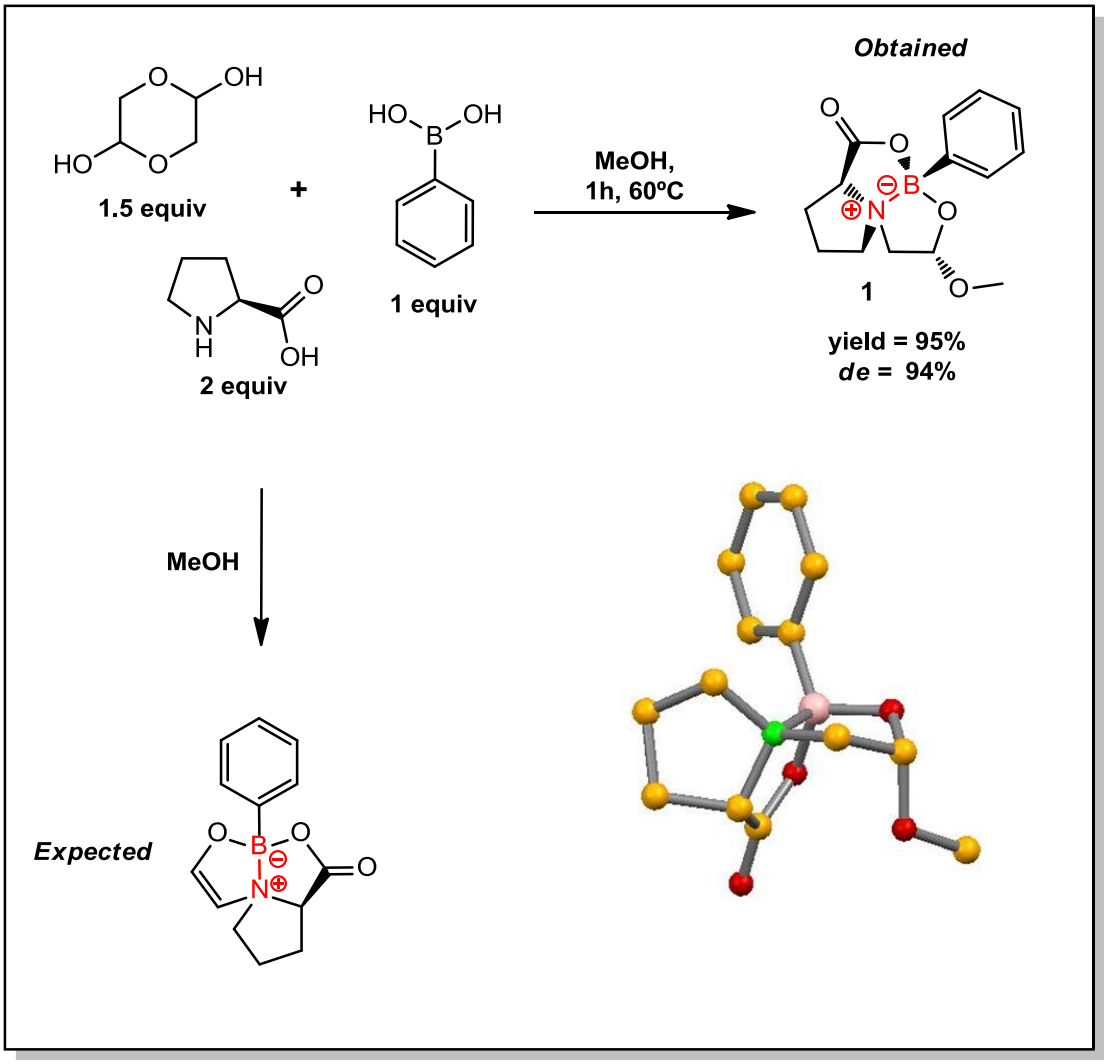

Figure 44 - Molecular diagram for molecule 1 of compound 1. Ellipsoids are set at 50% probability.

The mass spectrometry analysis, also confirmed the presence of a peak at 298 *m/z*, corresponding to the heterocycle molecular ion 275 *m/z*, typically coupled with Na^+ (Figure 46). The unanticipated inclusion of MeOH increased the final product structural similarity with the 5-oxofuro[2,3-b]furan unit and occurred either when using MeOH as the solvent or as a reagent in THF, though, in this case heterocycle **1** was obtained in a lower yield (88%) and diastereoselectivity (82%) as shown in Figure 45.

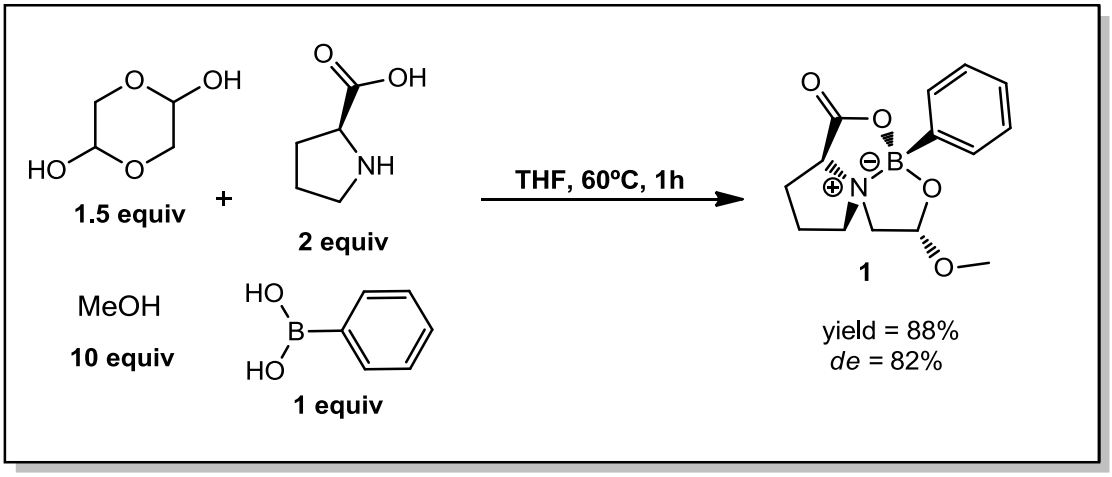

Figure 45 - Synthesis of boronate tricycle-heteroatom architecture using MeOH as reagent.

Recognizing that a higher homology between the target natural product 5-oxofuro[2,3-b]furan unit and the boron heterocycle could be achieve using other amino acids rather than L-proline, we performed the reaction using *N*-methyl-L-alanine as the nitrogen containing component. Disappointingly, this reaction afforded compound **2a** but only in 40% isolated yield and as a complex mixture of diastereoisomers (Figure 47). Similarly, using L-proline as the amino acid component, and 1-hydroxyacetone instead of glycolaldehyde dimer, also afforded a mixture of compounds 2b and 2c.

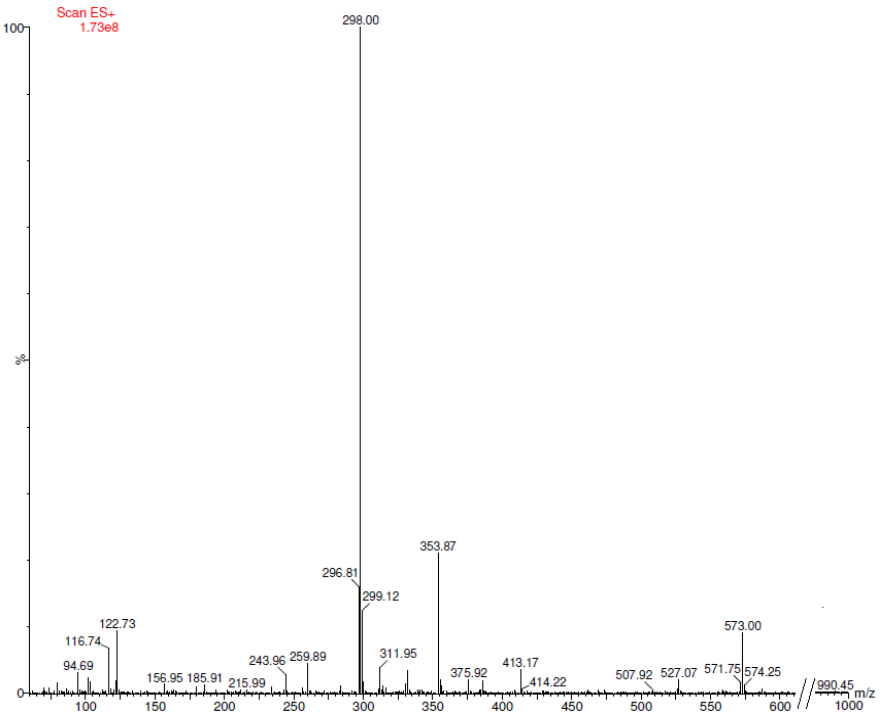

Figure 46 – ESI-MS of heterocycle 1.

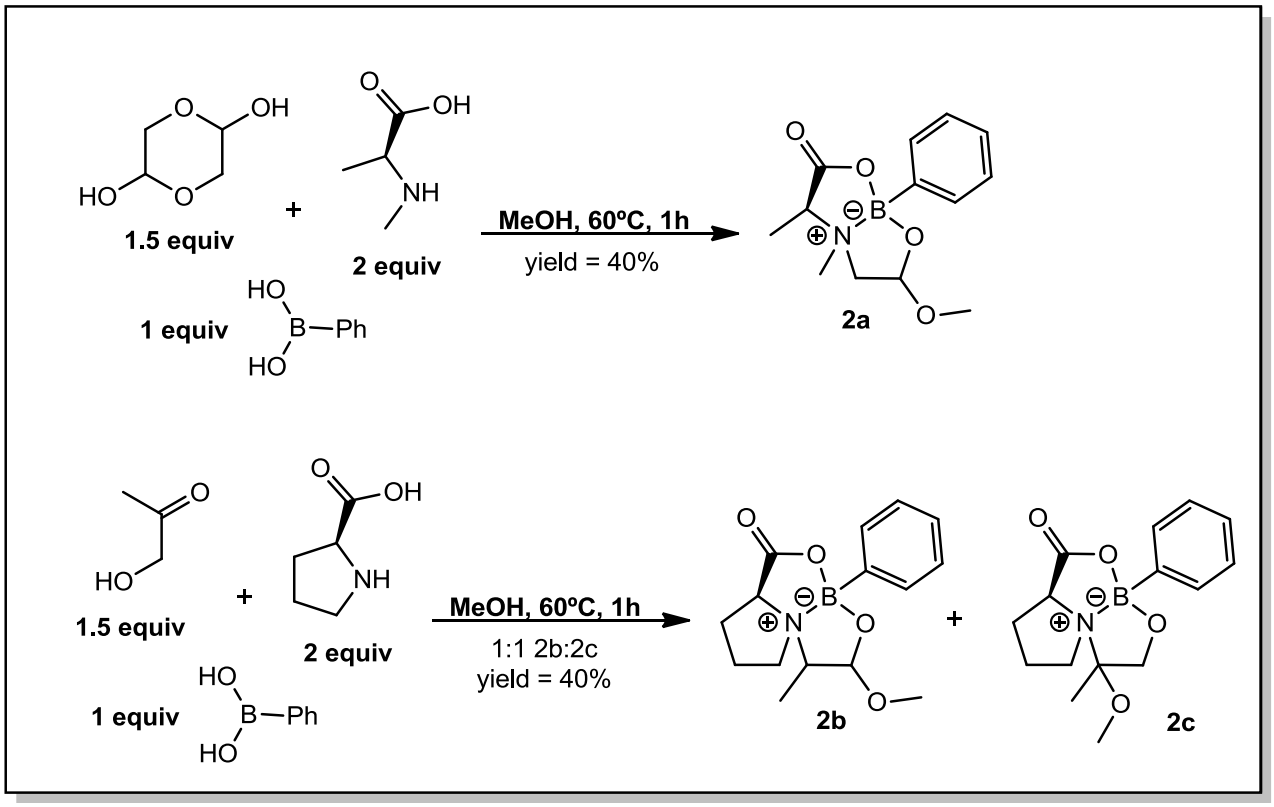

Figure 47 - Reaction with N-methyl-L-alanine instead of proline.

Based on these results, clearly the most efficient synthesis of the analogue for the 5-oxofuro[2,3-b]furan unit was obtained when using L-proline and glycolaldehyde dimer as the assembly partners in MeOH. Therefore, once the most efficient conditions to prepare these heterocycles were established, we evaluated the possibility of extending the protocol to different alcohols, using the same reaction conditions.

As showed in Figure 48 several alcohols generated the tricyclic heterocyclic structures in good yields and excellent diastereoselectivities, though the reaction was quite sensitive to the alcohol steric effect. A clear example of this effect, was the fact that when using EtOH as solvent, compound **5** was obtained in 89% yields, while with the bulkier *i*PrOH, heterocycle **6** was isolated in 72% yield and with *t*BuOH no reaction was observed. Despite this, hexanol, butanol, trifluoroethanol, and benzyl alcohols all afforded the expected heterocycles in yields ranging from 60% to 78% and diastereoselectivities in between 89% and >97%. In addition, unsaturated alcohols such as allyl, phenyl propargyl, and propargyl alcohols all yielded the expected products in good yields and excellent diastereoselectivities (Figure 48). After confirming the reaction tolerance toward a diverse set of alcohols, the assembly reaction was evaluated using different boronic acids. As in the case where different alcohols were tested, the boronic acids tested afforded the expected heterocycles in good yield and excellent diastereoselectivity, using aryl, heteroaryl, and alkyl boronic acids, and diastereoselectivities ranging from 90% to >97% (Figure 49).

Regarding the substitution profile on the aromatic ring, alkyl substituents afforded the desired products **12** and **13** in 88% and 75% yield and >97% and 95% *de* respectively, while 2-naphthyl boronic acid yielded the heterocycle **14** in 83% yield and 96% *de*. The reaction was slightly more sensitive toward the electronic profile of the aryl substituent. The substitution of the electron-donating para-methoxide in compound **16** by the electron-withdrawing para-fluoride in compound **17** increased the yield from 57% to 94% maintaining the high levels of diastereoselectivity. Finally, the *ortho*-substitution versus the *para*-substitution had an almost negligible effect in the reaction efficiency as the same isolated yield was obtained when using the *para*- and the *ortho*-bromo aryl boronic acids (Figure 49). Very gratifyingly, despite the possible reaction with proline, the method was tolerant to the presence of the ketone functionality as the 4-acetylphenylboronic acid afforded product **21** in 65% yield and 95% *de*. Finally, the 4-cyano-2-methylphenylboronic acid and the cyclohexyl boronic acid afforded heterocycles **22** and **23** in 65% yield, 96% *de* and 52% yield, >97% *de* respectively (Figure 49).

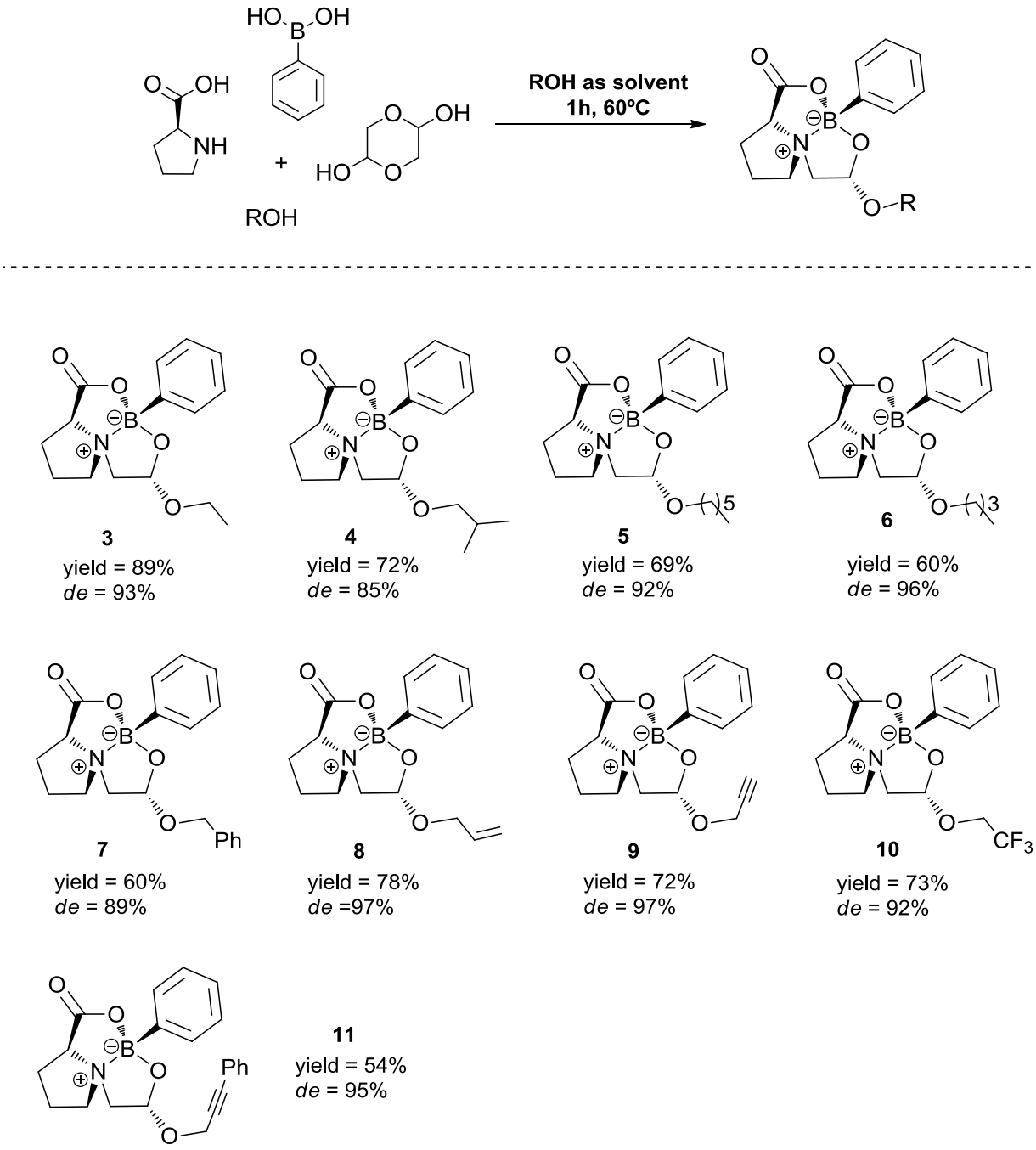

Figure 48 - Alcohol scope in the tricyclo-heteroatom architecture reaction.

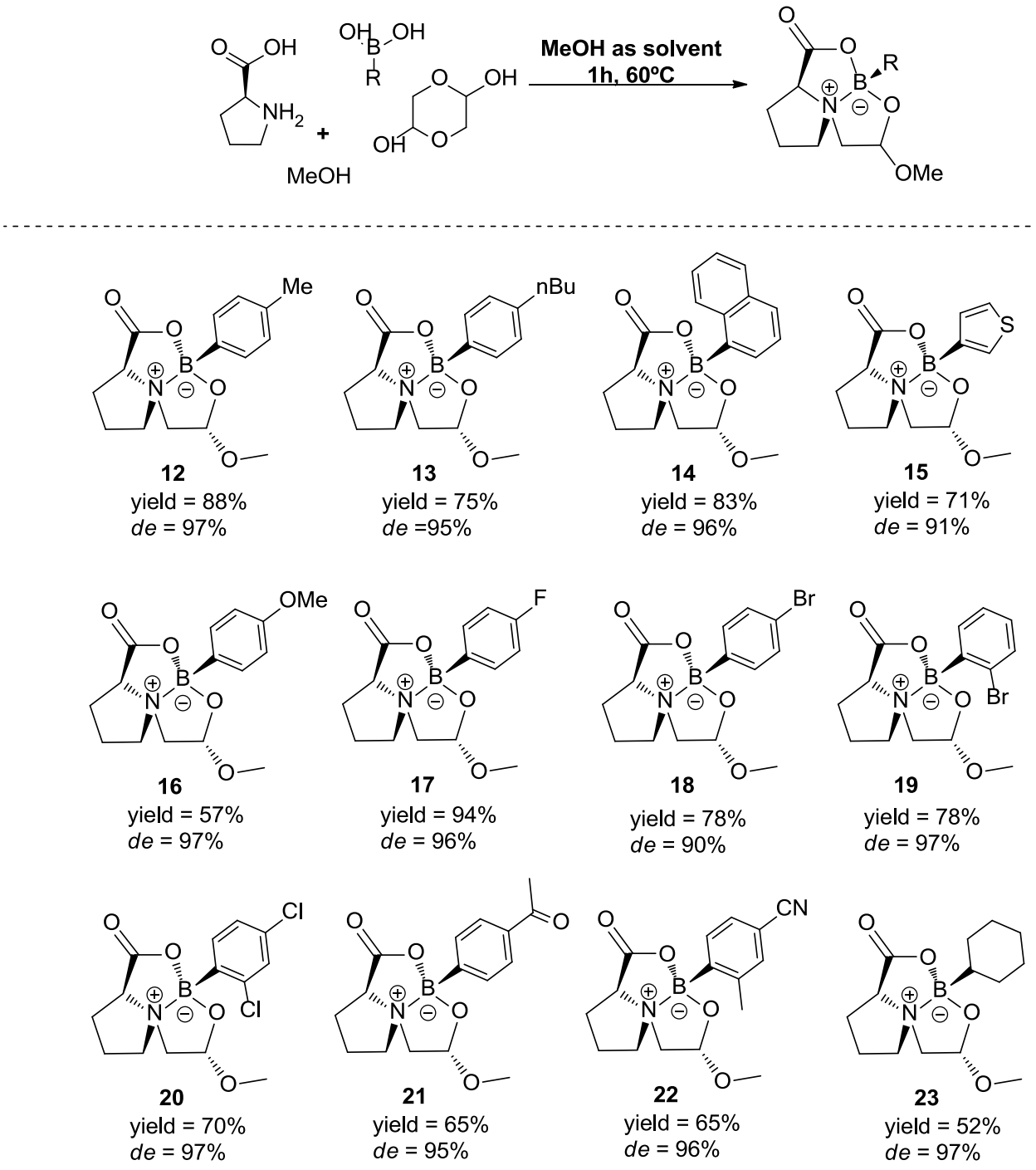

Figure 49 - Boronic acids scope in the tricycle-heteroatom architecture reaction.

Mechanistic studies

Once established the synthesis of 5-oxofuro[2,3,b]furan boronated analogues, we initiated a study to understand the reaction mechanism. Therefore, we studied the reaction mechanism using electrospray ionization mass spectroscopy (ESI-MS) (Figure 50). We performed the reaction between L-proline (2 equiv), phenyl boronic acid (1 equiv), glycolaldehyde dimer (1.5 equiv), and MeOH (10 equiv) in 2 mL of THF at 60°C. Aliquots of the reaction mixture, corresponding to the moment immediately after the addition of all reactants and after 10 min at 60°C, were collected and analyzed by ESI-MS.
As shown in Figure 50, the spectra obtained after the addition of all reactants shows an increased concentration of intermediates A and B formed between proline and phenyl boronic acid, while analysis of the spectra obtained after 10 min at 60°C revealed the formation of a new tricyclic intermediate C. This latter disappears in the spectrum recorded after 120 min to afford product **1**. Based on these results, the reaction mechanism was studied by means of DFT calculations, with the collaboration of prof Luis Veiros at IST, and the resulting highlights are shown in Figure 51.

The calculated mechanism starts with a complex of proline and boronic acid (B), and with its solvent adduct (A), both detected by ESI-MS data (Figure 51) in the initial aliquot. Addition of glycolaldehyde to B results in intermediate C. This step is assisted by OH coordination to the B-atom, first, and then by proton transfer from the alcohol to the O-atom in activating the carbonyl group to the nucleophilic atom from the nitrogen. Protonation of C leads to D with the corresponding activation of the B-O bond Then, the exchange between the two B-O bonds, from D to E, allows the activation of the C-O bond involving the C-atom R to the nitrogen and gives rise to the breaking of that bond and to the formation of the iminium ion that occurs in the

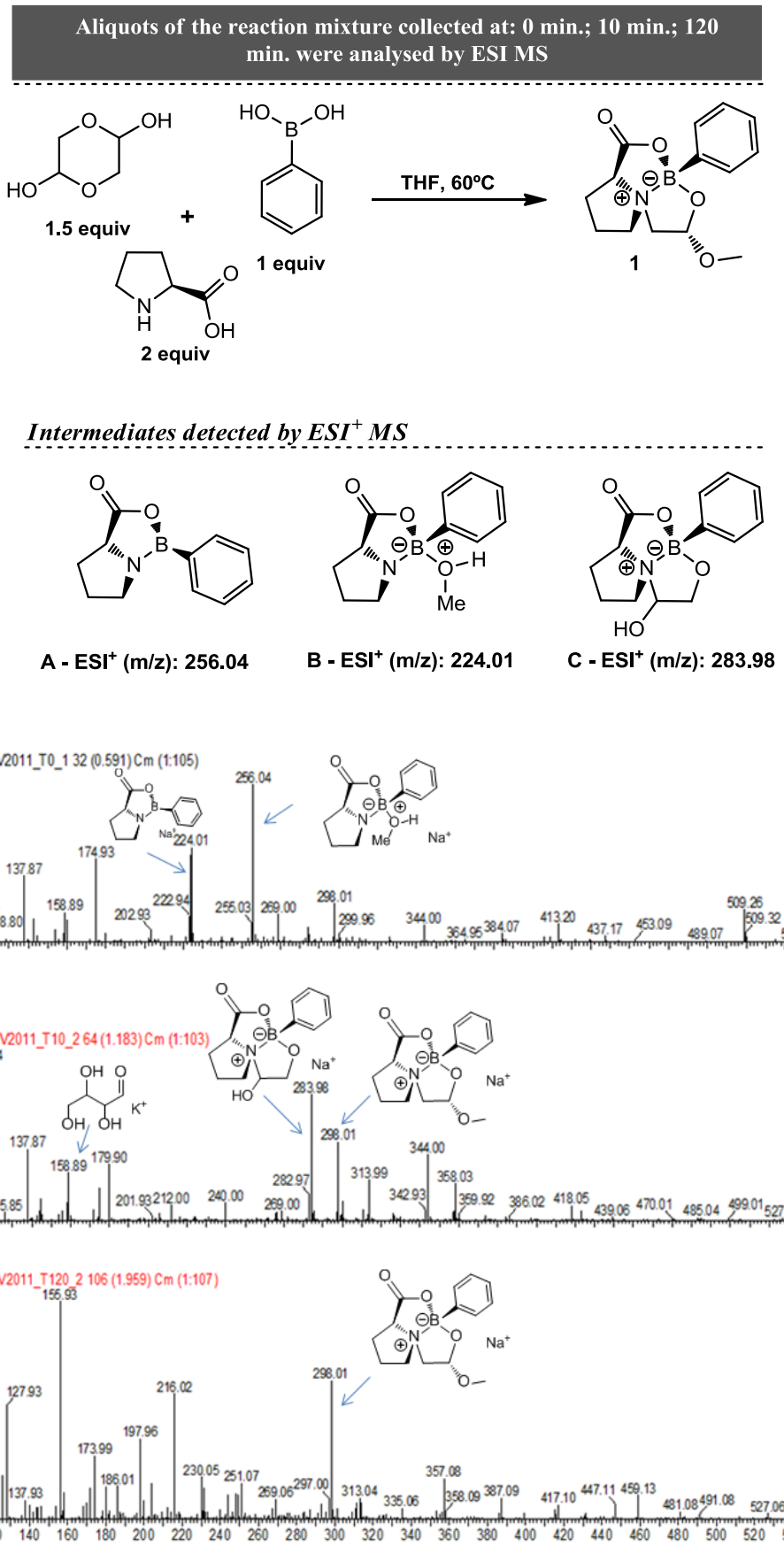

Figure 50- Mass Spectrum of reaction products at T_0, T_{10} and T_{120} (Full Scan *m/z* 60-600; ESI+; Capillary Potential 3,0kV; Source Potential 40V).

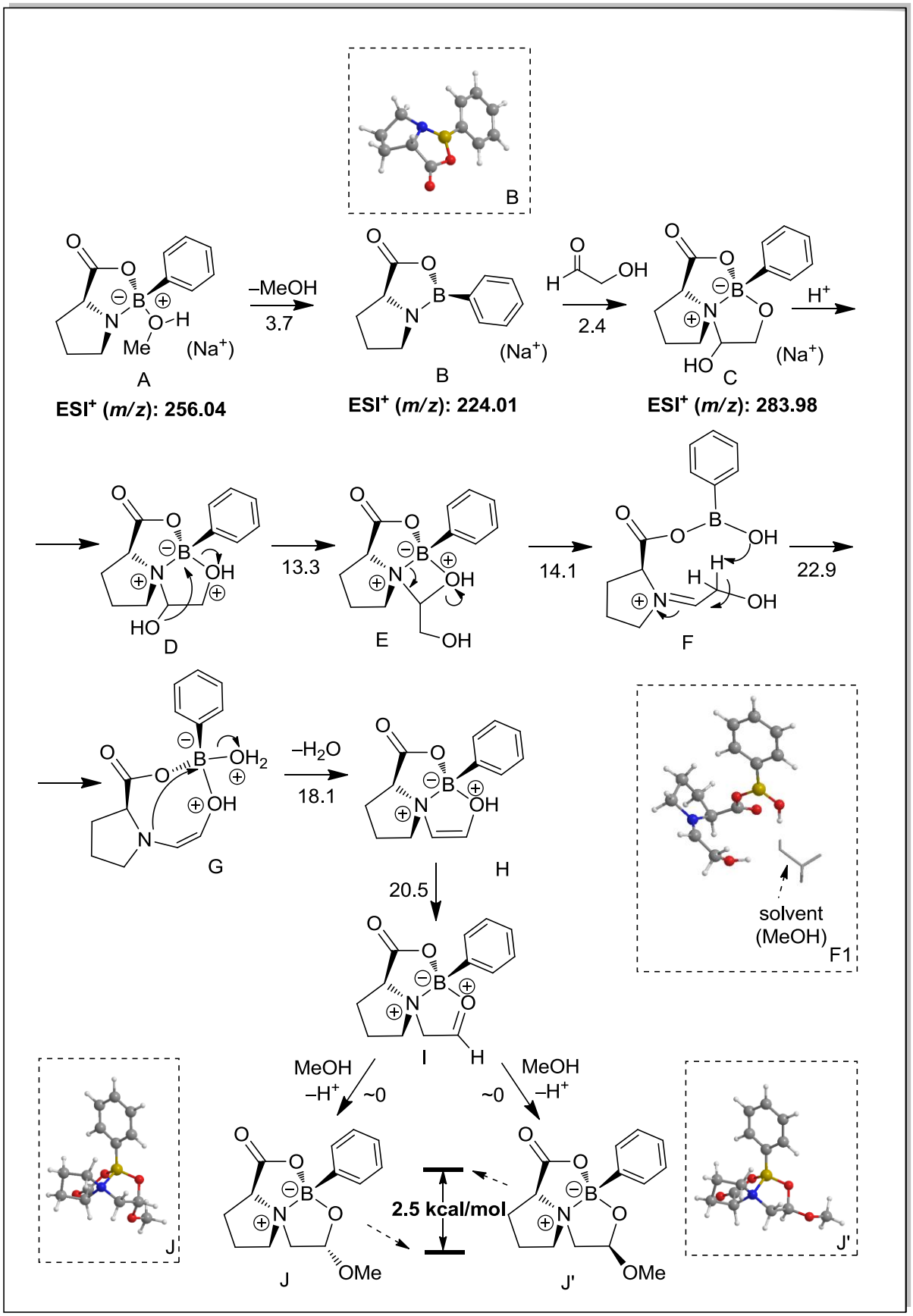

Figure 51 - Reaction mechanism proposed after DFT calculation.

following step, from E to F. Next, from F to G, there is abstraction of one proton by the OH group coordinated to boron, with the corresponding breaking of one C-H bond in the side chain. In G, there is regeneration of a neutral N-atom and formation of an enol (NCH=CHOH) that finally coordinates the boron through its O-atom (in G). From G to H, there is a nucleophilic attack from the N-atom to boron with the consequent loss of one water molecule. The coordinated enol (H) tautomerizes to the corresponding aldehyde, from H to I. The carbonyl group in I is activated by coordination to the B-atom and, thus, suffers nucleophilic attack from the solvent (methanol) yielding the final product of the reaction. It should be noticed that solvent plays an active and important role in the entire reaction path, through its assistance in all proton transfer steps, as expected for a protic solvent. Thus, in the calculated mechanism there was explicit consideration of one methanol that establishes an H-bond network with the various intermediates. In addition, in the section of the mechanism corresponding to enol formation from the iminium ion (F to G), a second methanol molecule was used in the calculations. The second solvent molecule coordinates the boron, allowing a tetrahedral environment around that atom that would other- wise remain trivalent as in F. The coordination of methanol enhances the electronic density in the B-atom and increases the basicity of the OH group that abstracts the proton from the C-H bond giving rise to the enol in G. In fact, the barrier calculated for this step without the B-OMeOH coordination is 6.6 kcal mol^{-1}higher than the one obtained considering methanol coordination. This indicates an active participation of the solvent along the reaction mechanism, and, in particular, in the enol formation step, the one with the highest calculated barrier: 22.9 kcal mol^{-1} Another interesting aspect of the reaction is the high diastereoselectivity found experimentally, especially taking into consideration the existence of four asymmetric centers in the product: the carbon from the proline, the N- and the B-atoms, and the acetal C-atom. On the other hand, the configuration observed for the N- and the B-atoms can be understood by the geometry of the intermediate B (Figure 51). In fact, the conformation of the amine five-membered ring, dictated by the configuration of the asymmetric C-atom and by the pyramidal geometry around the nitrogen, leaves only one side of the molecule available for the reaction with glycolaldehyde and determines the final configuration of both nitrogen and boron. Finally, the configuration on the acetal C-atom results from the relative stability of the two epimers. The last step is under thermodynamic control with negligible barriers calculated for the addition of methanol.

2.3.1 Biological evaluation

Once established the synthesis of these analogues of the 5 oxofuro[2,3-b]furan motif they were evaluated for their antitumor activity.Therefore, the newly synthesized boron heterocycles **7,15,18,20** and **21** were selected to be tested in a cell-based assay against a breast adenocarcinoma cell line (MCF-7)(Figure 52). The cells were incubated with the boron heterocycles for 24 hours previously to the assessment of the cell viability by a tetrazolium compound. This tetrazolium is reduced in metabolicaly active cells and is converted into a purple formazan detectable by UV at 570 nm. Based on the results obtained, compounds **4, 12, 14** and **15** did not change significantly the cell viability. Differently and to our delight, compound **9** exhibited a moderate activity in this assay decreasing the cell viability by 60% (Figure 52). Although it is premature to establish any structural-activity-relationship, the presence of the n-butyl substituent in the para position of the aryl group, appears to be determinant for the activity of this molecule as all other compounds tested, featuring different substituent's at the aryl moiety, displayed no relevant activity similarly to what occurred with compound 4 which as a long alkylic chain in the acetal moiety.

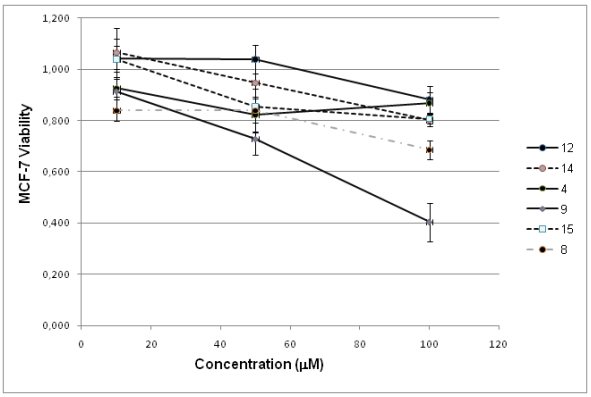

Figure 52 - cell-based assay against a breast adenocarcinoma cell line (MCF-7).

Encouraged by the "synthetic accomplishment of our goal" we decided to redirect our synthetic efforts towards a new biological target: human neutrophil elastase (HNE). HNE inhibitors spread over many different families of compounds with very distinct chemotypes, among these, fused cyclic lactones (Figure 53) have been described for the inhibition of

HNE with IC_{50}'s ranging from 0.024 to 1.603 μM.[84] Their bicyclo[3,3,0]octane unit closely resembles the structure of the oxofuro[2,3-b]furan unit, whose the boron heteroatom analogue was demonstrate to be easily synthesized through the boron tether strategy.

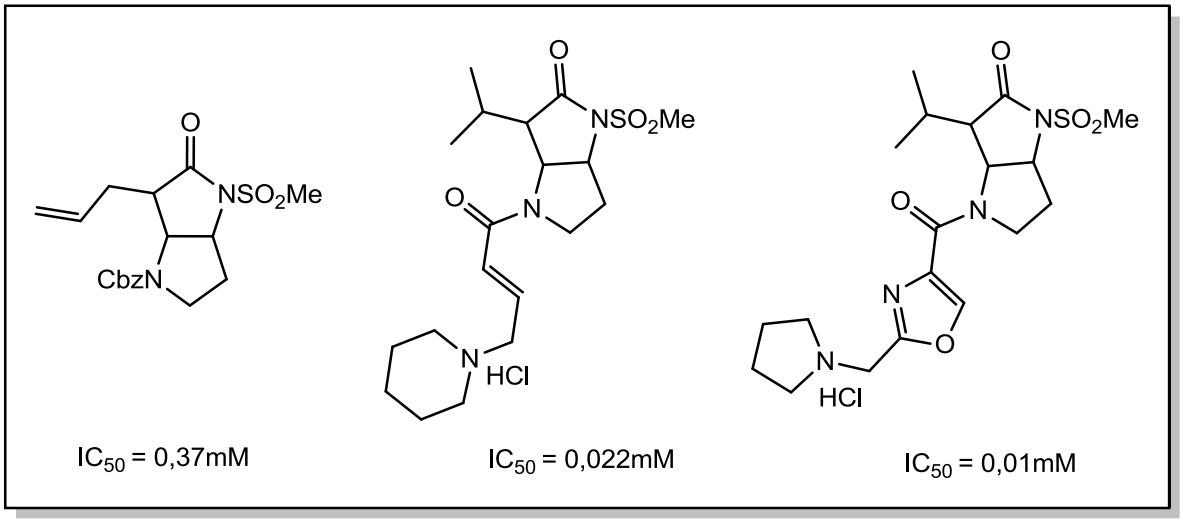

Figure 53 - Fused cyclic lactones as HNE inhibitors.

Despite the similarity between the two bicyclo-systems, we realized that the molecules of the boronate tricycle-heteroatom library miss the structural recognition requirement to properly fit in the active pocket of the HNE, which is widely known to possess extended molecular recognition binding sites (S1 is the most important with affinity for small hydrophobic groups).[85,86] A confirmation of this hypothesis came from the enzymatic assay of compound **3** against the HNE which was unable to induce any appreciable inhibition.

2.4 Conclusion

In summary we have developed a new one-pot four-component assembly of N-B heterocycles with a natural product-like framework similar to the 5-oxofuro[2,3-b]furan unit, which is a shared structure of many spongianian diterpenoids with an interesting range of biological activity. The reaction displayed a broad scope regarding the alcohol and boronic acid components. The N-B heterocycles were obtained in yields up to 95% and excellent diastereoselectivities (up to >97%). All of these results indicate that the use of boronic acid as a template to promote the assembly of several molecules in a multi component reaction (MCR) fashion, is an effective strategy to simply assemble collections of compounds with discrete molecular surfaces similar to those found in natural product frameworks. Despite this strategy being successful from the synthetic point of view, yielding the fused tricycle boronate heterocycles collection, it missed to effectively induce an appreciable biological response in the tumor cells.

3. Fused bicyclo-boronate heterocycles

3.1 Human neutrophil elastase (HNE) and boron based inhibitors

Inflammation is a complex process of the vascular system, which responds to deleterious stimuli such as: pathogens, injury and irritants. This mechanism is involved in the resolution of infective events and in tissue remodeling after injury occurrences. The human neutrophil elastase (HNE)(Figure 54) is one of the enzymes responsible for the destruction of the damaged proteins through hydrolysis of elastin that confers elasticity to the connective tissue.[85]

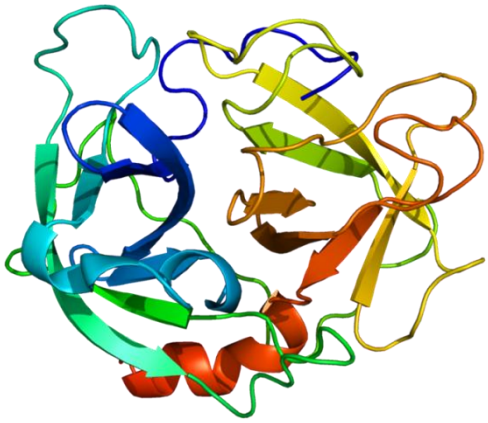

Figure 54 - The human neutrophil elastase (HNE).

This enzyme is contained into the azurophilic granules (primary granules) of the neutrophils, a phagocyte of the white blood cell system. More specifically, HNE is a serine protease that belongs to the chymotrypsin superfamily, constituted by 218 amino acids and a total weight of 29–33 kDa. The active site of this enzyme is a typical “catalytic triad” (Figure 55) machinery shared over all the large family of the proteases. It is composed by: aspartic acid 102, histidine 57 and serine 195.The triad is composed schematically by a nucleophile (the side chain –OH of the serine), a base (histidine) and an acid (aspartic acid)[87]. The objective of such machinery is to enhance the nucleophilic attitude of serine. The mechanism of the catalytic triad (Figure 56) starts with the aspartic acid that polarizes the histidine, which deprotonates the serine, making it a better nucleophile.

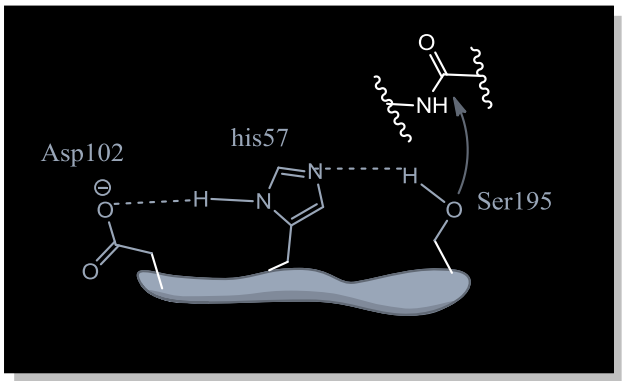

Figure 55- catalytic triad.

The deprotonated oxygen, from serine, can now easily attack the elected amide. The carbonyl of the amide changes the conformation from trigonal planar to tetrahedral. This new intermediate is stabilized by hydrogen bonding from Gly193 and a NH from the backbone of the Ser195, such region is commonly called the oxyanion hole. Histidine 57 assists the collapse of the tetrahedral intermediate to sp^2 acyl group, by proton donation to the amine leaving group. The enzyme activity is re-established through hydrolysis of the acyl-enzyme.[87]

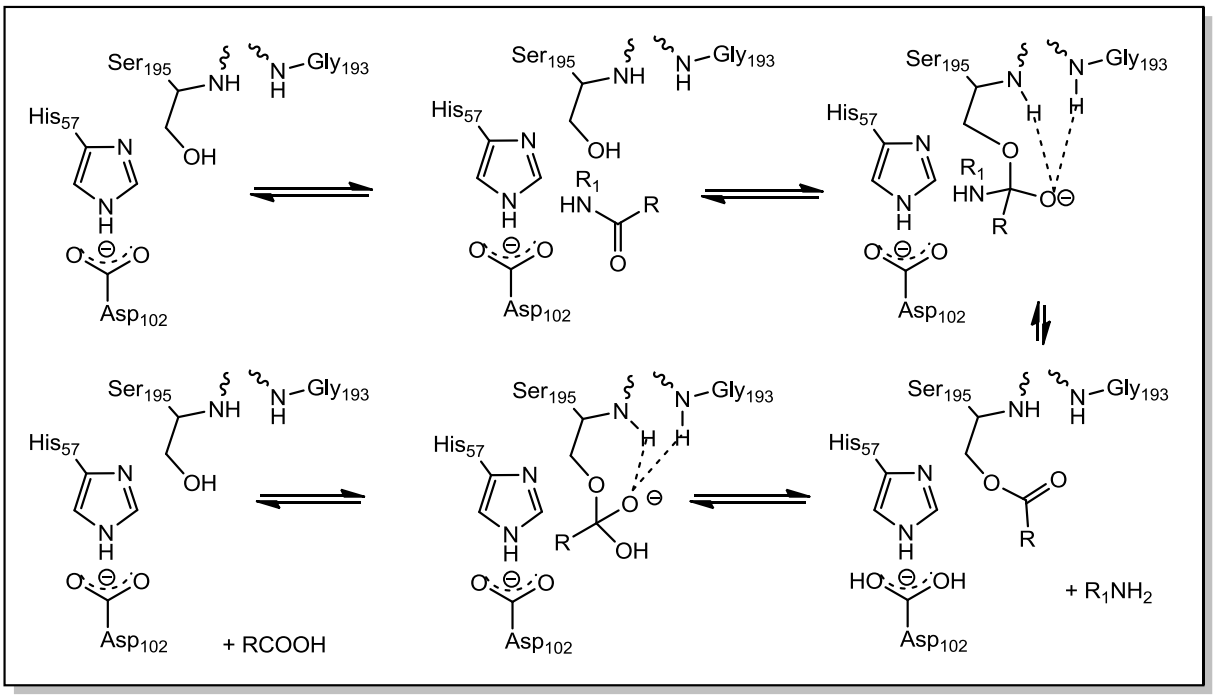

Figure 56 - Mechanism of the serine proteases.

The natural endogenous inhibitors of the HNE, are α1-proteinase inhibitor (α1-PI, α1-antitrypsin), secretory leukocyte protease inhibitor (SLPI) and elafin (ESI or SKALP).[88,89] They play the important role of protecting the health and functionality of the tissues from the destructive effects of extracellular HNE. An imbalance between the enzyme and its endogenous inhibitor could lead to an aberrant photolytic activity responsible for severe diseases such as: chronic obstructive pulmonary disease (COPD), rheumatoid arthritis, cystic fibrosis.[85] Nowadays, and just in Japan, Sivelestat is the only drug approved as HNE inhibitor. Since the lack of responses for such severe and urgent problems, organic chemists synthesized a number of inhibitor whose action could be ranked in three main categories according to their mode of action:

1. *Transition state analogues*
2. *Acylating agents*
3. *Mechanism like inhibitors*

Regardless of how an HNE inhibitor is classified, the initial steps of the inhibition mechanism always begin in a similar manner:

- *Nucleophilic attack of the serine 195 OH*
- *Creation of the tetrahedral Inhibitor-enzyme complex*

The evolution of this sp^3 intermediate is what makes the difference among the three different mechanisms.

Transition state analogues

An inhibitor is classified as a transition state agent, when the inhibitor-enzyme complex is stable enough to occupy the active pocket as long as an appreciable inhibition is produced. Among several drugs exploiting this mechanism ONO 6818 represents one of the most noteworthy examples. This molecule has shown to be active against: chronic obstructive pulmonary disease (COPD), acute lung injury (ALI) and acute respiratory distress syndrome (ARDS). With a K_i value of 12.16 nM, the aforementioned inhibitor was

active through oral administration (ED_{50}1.4 mg/kg). The crystal structure of the inhibitor-enzyme complex, suggests that the molecule acts as a transition state agent, with Ser 195 attacking the amidic carbonyl to generate a tetrahedral intermediate with a negative oxygen stabilized by the oxyanion hole (Figure 57). [85, 92] This promising molecule arrived to phase II clinical trials, To be discontinued when the an abnormal elevation in liver functions was revealed in the patients under the treatment with ONO 6818.[93]

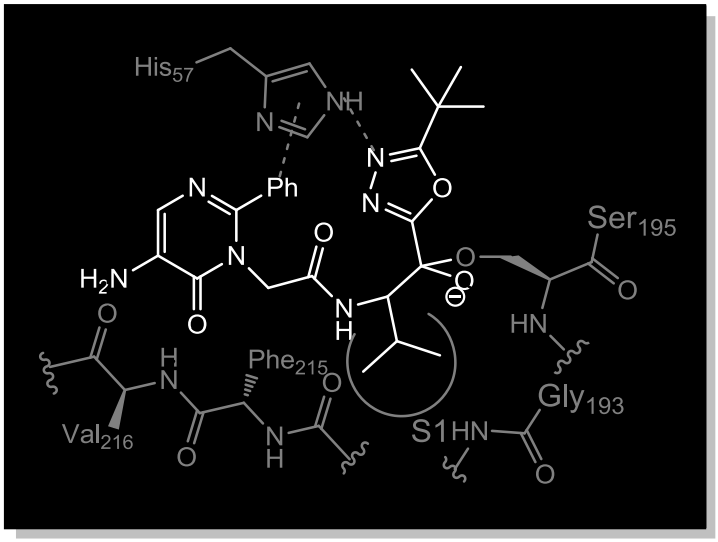

Figure 57 - schematic interaction between ono-6818 and PPE investigated through X-ray analysis.

Acylating agents

These compounds interact with the enzyme via the generation of a tetrahedral complex between the inhibitor and the enzyme. Differently from a transition state agent this complex is not stable and the enzymatic machinery continues its natural action catalyzing the release of the amine through proton donation of the hystidine 57, producing the acylated enzyme, which is a natural intermediate in the normal action of the HNE, which evolves a free enzyme through hydrolysis of the acyl group. What differentiates an acylitang agent from a natural substrate is the ability to produce an acyl-enzyme intermediate resistant to hydrolysis, disabling the enzyme form returning into its active form.

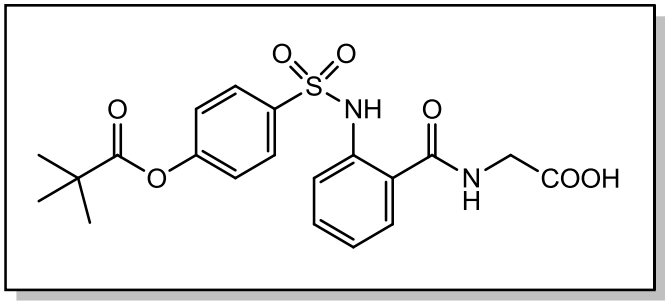

Figure 58 - ONO 5046.

ONO 5046 (Figure 58) is the most important HNE inhibitor, the only one to reach the commercialization (Japan only) and is an acylating agent. It is used for the treatment of ALI and ARDS. It has an IC_{50} of 0,0044 μM. The acylated enzyme was identified after 10 min of incubation with ONO 5046 by using LCESI-MS.[94,95]

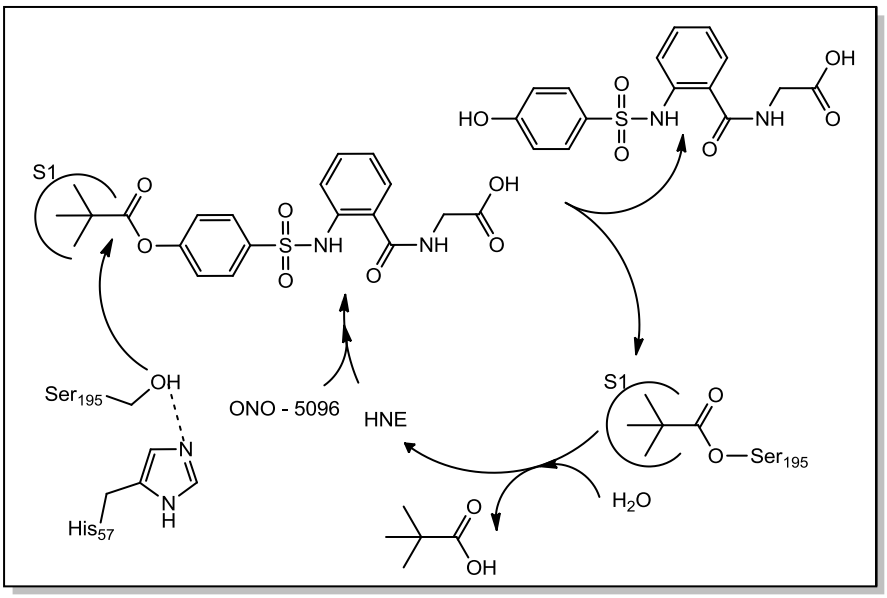

Figure 59 - ONO-5046 inhibition mechanism.

Mechanism based inhibitors

This class of compounds embodies in their structure a masked electrophilic functionality. The formation of the acyl intermediate triggers the unmasking of the hidden electrophilic moiety that can be attacked by a second nucleophile, which commonly is His 57. These inhibitors share the initial steps of the interaction with the enzyme, with the acyl-enzyme inhibitors. Indeed the first intermediate formed is an acyl enzyme that quickly evolves into

an electrophore. When such electrophore is attacked by a nucleophilebelonging to the enzyme the mechanism is classified as “double hit mechanism”.

An example of this is provided by the chloromethyl ketone that after activation is able to irreversibly alkylate the histidine residue of serine proteases (Figure 60).

This kind of activity it also called double hit mechanism since the presence of two nucleophilic attacks, the first from serine and the second from histidine.[96]

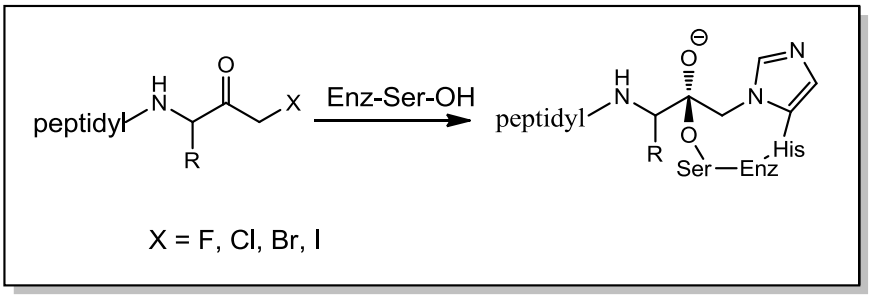

Figure 60 - Chloromethyl ketone double hit mechanism.

3.2 Synthesis and evaluation of fused byciclo-boronate heterocycles

Inspired by the proven inhibitory activity of the cyclic lactones against HNE,[97] we envisionedthat the Boron tether strategy could be exploited to create a series of boronated structures with similar architectures to the lactones, with a double fused ring system, in which electrophilic centers are incorporated in order to act as pharmacophore.
We figured that the lactone mimics could be readily assembled by combining a chelating aldehyde, a boronic acid and an amino acid.[98,99] These constructs could be simply tuned to promote a selective enzyme inhibition via formation of an acyl-enzyme complex as shown in Figure 61. Importantly, the boron construct depicted in Figure 61 can provide two major structural requirements for enzyme inhibition:

- *A substitution pattern appropriate for molecular recognition*
- *An increased reactivity of the 5-membered ring towards the catalytic serine.*

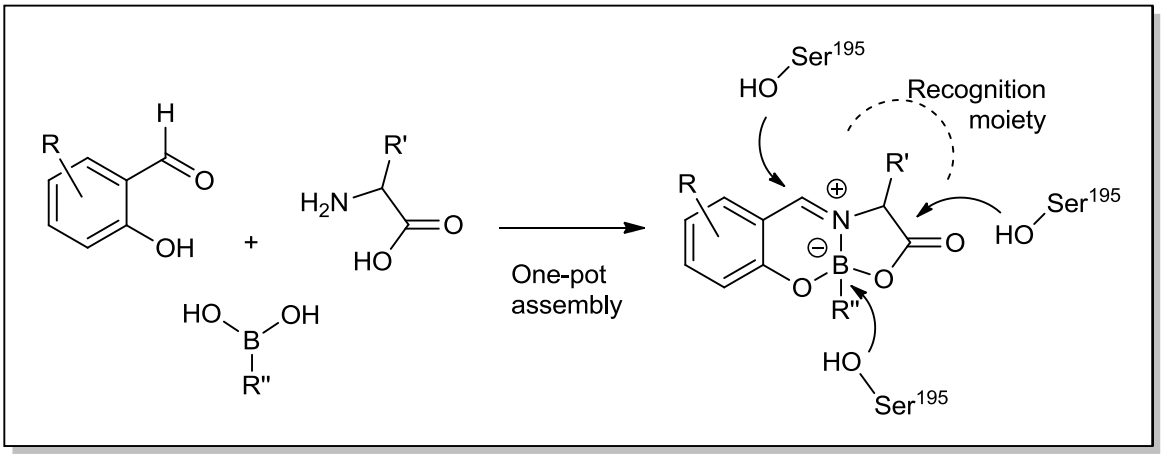

Figure 61 - bicycle-heteroatom architecture design.

As aforementioned, the topology of HNE active site comprises extended molecular recognition binding sites, of which the S1 is the primary specificity binding pocket with affinity for small hydrophobic groups.[86,87]Therefore as shown in Figure 61 a careful selection of the components may permit an optimal interaction with HNE active site.

Based on this, we selected amino acids with hydrophobic side chains like L-alanine, L-leucine and L- phenyl as partners, together with phenyl boronic acid and salicylaldehyde to generate the fused lactone mimic (Figure 62). Given the solubility issues related with the use of amino acids, the three components were combined in one-pot in water end reacted over 20 h at 90°C. As shown in Figure 62, this simple approach afforded the expected compounds in yield up to 76%. This protocol evidenced another advantage as the products precipitated from the aqueous phase and for that reason were simply collected by filtration in good to excellent yields and diastereoselectivities.[99] Once prepared, compounds **24-26** were readily evaluated against HNE using a fluorometric assay in which HNE activity is monitory using the fluorogenic substrate MeO-Suc-Ala-Ala-Pro-Val-AMC. Compounds **24** and **25**, were shown almost inactive (Figure 62). Very differently and to our delight, compound **26** synthesized with L-phenylalanine, displayed a very promising IC_{50} of 20.27μM. Foreseen a possible in situ hydrolysis of the complex into the assembly partners, the individual components phenyl boronic acid and salicylaldehyde were also evaluated against HNE and displayed no activity. These results clearly demonstrated that the recorded activity for compound **26** is indeed due to the heterocycle structure and not the individual components. Motivated by the identification of compound **26** as a HNE inhibitor, we embarked on a hit optimization program empowered by the chemical versatility offered by this synthetic strategy synthesizing the small collection of boronated compounds depicted in the Figure 64. A very satisfactory level of diasteroselectivity, measured by ^{1}H NMR, was achieved in all the reactions reported in 64. The X-ray crystallographic study data, and DFT calculations rendered a deeper insight over the structural characteristics of these molecules. Suitable crystals for X-ray analysis were obtained for heterocycles **26, 28, 29** (Figure 63). The first data evidenced by the crystallographic analysis was the importance of the stereo constrains of the boron-heterocycles architecture. Indeed despite the different boronic acids used to prepare **26**, **28** and **29** they all display similar N–B dative bond distances (1.577(2) Å (**26**), 1.574(3) Å (28) and 1.569(4) Å (29)). The DFT calculation of the optimized geometry of compounds **26, 28, 29** and were also in good agreement with the experimental X-ray data, the deviation of the N-B distances values in all three cases, was within 0.001Å. The similarity of the N-B bonds was also extended to the bond strength, confirmed by the Wiberg indices,[101]of 0.61, and the electronic distribution calculated for all the B-atoms of the three structures, with an atomic charge (NPA)[102-109,] 1.02.

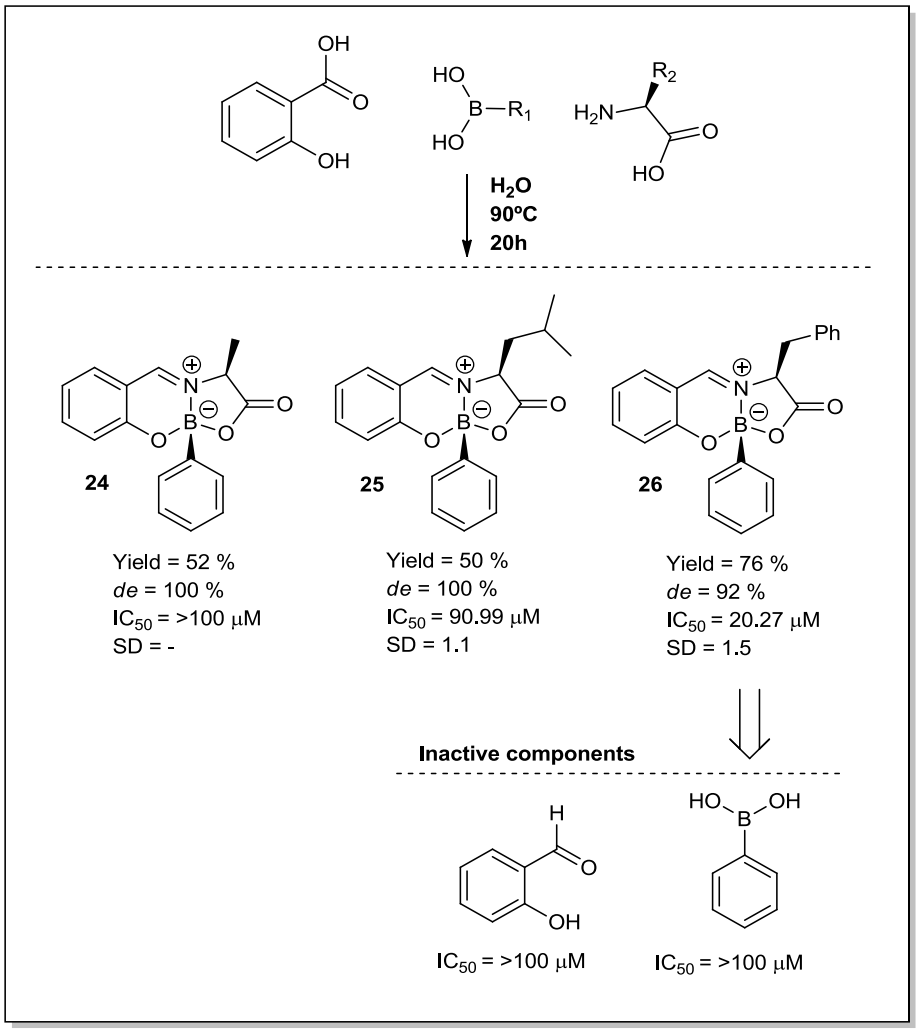

Figure 62 - Bicycle-heteroatom architecture with L-alanine, L-leucine, L-phenilalanine.

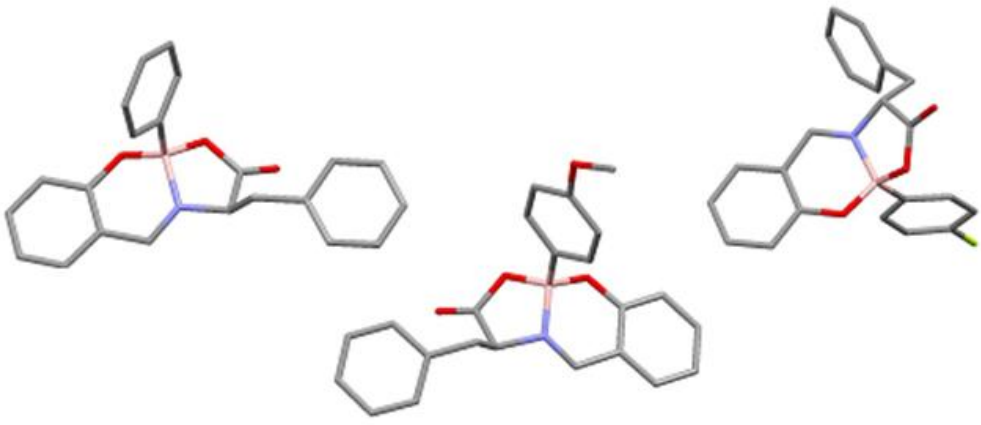

Figure 63 - Molecular diagrams of the complexes 26, 28 and 29 (from left to right) obtained by x-ray diffraction .

3.2.1 Inhibitor profile of fused bicyclo-boronate heterocycles

Regarding the biological activity as shown in figure 64, heterocycles **27**-**29** which were successfully prepared in 83%, 31% and 80% yields respectively and excellent diastereoselectivities (100%), using *para* substituted aromatic boronic acids, L-phenylalanine and salicylaldehyde, were readily tested against HNE. These compounds though, revealed no significant improvement in the inhibition profile of HNE, when compared with the inhibition obtained with compound **26**. Of this series the best result was obtained with compound **29** (IC_{50} = 16.06 μM) featuring a *para* fluorinated aromatic ring of the boronic acid component.

Based on this, the modification was extended to the aromatic moiety of the aldehyde. The inclusion of a methyl group only slightly improved the activity of compound **30** (IC_{50} = 15.39μM), while a methoxy function at the same position had a much more pronounced effect and reduced the IC_{50} up to 9.3μM. Therefore, compound **31** was selected as the starting point for another round of optimization in which functionally diverse boronic acids were explored as components of the assembly. Disappointingly compounds **32**-**33** displayed a poor inhibitory activity when compared with compound **31**. Very differently, the introduction of a bromine atom either in the *para* or *ortho* positions of the boronic acid aromatic moiety, greatly improved the potency up to 2μM. The same trend was observed in compounds **37** (IC_{50} = 2μM) and **38** which feature a chlorinated aromatic boronic acid *ortho* and *para* substituted and displayed an IC_{50} of 1.9 μM. Based on all modifications operated in this scaffold the methoxy substituent introduced in the aldehyde aromatic moiety was shown instrumental for potency. For this reason, compound **39** was prepared with 4-diethylamino-salicylaldehyde with the objective of improving the effect previously observed. Therefore, L-phenylalanine, 4-diethylamino-salicylaldehyde and 2,4-dichlorophenyl boronic acid were reacted in ethanol for 20 h at 70°C to yield **39** in 89 % yield and 98 % *de*. Very gratifyingly, the operated modification resulted in the improvement of the activity against HNE and **39**, with an IC_{50} = 1.1μM, becames the most efficient inhibitor prepared in this work. After this, we addressed the selectivity of **39** in the presence of other proteases like porcine pancreatic elastase (PPE), proteinase 3 (PR3) and Cathepsin G. As shown in Figure 48, compound **39** displayed a good selectivity towards HNE as at 50μM concentration only displayed an IC_{50} of 12μM against cathepsin G and was inactive towards PPE and PR3. Finally, the inhibitory activity of compound **39** towards HNE was also determined using the progress curve method (chapter 5

experimental). Significantly, a time-dependent inhibitory profile was observed and the corresponding pseudo first-order rate constant values, k_{obs}, varied linearly with the concentration of **39**, yielding a second-order rate constant of inactivation, k_{inact}/K_i, of 1.2×102 M^{-1} s^{-1}. This value compares well with those reported to other potent HNE inhibitors.[87] Overall, these results suggest that **39** inhibits HNE irreversibly, and contrasts sharply with compound **26**, for which reversible inhibition kinetics were observed.

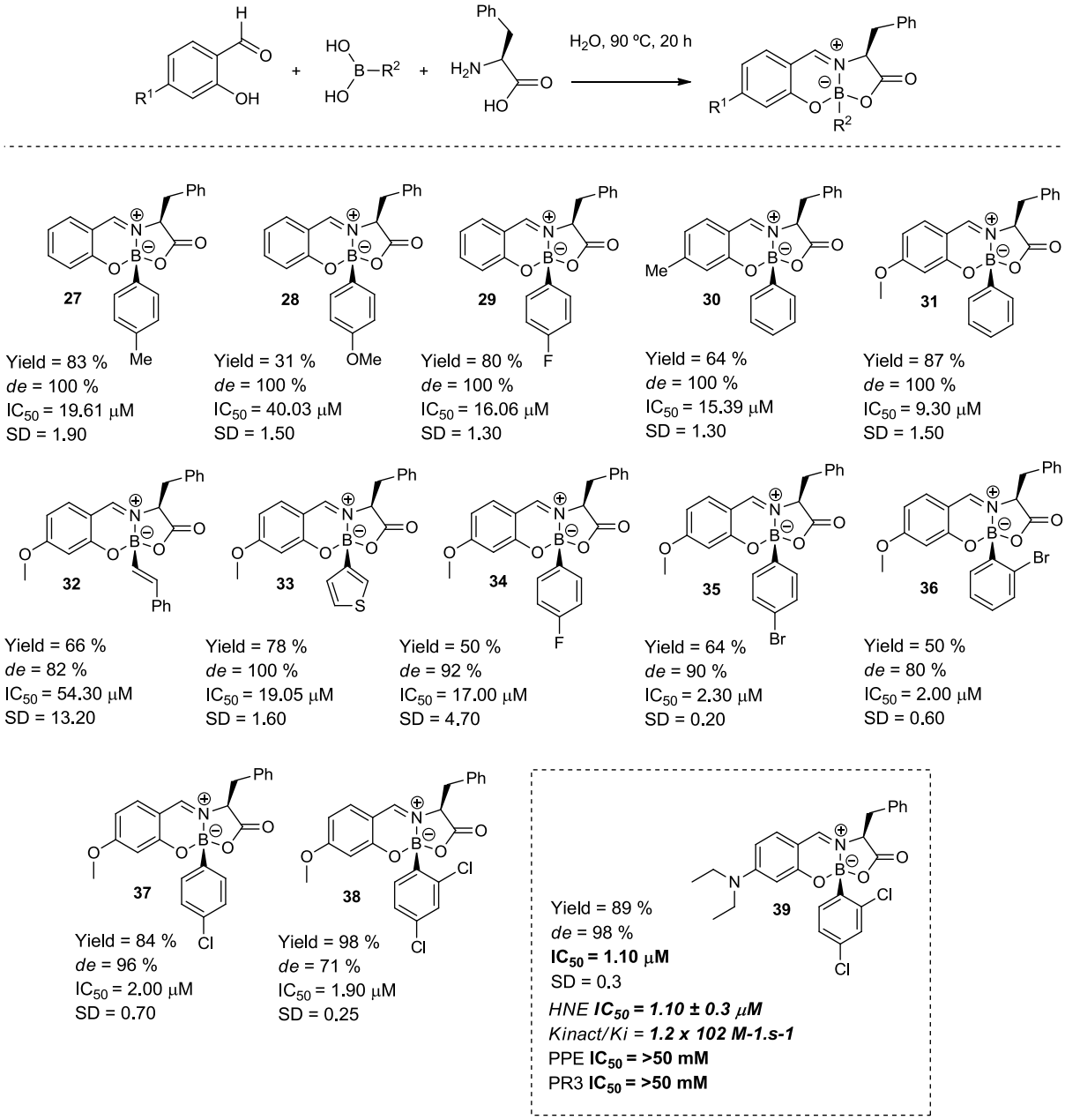

Figure 64 - Bicycle-heteroatom architecture library.

3.2.2 Mechanicistic studies

Once demonstrated the potential of this methodology to prepare new HNE inhibitors, we initiated a study to unravel their mechanism of action. Considering the general structure of this family of compounds we envisioned that the nucleophilic attack of the Ser195 hydroxyl oxygen atom to the lactone moiety would be the most likely mechanism of action. To confirm this assumption, we synthesized compound **41** in which the lactone mimic is absent and for which is expected no activity. The synthesis of this compound is based on two steps, the first affords the N-(2-hydroxybenzilidene)-2-amino-2-benzyl-ethanol (Figure 65**b**), by reaction of 2-amino-2-benzyl-ethanol and salicylaldehyde in ethanol and in the presence of molecular sieves. The second step is a condensation reaction in toluene that affords the boron heterocycles **41**. Very gratifyingly and as envisioned, the evaluation of compound **41** against HNE revealed the loss of activity when compared with the reference compound **26**. Encouraged by this result, we synthesized compound **40**, aiming to demonstrate that the lactone was indeed the reactive centre and not the imine moiety. The reaction proceeded through two steps, the first affords the N-(2-hydroxybenzil)-α-amino acid (Figure 65**a**), the in situ reduced product of the condensation between salicylaldehyde and the amino acid. The second step afforded the saturated boron heterocycle **40**. With compound **40** at hand it was evaluated against HNE. Surprisingly compound **40** was also shown inactive. Puzzled by these results, we considered that the saturation of the imine bond would significantly alter the electrophilicity of the lactone carbon, disfavoring by this way, the nucleophilic addition to this position. Nevertheless, the ^{11}B NMR of **26**, **40** and **41** did not expose any substantial differences between these molecules neither the atomic charges (NPA) calculated for **26**, **40** and **41** by means of DFT calculations,[110] corroborated this assumption (Figure 65).

Based on these results, we performed the evaluation of the stability of **39** in the presence of sodium methoxide, a strategy often used to mimic the action of the serine hydroxyl group at the active centre of the enzyme.[111]

The reaction was performed in methanol at room temperature and followed by mass spectrometry. Surprisingly, the product (ESI+ m/z = 386.10) formed in this transformation, indicates that two molecules of methoxide reacted with **39** (Figure 66**a**) and that the boronic acid component was released in the process (Figure 66). Interestingly, no product corresponding to the addition of just one molecule of methoxide to **39** was detected in the reaction mixture. This unexpected result indicated that the mechanism of action would

probably involve the addition to both the imine and the lactone moieties. Therefore, the mechanism of the reaction of O-nucleophilic attack on the heterocycles tested as HNE inhibitors was studied by means of DFT calculations in collaboration with professor Luis Veiros at IST (Figure 67). The system used was compound **26** as substrate and methanol as nucleophile, for computational convenience. The energy profile obtained is represented in (Figure 67).

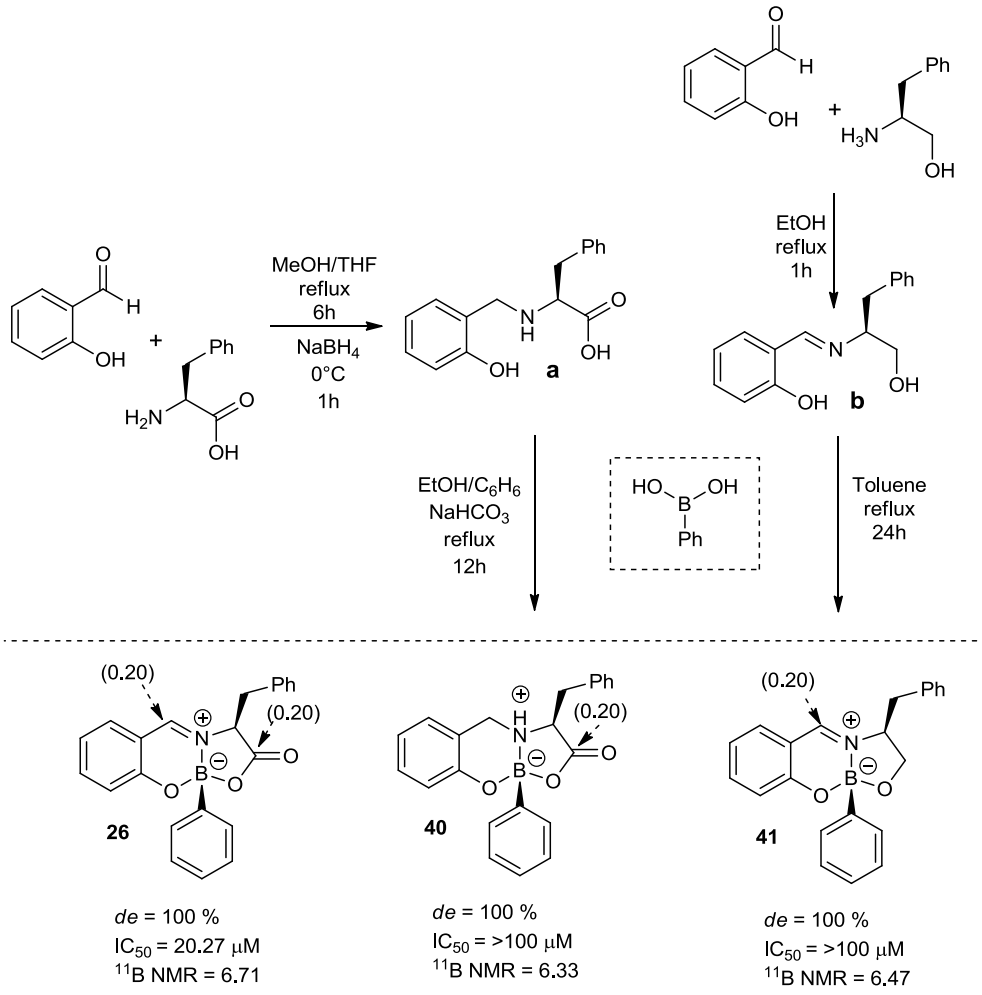

Figure 65 - biological evaluation, NPA atomic charges in parenthesis.

The mechanism starts with substrate **26** plus two molecules of methanol, represented by A in Figure 67. In the first step there is a nucleophilic attack of one methanol molecule on the imine C-atom, while at the same time the other MeOH molecule assists in the proton transfer from the OH bond in the nucleophile to the oxygen of the carbonyl group of the lactone. In the corresponding transition state, TS_{AB}, formation of the new C–O bond is almost accomplished, as shown by a distance of 1.58 Å, while the proton transfer is underway with the four relevant O– H bond lengths ranging from 1.07 and 1.40 Å.

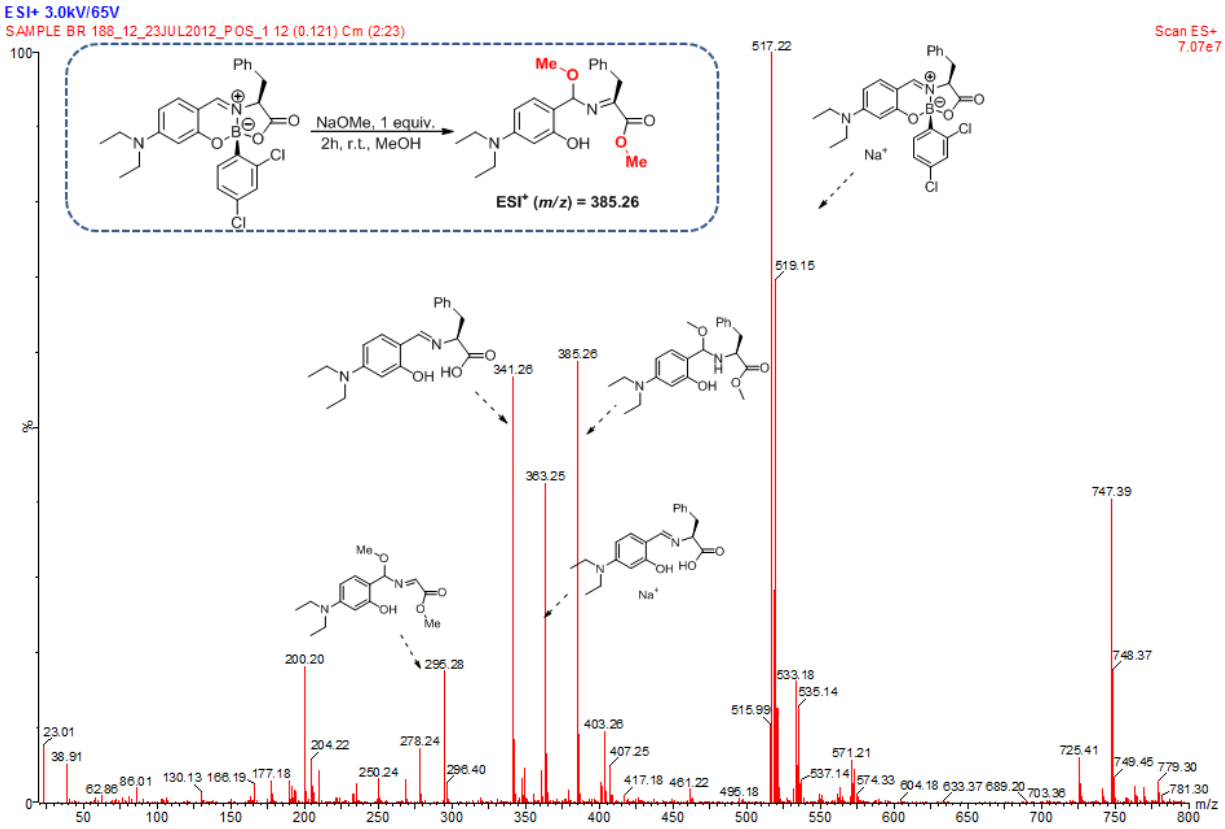

Figure 66 - Reaction of 39 with NaOMe in methanol followed by mass spectrometry.

Then, there is proton transfer from the oxygen, in B, to the nitrogen, in C, where there is a formally positive N-atom and the lactone C=O group is regenerated. Interestingly, this N-protonation step produces a significant stabilization of the intermediate, C being more stable than B by 21 kcal/mol. A third molecule of methanol is added to model, from C to D, as it will be required to assist the second nucleophilic attack. This attack occurs in the following step, from D to E, and the extra MeOH molecule assists in the protonation of the O in the carbonyl group of the lactone, while, at the same time, there is formation of the new C–O bond between the oxygen atom of methanol and the carbonyl C-atom. In the transition state, TSDE, formation of the new C–O bond is well advanced as indicated by a distance of 1.65 Å, while the process of proton transfer, from the methanol OH bond to the carbonyl O-atom, is half way through, as shown by the relevant O–H distances (1.11–1.32 Å).

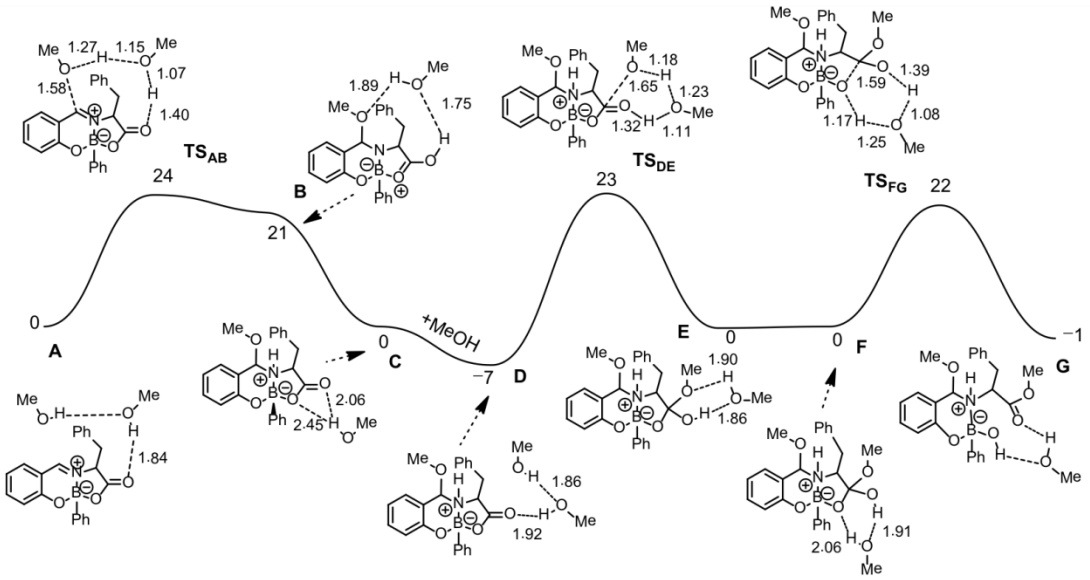

Figure 67 - The reaction of O-nucleophilic attack on the heterocycles tested as HNE inhibitors, studied by DFT calculations.

From E to F there is a rearrangement in the H-bonds between the intermediate and the neighbor MeOH molecule. Finally, in the last step there is proton transfer from the carbonyl O-atom to the oxygen connected to the boron atom, It is important to notice that the barriers calculated for the mechanism represented in Figure 67are rather high, presenting values of 24 and 30 kcal/mol for the two steps corresponding to nucleophilic attack. This is due to the use of methanol has nucleophile in the model employed in the calculations, a much poorer nucleophile than methoxide, the nucleophile used in the experiment described above. Nevertheless, the barriers obtained indicate a feasible reaction, especially taking into account an expected large excess of methanol if this species is used as solvent in the reaction medium. In addition, the similarity between the values calculated for the two energy barriers justify the existence of two consecutive methanol additions and, thus, the fact that the reaction cannot be stopped after the first attack, on the imine C-atom. Since there are two O-nucleophilic attacks in the reaction described above it is important to study the sequence of those attacks in order to gain insight into the mechanism of HNE inhibition. In other words, what occurs first, addition of the nucleophile to the carbonyl C-atom or attack on the imine C-atom? In order to answer this question the alternative path was explored by means of DFT calculations, i.e., a mechanism were the first step corresponds to methanol nucleophilic attack on the C=O of the lactone (Figure

68), while the entire path is presented as ESI (Figure 67). Corresponding hydrolysis of this bond and the opening of the former lactone ring. In the transition state, TSFG, scission of the C–O bond is just starting, with a distance (1.59 Å) that is only 0.19 Å longer than the corresponding one in intermediate F. Once again, assistance of the adjacent MeOH molecule is crucial to the H-transfer process that occurs along that step and the relevant O–H distances, indicate that, in fact, such process is underway in TSFG (1.08–1.39Å).

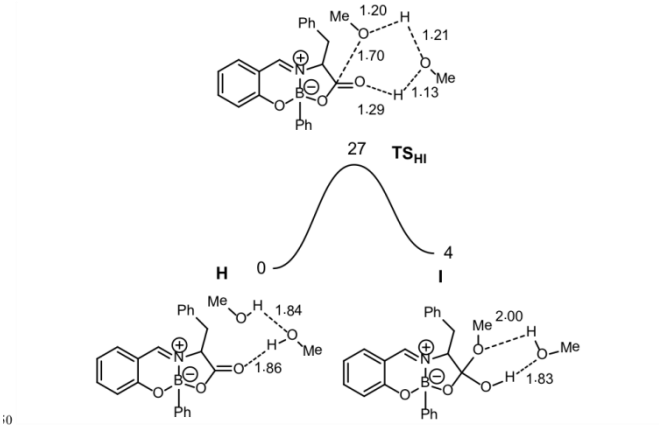

Figure 68 - Energy profile (kcal/mol) calculated for nucleophilic attack of methanol on C=O group.

The O-nucleophilic attack of methanol on the lactone C=O group of substrate 3 occurs similarly to the equivalent steps in the first mechanism addressed. Thus, there is methanol assisted proton transfer, from the incoming methanol molecule to the O-atom in the carbonyl group of the substrate, simultaneously to the formation of the new C–O between substrate and nucleophile. Formation of that bond is well advanced in the transition state, TSHI, with a C–O distance of 1.70 Å. Also, the process of H- transfer is evident in TSHI with the four relevant O–H distances between 1.13 and 1.29 Å. Most interestingly, the energy barrier calculated for this step is 3 kcal/mol higher than the one obtained for the attack on the imine C-atom, as first step of the reaction mechanism (TSAB Figure 67). This indicates the imine as the more favorable location on the substrate for the first O-nucleophilic attack, being a rather surprising result, taking into account the atomic charges calculated for 41(Figure 65), that show the carbonyl C-atom as more electrophilic than the imine one. However, the LUMO of the substrate (Figure 69) has a significant participation on the imine C=N bond, representing a π* interaction between those two atoms and

presenting 51% of the electron density of that orbital. The results above indicate that reaction is under orbital control, rather than being ruled by charge (Figure 69).

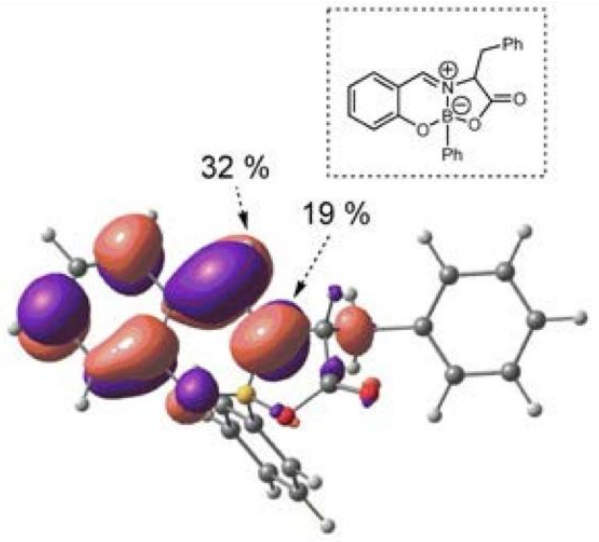

Figure 69 - Representation of the LUMO of the compound 26.

Aiming to explain the observed biological activity of the various heterocycles (Figure 64) and to get insight into their mechanisms of action at the molecular level, we also performed in silico molecular docking studies in the active site of HNE, using GOLD 5.1 software.[112] The coordinates of the enzyme structure were obtained from Protein Data Bank selecting the structure with accession code 1HNE (X-ray coordinates at 1.84 Å resolution, previously validated for docking procedures). Modelling the interaction of compounds 24, 26, 38 and 39 in HNE active site (Figure 70A, B, C and D, respectively), the most striking feature evidenced by the docking of all 4 compounds, is their distinct recognition by the enzyme's primary specificity binding pocket (S1). As shown in Figure 70A, the inactive compound 24 does not occupy S1, contrasting with the moderately active compound 26 (IC_{50} of 20μM), prepared with L-phenyl alanine, which sits the benzyl side chain well within the S1 pocket (Figure 70B). Interestingly, in this optimized conformation, the imine and lactone possible reactive sites are still quite distant from any HNE nucleophile. Regarding the most stable conformations obtained for the most potent inhibitors 38 and 39, inspection of Figure 70 C and D indicates that the L-phenyl alanine side chain is no longer occupying the S1 pocket, being replaced by the 4-methoxy or the 4-diethyl amino substituent of the aldehyde aromatic moiety. Interestingly, this arrangement visibly favours the proximity of the imine reactive site to the Ser195 (4.2Å

(38); 4.1Å (39)) and His57 (2.8Å (38); 2.9Å (39)).To validate this model and confirm the importance of the aldehyde aromatic substituent for the recognition and potency (Figure 71), compound 42 was prepared from glycine, 4-methoxy- salicylaldehyde and 2,4-dichlorophenylboronic acid in THF. Very gratifyingly, compound 42 that lacks the benzyl group displayed a 3.17μM IC50 which is comparable with the activity exhibited by compound 38 prepared from L-phenyl alanine.

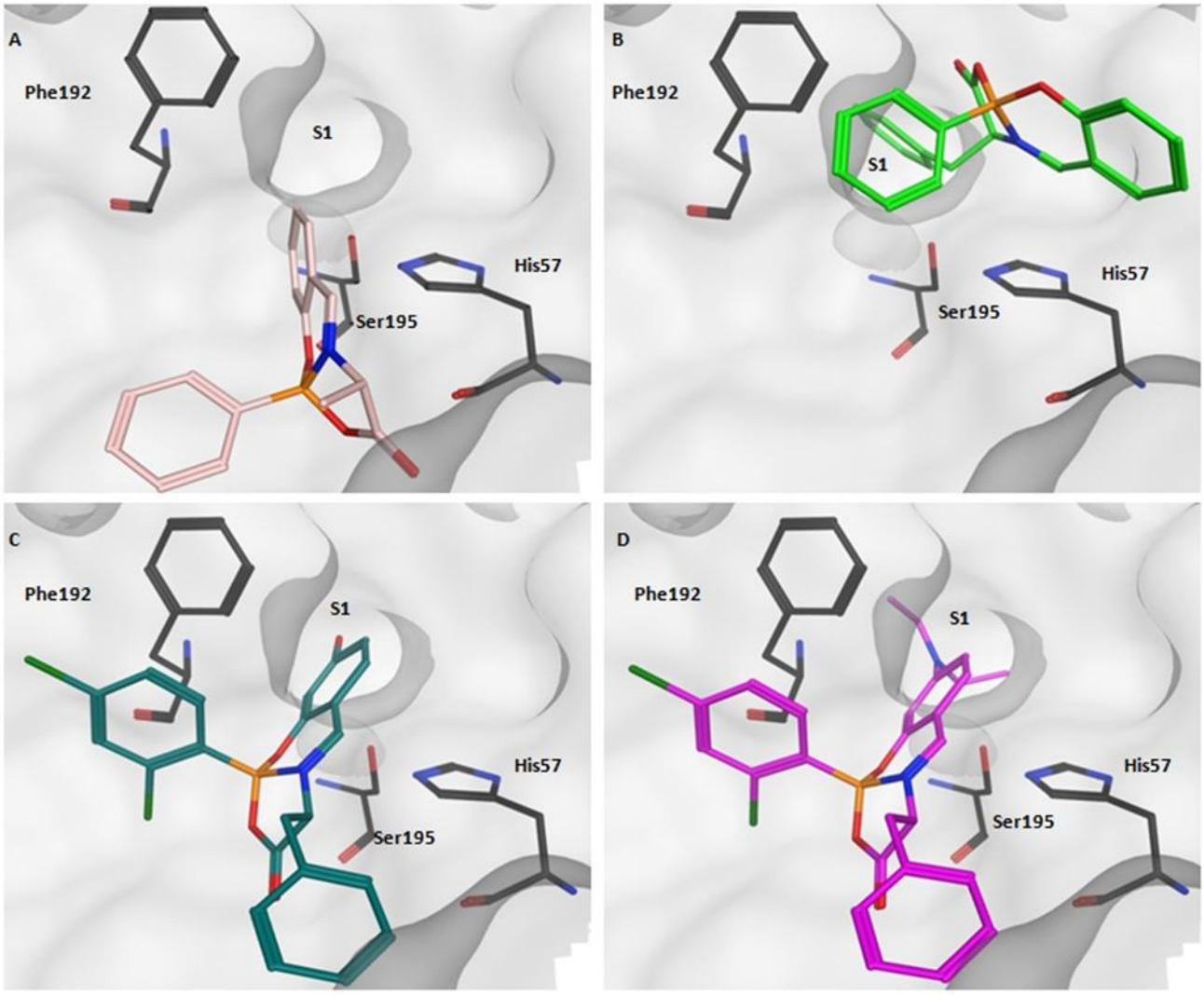

Figure 70 - Modelling the interaction of compounds 24, 26, 36, 39 in HNE active site (respectively A, B, C, D).

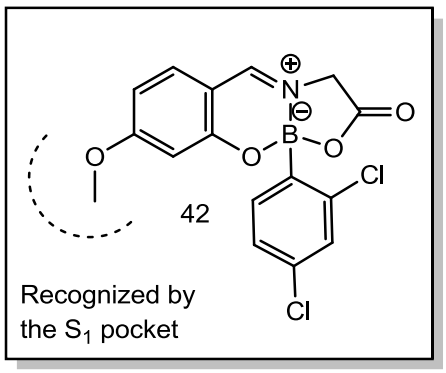

Figure 71 - The biological evaluation of compound 43 shows the importance of the aldehydic substituent for the recognition of the molecule in the active site of the HNE.

Regarding the mechanism of inhibition, the lack of activity of compounds **40** and **41** indicates that the reaction of the imine and lactone ring opening are both key events in the inhibitory process. Although it is uncertain the exact sequence of events of the mechanism, we envision that Ser195 hydroxyl group firstly adds to the nearby imine carbon centre to form an amino ketal (Figure 72 A), in line with the accepted first step of serine proteases mode of action,[113] and with the mechanism of methanol addition to 26, obtained by DFT calculations (see above). The O-nucleophilic attack on the imine neutralizes the nitrogen atom and generates a negatively charged intermediate, which may be readily protonated in the N-atom by the near His57, reestablishing the N-B ylide. This parallels the intermediate step in the mechanism of Figure 67, from B to C in which there is a gain of 21 kcal/mol. Subsequently, the proximity of the His57 to the amino ketal carbon centre (2.9Å) may assist in the dissociation of the hydroxyl group of Ser195 (Figure 72B), liberating this fragment for the following lactone ring opening that promotes the release of the boronic acid moiety as suggested by the reaction of 39 with sodium methoxide (Figure 72C). In agreement with this proposal, the minimized structure generated from the reaction of 39 with His57 and Ser195 in the HNE pocket (performed with MOE 2011.10 software27) shows the maintenance of the 4-diethyl amino substituent of the aldehyde aromatic moiety well fitted in to the S1 pocket as shown

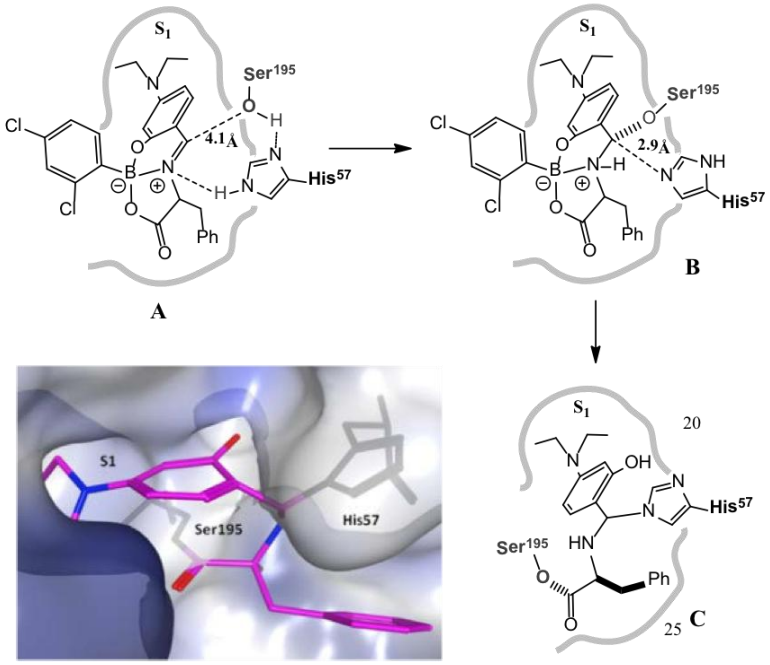

Figure 72 - Proposed mechanism of inhibition of the compound 39 against HNE.

Based on this proposal, we perform the LC-ESI-MS analysis of the reaction between inhibitor 39 and HNE (Figure 73). Very gratifyingly, we observed that 39 is completely consumed in the presence of HNE, at the same time that, compound **a** in the Figure 73 is formed in the reaction mixture (Figure 73). The *in situ* formation of **a**(Figure 73) is a particularly important observation as it is in good agreement with the aforementioned mechanism, in which imine **a** (Figure 73) maybe generated via hydrolysis of the intermediate depicted in Figure 72 A. Nevertheless, these results should be taken cautiously as the appearance of **a** (Figure 73) as a result of a spontaneous reaction of phenylalanine and salicylaldehyde formed via alternative pathways cannot be ruled out.

Once established the usefulness of this compounds to inhibit this important biological target, we addressed the toxicity of the leading compound **39** as well as the individual building blocks (Figure 74). The referred compounds were assayed against colon adeno-carcinoma cells (CaCo-2) and did not show any significant toxicity.

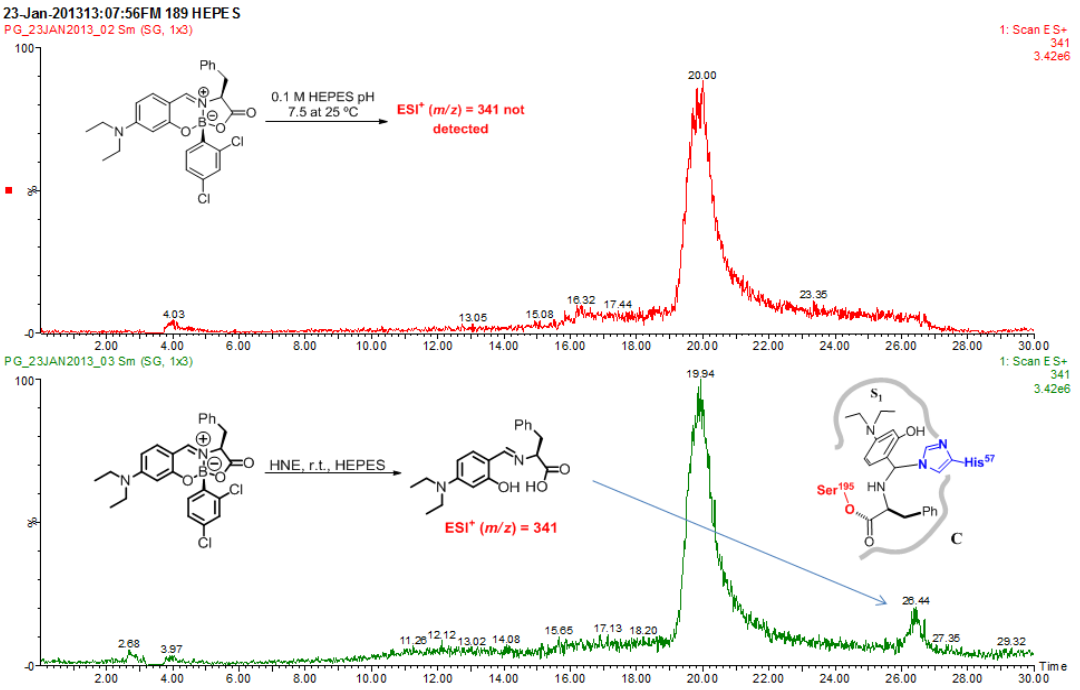

Figure 73 - LC-ESI-MS analysis of the reaction between inhibitor 39 and HNE.

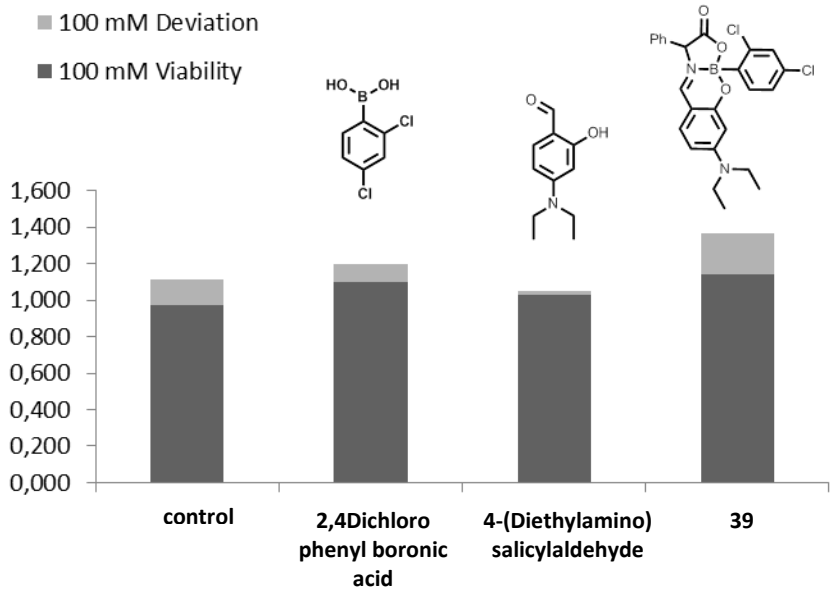

Figure 74 – Toxicity test over CaCo-2 cell line, with 100 µM concentration.

3.3 Conclusion

This study demonstrates that a boron promoted one-pot assembly reaction can be used to design novel bioactive scaffolds. This strategy was applied to the discovery of new HNE inhibitors generated from components like salicylaldehyde, aryl boronic acids and amino acids. The versatility of this assembly strategy allowed the synthesis of new HNE inhibitors in excellent yields, high diastereoselectivities and IC_{50} up to 1.1µM (compound 39). The combination of synthetic, biochemical, analytic and theoretical studies, allowed us to conclude that the boron tether can provide the structural requirements necessary for enzyme inhibition. Moreover, we were able to identify the 4-methoxy or the 4-diethyl amino substituent of the salicylaldehyde as the most important recognition moiety in the molecule, and the imine alkylation, lactone ring opening and release of the boronic acid as key events in the mechanism of inhibition.

4. Evaluation of fused bicycle-boronate heterocycles against the phenylalanine hydroxylase (PAH)

4.1 Overview

In the course of our studies, in which we explored the activities of fused bicyclo-boronated heterocycles against the HNE. A molecule found in the literature with some degree of structural analogy with bicyclo-boronate heterocycle architecture gathered our attention. This molecule is the 3-amino-2-benzyl-7-nitro-4-(2-quinolyl)-1,2-dihydroisoquinolin-1-one (Figure 75) and was reported to be a promising structure for the treatment of the phenylketonuria (PKU). [114]

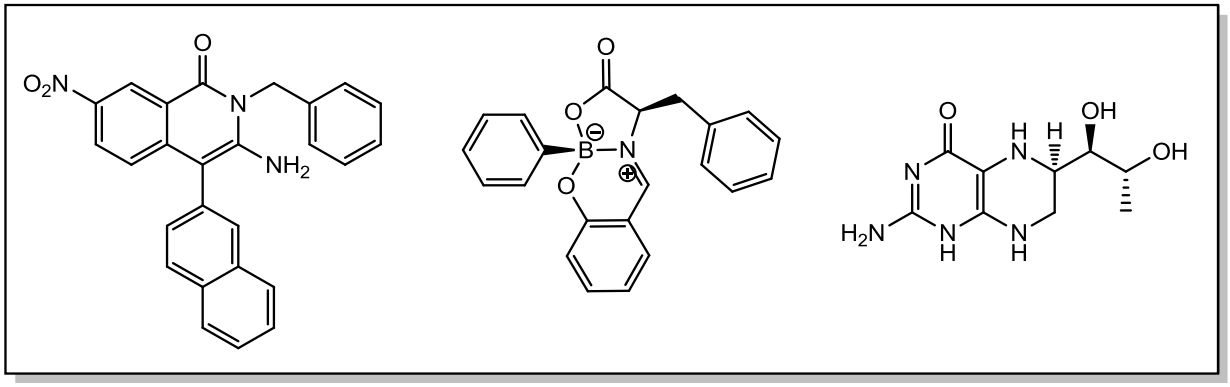

Figure 75 - Analogy between 3-amino-2-benzyl-7-nitro-4-(2-quinolyl)-1,2-dihydroisoquinolin-1-oneof and fused bicycle boronate heterocycle obtained with phenylalanine.

4.1.1 Phenylketonuria (PKU)

PKU is a metabolic genetic disorder characterized by high levels of phenylalanine, in all body tissues.[115]In most cases, PKU is related with dysfunctional activity of phenyl alanine hydroxylase (PAH) exhibiting conformational defects imposed by mutations in the PAH gene.[114,115.116,117]In humans the number of mutations responsible for a mistaken transcription of PAH gene is very large, nowadays they were numbered as over 500. A substantial part of these genetic modifications are classified as missense mutations,[116,118] which lead during the translation of the mRNA to include a wrong amino acid in the primary structure of the PAH. The final result is a muted and misfolded PAH protein with an decreased turnover in vivo. To understand the impact of PKU over our society, it is enough to quote the annual rate of incidence of this disease in the USA 1:16,000[120]. PKU is the most frequent of the amino acid metabolism inborn errors and, if untreated, leads to the disturbance of brain neurotransmitters levels that develops progressively into mental retardation, brain damage, epilepsy among other incapacitating neurological disorders.[115]PAH belongs to the family of aromatic amino acid hydroxylases and catalyses the oxidation of Phe to tyrosine (Tyr), which is the first step of the catabolic degradation of Phe.Consequently, a defective activity of PAH leads to Phe accumulation up to toxic levels, forcing PKU patients to stringently hold on to a Phe diet free, which often results on malnutrition and neurologic problems. For these, alternative strategies to control PKU are now beginning to emerge such as the diet supplementation with tetrahydrobiopterin (BH_4), which is a PAH natural cofactor that is able to act as a pharmacological chaperon stabilizing the mutated protein. In the 2008 Pey et *al* [114]. reported the possibility to use the 3-amino-2-benzyl-7-nitro-4-(2-quinolyl)-1,2-dihydroisoquinolin-1-one (Figure 75) as pharmacological chaperones of the PAH, in order to increase the correct folding of mutant form of the protein. Their study analyzed in deep the effect of the molecule in the Figure 75, in which disclosed the stabilizing effect on PAH enzyme kinetics; on the stability and folding of WT and mutant proteins. They found that the 3-amino-2-benzyl-7-nitro-4-(2-quinolyl)-1,2-dihydroisoquinolin-1-one:

- *Enhances the thermal stability of PAH without showing PAH inhibition activity.*
- *That it stabilizes the functional conformation of PAH either in the recombinant and mutants PAH.*
- *PAH liver levels activity of mouse, increased after a 12-day oral administration.*

They concluded their report writing:

"The fact that compound III (3-amino-2-benzyl-7-nitro-4-(2-quinolyl)-1,2-dihydroisoquinolin-1-one depicted in the Picture 59) does not display significant inhibitory effect indicates that the compound might be modified in order to increase its affinity for PAH. This would enhance its potency as pharmacological chaperone, therefore allowing potentially larger correction of the phenotype while still using relatively low concentrations."

Lured by the structural analogy between such promising structure and the bicyclo-heteroatom architecture library, and by the fact that, PAH, apart from BH_4, is also activated by Phe, which is embodied in the bicyclo-structures, we decided to test our compounds as chaperones of PAH in the attempt to investigate the possibility of an employment of these compounds in the treatment pf the PKU.

4.1.2 Evaluation of bicycle-boronate heterocycles collection for phenylalanine hydroxylase (PAH) inhibition

Apart from BH_4, the regulation of mammalian PAH is also operated via the cAPM-dependent protein kinase mediated phosphorylation at the Ser 16 and by the substrate Phe. PAH is activated several fold by pre-incubation with Phe. The mechanism for this activation is not yet comprehended and there is no agreement on whether it is caused by Phe binding to an allosteric site, in the regulatory domain, or to the active site. Regardless of its mode of action, activation by Phe is the most important mechanism for PAH regulation, and for this reason, Phe represents a very attractive structural starting point to develop new modulators of PAH. Based on this and on the fact that the bicycle boronate heterocycles incorporate the Phe in its structure, we tested this family of compounds against the PAH. We started our studies by evaluation of compounds **24-26** against PAH. The activity was measured with 100 µM L-Phe and 100 µM of each compound in 1% DMSO. Samples were preincubated with L-Phe and compound (substrate activated), not preincubated (non-activated), or preincubated with compound only (compound activated), respectively black white and dotted bars in the following figures, for 5 minutes at 25 ºC prior to the addition of BH4 to start the activity measurements. The reaction final concentrations were: 100 mM Na-Hepes, pH 7, 0.1 mg/ml catalase, 100 µM Fe2+, 5 mM ascorbic acid, 0.5 mM HCl, 100 µM L-Phe, 100 µM compound (in 1% DMSO), 75 µM BH4 and 5 µg (0.45 µM subunit) hPAH WT tetramer. The values were normalized by subtracted the background L-Tyr contribution from each compound (assay without substrate).

As shown in Figure 76, the iminoboronate 26 was able to modulate the activity of PAH. This compound clearly competed with the substrate Phe and, more importantly, exhibited the ability to activate PAH in the absence of Phe. Very differently, the iminoboronates **25** and **24**, prepared with L-leucine and L-alanine respectively, didn't show an activator profile. Taken these results together with the fact that the individual components, salicylaldehyde and phenyl boronic acid, were unable to activate the enzyme (Figure 76), they clearly suggest that the observed activity, is due to the incorporation of Phe into the structure of heterocycle **26**. Therefore we extended the study to other boron heterocycles as shown in Figure 77, compounds **27** featuring a methyl at the boronic acid aromatic para position demonstrated a similar substrate competitive profile as observed for 26, though with no activation.Very differently, compound 29 prepared with 4-fluorophenylboronic acid,

markedly activated PAH, on the other way, the introduction of a methoxide substituent in 28 resulted in a clear inhibition of PAH.

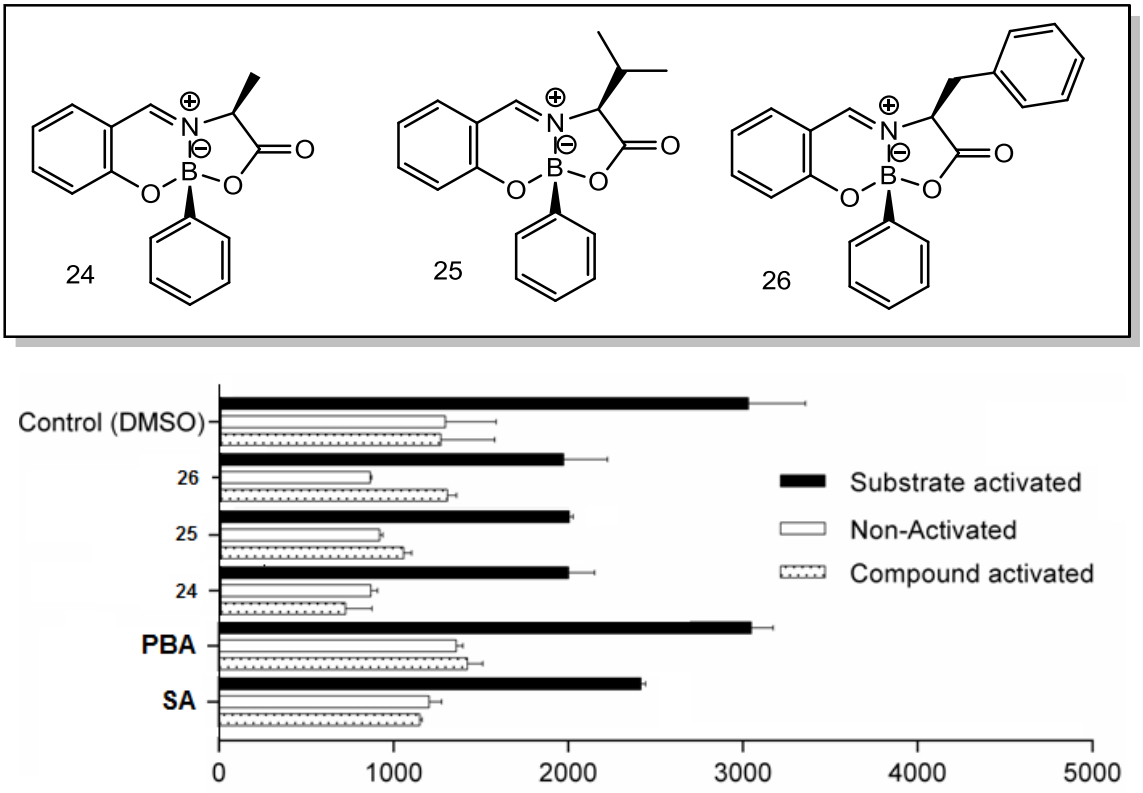

Figure 76 - Specific activity (nmol Tyr mg^{-1} mon^{-1}).

Further we evaluated the substitution at the aromatic ring of the aldehyde (Figure 78). Compound 30 is a variation of 26 with a methyl at the para position of the aldehyde moiety, such functionalization decreased the activation profile of the molecule. In the compound 31 the inclusion of a methoxide at the same position lead to an improved ability to activated the enzyme when comparing with **26**. This molecule was consider as new lead compound and as new benchmark in the functionalization process, for a second round of evaluation. Compounds **32, 33, 34, 35, 36** and 37 were tested (Figure 78,). Unfortunately, compounds 33 and 37 displayed only a very modest activation profile, whereas **35** and **32** only moderately compete with the substrate for the access to the enzyme active site. More interestingly the isomer of compound **35** bearing a bromo orto substituted boronic acid aromatic moiety (compound **36**) only moderately competed with the substrate at the same time that was able to activate the enzyme towards the hydroxylation of Phe alanine. As shown is the combination of para-methoxy-salicylaldehyde with different aromatic and vinylicboronic acids didn't improved the activation previously observed with compound **31**.

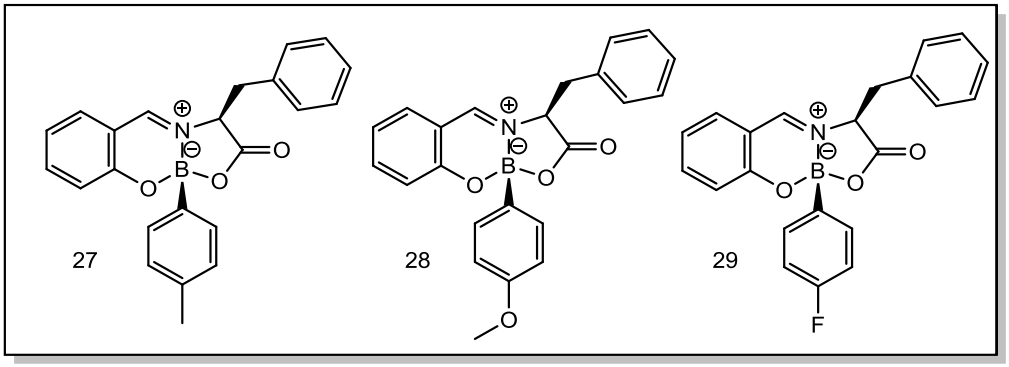

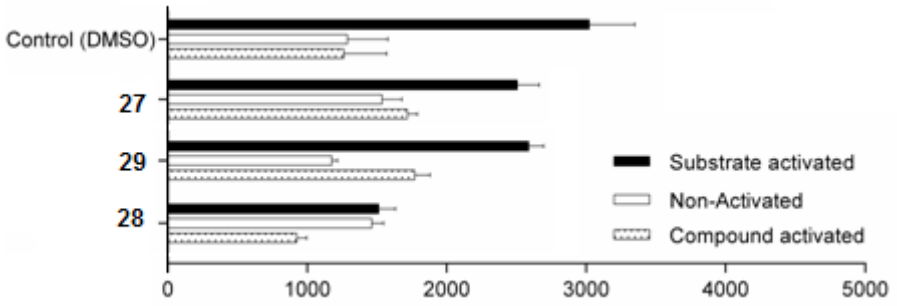

Figure 77 - comparation among the specific activity of compounds 27, 29, 28(nmol Tyr mg^{-1} min^{-1}).

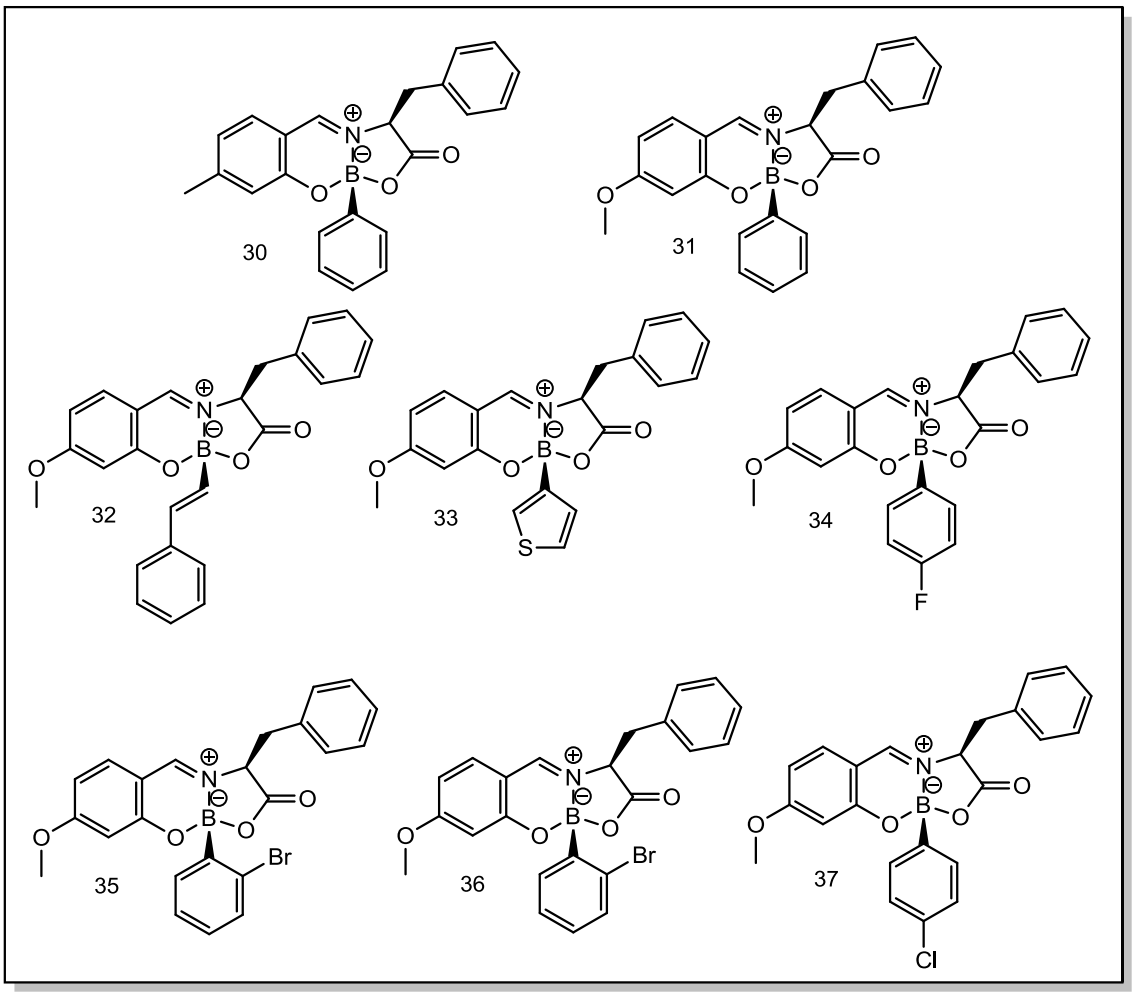

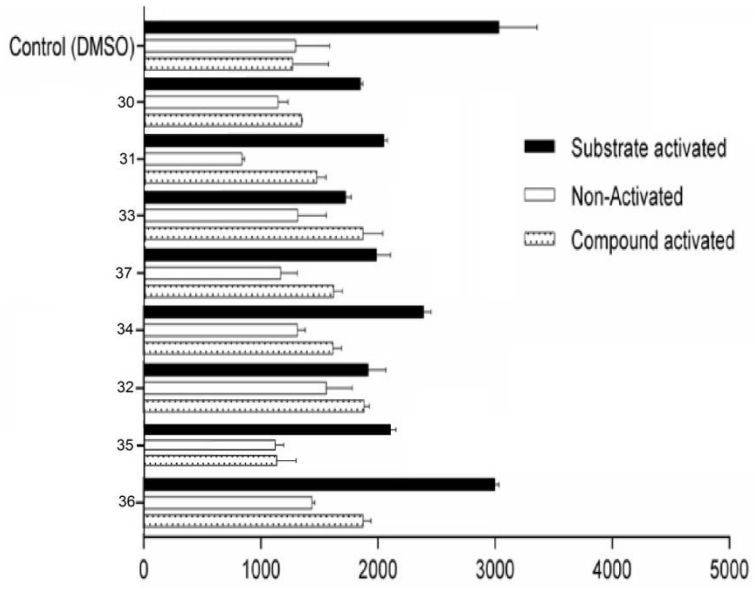

Figure 78 - Comparison among the specific activity of compounds 30, 31, 32, 33, 34, 35, 37 (nmol Tyr mg^{-1} min^{1}).

4.1.3 Conclusion

The profile of the molecules tested against the wild type of PHA showed a clear ability to modulate the biological activity of PHA despite this study still stand in a preliminary phase they shows that fused bicycle boronate heterocycles are an interesting scaffold able to interact with PHA and they may be considered as a benchmark for next round of optimization process.

5. Diazoborine as inhibitor of HNE

5.1 Overview

The diazoborine is a well-known class of chemical compounds structurally characterized by an etheroatomic ring that embodies boron and two nitrogens. Until today these heterocycles have been described as antibacterial, limited to the gram-negative population. Two characteristics of this compounds attracted our attention: the general architecture of the diazaborines and the speculation proposed by Baldock in 1998 according to which the boron of diazoborine undergoes a sp2-sp3 transformation while interacting with an –OH functionality of its biological target.[121] Intrigued by these two considerations we wonder if the diazaborine could be employed as a HNE inhibitors.

Beyond the putative activity against HNE, this family of compounds is also eligible to be prepared via a simple assembly reaction in line with our boron tether strategy. In 1963 Dewar and Dougherty reported the possibility to obtain the (1,2,3) diazaborine through an easy one-pot reaction between a formylboronic acid and hydrazine (Figure 79) in ethanol, followed by product precipitation in water. A more carefully analysis of this synthesis reveal even more analogies between the reactions discussed in the previous chapters and the one disclosed by Dewar and Dougherty. To synthesize either the tricyclo and the bicyclo-boronated heterocycle architectures three important components are required: an aldehyde, a boronic acid and a compound with reactive nitrogenated and oxygenated functionalities, which work as connectors. In the reaction for the synthesis of the diazaborine this pattern is partially maintained, the boronic acid and the aldehyde are fused in one molecule. Based on this we envisioned that this methodology and scaffold could be used to test against HNE.

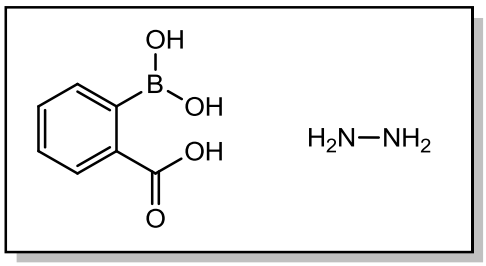

Figure 79 Reaction components of Dewar's protocol.

Regarding the structure of diazaborines, it is possible to highlight the characteristic heteroatom ring that is often fused with a second ring system (Figure 80a), and the nature

of such ring system may vary (benzene, naphthalene, thiophene, furan, pyrrole).[121] The positions of the heteroatoms in the ring system is not set, and it can have several variants (Figure 80).

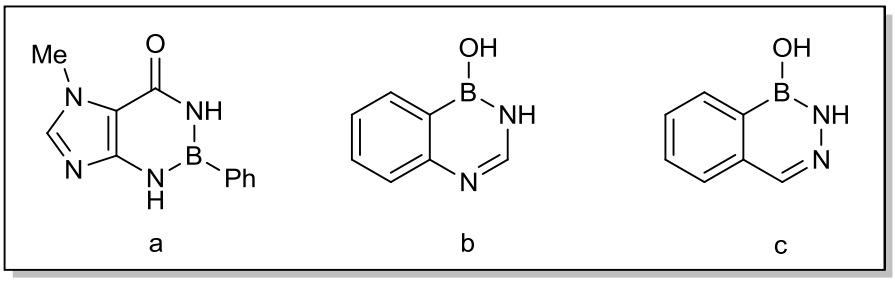

Figure 80 - examples of the variable arrangement of the heteroatoms in the diazoborines.

The systematic name for such molecules indicates the position of each etheroatom in the cycle, (1,3,2) diazaborine for the structure **a**, (2,4,1) diazaborine for the structure **b**[122]and (1,2,3) diazaborine for the **c.** ,[121]

Regarding the biological activity of these compounds, they are reported to be selectively active against gram-negative bacteria,[121]which suggests the biological target of these molecules to be related with the cell wall. Turnowsky et al. [123] identified and proved that the cellular target of the diazaborine is NAD(P)H-dependent enoyl acyl carrier protein reductase (ENR), an enzyme responsible for the last step of fatty acid synthase. The diazaborine inhibition of the ENR requires the presence of the $NADP^+$ that is a pivotal element either in the binding of the diazaborine and in the inhibitory mechanism in itself.[124] Baldock et al. reported a x-ray crystallographic analysis of the enzyme incubated with the cofactor and the diazaborine, showing that they form a bisubstrate due to a covalent bond between the boron and the 2' OH of the nicotinamide ribose a rearrangement of the boron from trigonal planar to tetrahedral geometry.[121]

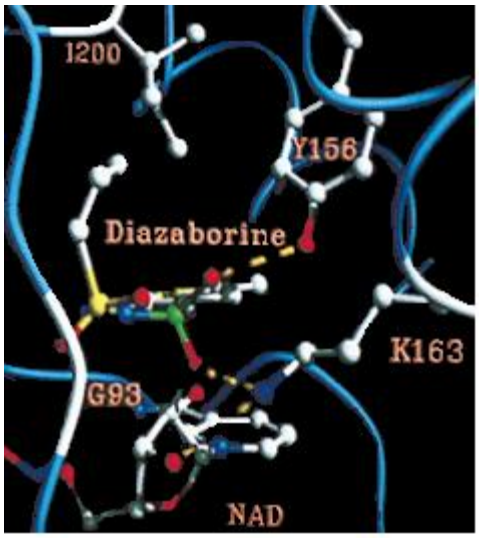

Figure 81 - X-ray crystallographic analysis of the enzyme, the cofactor and the diazaborine.

To support their data, Baldock et al, suggested an analogy between the mechanisms that leads to the tetrahedral borate in the diazaborine/NADP+ disubstrate and the boronic acid/serine proteases. As far as our knowledge goes the diazaborine have been exclusively employed as antimicrobic for the treatment of the tubercolosis. Despite the analogy suggested by Baldock and co-workers, this class of compounds has not been tested as serine proteases inhibitor, even though the correspondence between the boronate formed by diazaborine/NADP+ and boronic acid inhibotrs/serine proteases is real: B-O covalent bond formation, tetrahedral rearrangement of the boron, formal negative charge formally placed onto the boron.

5.1.1 Synthesis of a diazaborine library and its enzymatic evaluation against HNE

Bearing in mind the considerations discussed above, we started our study by synthesizing molecules **43, 44, 45, 46** depicted in the Figure 82. The products were prepared by combining different boronated aldehyde (2-Formylphenylboronic acid; 3-fluoro-2-formylphenylboronic acid; 2-formyl-3-thiopheneboronic acid) with hydrazine hydrate 64%. The reaction was performed following Dewar's procedure and using methanol as solvent, the product was simply precipitated from the reaction mixture with cold water, a simple filtration afforded the product, in good yield, [125] that required no extra purification steps. With these products in hands we readily tested them against HNE.

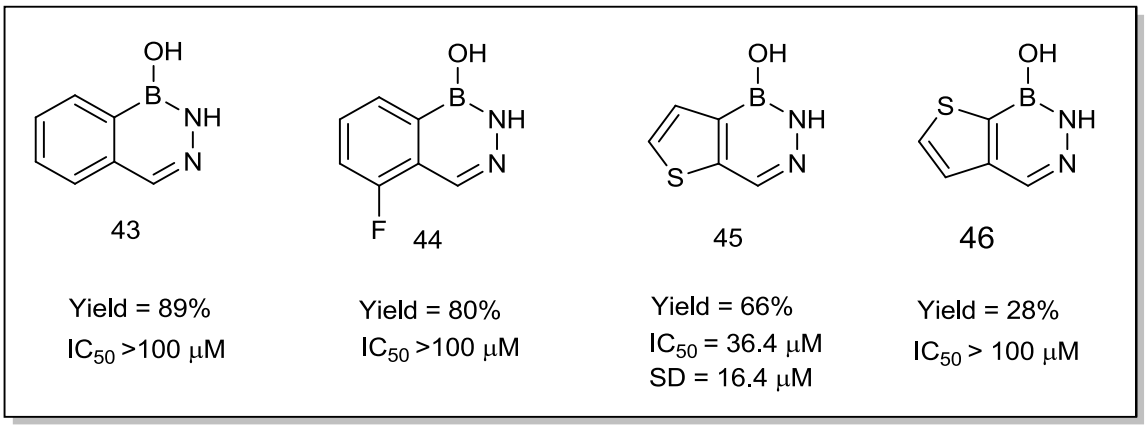

Figure 82 Activity of compounds 43-46 against HNE.

As shown in Figure 82 compounds **43, 44** and **46** did not show any inhibitory activity against the enzyme, but compound **45**, even if in small magnitude, shown some inhibition of HNE. Encouraged by this result we wonder if the modulation of the inhibitory activity could be achieved by functionalization of the N bonded to B with a phenyl group. We also questioned whether the relative position of the sulphur in the diazaborine could also improve the biological activity. Motivated by these questions, we synthesized molecules **47** and **48** shown in Figure 83, using either the 2/3-formyl-2/3-thiopheneboronic acid; hydrazine and phenyl hydrazine.

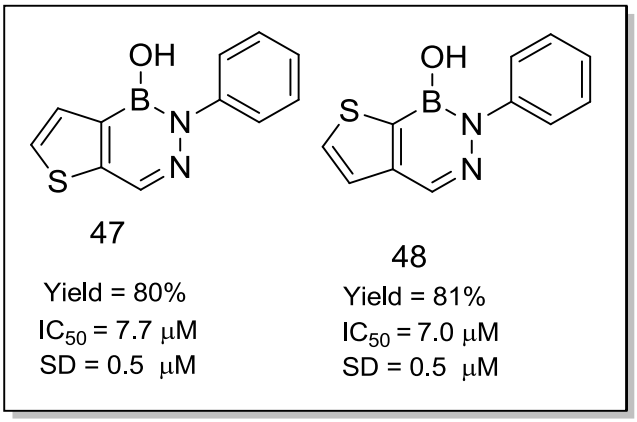

Figure 83 Activity of compounds 47, 48 against HNE.

The enzymatic evaluation of the products illustrated in the Figure 83, revealed a dramatic increase of the inhibitory activity of the diazaborines prepared with phenyl hydrazine. However, despite this interesting result, the interpretation of the relation between the inhibitory activity and the structures of the diazaborine **45, 46, 47, 48** remained controversial. Indeed comparing the molecule **45** and **46** it appears that the position of the sulphur has a very deep effect on the ability of the molecule to inhibit the HNE, differently compounds **47** and **48** show almost the same activity against the enzyme. A partial explanation could come from the observation that the inhibitory activity is affected by the phenyl group and the sulphur position in the aromatic ring in a divergent sense. Nevertheless the importance of the phenyl appear to be more decisive for the activity. At this point, we considered how other substituents at the nitrogen could alter the biological activity of the diazaborine. Therefore we prepared compounds **49** and **50** (Figure 84), though the presence of a electron withdrawing group sulphone did not improve the previous observed activity.

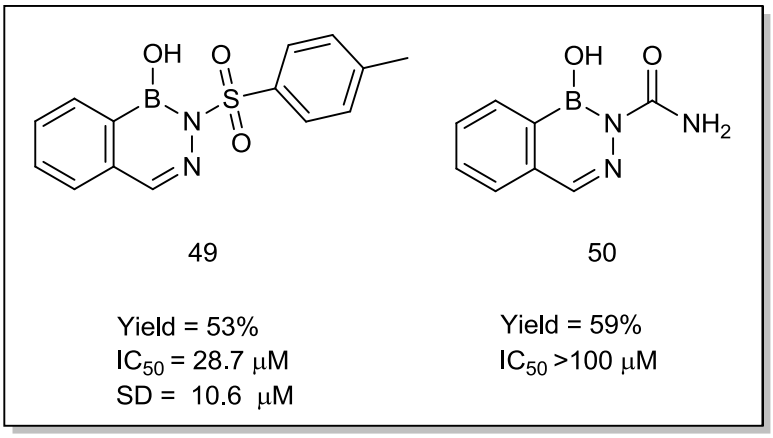

Figure 84 - Activity of compounds 49-50 against HNE.

Once established that the phenyl was indeed pivotal for the activity, we wonder if the phenyl functionality could also improve the biological profile of molecules **43** and **44** similarly to what happened with the compounds **47** and **48**.

Therefore we synthesized diazaborines **51**, **52** and **53** (Figure 85) and tested them against HNE, unfortunately in this case, the phenyl group did not enhance the biological activity of these new molecules.

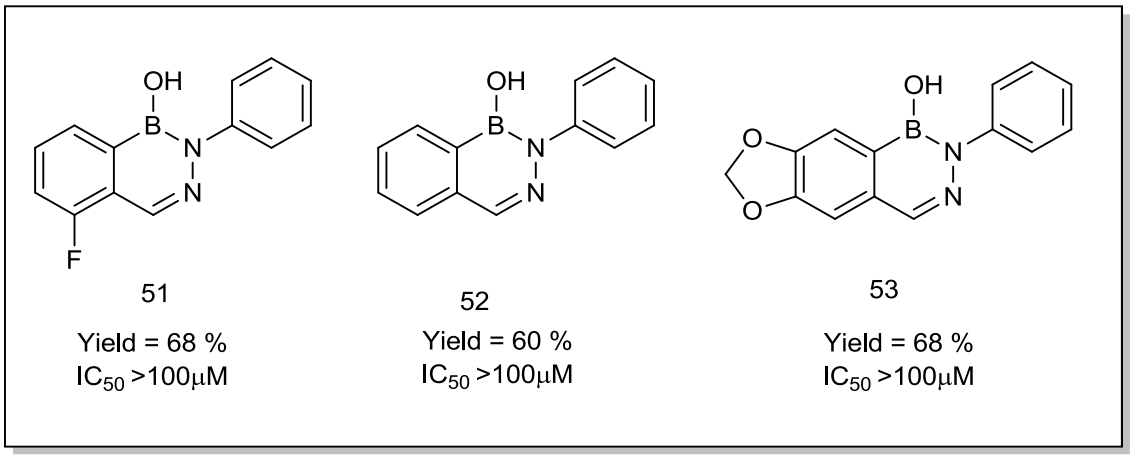

Figure 85 - Activity of compounds 51-53 against HNE.

Taken these results in consideration we move on and synthesize two new diazaborines (Figure 86) combining 2-acetyl phenylboronic acid and phenyl hydrazine (**54, 55**). Once prepared these compounds were tested in an assay against HNE. Very gratifyingly this evaluation rendered an activity of 2.5 μM for compound **54**, which until now is the most

potent compound of the library. Interestingly compound 55 featuring no substitution at the nitrogen had no activity outlining, once again, the importance of this function. The comparison among the structures and the inhibition induced in the HNE by molecules **43, 52, 54, 55** suggest that to have inhibitory activity against the enzyme a phenyl and a methyl group are required respectively at the positions 2 and 4 of the heterocycle. To better understand the contribution of the methyl and phenyl groups over the activity of these diazaborine, we evaluated molecules **43, 52, 54, 55** in a preliminary docking study.

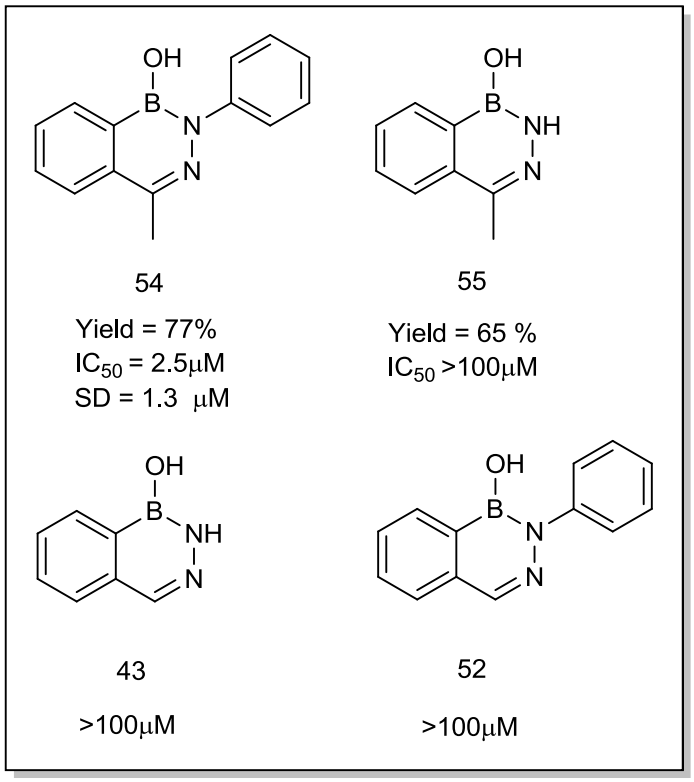

Figure 86 - Effect on the inhibitorial activity of the methyl as substituent in compounds 43 and 52.

Docking studies

In order to understand how the diazaborines interact with reactive site of HNE we performed in silico molecular docking studies of the diazaborine **52, 54** and **55** (Figure 86), using GOLD 5.1 software.[112]

The coordinates of the enzyme structure were obtained from Protein Data Bank selecting the structure with accession code 1HNE (X-ray coordinates at 1.84 Å resolution, previously validated for docking procedures). Once again the S1 binding pocket plays a pivotal role for the recognition of the molecules into the active site. The diazaborine **55** does not have any specific interaction with the S1 (Fig 87 **a**), which in turn is in good accordance with the lack of inhibitory activity of this compound. Differently both compounds 52 and 54 (Figure 87 **b**, **c**) place their phenyl substituent into the S1 region, but according the enzymatic assays only the compound 52 displayed a reasonable activity.

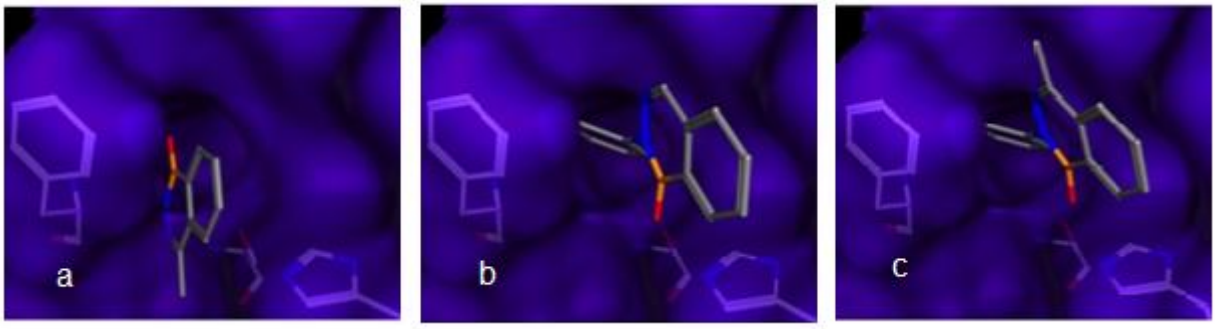

Figure 87 – Docking of compounds 52, 54, 55, cyclic form .

interestingly, despite compounds 52 and 54 siting their N-phenyl substituent inside the S1 binding pocket, the distances between the boron and the oxygen of the Ser 195, which is the nucleophile responsible for the biological activity of the enzyme, is too large to predict an efficient covalent interaction between the two atoms. Surprisingly, despite the distances could be considered almost equal (3.81Å for compound 52, 3.85 Å for compound 54), is the inactive compound 52 to set in closer proximity the boron closer to the oxygen of ser 195.

Puzzled by the discordance between docking studies and experimental evidences, we envisioned the possibility of the diazaborine to actually act as a prodrug. As shown in figure 88 diazaboorines could exist in equilibrium with is open form and it is this latter that

could be the responsible of the enzymatic activity. This concept was already disclosed by Bachovchin as already mentioned in the first chapter.

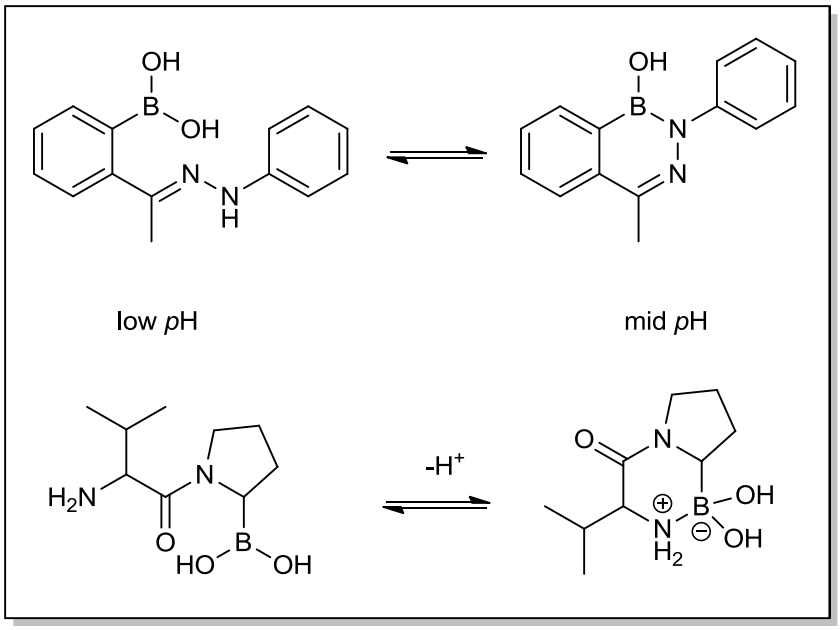

Figure 88 - Comparison between the Bachovchin soft-drug cyclizatoin which decrease the activity of the molecule and diazaborine pro-drug chain opening responsible of the putative activity of these compounds.

Bachovchin exploited this cyclization as a time dependent mechanism to decrease the side effect of the boropeptide.

Despite such speculation needs deeper investigation, a positive feedback seems to come from the docking studies of the open forms of the molecules **43, 52, 54, 55**. The first notable feature is that the moiety of the diazaborines responsible of the molecular recognition to the S1-binding pocket (Figure 89) is now the aromatic ring bonded to the boron and no longer the phenyl group, which now is available for a π-π interaction with the Hys 57 . Despite the molecule 43 and 55 were able to interact with the pocket S1 (Figure 89 **a**, **b**) they miss any π-π interaction with the Hys 57, data that eventually explain the lack of inhibitory activity. In addition molecules **52** and **54** possess either an aromatic moiety to fit in the S1 pocket and a phenyl group that may interact through π-π interaction with the hys 57 (Figure 89 **c, d**) but only **54** is active.

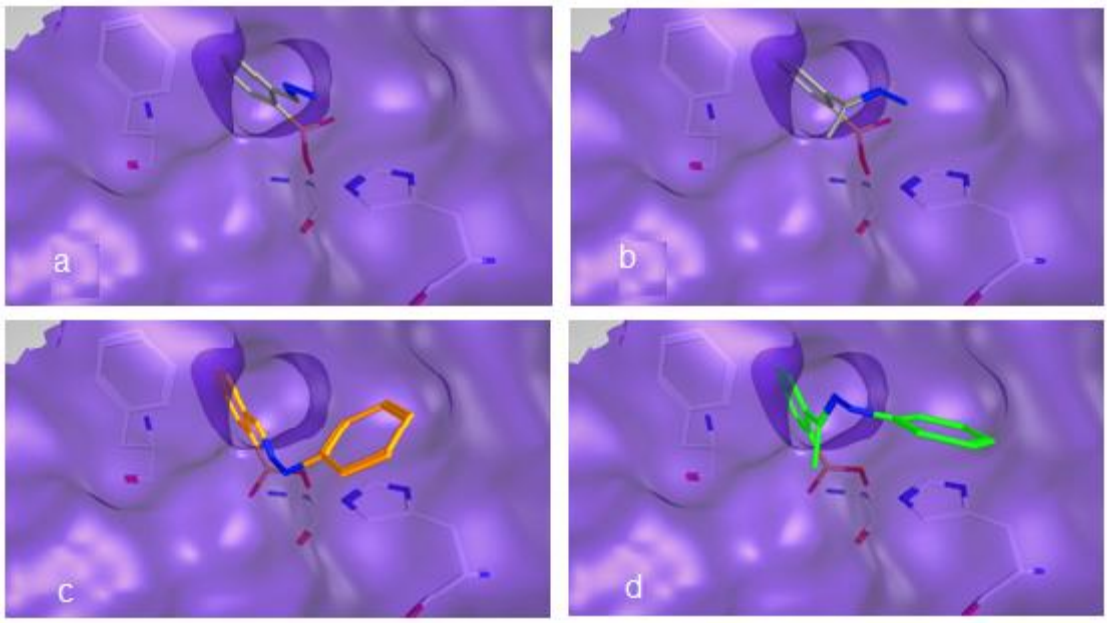

Figure 89 - Docking of compounds 43, 52, 54, 55, in opened form.

A more carefully inspection of the Figure 89, reveals that the serine 195 is present at the entrance of the S1 pocket and that, if may efficiently bind to the boron atoms of the two structures. This shows that both structures are able to place their pharmacophores in close proximity with the serine 195 not explaining the dramatic difference in the inhibitor activity between the two diazaborines. Instead the diazophenyl side chains of the molecules **52** and **54**, present a different arrangement, more evident in Figure 90, specifically the molecule 54 shows an orientation of the N-phenyl substituent that favors a stronger π-π interaction with the Hys 57. Despite this data is in accordance with the enzymatic assay, the difference between the π-π interactions between the N-phenyl group of the two molecules is sufficiently large to justify a difference in the biological activity of 2.5 μM for diazaborina **54** and >100 μM for diazaborine **52**. A possible explanation may be the steric hindrance provided by the methyl group which block the entrance of the S1 pocket protecting the boronate complex (diazaborine-enzyme) from hydrolysis enough to produce a sensible enzymatic inhibition. As already mentioned in "*What characterizes an acylating agent from a natural substrate is the ability to produce an acyl-enzyme intermediate resistant to the hydrolysis, disabling the enzyme to return into its active form".* Among all diazaborines tested so far, compound **54** is not the only one to incorporate a 4-methyl group. The diazaborine 55 also embodies this functionality but still miss any biological

response. The difference of activity between molecules **54** and **55** (respectively 2.5 μM and >100μM) maybe sit in the double presence of the N-phenyl and the 4-methyl groups, which together afford an effective protection from the hydrolysis (Figure 91). The Figure 91 a is the optimized structure of the compound **55** in to the active site of HNE, the methyl group and the diazo moiety seems also to close the entrance of the S1 pocket. Differently from the docking model, in the reality, the protein and the molecule are dynamic entities and a certain degree of rotation, along the bond Ar---$C(CH_3)NN_2H$ that allows alternative conformations with reduced steric hindrance, should be taken in count. In compound **54** the π-π interaction between the N-phenyl group and the his 57 may prevent or limit possible rotations along the Ar---$C(CH_3)NN_2Ph$ bond, conferring a certain degree of structural rigidity, which in turn, enhance the protective hindrance from hydrolysis , provided by the 4-methyl group.

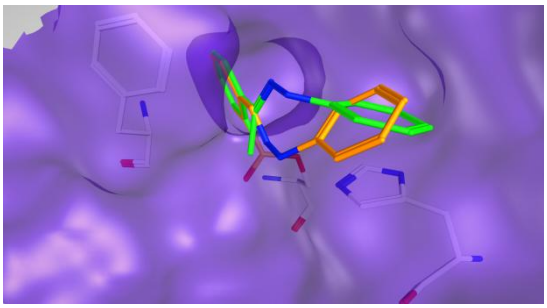

Figure 90 – Overlapped structures of compounds 52 and 54.

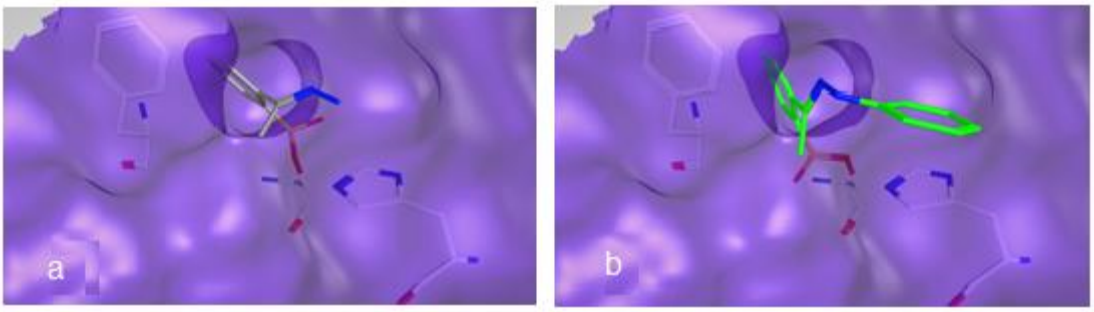

Figure 91 – Comparison between molecules 54 and 55.

5.2 Conclusion

Despite the exploitation of diazaborine as new inhibitor of HNE is still in a preliminary phase we shown that this class of compounds can offer, under the synthetic point of view, an easily accessible scaffold able to modulate the HNE activity. Nevertheless further experiments are required either to enlighten the pharmacokynetic and pharmacodynamic of this family of molecules and also to continue exploring the functionalization process that can improve the activity of diazaborines as inhibitor of HNE.

6.Conclusion

In conclusion, with the synthesis of the tricycle heteroatoms, the bicycle heteroatoms and the diazaborine collections, we demonstrate the efficiency of the Boron tether strategy as alternative route to discovery new hit compounds and evolve the optimization toward lead compounds. The Boronate tether strategy fall inside the groove already tracked by the combinatorial chemistry, representing a specific section of this relatively new branch of chemistry. The boron tether strategy rapresent an intriguing tool a disposal of the chemists, in which the main strong points of this alternative synthetic approach are: a more logical employment of the resources, through a high atom economy, exploiting in many cases of environmental friendly solvents, such as water and ethanol, and a more economic approach made of easy purification procedures. The boron tether strategy represent one of the many branches of chemistry, which with the aforementioned characteristics try to better respond to the nowadays resource waste and ecological needs.

7. Experimental

7.1 General Remarks

Tetrahydrofuran (THF) was distilled over calcium hydride/benzophenone immediately prior to use and ethyl acetate was distilled over potassium carbonate. All reactions were performed in oven-dried glassware under argon. Methanol and ethanol as reaction solvents were used as distilled. All the other superior alcohols used were analytical grade. The aldehydes, boronic acids and L-proline were purchased from Aldrich and used without further purification. Flash chromatography was carried out on silica gel 60 M Merck (Ref.107734). Reaction mixtures were analyzed by TLC using F254 from Merck (Ref. 105554, silica gel 60), and visualization of TLC spots was effected using UV and phosphomolybdic acid solution. Proton nuclear magnetic resonance spectra (1H NMR) were recorded on Bruker AMX 400 spectrophotometer with CDCl3 as solvent. Chemical shifts for 1H NMR spectra are reported as δ in units of parts per million (ppm) downfield from SiMe4 (δ 0.0) and relative to the signal of chloroform (δ 7.26, singlet). Multiplicities are given as: s (singlet), d (doublet), t (triplet), q (quartet), dd (double of doublet), td (triplet of doublets) or m (multiplets). The number of protons (n) for a given resonance is indicated by nH. Coupling constants are reported as a J value in Hertz. Carbon nuclear magnetic resonance spectra (13C NMR) are reported as δ in units of parts per million (ppm) downfield from SiMe4 (δ 0.0) and relative to the signal of chloroform (δ 77.16, triplet). The diastereomeric excess was determined based on the 1H integration of the acetal moiety proton. Infrared spectra (IR) spectra were recorded with FTIR spectrometer as thinly dispersed films.

7.2 Preparation and characterization of boronate heterocycles

General Procedure for Preparation of fused tricycle boronate heterocycles collection using alcohol as a solvent

A round bottom flask equipped with a magnetic stirrer was charged with proline (2.0 eq), glycolaldehyde dimer (1.5eq), boronic acid (0,206 mmol) and the corresponding alcohol (2.0 ml). This suspension was stirred at 60 °C for 1 h. The reaction mixture was concentrated under reduced pressure to 1 ml. The obtained residue was purified through silica flash chromatography eluted with gradient AcOEt/Hexane (3.5:1.5);(4:1).

General Procedure for Preparation of fused tricycle boronate heterocycles collection using alcohol as a reactant

A round bottom flask equipped with a magnetic stirrer was charged with proline (2.0 eq), glycolaldehyde dimer (1.5eq), boronic acid (0,206 mmol), the corresponding alcohol (10 eq) and THF (2.0 ml). This suspension was stirred at 60 °C for 1 h. The reaction mixture was concentrated under reduced pressure to 1 ml. The obtained residue was purified through silica flash chromatography eluted with gradient AcOEt/Hexane (3.5:1.5);(4:1).

General Procedure for Preparation of fused bicycle boronate heterocycles collection using alcohol as a reactant

A round bottom flask equipped with a magnetic stirrer was charged with amino acid (2.0 equiv.), aldehyde (1.5 equiv.) and distilled water (2.0 mL). This suspension was stirred at 90ºC for 1 h after which the boronic acid (0.41 mmol) was added, the mixture was then stirred at 90ºC for 20 h. The reaction mixture, which appears as a biphasic composition of precipitate and a supernatant liquid, was filtered and the solid retained in the filter was then washed with water followed by hexane. The desired compound was recovered with dichloromethane, which was subsequently removed under reduced pressure.

General Procedure for Preparation of 1 hydroxy 2,3,1 benzodiazaborine collection

A round bottom flask equipped with a magnetic stirrer was charged with the boronic acid (1.0 equiv.), hydrazine (1.0 equiv.) and the methanol (2.0 ml). This suspension was stirred at RT, *18h in the* ***procedure A***, *72h in the* ***procedure B***. After the appropriate amount of time, the reaction was quenched with 6ml of a mixture of water and ice, in order to promote the precipitation of the product, stirred for few minutes, and stored overnight into the refrigerator to complete the precipitation process. The mixture of surnatant and precipitate was filtered, the solid onto the filter washed with few ml of fresh water, followed by few ml of hexane. The product was recovered from the filter through dissolution with DCM, the residuals of water were eliminated by sodium sulfate anhydrous. The resulted dry solution free of the drying agent sodium sulfate was evaporated through the rotavapor, the residual traces of solvent were removed by high vacuum pomp.

Compounds Characterization

Compound 1

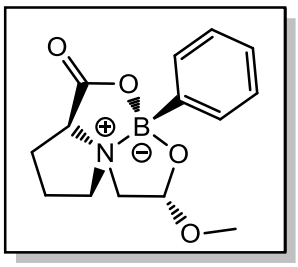

Isolated yield = 95% ***de* =** 94% (flash chromatography eluent AcOEt\Hexane)

$[\alpha]_D^{20°}$= + 5.35 (c 2, $CHCl_3$)

IR (film): ν_{max} (cm^{-1}): 3053, 2976, 2926, 2362, 2328, 1747, 1732, 1651, 1633 1456, 1435.

^{1}H NMR (400 MHz, $CDCl_3$, 25 °C, TMS): δ =1,37-1.48 (m, 1H, $NCHCH_2CH_2$), 1.55-1.62 (m, 1H, $NCHCH_2CH_2$),2.11-2,22 (m, 1H, $NCH_2CH_2CH_2$), 2.29-2,33 (m, 1H, $NCH_2CH_2CH_2$), 2.64 (dt, *J* = 11.4, 6.0 Hz,1H, $NCHCH_2CH_2CH_2$), 2.96 (dd, *J* = 10.1, 6.5 Hz, 1H, $NCHCH_2CH_2CH_2$), 3.15 (dd, *J* = 11.8, 3.7 Hz, 1H, $NBOCHCH_2$), 3.27 (d, *J* = 11.8 Hz, 1H, $NBOCHCH_2$), 3.32 (s, 3H, $CHOCH_3$), 4.17 (d, *J* = 8.7 Hz, 1H, $NCH_2CH_2CH_2CH$), 5.22 (d, *J* = 3.6 Hz, 1H, NBOCH), 7.21-7.29 (m, 3H, C_6H_5), 7.46-7.49 (m, 2H, C_6H_5).

^{13}C NMR (100 MHz, $CDCl_3$, 25 °C): δ = 23.95($NCHCH_2CH_2$), 29.88($NCH_2CH_2CH_2$), 54.09($BOCHOCH_3$), 59.83 ($NCHCH_2CH_2CH_2$), 65.76 ($NBOCHCH_2$), 72.46 ($NCH_2CH_2CH_2CH$), 99.76 (NBOCH), 127.73, 128.72, 132.79 (C_6H_5), 174,25(C=O).

^{11}B NMR(300 MHz, $CDCl_3$, 25°C): δ = 12.83

HMRS (ESI):*m*/*z* calculated $[M+Na]^+$ = 298.122363, found $[M+Na]^+$ = 298.120816.

Compound 1 prepared in THF experiment

Isolated yield = 88% ***de***= 88%(flash chromatography eluent AcOEt\Hexane)

^{1}H NMR (400 MHz, $CDCl_3$, 25 °C, TMS): δ =1,35-1.48 (m, 1H, $NCHCH_2CH_2$), 1.55-1.62 (m, 1H, $NCHCH_2CH_2$),2.11-2,25 (m, 1H, $NCH_2CH_2CH_2$), 2.31 (dd, J = 12.9, 6.6 Hz, 1H, $NCH_2CH_2CH_2$), 2.61-2.68 (m, 1H, $NCHCH_2CH_2CH_2$), 2.94-2.98 (m, 1H, $NCHCH_2CH_2CH_2$), 3.15 (dd, J = 11.8, 3.7 Hz, 1H, $NBOCHCH_2$), 3.27 (d, *J* = 11.8 Hz, 1H, $NBOCHCH_2$), 3.32 (s, 3H, $CHOCH_3$), 4.17 (d, J = 8.7 Hz, 1H, $NCH_2CH_2CH_2CH$), 5.22 (d, J = 3.6 Hz, 1H, NBOCH), 7.24-7.26 (m, 3H, C_6H_5), 7.46-7.49 (m, 2H, C_6H_5).

Compound 2 a

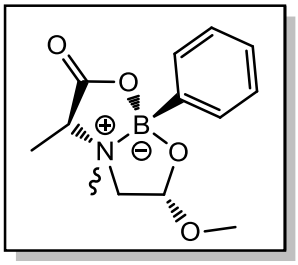

Isolated yield = 40% (flash chromatography eluent AcOEt\Hexane)

$[\alpha]_D^{20°}$= +2 (c 1.8, $CHCl_3$)

IR (film):$\tilde{\nu}$ max = 3053, 2985, 2918, 2835, 2684, 2304, 1747, 1600, 1651, 1458, 1421cm^{-1}

^{1}H NMR (400 MHz, $CDCl_3$, 25 °C, TMS):δ = 1.49 (d, J = 7.1 Hz, 3H, NCHC*H*$_3$),2.54 (s, 3H, NC*H*$_3$), 2.97 (d, J = 12.5 Hz, 1H, NC*H*$_2$), 3.24-3.34 (m, 1H, NC*H*$_2$), 3.54-3.59 (m, 1H, NC*H*), 3.59 (s, 3H, CHOC*H*$_3$), 5.27 (d, J = 4.9 Hz, 1H, NBOC*H*), 7.33-7.38 (m, 3H, C_6H_5), 7.54-7.57 (m, 2H, C_6H_5).

^{13}C NMR (100 MHz, $CDCl_3$, 25 °C): δ = 8.85(NCH*C*H$_3$), 44.81 (CHO*C*H$_3$), 54.80 (N*C*H$_3$), 59.23 (N*C*H$_2$), 65.61 (N*C*H), 100.36 (NBO*C*H), 127.76, 128.77,132.83 (C_6H_5), 170.86 (*C*=O).

^{11}B NMR (300 MHz, $CDCl_3$, 25°C): δ = 11.68

HMRS (ESI):*m*/*z* calculated $[M+Na]^+$ =286.122345, found $[M+Na]^+$ = 286.121857

Compound 2 b, 2 c

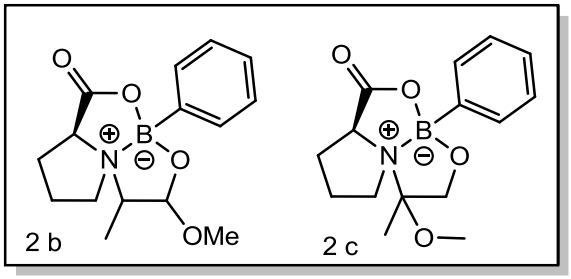

Isolated yield = 50% as mixture of two position isomers (flash chromatography eluent AcOEt\Hexane)

IR (film): $\tilde{\nu}$ max = 3053, 2976, 2926, 2362, 2328, 1747, 1732, 1651, 1633 1456, 1435 cm^{-}

Compound 2b

^{13}C NMR (100 MHz, $CDCl_3$, 25 °C): δ = 17.97 ($NCHCH_3$), 23.28 ($NCHCH_2CH_2$), 30.47 ($NCH_2CH_2CH_2$), 54.17 ($BOCHOCH_3$), 57.19 ($NCHCH_2CH_2CH_2$), 66.46 ($NCH_2CH_2CH_2CH$), 72.35 (NBOCHCH), 101.07 (NBOCH), 127.68, 127.75, 127.80, 127.90, 128.66, 128.68, 128.69, 129.01, 132.72, 138.82, 132.85, 135.06 (C_6H_5, peaks of the two position isomers), 174.33, 174.36 (C=O, peaks of the two position isomers).

Compound 2c

^{13}C NMR (100 MHz, $CDCl_3$, 25 °C): δ = 20.77 ($NCCH_3$), 23.74 ($NCHCH_2CH_2$), 29.98 ($NCH_2CH_2CH_2$), 48.28 ($NCOCH_3$), 59.92 ($NCHCH_2CH_2CH_2$), 63.90 ($NCH_2CH_2CH_2CH$), 72.35 ($NBOCH_2$), 103.05 (NC), 127.68, 127.75, 127.80, 127.90, 128.66, 128.68, 128.69, 129.01, 132.72, 138.82, 132.85, 135.06 (C_6H_5, peaks of the two position isomers), 174.33, 174.36 (C=O, peaks of the two position isomers).

HMRS (ESI): *m/z* calculated $[M+Na]^+$ = 312.138030, found $[M+Na]^+$ = 312.137595

Compound 3

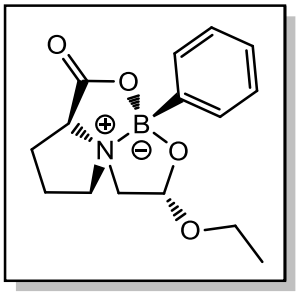

Isolated yield = 89% ***de*** = 93% (flash chromatography eluent AcOEt\Hexane)

IR (film): ν_{max} (cm^{-1}): 3053, 2958, 2924, 2304, 1743, 1734, 1598, 1458.

$[\alpha]_D^{20°}$= +4.1 (c 1.2, $CHCl_3$)

^{1}H NMR (400 MHz, $CDCl_3$, 25 °C, TMS): δ = 1.21 (t, *J* = 7.1 Hz, 3H, $BOCHOCH_2CH_3$), 1.46-1.59 (m, 1H, $NCHCH_2CH_2$), 1,66-1,72 (m, 1H, $NCHCH_2CH_2$), 2.18-2.32 (m, 1H, $NCH_2CH_2CH_2$), 2.43 (dd, *J* = 13.1, 6.6 Hz, 1H, $NCH_2CH_2CH_2$), 2.69-2.80 (m, 1H, $NCHCH_2CH_2CH_2$), 3.08 (dd, *J* = 10.4,6.3 Hz, 1H, $NCHCH_2CH_2CH_2$), 3.26 (dd, *J* = 11.6, 3.7 Hz, 1H, $NBOCHCH_2$), 3.36 (d, *J* = 11.6 Hz, 1H, $NBOCHCH_2$), 3.43-3.54 (m, 1H, $BOCHOCH_2$), 3.92 (dq, *J* = 9.4, 7.1 Hz, 1H, $BOCHOCH_2$), 4.32 (dd, *J* = 10.3, 1.5 Hz, 1H, $NCH_2CH_2CH_2CH$), 5.43 (d, *J* = 3.6 Hz, 1H, NBOCH), 7.32-7.38 (m, 3H, C_6H_5), 7.58 (dd, J = 6.4, 2.9 Hz, 2H, C_6H_5).

^{13}C NMR (100 MHz, $CDCl_3$, 25 °C): 14.97 ($BOCHOCH_2CH_3$), 23.95 ($NCHCH_2CH_2$), 29.91 ($NCH_2CH_2CH_2$), 59.84 ($NCHCH_2CH_2CH_2$), 62.19 ($BOCHOCH_2$), 65.88 ($NBOCHCH_2$), 72.52 ($NCH_2CH_2CH_2CH$), 98.34 (NBOCH), 127.73, 128.70, 132.80 (C_6H_5), 174.28 (*C*=O).

^{11}B NMR (300 MHz, $CDCl_3$, 25°C): δ = 13.96

HMRS (ESI): *m*/*z* calculated $[M+Na]^+$ = 312.138030, found $[M+Na]^+$ = 312.136847.

Compound 4

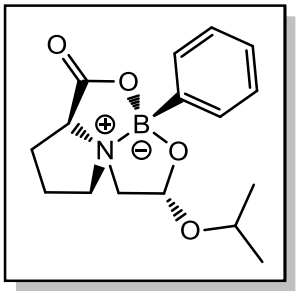

Isolated yield = 72% ***de*** = 85% (flash chromatography eluent AcOEt\Hexane)

IR (film): ν_{max} (cm^{-1}): 3053, 2974, 2927, 2360, 2330, 1743, 1598, 1458, 1435.

$[\alpha]_D^{20°}$ = + 3.12 (c 1.6, $CHCl_3$)

^{1}H NMR (400 MHz, $CDCl_3$, 25 °C, TMS):δ = 1.07 (d, *J* = 6.1 Hz, 3H, BOCHOCH(CH_3)$_2$), 1.12 (d, *J* = 6.3 Hz, 3H, BOCHOCH(CH_3)$_2$), 1.37-1.49 (m, 1H, NCHCH$_2$CH_2), 1.60 (dt, *J* = 12.1, 6.0 Hz, 1H, NCHCH$_2$CH_2), 2.17-2.21 (m, 1H, NCH$_2$CH$_2$CH_2), 2.36 (dd, J = 13.1, 6.4 Hz, 1H, NCH$_2$CH$_2$CH_2), 2.58-2.70 (m, 1H, NCHCH$_2$CH$_2$CH_2), 3.00 (dd, *J* = 10.5, 6.2 Hz, 1H, NCHCH$_2$CH$_2$CH_2), 3.17 (dd, *J* = 11.6, 3.7 Hz, 1H, NBOCHCH_2), 3.24 (d, *J* = 11.6 Hz, 1H, NBOCHCH_2), 4.06 (dt, *J* = 12.3, 6.2 Hz, 1H, BOCHOC*H*), 4.26 (dd, *J* = 10.3, 1.5 Hz, 1H, NCH$_2$CH$_2$CH$_2$C*H*), 5.46 (d, *J* = 3.6 Hz, 1H, NBOC*H*), 7.25-7.26 (m, 3H, C_6H_5), 7.48 (dt, *J* = 6.9, 3.3 Hz, 2H, C_6H_5).

^{13}C NMR (100 MHz, $CDCl_3$, 25 °C): δ = 20.72, 23,21 (BOCHOCH(CH_3)$_2$), 23,96 (NCHCH$_2$*C*H$_2$), 29.75 (NCH$_2$CH$_2$*C*H$_2$), 59.94 (NCHCH$_2$CH$_2$*C*H$_2$), 66.02 (NBOCH*C*H$_2$), 67.73 (BOCHO*C*H), 72.74 (NCH$_2$CH$_2$CH$_2$*C*H), 96.10 (NBO*C*H), 127.73, 128.67, 132.81 (*C*$_6$H$_5$), 174.43 (*C*=O).

^{11}B NMR (300 MHz, $CDCl_3$, 25°C): δ = 12.95

HMRS (ESI): *m*/*z* calculated $[M+Na]^+$ = 326.153698, found $[M+Na]^+$ = 326.152009.

Compound 5

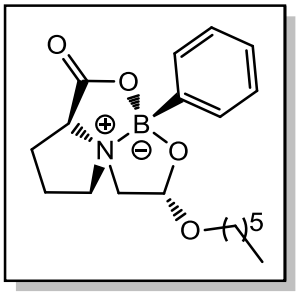

Isolated yield = 69% ***de***= 92% (flash chromatography eluent AcOEt\Hexane)

IR (film): ν_{max} (cm^{-1}): 3051, 2954, 2931, 2358, 2341, 1747, 1687, 1458, 1435.

$[\alpha]_D^{20°}$= + 6.5 (c 0.2, $CHCl_3$)

^{1}H NMR (400 MHz, $CDCl_3$, 25 °C, TMS): δ = 0.75-0.85 (m, 3H, $BOCHO(CH_2)_5CH_3$), 1.18-1.54 (m, 8H, $BOCHOCH_2(CH_2)_4CH_3$), 1.57-1.63 (m, 2H, $NCHCH_2CH_2$), 2,11-2,22 (m, 1H, $NCH_2CH_2CH_2$) 2.33-2,38 (m, 1H, $NCH_2CH_2CH_2$), 2.61-2,69 (m, 1H, $NCHCH_2CH_2CH_2$) 2.99 (dd, *J* = 10.5, 6.1 Hz, 1H, $NCHCH_2CH_2CH_2$), 3.17 (dd, *J* = 11.7, 3.8 Hz, 1H, $NBOCHCH_2$) 3.26-3.36 (s, 2H, $NBOCHCH_2$, $BOCHOCH_2$, overlapped), 3.75-3.80 (m, 1H, $BOCHOCH_2$), 4.23 (dd, *J* = 10.2, 1.5 Hz, 1H, $NCH_2CH_2CH_2CH$), 5.33 (d, *J* = 3.7 Hz, 1H, NBOCH), 7.16-7.33 (m, 3H, C_6H_5), 7.48-7.50 (m, 2H, C_6H_5).

^{13}C NMR (100 MHz, $CDCl_3$, 25 °C): δ = 14.09 ($BOCHO(CH_2)_5CH_3$), 22.61 ($BOCHO(CH_2)_4CH_2CH_3$), 23.98 ($NCHCH_2CH_2$), 25.84 ($BOCHO(CH_2)_3CH_2CH_2CH_3$), 29.31 ($BOCHO(CH_2)_2CH_2(CH_2)_2CH_3$), 29.90 ($NCH_2CH_2CH_2$), 31.64 ($BOCHOCH_2CH_2(CH_2)_3CH_3$), 59.86 ($NCHCH_2CH_2CH_2$), 65.88 ($NBOCHCH_2$), 67.05 ($BOCHOCH_2(CH_2)_4CH_3$), 72.49 ($NCH_2CH_2CH_2CH$), 98.63 (NBOCH), 127.72, 128.67, 132.79 (C_6H_5), 174.08 (C=O).

HMRS (ESI): *m*/*z* calculated $[M+Na]^+$ = 368.200699, found $[M+Na]^+$ = 368.200393.

Compound 6

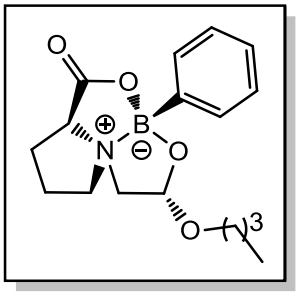

Isolated yield = 60% ***de*** = 96% (flash chromatography eluent AcOEt\Hexane)

IR (film): ν_{max} (cm^{-1}): 3051, 2958, 2931, 2360, 2341,1747, 1687, 1458, 1435.

$[\alpha]_D^{20°}$ = + 2 (c 0.2, $CHCl_3$)

^{1}H NMR (400 MHz, $CDCl_3$, 25 °C, TMS): δ = 0.83 (t, *J* = 7.4 Hz, 3H, $BOCHO(CH_2)_3CH_3$), 1.26 (dq, *J* = 14.8, 7.4 Hz, 2H, $BOCHO(CH_2)_2CH_2CH_3$), 1.34-1.53 (m, 3H, $BOCHOCH_2CH_2CH_2CH_3$, $NCHCH_2CH_2$ overlapped) 1.56-1.62 (m, 1H, $NCHCH_2CH_2$), 2,10-2,22 (m, 1H, $NCH_2CH_2CH_2$) 2.34 (dd, *J* = 13.1, 6.5 Hz, 1H, $NCH_2CH_2CH_2$), 2.64 (td, *J* = 12.2, 10.8, 5.5 Hz, 1H, $NCHCH_2CH_2CH_2$), 2.97 (dd, *J* = 10.5, 6.3 Hz, 1H, $NCHCH_2CH_2CH_2$), 3.15 (dd, *J* = 11.7, 3.8 Hz, 1H, $NBOCHCH_2$), 3.26 (d, *J* = 11.7 Hz, 1H, $NBOCHCH_2$), 3.32 (dt, J = 9.6, 6.7 Hz, 1H, $BOCHOCH_2$), 3.77 (dt, *J* = 9.4, 6.7 Hz, 1H, $BOCHOCH_2$), 4.22 (dd, *J* = 10.3, 1.6 Hz, 1H, $NCH_2CH_2CH_2CH$), 5.32 (d, *J* = 3.7 Hz, 1H, NBOC*H*),7.24-7.27 (m, 3H, C_6H_5) 7.46-7.49 (m, 2H, C_6H_5).

^{13}C NMR (100 MHz, $CDCl_3$, 25 °C): δ = 13.90 ($BOCHO(CH_2)_3CH_3$), 19.35 ($BOCHO(CH_2)_2CH_2CH_3$), 23.97 ($NCHCH_2CH_2$), 29.87 ($NCH_2CH_2CH_2$), 31.49 ($BOCHOCH_2CH_2CH_2CH_3$), 59.84 ($NCHCH_2CH_2CH_2$), 65.85 ($NBOCHCH_2$), 66.74 ($BOCHOCH_2$), 72.47 ($NCH_2CH_2CH_2CH$), 98.70 (NBOCH), 127.71, 128.67, 132.78 (C_6H_5), 174.10 (*C*=O).

HMRS (ESI): *m*/*z* calculated $[M+Na]^+$ = 340.169365, found $[M+Na]^+$ = 340.168926.

Compound 7

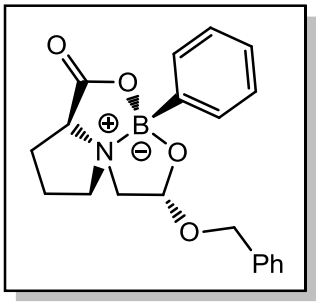

Isolated yield = 78% ***de***= 89% (flash chromatography eluent AcOEt\Hexane)

IR (film): ν_{max} (cm^{-1}): 3053, 2958, 2926, 2370, 2330, 2310,1743, 1629, 1598 1452, 1435.

$[\alpha]_D^{20^\circ}$ = + 7.5 (c 2.2, $CHCl_3$)

^{1}H NMR (400 MHz, $CDCl_3$, 25 °C, TMS): δ = 1.33-1.46 (m, 1H, $NCHCH_2CH_2CH_2$), 1.52-1.59 (m, 1H, $NCHCH_2CH_2CH_2$), 2.05-2.15 (m, 1H, $NCH_2CH_2CH_2CH_2$), 2.29 (dd, *J* = 12.8, 6.1 Hz, 1H, $NCH_2CH_2CH_2CH_2$), 2.57-2.64 (m, 1H, $NCHCH_2CH_2CH_2CH_2$), 2.87-3.03 (m, 1H, $NCHCH_2CH_2CH_2CH_2$), 3.12 (d, *J* = 11.7 Hz, 1H, $NBOCHCH_2$), 3.26 (d, *J* = 11.8 Hz, 1H, $NBOCHCH_2$), 4.21 (d, *J* = 10.2 Hz, 1H, $NCH_2CH_2CH_2CH$), 4.36 (d, *J* = 11.3 Hz, 1H, $BOCHOCH_2$), 4.77 (d, *J* = 11.3 Hz, 1H, $BOCHOCH_2$), 5.38 (s, 1H, NBOCH), 7.26 (s, 8H, C_6H_5), 7.48 (s, 2H, C_6H_5).

^{13}C NMR (100 MHz, $CDCl_3$, 25 °C): δ = 22.92 ($NCHCH_2CH_2CH_2$), 28.82 ($NCH_2CH_2CH_2CH_2$), 58.71 ($NCHCH_2CH_2CH_2CH_2$), 64.66 ($NBOCHCH_2CH_2$), 67.42 ($BOCHOCH_2CH_2$), 71.28 ($NCH_2CH_2CH_2CH$), 97.08 (NBOCH), 126.73, 126.82, 127.43, 127.47, 127.66, 127.73, 131.77 (C_6H_5), 173.11 (C=O).

^{11}B NMR (300 MHz, $CDCl_3$, 25°C): δ = 13.14

HMRS (ESI): *m*/*z* calculated $[M+Na]^+$ = 374.153766, found $[M+Na]^+$ = 374.152043.

Compound 8

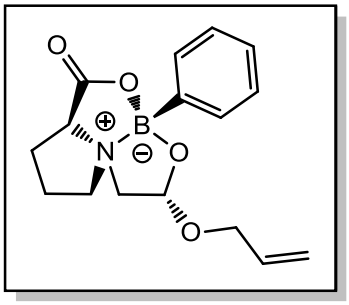

Isolated yield = 88% ***de*** > 97% (flash chromatography eluent AcOEt\Hexane)

IR (film): ν_{max} (cm^{-1}): 3051, 2958, 2929, 2358, 2322, 1747, 1732, 1645, 1598, 1452, 1435.

$[\alpha]_D^{20°}$= +3.9 (c 2.8, $CHCl_3$)

^{1}H NMR (400 MHz, $CDCl_3$, 25 °C, TMS): δ = 1.45-1.54 (m, 1H, $NCHCH_2CH_2$), 1.63-1.69 (m, 1H, $NCHCH_2CH_2$), 2,19-2.30 (m, 1H, $NCH_2CH_2CH_2$), 2.36-2.41 (m, 1H, $NCH_2CH_2CH_2$), 2.69-2.76 (m, 1H, $NCHCH_2CH_2CH_2$), 3.03 (dd, *J* = 10.0, 6.0 Hz, 1H, $NCHCH_2CH_2CH_2$), 3.24 (dd, *J* = 11.8, 3.8 Hz, 1H, $NBOCHCH_2$), 3.38 (d, *J* = 11.8 Hz, 1H, $NBOCHCH_2$), 3.99 (dd, *J* = 12.6, 6.5 Hz, 1H, $BOCHOCH_2$), 4.18-4.38 (m, 1H, $BOCHOCH_2$), 4.18-4.38 (m, 1H, $NCH_2CH_2CH_2CH$), 5.17 (d, *J* = 10.3 Hz, 1H, $BOCHOCH_2CHCH_2$), 5.27 (d, *J* = 17.2 Hz, 1H, $BOCHOCH_2CHCH_2$), 5.44 (d, *J* = 3.6 Hz, 1H, NBOCH), 5.85-5.96 (m, 1H, $BOCHOCH_2CH$), 7.32-7.33 (m, 3H, C_6H_5), 7.53-7.56 (m, 2H, C_6H_5).

^{13}C NMR (100 MHz, $CDCl_3$, 25 °C): δ = 23.95 ($NCHCH_2CH_2$), 29.88 ($NCH_2CH_2CH_2$), 59.86 ($NCHCH_2CH_2CH_2$), 65.73 ($NBOCHCH_2$), 67.25 ($BOCHOCH_3$), 72.51 ($NCH_2CH_2CH_2CH$), 97.99 (NBOCH), 117.44 ($BOCHOCH_2CHCH_2$), 127.73, 128.62, 132.81 (C_6H_5), 133.91 ($BOCHOCHCH_2$), 174.15 (C=O).

^{11}B NMR (300 MHz, $CDCl_3$, 25°C): δ = 12.98

HMRS (ESI):*m*/*z* calculated $[M+Na]^+$ = 324.138048, found $[M+Na]^+$ = 320.136345.

Compound 9

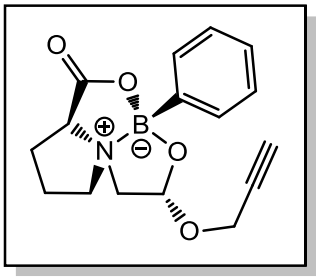

Isolated yield = 72% ***de***= 97% (flash chromatography eluent AcOEt\Hexane)

IR (film):$\tilde{\nu}$ max = 3053, 2960, 2924, 2852, 23492, 2304, 1734, 1472, 1340, 1398 cm^{-1}.

$[\alpha]_D^{20°}$= + 4.1 (c 2.4, $CHCl_3$)

^{1}H NMR (400 MHz, $CDCl_3$, 25 °C, TMS) δ = 1.48-1.60 (m, 1H, $NCHCH_2CH_2$), 1.67-1.74 (m, 1H, $NCHCH_2CH_2$), 2.22-2.32 (m, 1H, $NCH_2CH_2CH_2$), 2.42-2.50 (m, 2H, $NCH_2CH_2CH_2$, OCH_2CCH), 2.73-2.80 (m, 1H, $NCHCH_2CH_2CH_2$), 3.11 (dd, J = 10.5, 6.3 Hz, 1H, $NCHCH_2CH_2CH_2$), 3.33 (dd, J = 11.9, 3.8 Hz, 1H, $NBOCHCH_2$), 3.43 (d, J = 11.9 Hz, 1H, $NBOCHCH_2$), 4.24-4.32 (m, 1H, $NCH_2CH_2CH_2CH$), 4.33 (d, J = 2.4 Hz, 1H, $CHOCH_2$), 4.39 (d, J = 2.3 Hz, 1H, $CHOCH_2$), 5.69 (d, J = 3.7 Hz, 1H, NBOCH), 7.34-7.37 (m, 3H, C_6H_5), 7.56-7.60 (m, 2H, C_6H_5).

^{13}C NMR (100 MHz, $CDCl_3$, 25 °C): δ = 23.98 ($NCHCH_2CH_2$), 29.68 ($NCH_2CH_2CH_2$), 29.68 (OCH_2CCH), 53.07 ($OCHOCH_2$), 60.02 ($NCHCH_2CH_2CH_2$), 65.61 ($NBOCHCH_2$), 72.50 ($NCH_2CH_2CH_2CH$), 74.69 (OCH_2CCH), 78.93(OCH_2CCH), 96.77 (NBOCH), 127.77, 128.82, 132.77 (C_6H_5), 173.82 (C=O)

^{11}B NMR (300 MHz, $CDCl_3$, 25°C): δ = 13.14

HMRS (ESI):*m/z* calculated $[M+Na]^+$ =322.122398, found $[M+Na]^+$ = 322.120800

Compound 10

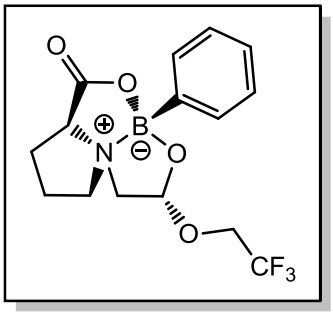

Isolated yield = 73% ***de***= 92% (flash chromatography eluent AcOEt\Hexane)

IR (film):$\tilde{\nu}$ max = 3444, 2960, 2347, 1747, 1637, 1633 1458, 1435 cm^{-1}.

$[\alpha]_D^{20°}$= +2 (c 1.8, $CHCl_3$)

^{1}**H NMR** (400 MHz, $CDCl_3$, 25 °C, TMS) δ = 1.44-1.59 (m, 1H, $NCHCH_2CH_2$), 1.68-1.75 (m, 1H, $NCHCH_2CH_2$), 2.22-2.36 (m, 1H, $NCH_2CH_2CH_2$), 2.41-2.47 (m, 1H, $NCH_2CH_2CH_2$), 2.77(td, *J* = 12.3, 10.8, 5.5 Hz, 1H, $NCHCH_2CH_2CH_2$), 3.10 (dd, *J* = 10.5, 6.3 Hz, 1H, $NCHCH_2CH_2CH_2$), 3.31 (dd, *J* = 12.2, 3.7 Hz, 1H, $NBOCHCH_2$), 3.50 (d, *J* = 12.2 Hz, 1H, $NBOCHCH_2$), 3.97-4.10 (m, 2H, $CHOCH_2$), 4.30 (dd, *J* = 10.2, 1.7 Hz, 1H, $NCH_2CH_2CH_2CH$), 5.57 (d, *J* = 3.6 Hz, 1H, NBOCH), 7.35-7.40 (m, 3H, C_6H_5), 7.53-7.56 (m, 2H, C_6H_5).

^{13}**C NMR** (100 MHz, $CDCl_3$, 25 °C): δ = 23.86 ($NCHCH_2CH_2$), 30.12 ($NCH_2CH_2CH_2$), 58.52 ($OCHCF_3$), 60.18 ($NCHCH_2CH_2CH_2$) 63.09 (q, *J* = 34,7 $OCHCF_3$), 65.38 ($NBOCHCH_2$), 72.79 ($NCH_2CH_2CH_2CH$), 99.14 (NBOCH), 127.80, 128.90, 132.86(C_6H_5), 173.48 (C=O).

^{11}**B NMR** (300 MHz, $CDCl_3$, 25°C): δ = 13.13

HMRS (ESI):*m*/*z* calculated $[M+Na]^+$ = 366.10976, found $[M+Na]^+$ = 366.10933.

Compound 11

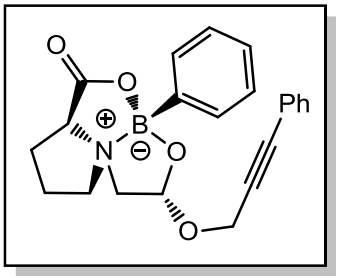

Isolated yield = 54% ***de***= 95% (flash chromatography eluent AcOEt\Hexane)

IR (film):$\tilde{\nu}$ max = 3053, 2985, 2958, 2926, 2854, 2684, 2411, 2304, 1747, 1598, 1489, 1456, 1442, 1421, 1352 1358cm^{-1}.

$[\alpha]_D^{20°}$= + 4.3 (c 1, $CHCl_3$)

^{1}H NMR (400 MHz, $CDCl_3$, 25 °C, TMS) δ = 147-1.58 (m, 1H, $NCHCH_2CH_2$), 1.62-1.77 (m, 1H, $NCHCH_2CH_2$), 2.21-2.31 (m, 1H, $NCH_2CH_2CH_2$), 2.40-2.46 (m, 1H, $NCH_2CH_2CH_2$), 2.70-2.79 (m, 1H, $NCHCH_2CH_2CH_2$), 3.06-3.11 (m, 1H, $NCHCH_2CH_2CH_2$), 3.31 (dd, J = 12.0, 3.7 Hz, 1H, $NBOCHCH_2$), 3.44 (d, J = 11.9 Hz, 1H, $NBOCHCH_2$), 4.32 (d, J = 9.0 Hz, 1H, $NCH_2CH_2CH_2CH$), 4.53 (d, J = 16.1 Hz, 1H, $BOCHOCH_2$), 4.62 (d, J = 16.0 Hz, 1H, $BOCHOCH_2$), 5.75 (d, J = 3.6 Hz, 1H, NBOCH), 7.26-7.41 (m, 6H, C_6H_5), 7.43-7.54 (m, 2H, C_6H_5), 1.57-160 (m, 2H, C_6H_5)

^{13}C NMR (100 MHz, $CDCl_3$, 25 °C): δ = 23.98 ($NCHCH_2CH_2$), 29.93 ($NCH_2CH_2CH_2$), 53.85 ($BOCHOCH_2$), 59.99 ($NCHCH_2CH_2CH_2$), 65.62 ($NBOCHCH_2$), 72.50 ($NCH_2CH_2CH_2CH$), 84.33 (CCC_6H_5), 86.36 (CCC_6H_5), 96.83 (NBOCH), 122.51,127.78 ,128.56, 131.68,132.91 (C_6H_5), 174.02 (C=O).

^{11}B NMR (300 MHz, $CDCl_3$, 25°C): δ = 11.97

HMRS (ESI):*m*/*z* calculated $[M+Na]^+$ =398.158800, found $[M+Na]^+$ = 398.152946

Compound 12

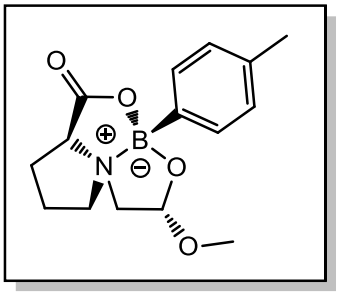

Isolated yield = 88% ***de***>97% (flash chromatography eluent AcOEt\Hexane)

IR (film): ν_{max} (cm^{-1}): 2956, 2922, 1735, 1608, 1456.

$[\alpha]_D^{20°}$ = + 7.5 (c 1, $CHCl_3$)

^{1}H NMR (400 MHz, $CDCl_3$, 25 °C, TMS): δ = 1.57 (td, *J* = 19.3, 12.8, 6.4 Hz, 1H, $NCHCH_2CH_2$), 1.64-1.76 (m, 1H, $NCHCH_2CH_2$), 2.18-2.33 (m, 1H, $NCH_2CH_2CH_2$), 2.36 (s, 3H, $C_6H_4CH_3$), 2.45 (dd, *J* = 13.2, 6.6 Hz, 1H, $NCH_2CH_2CH_2$), 2.67-2.81 (m, 1H, $NCHCH_2CH_2CH_2$), 3.12 (dd, *J* = 10.4, 6.3 Hz, 1H, $NCHCH_2CH_2CH_2$), 3.26 (dd, *J* = 11.7, 3.7 Hz, 1H, $NBOCHCH_2$), 3.36 (d, *J* = 11.7 Hz, 1H, $NBOCHCH_2$), 3.43 (s, 3H, $BOCHOCH_3$), 4.28 (dd, *J* = 10.4, 1.8 Hz, 1H, $NCH_2CH_2CH_2CH$), 5.34 (d, *J* = 3.6 Hz, 1H, NBOCH), 7.17 (d, *J* = 7.5 Hz, 2H, C_6H_4), 7.48 (d, *J* = 7.8 Hz, 2H, C_6H_4).

^{13}C NMR (100 MHz, $CDCl_3$, 25 °C): δ = 21.43 ($NCHCH_2CH_2$), 23,99 ($NCH_2CH_2CH_2$), 29,95 ($C_6H_4CH_3$), 54,09 ($BOCHOCH_3$), 59.89 ($NCHCH_2CH_2CH_2$), 65.77 ($NBOCHCH_2$), 72.42 ($NCH_2CH_2CH_2CH$), 99.63 (NBOCH),128.54 ,132.81, 138.35 (C_6H_4), 174.03 (C=O).

^{11}B NMR (300 MHz, $CDCl_3$, 25°C): δ = 12.97

HMRS (ESI): *m*/*z* calculated $[M+Na]^+$ = 312.138030, found $[M+Na]^+$ = 312.136382.

Compound 13

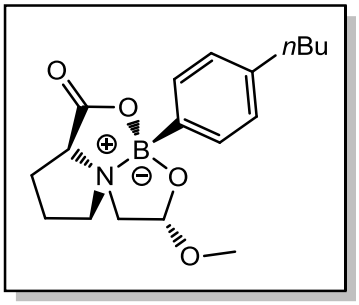

Isolated yield = 75% ***de*** = 95% (flash chromatography eluent AcOEt\Hexane)

IR (film): ν_{max} (cm^{-1}): 3053, 2956, 2929, 2684, 2304, 1743, 1734, 1598, 1458.

$[\alpha]_D^{20°}$ = +3 (c 0.2, $CHCl_3$)

^{1}H NMR (400 MHz, $CDCl_3$, 25 °C, TMS): δ = 0.84 (t, *J* = 7.3 Hz, 3H, $C_6H_4(CH_2)_3CH_3$), 1.19-1.64 1,38-1.64 (m 6H, $NCHCH_2CH_2$, $C_6H_4(CH_2)_2CH_2$, $C_6H_4CH_2CH_2$ overlapped), 2.11–2.21 (m, 1H, $NCH_2CH_2CH_2$), 2.25-2.38 (m, 1H, $NCH_2CH_2CH_2$), 2.44-2.57 (m, 2H, $C_6H_4\,CH_2$), 2.60-2,67(m, 1H, $NCHCH_2CH_2CH_2$), 2,97-3.01 (m, 1H, $NCHCH_2CH_2CH_2$), 3.13 (dd, *J* = 11.8, 3.4 Hz, 1H, $NBOCHCH_2$), 3.25 (d, *J* = 11.8 Hz, 1H, $NBOCHCH_2$), 3.31 (s, 3H, $NBOCHOCH_3$), 4.16 (d, *J* = 10.2 Hz, 1H, $NCH_2CH_2CH_2CH$), 5.21 (d, *J* = 2.8 Hz, 1H, NBOCH), 7.07 (d, *J* = 7.7 Hz, 2H, C_6H_4), 7.37 (d, *J* = 7.6 Hz, 2H, C_6H_4).Relevant peaks from minor diastereoisomer: 6.66-6.68; 6.91-6.93.

^{13}C NMR (100 MHz, $CDCl_3$, 25 °C): δ = 13.93 ($C_6H_4(CH_2)_3CH_3$), 22,28 ($C_6H_4(CH_2)_2CH_2$), 23.97 ($NCHCH_2CH_2$), 29.89 ($NCH_2CH_2CH_2$), 33.60 ($C_6H_4CH_2CH_2$), 35.60 ($C_6H_4CH_2$), 54.04 ($BOCHOCH_3$), 59.83 ($NCHCH_2CH_2CH_2$), 65.69 ($NBOCHCH_2$), 72.42 ($NCH_2CH_2CH_2CH$), 99.72 (NBOCH), 127.87 132.77 143.93 (C_6H_4), 174.30 (C=O).Relevant peaks from minor diastereoisomer 115, 129.

^{11}B NMR (300 MHz, $CDCl_3$, 25°C): δ = 12.0

HMRS (ESI): *m*/*z* calculated $[M+Na]^+$ = 354.185032, found $[M+Na]^+$ = 354.182812.

Compound 14

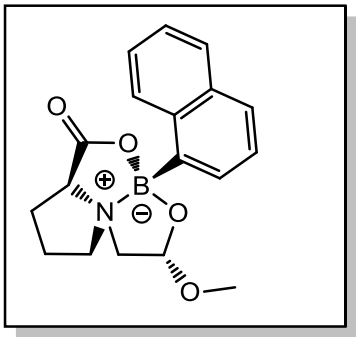

Isolated yield = 83% ***de*** = 91% (flash chromatography eluent AcOEt\Hexane)

IR (film): ν_{max} (cm^{-1}): 3051, 2956, 2927, 2308, 1745, 1627, 1595, 1456, 1344.

$[\alpha]_D^{20°}$ = + 3.3 (c 0.6, $CHCl_3$)

^{1}H NMR (400 MHz, $CDCl_3$, 25 °C, TMS): δ = 1.42-1.67 (m, 2H, $NCHCH_2CH_2CH_2$), 2.19-2.29 (m, 1H, $NCH_2CH_2CH_2CH_2$), 2.43 (dd, *J* = 13.1 Hz, 1H, $NCH_2CH_2CH_2CH_2$), 2.68 (td, *J* = 11,5 Hz, 1H, $NCHCH_2CH_2CH_2CH_2$) 3.03 (d, *J* = 12.0 Hz, 1H, $NCHCH_2CH_2CH_2CH_2$), 3.29 (dd, *J* = 11.8 Hz, 1H, $NBOCHCH_2$), 3.37 (d, *J* = 11.8 Hz, 1H, $NBOCHCH_2$), 3.44 (s, 3H, $BOCHOCH_3$),4.30 (d, *J* = 10.1 Hz, 1H, $NCH_2CH_2CH_2CH$), 5.37 (d, *J* = 3.4 Hz, 1H, NBOCH), 7.43-7.53 (m, 2H, $C_{10}H_7$), 7.64 (d, *J* = 8.2 Hz, 1H, $C_{10}H_7$) 7.77-7.90 (m, 3H, $C_{10}H_7$) 8.10 (s, 1H, $C_{10}H_7$).

^{13}C NMR (100 MHz, $CDCl_3$, 25 °C): δ = 24.02 ($NCHCH_2CH_2$), 29.1 ($NCH_2CH_2CH_2$), 54.18 ($BOCHOCH_3$), 59.88 ($NCHCH_2CH_2CH_2$), 65.85 ($NBOCHCH_2$), 71.57 ($NCH_2CH_2CH_2CH$), 98.87 (NBOCH), 125.57, 126.02, 127.07, 127.61, 128.31, 129.82, 132.04, 133.08, 133.83 ($C_{10}H_7$), 174.20 (C=O).

^{11}B NMR (300 MHz, $CDCl_3$, 25°C): δ = 13.71

HMRS (ESI): *m/z* calculated $[M+Na]^+$ = 348.138082, found $[M+Na]^+$ = 348.136111.

Compound15

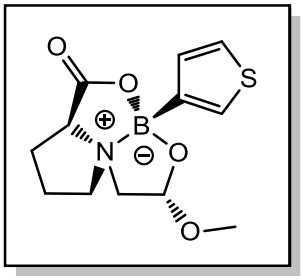

Isolated yield = 71% ***de***= 91% (flash chromatography eluent AcOEt\Hexane)

IR (film): ν_{max} (cm^{-1}): 3055, 2958, 2926, 2362, 1741, 1637, 1629, 1508, 1456.

$[\alpha]_D^{20°}$= +2.15 (c 1.9, $CHCl_3$)

^{1}H NMR (400 MHz, $CDCl_3$, 25 °C, TMS):δ = 1.41-1.53 (m, 1H, $NCHCH_2CH_2$), 1.63-1.69 (m,1H, $NCHCH_2CH_2$), 2.13-2.25 (m, 1H, $NCH_2CH_2CH_2$), 2.33 (dd, *J* = 13.1, 6.5 Hz, 1H, $NCH_2CH_2CH_2$), 2.65-2.73 (m, 1H, $NCHCH_2CH_2CH_2$), 3.03-3.08 (m, 1H, $NCHCH_2CH_2CH_2$), 3.17 (dd, *J* = 11.8, 3.7 Hz, 1H, $NBOCHCH_2$), 3.28 (d, *J* = 11.8 Hz, 1H, $NBOCHCH_2$), 3.31 (s, 3H, $BOCHOCH_3$), 4.19-4.13 (m, 1H, $NCH_2CH_2CH_2CH$), 5.18 (d, *J* = 3.5 Hz, 1H, NBOCH), 7.10 (d, *J* = 4.8 Hz, 1H, thiophenyl), 7.26 (dd, *J* = 4.5, 2.8 Hz, 1H, thiophenyl), 7.42 (d, *J* = 2.5 Hz, 1H, thiophenyl).

^{13}C NMR (100 MHz, $CDCl_3$, 25 °C): δ = 24.12 ($NCHCH_2CH_2$), 29.68 ($NCH_2CH_2CH_2$), 54.10 ($BOCHOCH_3$), 59.94 ($NCHCH_2CH_2CH_2$), 65.62 ($NBOCHCH_2$), 72.42 ($NCH_2CH_2CH_2CH$), 99.54 (NBOCH), 125.60 130.70 131.28 (thiophenyl), 173.95 (*C*=O).Relevant peaks from minor diastereoisomer: 23.08, 24.76, 29.43, 30.03, 68.26, 128,85.

^{11}B NMR (300 MHz, $CDCl_3$, 25°C): δ = 11.79

HMRS (ESI):*m*/*z* calculated $[M+Na]^+$ = 304.078754, found $[M+Na]^+$ = 304.077574.

Compound 16

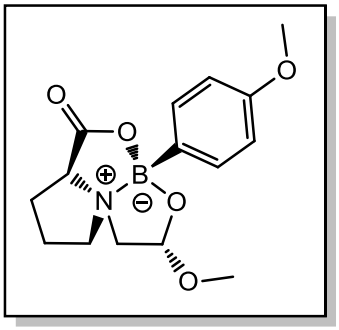

Isolated yield = 57% ***de*** = 97% (flash chromatography eluent AcOEt\Hexane)

IR (film): ν_{max} (cm^{-1}): 3053, 2974, 2927, 2360, 2343, 1743, 1450, 1435, 1340.

$[\alpha]_D^{20°}$= + 6.12 (c 0.8, $CHCl_3$)

^{1}H NMR (400 MHz, $CDCl_3$, 25 °C, TMS): δ = 1.38-1.49 (m, 1H, $NCHCH_2CH_2$), 1.58-1.64 (m, 1H, $NCHCH_2CH_2$), 2.12-2.22 (m, 1H, $NCH_2CH_2CH_2$), 2.33 (dd, *J* = 13.1, 6.5 Hz, 1H, $NCH_2CH_2CH_2$), 2.61-2.70 (m, 1H, $NCHCH_2CH_2CH_2$), 3.01 (dd, *J* = 10.2, 6.4 Hz, 1H, $NCHCH_2CH_2CH_2$), 3.15 (dd, *J* = 11.7, 3.7 Hz, 1H, $NBOCHCH_2$), 3.26 (d, *J* = 11.7 Hz, 1H, $NBOCHCH_2$), 3.31 (s, 3H, $BOCHOCH_3$), 3.74 (s, 3H, C_6H_4 OCH_3), 4.18 (d, *J* = 10.1 Hz, 1H, $NCH_2CH_2CH_2CH$), 5.22 (d, *J* = 3.7 Hz, 1H, NBOCH), 6.81 (d, *J* = 8.3 Hz, 2H, C_6H_4), 7.41 (d, *J* = 8.2 Hz, 2H, C_6H_4).

^{13}C NMR (100 MHz, $CDCl_3$, 25 °C): δ = 23.93 ($NCHCH_2CH_2$), 29.95 ($NCH_2CH_2CH_2$), 54.04 ($BOCHOCH_3$), 54.96 ($C_6H_4OCH_3$), 59.83 ($NCHCH_2CH_2CH_2$), 65.68 ($NBOCHCH_2$), 72.38 ($NCH_2CH_2CH_2CH$), 99.62 (NBOCH), 113.29, 134.16, 160.20 (C_6H_4), 174.17 (C=O).

^{11}B NMR (300 MHz, $CDCl_3$, 25°C): δ = 13.06

HMRS (ESI):*m*/*z* calculated $[M+Na]^+$ = 328.132945, found $[M+Na]^+$ = 328.131426.

Compound 17

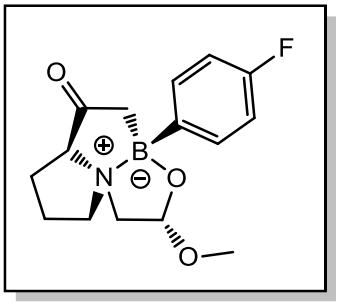

Isolated yield = 94% ***de***= 96% (flash chromatography eluent AcOEt\Hexane)

IR (film): ν_{max} (cm^{-1}): 3003, 2964, 2916, 2351, 2320, 1745, 1598, 1504, 1454.

$[\alpha]_D^{20^\circ}$ = + 6.5 (c 0.9, $CHCl_3$)

^{1}H NMR (400 MHz, $CDCl_3$, 25 °C, TMS):δ = 1.32-1.44 (m, 1H, $NCHCH_2CH_2CH_2$), 1.54-1.65 (m, 1H, $NCHCH_2CH_2CH_2$), 2.13-2.24 (m, 1H, $NCH_2CH_2CH_2CH_2$), 2.28-2.33 (m, 1H, $NCH_2CH_2CH_2CH_2$), 2.60-2.75 (m, 1H, $NCHCH_2CH_2CH_2CH_2$), 2.85-2.99 (m, 1H, $NCHCH_2CH_2CH_2CH_2$), 3.15 (dd, *J* = 11.8, 3.5 Hz, 1H, $NBOCHCH_2$), 3.27-3.31 (m, 4H, $NBOCHCH_2$, $BOCHOCH_3$ overlapped), 4.18 (d, *J* = 10.2 Hz, 1H, $NCH_2CH_2CH_2CH$), 5.21 (d, *J* = 3.1 Hz, 1H, NBOCH), 6.94 (t, *J* = 8.8 Hz, 2H, C_6H_4), 7.45 (t, *J* = 7.2 Hz, 2H, C_6H_4).

^{13}C NMR (100 MHz, $CDCl_3$, 25 °C): δ = 23.91 ($NCHCH_2CH_2CH_2$), 29.85 ($NCH_2CH_2CH_2CH_2$), 54.10 ($BOCHOCH_3$), 59.78 ($NCHCH_2CH_2CH_2CH_2$), 65.71 ($NBOCHCH_2$), 72.41 ($NCH_2CH_2CH_2CH$), 99.71 (NBOCH), 114.55, 134.67, 162.39, 163.59, 164.82 (C_6H_4), 174.03 (C=O).

^{11}B NMR (300 MHz, $CDCl_3$, 25°C): δ =12.45

HMRS (ESI): *m*/*z* calculated $[M+Na]^+$ = 316.112941, found $[M+Na]^+$ = 316.111601.

Compound 18

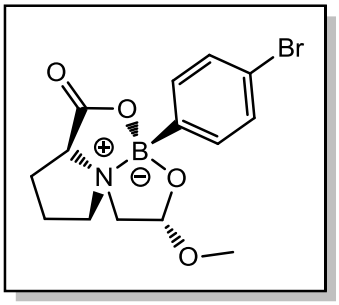

Isolated yield = 78% ***de*** = 90% (flash chromatography eluent AcOEt\Hexane)

IR (film): ν_{max} (cm^{-1}): 3051, 2956, 2926, 2362, 2322, 1743, 1602, 1581, 1458.

$[\alpha]_D^{20°}$ = + 0.4 (c 1, $CHCl_3$)

^{1}H NMR (400 MHz, $CDCl_3$, 25 °C, TMS): δ = 1.33-1.46 (m, 1H, $NCHCH_2CH_2$), 1,61-1,67 (m, 1H, $NCHCH_2CH_2$), 2.13-2.24 (m, 1H, $NCH_2CH_2CH_2$), 2.31-2.36 (m, 1H, $NCH_2CH_2CH_2$), 2.64-2.72 (m, 1H, $NCHCH_2CH_2CH_2$), 2.93-2.97 (m, 1H, $NCHCH_2CH_2CH_2$), 3.15 (dd, *J* = 11.8, 3.6 Hz, 1H, $NBOCHCH_2$) 3.29 (d, *J* = 11.8 Hz, 1H, $NBOCHCH_2$), 3.32 (s, 3H, $BOCHOCH_3$), 4.19 (d, *J* = 10.3 Hz, 1H, $NCH_2CH_2CH_2CH$), 5.22 (d, *J* = 3.5 Hz, 1H, NBOCH), 7.30-7.47 (m, 4H, C_6H_4).

^{13}C NMR (100 MHz, $CDCl_3$, 25 °C): δ = 23.99 ($NCHCH_2CH_2$), 29.88 ($NCH_2CH_2CH_2$), 54.19 ($BOCHOCH_3$), 59.87 ($NCHCH_2CH_2CH_2$), 65.81 ($NBOCHCH_2$), 72.51 ($NCH_2CH_2CH_2CH$), 99.73 (NBOCH), 123.45, 130.91, 134.57 (C_6H_4), 173.91 (C=O).

HMRS (ESI): *m/z* calculated $[M+Na]^+$ = 376.032876, found $[M+Na]^+$ = 376.031248.

Compound 19

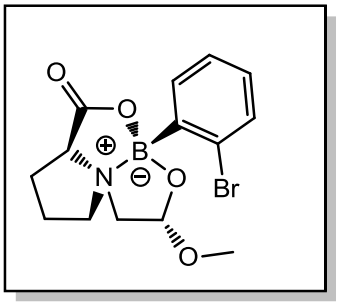

Isolated yield = 78% ***de***> 97% (flash chromatography eluent AcOEt\Hexane)

IR (film):$\tilde{\nu}$ max = 3051, 2956, 2926, 2362, 2322, 1743, 1602, 1581, 1458.

$[\alpha]_D^{20^\circ}$= + 11 (c 1, $CHCl_3$)

^{1}H NMR(400 MHz, $CDCl_3$, 25 °C, TMS): δ = 1.29-1.38 (m, 1H, $NCHCH_2CH_2$), 1.65-1.70 (m, 1H, $NCHCH_2CH_2$), 2.15-2.31 (m, 2H, $NCH_2CH_2CH_2$), 2.87 (td, *J* = 11.5, 5.4 Hz, 1H, $NCHCH_2CH_2CH_2$), 3.32 (s, 3H, $BOCHOCH_3$), 3.34 (s, 1H, $NBOCHCH_2$), 3.38-3.42 (m, 1H, $NCHCH_2CH_2CH_2$), 3.82 (dd, *J* = 11.5, 3.3 Hz, 1H, $NBOCHCH_2$), 4.09-4.21 (m, 1H, $NCH_2CH_2CH_2CH$), 5.25 (d, *J* = 3.3 Hz, 1H, NBOCH), 7.11 (t, *J* = 7.5 Hz, 1H, C_6H_4), 7.20 (t, *J* = 7.3 Hz, 1H, C_6H_4), 7.48 (d, *J* = 7.9 Hz, 1H, C_6H_4), 7.63 (d, *J* = 7.4 Hz, 1H, C_6H_4).

^{13}C NMR (100 MHz, $CDCl_3$, 25 °C): δ = 24.46 ($NCHCH_2CH_2$), 29.73 ($NCH_2CH_2CH_2$), 54.00 ($BOCHOCH_3$), 59.59 ($NCHCH_2CH_2CH_2$),66.79 ($NBOCHCH_2$), 73.73 ($NCH_2CH_2CH_2CH$), 100.32 (NBOCH), 126.72, 129.11, 130.64, 133.58, 136.52 (C_6H_4), 173.45 (C=O).

^{11}B NMR (300 MHz, $CDCl_3$, 25°C): δ = 12.33

HMRS (ESI):*m*/*z* calculated $[M+Na]^+$ = 376.032876, found $[M+Na]^+$ = 376.030680.

Compound 20

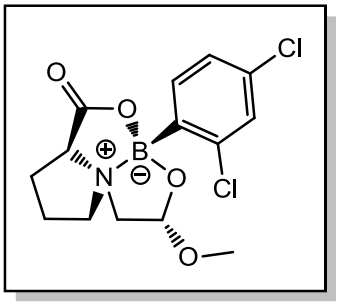

Isolated yield = 70% ***de***> 99% (flash chromatography eluent AcOEt\Hexane)

IR (film):$\tilde{\nu}$ max = 3053, 2985, 2960, 2927, 2304, 1749, 1732, 1579, 1421, 1346 cm^{-1}.

$[\alpha]_D^{20^\circ}$= + 10.27 (c 1.4, $CHCl_3$)

^{1}H NMR (400 MHz, $CDCl_3$, 25 °C, TMS) δ = 1.34-1.42 (m, 1H, $NCHCH_2CH_2$), 1.72-1.86 (m, 1H, $NCHCH_2CH_2$), 2.23-2.43 (m, 2H, $NCH_2CH_2CH_2$), 2.97 (td, J = 11.5, 5.4 Hz, 1H, $NCHCH_2CH_2CH_2$), 3.38-3.45 (m, 5H, $NCHCH_2CH_2CH_2$, $NBOCHCH_2$,$CHOCH_3$ overlapped peaks),), 3.74 (dd, J = 11.5, 3.7 Hz, 1H, $NBOCHCH_2$), 4.28 (dd, J = 9.9, 2.7 Hz, 1H, $NCH_2CH_2CH_2CH$), 5.31 (s, 1H, NBOCH), 7.17-7-30 (m, 1H, C_6H_3), 7.37 (d, J = 1.5 Hz, 1H, C_6H_3), 7.66 (d, J = 8.1 Hz, 1 H, C_6H_3).

^{13}C NMR (100 MHz, $CDCl_3$, 25 °C): δ = 24.53 ($NCHCH_2CH_2$), 29.76($NCH_2CH_2CH_2$), 54.00 ($BOCHOCH_3$), 59.56 ($NCHCH_2CH_2CH_2$), 66.42 ($NBOCHCH_2$), 73.61 ($NCH_2CH_2CH_2CH_2$), 100.15 (NBOCH), 126.53, 129.71, 135.56, 136.90, 139.61 (C_6H_3), 173.18 (C=O)

^{11}B NMR (300 MHz, $CDCl_3$, 25°C): δ = 12.07

HMRS (ESI):*m*/*z* calculated $[M+K]^+$ = 382.01835, found $[M+K]^+$ = 382.01812

Compound 21

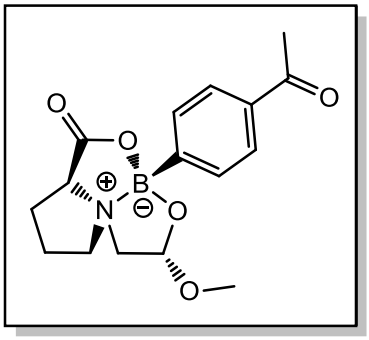

Isolated yield = 65% ***de***= 95% (flash chromatography eluent AcOEt\Hexane)

IR (film):$\tilde{\nu}$ max = 3053, 2976, 2926, 2362, 2328, 1747, 1732, 1651, 1633 1456, 1435 cm^{-1}

$[\alpha]_D^{20°}$= + 2.43 (c 2.3, $CHCl_3$)

^{1}H NMR (400 MHz, $CDCl_3$, 25 °C, TMS) δ = 1.39-1.60 (m, 1H, $NCHCH_2CH_2$), 1.67-1.77 (m, 1H, $NCHCH_2CH_2$),2.28 (m, 1H, $NCH_2CH_2CH_2$), 2.38-2.50 (m, 1H, $NCH_2CH_2CH_2$), 2.61 (s, 3H, $C_6H_4COCH_3$), 2.72-2.85 (m, 1H, $NCHCH_2CH_2CH_2$), 2.96-3.07 (m, 1H, $NCHCH_2CH_2CH_2$), 3.29 (dd, J = 11.8, 3.5 Hz, 1H, $NBOCHCH_2$), 3.36-3.45 (m, 4H, $NBOCHCH_2$, $CHOCH_3$,overlapped peaks,4.30 (d, J = 10.2 Hz, 1H, $NCH_2CH_2CH_2CH$), 5.34 (d, J = 1.8 Hz, 1H, NBOCH), 7.68(d, J = 7.0 Hz, 2H C_6H_4), 7.90-7.94 (m, 2H, C_6H_4).

^{13}C NMR (100 MHz, $CDCl_3$, 25 °C): δ = 24.01 ($NCHCH_2CH_2$), 26.73 ($C_6H_4COCH_3$), 29.85 ($NCH_2CH_2CH_2$), 54.19 ($BOCHOCH_3$), 59.85 ($NCHCH_2CH_2CH_2$), 65.91 ($NBOCHCH_2$), 72.56 ($NCH_2CH_2CH_2CH$), 99.83 (NBOCH), 127.46 (C_6H_4), 133.04 (C_6H_4), 137.33 (C_6H_4), 173.79 (CH*C*=O), 198.76 (C_6H_4CO).

HMRS (ESI):*m*/*z* calculated $[M+Na]^+$ =339.13631, found $[M+Na]^+$ = 339.13623

Compound 22

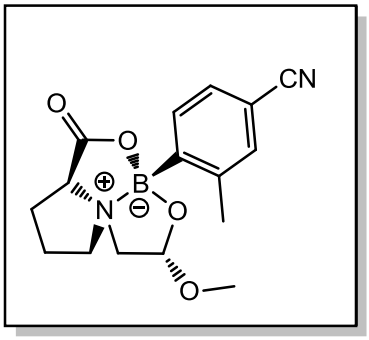

Isolated yield = 65% ***de***= 96% (flash chromatography eluent AcOEt\Hexane)

IR (film):$\tilde{\nu}$ max = 3053, 2976, 2926, 2362, 2328, 1747, 1732, 1651, 1633 1456, 1435 cm^{-1}

$[\alpha]_D^{20°}$= + 8.9 (c 1, $CHCl_3$)

^{1}H NMR (400 MHz, $CDCl_3$, 25 °C, TMS) δ = 1.34-1.45 (m, 1H, $NCHCH_2CH_2$), 1.73-1.80 (m, 1H, $NCHCH_2CH_2$), 2.27-2.42 (m, 2H, $NCH_2CH_2CH_2$), 2.51 (s, 3H, $C_6H_3CH_3$), 2.87-2.94 (m, 1H, $NCHCH_2CH_2CH_2$), 3.04-3.08 (m, 1H, $NCHCH_2CH_2CH_2$), 3.34-3.54 (m, 5H, $NBOCHCH_2$, $CHOCH_3$, overlapped signals), 4.27 (dd, J = 10.1, 2.7 Hz, 1H, $NCH_2CH_2CH_2CH$), 5.34 (d, J = 3.3 Hz, 1H, NBOCH), 7.39-7.46 (m, 2H, C_6H_3), 7.71 (d, J = 7.6 Hz, 1H, C_6H_3).

^{13}C NMR (100 MHz, $CDCl_3$, 25 °C): δ = 22.46 ($C_6H_3CH_3$), 24.40 ($NCHCH_2CH_2$), 29.72 ($NCH_2CH_2CH_2$), 54.11 ($BOCHOCH_3$), 59.63 ($NCHCH_2CH_2CH_2$), 66.62 ($NBOCHCH_2$), 73.41 ($NCH_2CH_2CH_2CH$), 99.88 (NBOCH), 112.31 (C_6H_3), 119.26 (C_6H_3CN), 128.45, 133.68, 135.04(C_6H_3), 173.18(C=O)

^{11}B NMR (300 MHz, $CDCl_3$, 25°C): δ = 12.82

HMRS (ESI):*m/z* calculated $[M+K]^+$ =353.10723, found $[M+K]^+$ = 353.10700

Compound 23

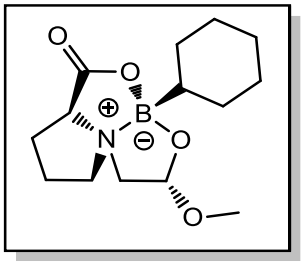

Isolated yield = 52% ***de***> 99% (flash chromatography eluent AcOEt\Hexane)

IR (film):$\tilde{\nu}$ max = 3053, 2985, 2960, 2927, 2304, 1749, 1579, 1421cm^{-1}.

[α]$_D^{20°}$= +2 (c 1, $CHCl_3$)

^{1}H NMR (400 MHz, $CDCl_3$, 25 °C, TMS) δ = 1.08-1.40 (m, 6H, C_6H_{11}), 1.52 (d, J = 11.1 Hz, 1H, C_6H_{11}), 1.64-1.80 (m, 3H, C_6H_{11}), 1.80-1.95 (m, 2H, C_6H_{11}, $NCHCH_2CH_2$, overlapped peaks), 2.00-2.07 (m, 1H, $NCHCH_2CH_2$), 2.19-2.32 (m, 1H, $NCH_2CH_2CH_2$), 2.32-2.44 (m, 1H, $NCH_2CH_2CH_2$), 2.98 (td, J = 11.0, 5.8 Hz,1H, $NCHCH_2CH_2CH_2$), 3.08 (dd, J = 11.5, 4.0 Hz, 1H, $NBOCHCH_2$), 3.28 (d, J = 11.5 Hz, 1H, $NBOCHCH_2$), 3.35 (s, 3H, $CHOCH_3$) 3.66-3.78 (m, 1H, $NCHCH_2CH_2CH_2$),4.33 (dd, J = 9.8, 2.9 Hz, 1H, $NCH_2CH_2CH_2CH$), 5.11 (d, J = 3.9 Hz, 1H, NBOCH).

^{13}C NMR (100 MHz, $CDCl_3$, 25 °C): δ = 25.14 ($NCHCH_2CH_2$), 27.05, 27.66, 27.17, 28.62, 28.99 (C_6H_{11}), 29.32 ($NCH_2CH_2CH_2$), 54.02 ($BOCHOCH_3$), 58.36 ($NCHCH_2CH_2CH_2$), 66.28 ($NBOCHCH_2$), 73.01 ($NCH_2CH_2CH_2CH$), 99.11 (NBOCH), 173.54 (C=O)

^{11}B NMR (300 MHz, $CDCl_3$, 25°C): δ = 12.50

HMRS (ESI):*m*/*z* calculated $[M+Na]^+$ =304.16931, found $[M+Na]^+$ = 304.16911

Compound 24

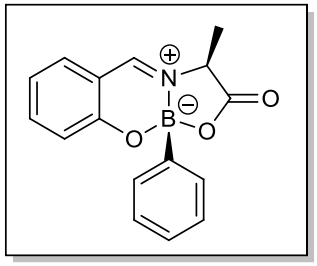

Isolated yield = 52 % *de*100%, after 20 h at 90 ºC (0.142 g).

^{1}H NMR (400 MHz, CDCl3, 25ºC, TMS): δ 1.73 (d, 3H, J = 6.8 Hz, -CHCH3), 4.62 (qd, 1H,J = 6.7, 2.3 Hz, -CHCH3), 6.93 –7.08 (m, 1H, Ar), 7.16 (d, 1H, J = 8.4 Hz, Ar), 7.20 – 7.33 (m, 3H, Ar), 7.40 (dd, 2H,J = 7.5, 1.7 Hz, Ar), 7.45 (dd, 1H,J = 7.8, 1.6 Hz, Ar), 7.55–7.71 (m, 1H, Ar), 8.17 (d, 1H, J = 2.2 Hz, Ar)

^{13}C-RMN (100MHz, CDCl3, 25ºC, TMS): δ 12.98 (-CHCH3), 58.59 (-NCHCH3-), 117.30, 120.22, 120.35, 125.83, 127.83, 128.48, 130.74, 131.60, 139.07 (Ar), 156.61 (Ar, quaternary), 159.79 (ArCHN-), 170.66 (-CHCOO-).

^{11}B NMR (300 MHz, CDCl3, 25°C): δ = 6.99

ESI+: 318, 302, 280, 122.

HMRS (EI): m/z calc. [M+] = 279.1067, found [M+] = 279.1066.

Compound 25

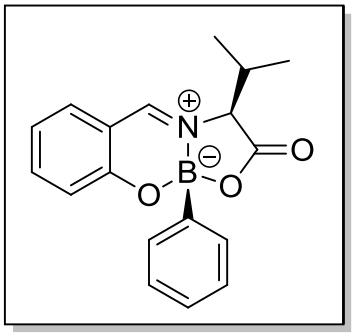

Isolated yield = **50 %***de* 100%,after 20 h at 90 ºC (0.142 g).

^{1}H NMR (400 MHz, $CDCl_3$, 25ºC, TMS): δ 1.05 (dd, 6H, *J* = 12.9, 6.4 Hz, -$CHCH_2CH(CH_3)_2$), 1.77–1.96 (m, 1H, -$CHCH_2CH(CH_3)_2$), 2.03– 2.27 (m, 2H, -$NCHCH_2CH(CH_3)_2$), 4.53 (td, 1H, *J* = 5.7, 2.3 Hz, -$NCHCH_2CH(CH_3)_2$),6.96 – 7.07 (m, 1H, Ar), 7.16 (d, 1H,*J* = 8.4 Hz, Ar), 7.21 - 7.35 (m, 4H, Ar), 7.39 (dd, 2H, *J* = 7.5, 1.8 Hz, Ar), 7.44 (dd, 1H, *J* = 7.8, 1.6 Hz,Ar), 7.62 (td, 1H, *J* = 8.7, 7.4, 1.7 Hz, Ar);

^{13}C-RMN (100MHz, $CDCl_3$, 25ºC, TMS): δ 22.50(-$CHCH_2(CH3)_2$), 22.93 (-$CHCH_2(CH3)_2$), 25.16 (-$NCHCH_2CH$-), 37.16 (-$NCHCH_2$-), 60.64 (-$NCHCH_2$ -), 117.49, 120.21, 120.27, 125.98, 127.83, 128.43, 130.89, 131.65 (Ar), 139.02 (-NCHAr-), 156.70, 159.70 (Ar, quaternary), 170.79 (-CHCOO-).

^{11}B NMR (300 MHz, $CDCl_3$, 25°C): δ = 6.73

ESI^{+}: 360, 344, 322, 274, 236

HMRS (EI): m/z calc.[M^{+}] = 321.1536, found [M^{+}] = 321.1534

Compound 26

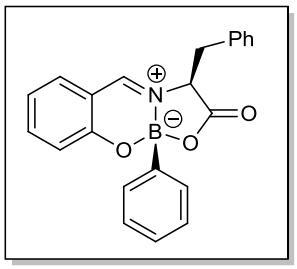

Isolated yield = 86% ***de*** 91%, after 20 h at 90ºC (0.125 g).

^{1}H NMR (400 MHz, CDCl3, 25ºC, TMS): δ 2.71 (t, 1H, *J*= 13.2, –CHC*H*$_2$Ph), 3.41 (dd, 1H, *J*=3.6, 14.0, –CHC*H*$_2$Ph), 4.34 (dd, 1H, *J*= 3.6, 12.4, –NC*H*CH2Ph), 6.87–6.95 (m, 3H, Ar), 7.02–7.05 (m, 1H, Ar), 7.11– 7.16 (m, 2H, Ar), 7.27–7.34 (m, 6H, Ar), 7.43–7.55 (m, 3H, Ar);

^{13}C-NMR (100 MHz, CDCl3, 25ºC, TMS): δ 37.73 (–CH*C*H$_2$Ph), 66.92 (–N*C*HCOCH$_2$–), 117.57, 120.19, 120.32, 127.79, 127.90, 128.58, 129.16, 129.21, 130.55, 131.45, 135.11, 139.04 (Ar), 159.95 (-N*C*HAr-), 160.43(Ar, quaternary), 170.22 (–CH*C*OO–).

^{11}B NMR (300 MHz, $CDCl_3$, 25°C): δ = 6.71

ESI^{+}: 394, 378, 356, 270, 248.

HMRS (EI): m/z calc. [M+H^{+}] = 356.1458, found [M+H^{+}] = 356.1466

Compound 27

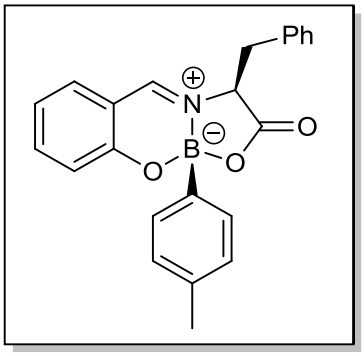

Isolated yield = 83 % yield, ***de*** 100%, after 20 h at 90 ºC (0.126 g).

^{1}H NMR (400 MHz, $CDCl_3$, 25ºC, TMS): δ 2.34 (s, 3H, -ArC*H*$_3$), 2.73 (t, 1H, *J*= 12.0, -CHC*H*$_2$Ph), 3.42 (dd, 1H, *J*= 4.0, 14.0, -CHC*H*$_2$Ph), 4.35 (dd, 1H, *J*= 4.0, 12.0, -NC*H*CH$_2$Ph), 6.91 (t, 1H, *J*= 8.0, Ar), 6.99-7.04 (m, 3H, Ar), 7.12-7.16 (m, 4H, Ar), 7.28-7.38 (m, 5H, Ar), 7.50-7.56 (m, 1H, Ar);

^{13}C-RMN (100MHz, $CDCl_3$, 25ºC, TMS): δ 21.44 (-Ar*C*H$_3$), 37.78 (-CH*C*H$_2$Ph), 66.90 (-N*C*HCH$_2$Ph-), 117.62, 120.14, 120.32, 127.80, 128.67, 129.16, 129.28, 130.61, 131.46, 135.21, 138.19, 138.94 (Ar), 159.94 (Ar, quaternary), 160.35 (Ar*C*HN-), 170.35 (-CH*C*OO-).

^{11}B NMR (300 MHz, $CDCl_3$, 25°C): δ = 6.97

ESI^{+}: 392, 370, 300, 188.

HMRS (EI): m/z calc. [M+H^{+}] = 370.1614, found [M+H^{+}] = 370.1620.

Compound 28

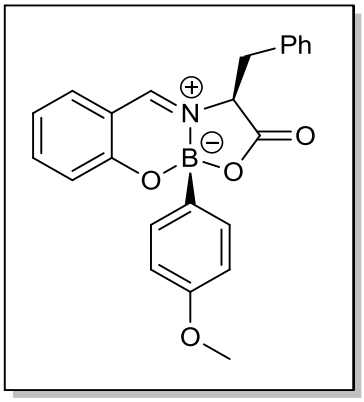

Isolated yield =**31 %** ***de*** 97%, after 20 h at 90 ºC (0.048 g)

^{1}H NMR (400 MHz, $CDCl_3$, 25ºC, TMS): δ 2.72 (t, *J*= 13.0, 1H, -CHC*H*$_2$Ph), 3.42 (dd, 1H,*J*= 3.2, 13.6, -CHC*H*$_2$Ph), 3.81 (s, 3H, -ArOC*H*$_3$), 4.34 (dd, 1H,*J*= 3.2, 12.4, -NC*H*COCH$_2$-), 6.80-7.35 (m, 14H, Ar);

^{13}C-RMN (100MHz, $CDCl_3$, 25ºC, TMS): δ 37.87 (-CH*C*H$_2$Ph), 55.04 (-ArO*C*H$_3$), 66.82 (-N*C*HCOCH$_2$-), 113.42, 117.55, 120.15, 120.27, 127.80, 129.16, 129.28, 131.48, 131.96, 135.14, 138,92 (Ar), 159.94(Ar*C*HN-), 159.98, 160.22 (Ar, quaternary), 170.42 (-CH*C*OO-).

^{11}B NMR (300 MHz, $CDCl_3$, 25°C): δ = 6.95

ESI^{+}: 408, 386, 288, 270.

HMRS (EI): m/z calc. [M+H^{+}] = 386.1564, found [M+H^{+}] = 386.1556.

Compound 29

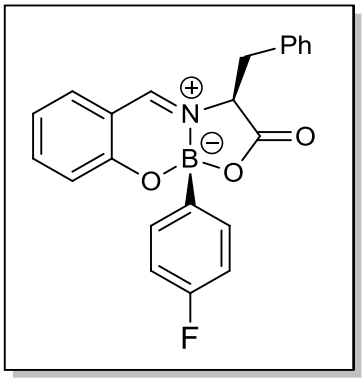

Isolated yield = 80 % ***de*** 100%, after 20 h at 90 ºC (0.122 g).

^{1}H NMR (400 MHz, $CDCl_3$, 25ºC, TMS): δ 2.68 (t, *J*= 13.2,, 1H -CHC*H*$_2$Ph), 3.45 (dd, 1H,*J*= 3.4, 13.8, -CHC*H*$_2$Ph), 4.36 (dd, 1H,*J*= 3.2, 12.4, -NC*H*CH_2Ph-), 6.80-7.71 (m, 14H, Ar);

^{13}C-RMN (100MHz, $CDCl_3$, 25ºC, TMS): δ 37.79 (-CH*C*H_2Ph), 66.87 (-N*C*HCH_2-), 114.74, 114.94, 117.47, 120.32, 120.38, 127.91, 129.16, 129.24, 131.53, 132.34, 132.41, 134.97, 139.23 (Ar), 159.84 (Ar, quaternary), 160.56 (Ar, quaternary), 170.13 (-H*C*OO).

^{11}B NMR (300 MHz, $CDCl_3$, 25°C): δ = 6.50

ESI^{+}: 412, 374, 270.

HMRS (EI): m/z calc. [M+H^{+}] = 374.1364, found [M+H^{+}] = 374.1367

Compound 30

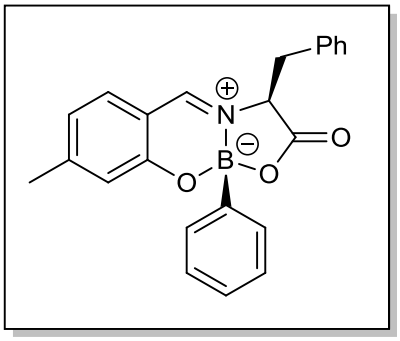

Isolated yield = 63 % ***de***. 100% , after 20 h at 90 ºC (0.095 g).

^{1}H NMR (400 MHz, $CDCl_3$, 25ºC, TMS): δ 2.35 (s, 3H, -ArC*H*$_3$), 2.70 (t, 1H, *J*= 12.0, -CHC*H*$_2$Ph), 3.41 (dd, 1H, *J*= 2.0, 14.0, -CHC*H*$_2$Ph), 4.34 (dd, 1H, *J*= 4.0, 12.0, -C*H*CH$_2$Ph), 6.73 (d, 1H, *J*= 8.0Hz, Ar), 6.85 (s, 1H, Ar), 6.97-7.03 (m, 3H, Ar), 7.12 (s, 1H, AR), 7.28-7.38 (m, 6H, Ar), 7.45-7.47 (m, 2H, Ar).

^{13}C-RMN (100MHz, $CDCl_3$, 25ºC, TMS): δ 22.50 (-Ar*C*H$_3$), 37.75(-CH*C*H$_2$Ph), 66.75 (-N*C*HCOCH$_2$-), 115.41, 120.38, 121.74, 127.74, 127.88, 128.48, 129.14, 129.24, 130.58, 131.23, 135.28 (Ar), 151.41 (Ar, quaternary), 159.95 (Ar, quaternary), 159.99 (Ar*C*HN-), 170.58 (-CH*C*OO-).

^{11}B NMR (300 MHz, $CDCl_3$, 25°C): δ = 6.94.

ESI^{+}: 408, 392, 370, 284.

HMRS (EI): m/z calc. [M+H^{+}] = 370.1614, found [M+H^{+}] = 370.1615.

Compound 31

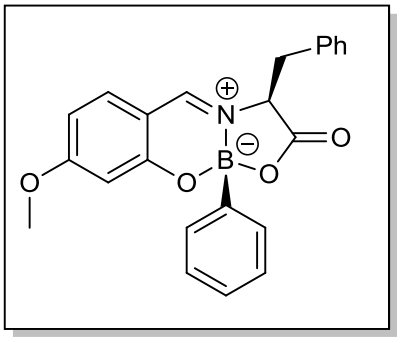

Isolated yield = 88 % yield, de 100%, after 20 h at 90 ºC (0.133 g).

^{1}H NMR (400 MHz, $CDCl_3$, 25ºC, TMS): δ 2.69 (t, 1H, *J*= 13.0, -CHC*H*$_2$Ph), 3.39 (dd, 1H, *J*= 3.6, 14.0, -CHC*H*$_2$Ph), 3.84 (s, 3H, -ArOC*H*$_3$), 4.31 (dd, 1H, *J*= 3.2, 12.4, -NC*H*CH_2Ph-), 6.45-6.50 (m, 2H, Ar), 6.97-7.09 (m, 4H, Ar), 7.28-7.48 (m, 6H, Ar), 7.49-7.50 (m, 2H, Ar);

^{13}C-RMN (100MHz, $CDCl_3$, 25ºC, TMS): δ 37.78 (-CH*C*H_2Ph), 55.87 (-ArO*C*H_3), 66.54 (-N*C*HCOCH_2-), 102.62, 110.12, 111.47, 127.65, 127.88, 128.42, 129.10, 129.24, 130.57, 132.88, 135.47 (Ar), 158.98 (Ar*C*HN-), 162.65 (Ar, quaternary), 168.80 (Ar, quaternary), 170.91 (-CH*C*OO-).

^{11}B NMR (300 MHz, $CDCl_3$, 25°C): δ = 7.62

ESI^{+}: 424, 408, 386, 300.

HMRS (EI): m/z calc. [M+H^{+}] = 386.1564, found [M+H^{+}] = 386.1571.

Compound 32

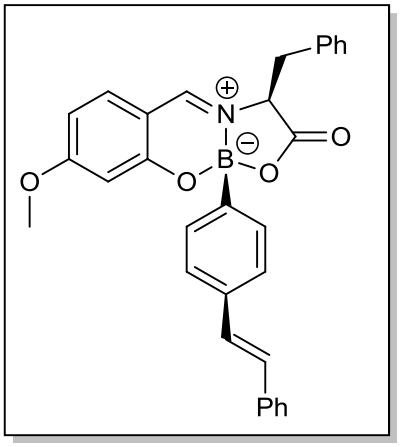

Isolated yield = 66 % ***de*** 77%, after 20 h at 90 ºC (0.111 g).

^{1}H NMR (400 MHz, $CDCl_3$, 25ºC, TMS): δ3.08 – 3.18 (m, 1H, -NC*H*CH_2Ph-), 3.55 (dt, 1H,*J*= 8.6, 4.3 Hz, -CHC*H*$_2$Ph), 3.85 (s, 3H, -OC*H*$_3$), 4.34 (dd, 1H, *J*= 11.9, 3.7 Hz, -CHC*H*$_2$Ph), 7.46 – 6.71 (m, 16H, Ar).

^{13}C-RMN (100MHz, $CDCl_3$, 25ºC, TMS): δ 38.8 (-CH*C*H_2Ph), 56.2 (-O*C*H_3), 66.0 (-N*C*HCOCH_2-), 103.0, 110.3, 112.0, 126.8, 127.8, 128.1, 128.7, 129.5, 129.7, 133.2, 135.7, 138.9, 158.6 (Ar, quaternary), 162.8 (Ar, quaternary), 168.9 (Ar, quaternary), 171.4 (-CH*C*OO-).

^{11}B NMR (300 MHz, $CDCl_3$, 25°C): δ = 6.36.

ESI$^+$: 300, 188, 166, 120.

HMRS (EI): m/z calc. [M^+] = 411.1642, found [M^+] = 411.1638.

Compound 33

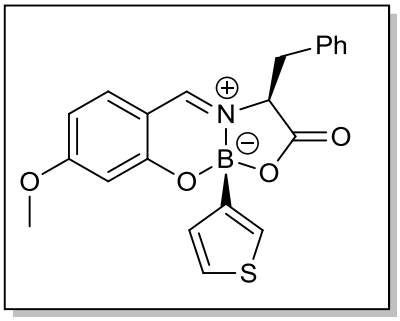

Isolated yield = 78 %***de*** 100%, after 20 h at 90 ºC (0.125 g).

^{1}H NMR (400 MHz, $CDCl_3$, 25ºC, TMS): δ 2.73 (t, 1H, *J*= 13.0, -CHC*H*$_2$Ph), 3.44 (dd, 1H. *J*= 3.6, 14.0, -CHC*H*$_2$Ph), 3.85 (s, 3H, -ArOC*H*$_3$). 4.31 (dd, 1H, *J*= 3.4, 12.2, -NC*H*CH_2Ph-), 6.47-6.52 (m, 2H, Ar), 6.95-7.04 (m, 5H, Ar), 7.28-7.40 (m, 5H, Ar).

^{13}C-RMN (100MHz, $CDCl_3$, 25ºC, TMS): δ 38.22 (-CH*C*H_2Ph), 55.89 (-ArO*C*H_3), 66.02 (-N*C*HCOCH_2-), 102.72, 110.19, 111.50, 125.71, 127.70, 127.75, 129.11, 129.34, 129.80, 132.82, 135.32 (Ar), 158.24 (Ar*C*HN-), 162.34 (Ar, quaternary), 168.70 (Ar, quaternary), 171.05 (-CH*C*OO-).

^{11}B NMR (300 MHz, $CDCl_3$, 25°C): δ = 5.70

ESI^{+}: 430, 392, 338, 300.

HMRS (EI): m/z calc. [M+H^{+}] = 392.1128, found [M+H^{+}] = 392.1138.

Compound 34

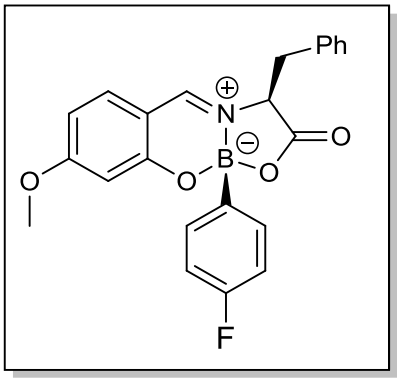

Isolated yield = 50 %***de*** 91% , after 20 h at 90 ºC (0.08 g).

^{1}H NMR (400 MHz, $CDCl_3$, 25ºC, TMS): δ 2.54 (dd, 1H,*J* = 14.1, 12.3 Hz, -NC*H*CH_2Ph), 3.23 (dd, 1H,*J* = 14.2, 3.0 Hz, -CHC*H*$_2$Ph), 3.83 (s, 3H, -OC*H*$_3$), 4.32 (dd, 1H,*J* = 12.2, 3.1 Hz, -CHC*H*$_2$Ph), 6.39 – 6.46 (m, 2H, Ar), 6.99 (d, 1H, *J* = 8.7 Hz, Ar), 7.03 – 7.17 (m, 2H, Ar), 7.07-7.39(m, 5H, Ar), 7.61 (dd, 1H, *J* = 7.9, 0.9 Hz, Ar), 7.68 (dd, 1H,*J* = 7.5, 1.7 Hz, Ar).

^{13}C-RMN (100MHz, $CDCl_3$, 25ºC, TMS): δ 37.82 (-CH*C*H_2Ph), 55.89 (-O*C*H_3), 66.49 (-N*C*HCOCH_2-), 102.60, 110.27, 114.76, 127.73, 127.63, 129.15, 129.5, 132.34, 132.25, 132.89, 135.32, 158.99 (Ar), 162.57 (-CH*C*OO-).

^{11}B NMR (300 MHz, $CDCl_3$, 25°C): δ = 6.48

ESI^{+}: 442, 426, 360, 300.

HMRS (EI): m/z calcd. [M+H^{+}] = 404.1464, found [M+H^{+}] 404.1455.

Compound 35

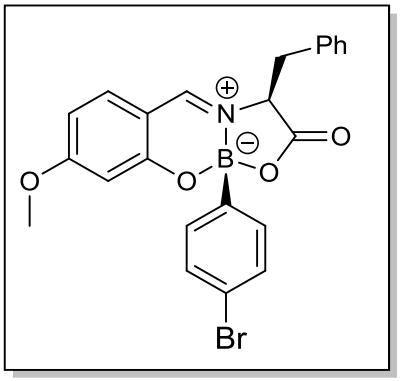

Isolated yield = 66 %, ***de*** 88% , after 20 h at 90 ºC (0.12 g).

^{1}H NMR (400 MHz, $CDCl_3$, 25ºC, TMS): δ 2.59–2.69 (m, 1H, -NC*H*CH_2Ph-), 3.40 (dd, 1H, *J*= 13.8, 3.2 Hz, -NCHC*H*$_2$Ph), 3.84 (s, 3H, -OC*H*$_3$), 4.34 (dd, 1H, *J*= 12.3, 3.3 Hz, -NCHC*H*$_2$Ph), 6.17-6.51 (m, 2H, Ar), 6.92-7.07 (m, 3H, Ar), 7.19–7.50 (m, 7H, Ar).

^{13}C-RMN (100MHz, $CDCl_3$, 25ºC, TMS): δ 38.1 (-CH*C*H_2Ph), 56.2 (-O*C*H_3), 66.8 (-N*C*HCH$_2$Ph-), 103.0, 110.7, 111.7, 123.1, 129.5, 131.3, 132.7, 133.3, 135.6, 159.5 (Ar), 162.8 (Ar, quaternary), 169.4 (Ar, quaternary), 169.3 (-CH*C*OO-).

^{11}B NMR (300 MHz, $CDCl_3$, 25°C): δ =6.48

ESI^{+}: 502, 486, 464,152.

HMRS (EI): m/z calcd. [M^{+}] = 463.0590, found [M^{+}] 463.0583.

Compound 36

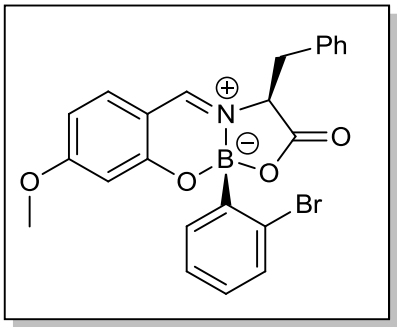

Isolated yield = 50 % ***de*** 77%, after 20 h at 90 ºC (0.09 g).

^{1}H NMR (400 MHz, $CDCl_3$, 25ºC, TMS): δ 2.54 (dd, 1H, *J* = 14.1, 12.4 Hz, -NC*H*CH_2Ph-), 3.24 (dd, 1H, *J* = 14.1, 2.9 Hz, -CHC*H*$_2$Ph), 3.84 (s, 3H, -OC*H*$_3$), 4.30 (dd, 1H, *J*= 12.3, 3.3 Hz, -CHC*H*$_2$Ph), 6.43-6.46 (m, 2H, Ar), 7.07 – 7.30 (m, 3H, Ar), 7.28-7.40(m, 5H, Ar), 7.61 (dd, 1H, *J* = 7.9, 1.0 Hz, Ar), 7.70 (dd,1H, *J* = 7.5, 1.7 Hz, Ar) ; **^{13}C-RMN** (100MHz, $CDCl_3$, 25ºC, TMS): δ 37.26 (-CH*C*H_2Ph), 55.9 (-O*C*H_3), 68.38 (-N*C*HCOCH_2-), 101.78, 110.33, 112.6, 126.8, 127.8, 129.0, 129.3, 129.86, 133.0, 134.2, 133.5, 135.6, 161.7, 169.41 (Ar, quaternary), 162.8 (Ar, quaternary), 169.7 (Ar, quaternary), 170.4 (-CH*C*OO-).

^{11}B NMR (300 MHz, $CDCl_3$, 25°C): δ =6.29

ESI^{+}: 502, 486, 464, 256.

HMRS (EI): m/z calcd. [M^{+}] = 463.0591, found [M^{+}] 463.0580.

Compound 37

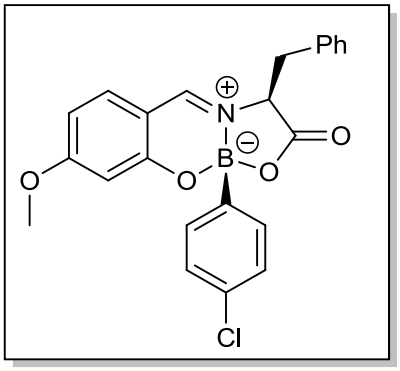

Isolated yield = 84%, ***de*** 96%, after 20 h at 90 ºC (144 mg).

^{1}H NMR (400 MHz,CDCl3, 25ºC, TMS): δ 2.62 (t, 1H,*J*= 13.2 Hz, -NCHCOC*H*$_2$-), 3.38 (d, 1H,*J*= 13.9 Hz, -CHC*H*$_2$Ph-), 3.82(s, 3H, -OC*H*$_3$), 4.28 (d, 1H,*J*= 11.7 Hz, -C*H*CH$_2$Ph-), 6.36 – 7.45 (m, 14H, Ar).

^{13}C NMR (100 MHz, CDCl3) δ38.1 (-CH*C*H2Ph-), 56.2 (-O*C*H3), 66.8 (-N*C*HCH$_2$Ph-), 102.9, 110.7, 111.7, 128.1, 128.4, 129.5, 132.3, 133.3, 134.6, 135.6 (Ar), 159.5 (Ar, quaternary), 162.8 (Ar, quaternary), 169.3 (Ar, quaternary), 171.0 (-CHCO)

^{11}B NMR (300 MHz, $CDCl_3$, 25°C): δ = 6.48

ESI^{+}: 442, 322, 300, 166.

HMRS (EI): m/z calcd. [M^{+}] = 419.1096, found [M^{+}] 419.1106.

Compound 38

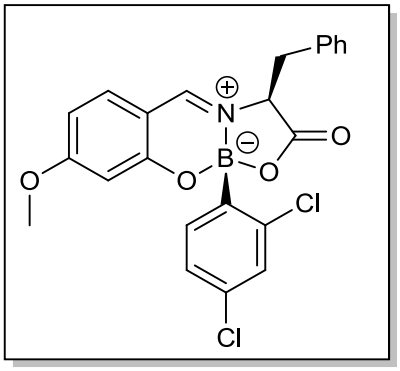

Isolated yield = 98 % ***de*** 68%, after 20 h at 90 ºC (183 mg).

^{1}H NMR (400 MHz,CDCl3, 25ºC, TMS): δ 2.47 (dd, 1H, *J* = 14.0, 12.4 Hz, -NCHC*H*$_2$Ph-), 3.23 (dd, 1H,*J*= 14.1, 3.0 Hz, -NCHC*H*$_2$Ph-), 3.83 (d, 3H,*J*= 9.5 Hz, -OCH3), 4.25 (dd, 1H,*J*= 12.2, 3.1 Hz, -C*H*CH2Ph-),6.27–6.41 (m, 2H, Ar), 6.91 – 7.07 (m, 4H, Ar), 7.14 – 7.34 (m, 6H, Ar).

^{13}C NMR (100 MHz, CDCl3) δ 37.8 (-CH*C*H$_2$Ph-), 56.2 (-O*C*H3), 68.5 (-N*C*HCH$_2$Ph-), 102.0, 110.7, 112.1, 126.8, 127.9, 128.5, 129.4, 129.5, 129.7, 129.8, 133.2, 135.0, 135.1,135.4, 135.7, 139.7 (Ar), 161.8 (Ar, quaternary), 162.3 (Ar, quaternary), 162.6 (Ar, quaternary), 169.8 (-CHCOO).

^{11}B NMR (300 MHz, $CDCl_3$, 25°C): δ = 6.31

ESI^{+}: 492, 454, 300.

HMRS (EI): m/z calcd. [M+H^{+}] = 454.0779, found [M+H^{+}] 454.0763.

Compound 39

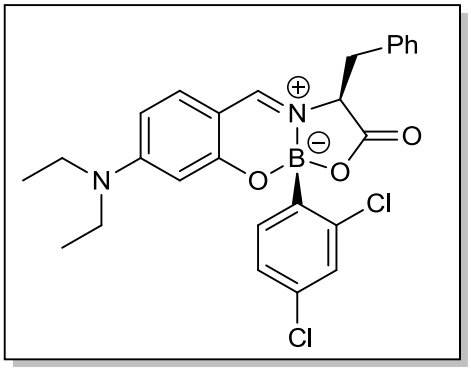

A round bottom flask equipped with a magnetic stirrer was charged with amino acid (2.0 equiv.), aldehyde (1.5 equiv.) and distilled ethanol (2.0 mL). This suspension was stirred at 90ºC for 1 h after which the boronic acid (0.41 mmol) was added, the mixture was then stirred at 75ºC for 20 h. The reaction mixture, which appears as a biphasic composition of precipitate and a supernatant liquid, was filtered and the solid retained in the filter, was then washed with water followed by hexane. The desired compound was recovered with dichloromethane, which was subsequently removed under reduced pressure.

Isolated yield = 89 %, ***de*** 98%, after 20 h at 75 ºC (0.08 g).

^{1}H NMR (400 MHz, $CDCl_3$, 25ºC, TMS): δ 1.11 (t, 6H, *J* = 6.8 Hz, –N(CH_2CH_3)$_2$, 2.37 (t, 1H,*J* = 13.0 Hz, -CHCH_2Ph), 3.10 (d, 1H,*J* = 13.6 Hz, -CHCH_2Ph), 3.18 – 3.45 (m, 4H, –N(CH_2CH_3)$_2$), 4.10 (d, 1H,*J* = 10.3 Hz, -C*H*CH_2Ph), 5.98 (s, 1H, Ar), 6.12 (d, 1H,*J* = 8.4 Hz, Ar), 6.84 (d, 1H,*J* = 8.6 Hz, Ar), 6.96 (s, 1H, Ar), 7.03 (d, *J* = 7.0 Hz, 2H, Ar), 7.42 – 7.08 (m, 6H, Ar).

^{13}C-RMN (100MHz, $CDCl_3$, 25ºC, TMS): δ 45.08 (–N(CH_2CH_3), 67.72 (-CH*C*H_2Ph), 98.12 (-N*C*HCOCH_2-), 105.97, 108.34, 126.30, 127.33, 128.27, 128.94, 129.24, 133.50, 134.26, 134.70, 135.09, 136.18, 139.46, 156.56, 158.90, 161.43, (Ar), 171.47 (-CH*C*OO).

^{11}B NMR (300 MHz, $CDCl_3$, 25°C): δ = 5.96

ESI^{+}: 517, 495, 341.

HMRS (EI): m/z calcd. [M^{+}] = 494.1335, found [M^{+}] = 494.1330.

Compound 40

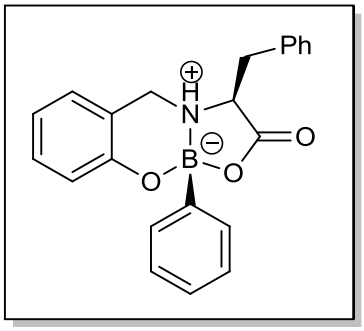

A round bottom flask equipped with a magnetic stirrer was charged with amino acid (0,82 mmol), Cl_2SO (1equiv.), distilled methanol (3.0 mL) after which the suspension was stirred at reflux for 12 h. Then the volatiles were removed under reduced pressure and the remaining solid was solubilized with a mixture of methanol and THF (3.0 mL, 1:1), the aldehyde was then added (1eqiv) and the reaction was stirring for 6 h at reflux to yield the schiff base. Subsequently, $NaBH_4$ (3 equiv.) was slowly added at 0ºC to the reaction mixture which was then allowed to react at this temperature for 1 h after which the reaction was quenched with HCl (3 equiv.). The reaction mixture volatiles were then evaporated under reduced pressure. The residue was then solubilized with NaOH (1,5ml 3 M) and the mixture stirred for 2 h at rt, after which HCl was added until PH 7 was obtained. The mixture than was evaporated by reduced pressure. The product was solubilized with CH_2Cl_2, the insoluble material was discarded. The product was dried by reduced pressure. Further 0,41mmol of this compounds were solubilized by 1/1 mixture of ethanol and benzene (2mL) and reacted with phenyl boronic acid (1equiv.) in presence of $NaHCO_3$(1,5equiv.) for 12h at reflux.

Isolated yield = 48%,***de*** 100%.

^{1}H NMR (400 MHz, CDCl3, 25"C, TMS): 3.13-3.25 (m, 2H,–CHC*H*$_2$Ph), 3.37 (d, 1H, *J* = 13.5 Hz, –NHC*H*$_2$C$_6$H$_4$–), 3.77 (d, 1H, *J* = 7.4 Hz,–NC*H*CH2–), 4.15 (d, *J* = 11.9 Hz, 1H –NHC*H*$_2$C$_6$H$_4$–), 4.63 (s, 1H -N*H*-), 7.38 – 6.80 (m, 14H, Ar),

^{13}C-NMR (100 MHz, CDCl3, 25ºC, TMS): δ 34.53 (–CH*C*H$_2$Ph), 47.03 (–NH*C*H$_2$C$_6$H$_4$), 60.36(-NH*C*HCH$_2$-)117.07, 119.93, 120.78, 127.94, 128.38, 128.73, 129.21, 129.29, 131.34, 133.47 (Ar), 155.77 (Ar, quaternary), 171.67 (–CH*C*OO–).

^{11}B NMR (300 MHz, $CDCl_3$, 25°C): δ = 6.33.

ESI$^+$: 358, 294, 272.

HMRS (EI): m/z calcd. [M^+] 357.1536, found [M^+] = 357.1541 .

Compound 41

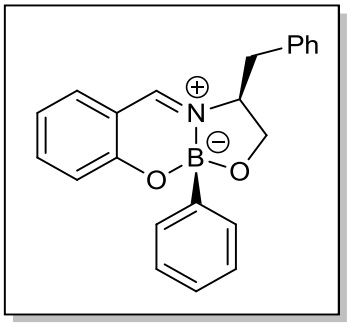

A round bottom flask equipped with a magnetic stirrer and molecular sieves, was charged with amino alcohol (0.41 mmol), aldehyde (1.0equiv.) and distilled ethanol (2.0 mL). This suspension was stirred at reflux for 1 h, after which the solvent was evaporated under educed pressure. Toluene (2 mL) and boronic acid (1.0 equiv.) was then added and the mixture was stirred at reflux for 24 h. The mixture reaction that appears as yellow clear solution was filtered at room temperature through a silica column and the expected compound was precipitated from this mixture by low temperature.

Isolated yield = 20 % (0.133 g).

^{1}H NMR (400 MHz, $CDCl_3$, 25ºC, TMS): δ2.77 – 3.04 (m, 2H, *J*= 13.0, -CHC*H*$_2$Ph), 4.09 (d, 2H,*J* = 8.9 Hz, -NCHC*H*$_2$O-, -NC*H*CH$_2$O-), 4.34 (dd, 1H,*J* = 9.7, 6.8 Hz, -NCHC*H*$_2$O-), 6.83 (t, 1H,*J* = 7.4 Hz, -Ar), 6.99 (dd, 3H,*J* = 11.7, 8.1 Hz, Ar), 7.14 (d, 1H,*J* = 7.7 Hz, Ar), 7.22 – 7.38 (m, 7H, Ar), 7.45 – 7.53 (m, 3H, Ar).

^{13}C-RMN (100MHz, $CDCl_3$, 25ºC, TMS): δ 39.84 (-CH*C*H$_2$Ph), 66.15 (-N*C*HCH$_2$-), 67.87 (-NCH*C*H$_2$-), 117.62, 118.94, 120.34, 127.15, 127.46, 127.51, 128.84, 129.22, 130.80, 131.00, 136.67, 137.64, 159.03, 160.39 (Ar).

^{11}B NMR (300 MHz, $CDCl_3$, 25°C): δ = 6.47

ESI^{+}: 380, 364, 342, 256.

HMRS (EI): m/z calcd. [M^{+}] = 341.1587, found [M^{+}] = 341.1544

Compound 42

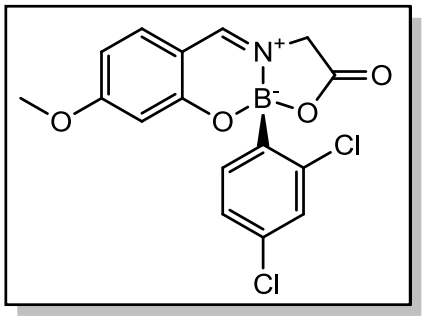

Isolated yield = 17 %

^{1}H NMR (400 MHz, $CDCl_3$, 25ºC, TMS): δ, 3.80 (s, 3H, -OC*H*$_3$), 4.14 (d, 1H, *J* = 16.9 Hz, -NC*H*$_2$-), 4.48 (d, 1H, *J* = 16.9 Hz, NC*H*$_2$-), 6.41 – 6.56 (m, 1H, Ar), 7.09 (d, *J*= 8.0 Hz, 1H, Ar), 7.21 (d, *J*= 11.6 Hz, 4H, Ar), 7.41 (d, *J* = 8.1 Hz, 1H, Ar);

^{13}C-RMN (100MHz, $CDCl_3$, 25ºC, TMS): δ 54.28 (-N*C*H-), 56.00 (-O*C*H$_3$), 102.18, 110.68, 126.21, 129.29, 132.99, 135.10 (Ar), 138.58, 159.95, 161.92 (Ar, quaternary), 169.39 (-CH*C*OO-).

^{11}B NMR (300 MHz, $CDCl_3$, 25°C): δ =

ESI^{+}: [Mþ1H] , found 364.15 [Mþ1H] .

HMRS (EI): m/z calcd [Mþ1H] 363.0236, found [Mþ1H].

Compound 43 procedure A

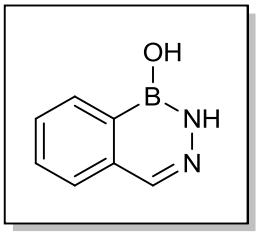

Isolated yield = 90%

^{1}H NMR (400 MHz, DMSO, 25 °C, TMS): δ =2.48 (s, 3H, HOBNHNCHC*H*$_3$C$_6$H$_4$), 7.52–7.64 (m, 1H)7.73–7.86 (m, 1H)7.78 (d, *J* = 8.0 Hz, 1H)8.31 (d, *J* = 7.5 Hz, 1H) (HOBNHNCHCH$_3$C$_6$*H*$_4$), 8.19 (s, 1H, *H*OBNHNCHCH$_3$C$_6$H$_4$),

^{13}C NMR (100 MHz, DMSO, 25 °C): δ = 21.45 (HOBNHNCH*C*H$_3$C$_6$H$_4$),129.14 131.85, 132.31, 135.22, 142.23 (HOBNC$_6$H$_5$N*C*HCH$_3$*C*$_6$H$_4$)

^{11}B NMR (300 MHz, DMSO, 25°C): δ = 27.05

Compound 44 procedure A

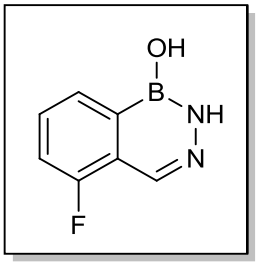

Isolated yield = 80%

^{1}H NMR (400 MHz, DMSO, 25 °C, TMS): δ = 7.59(s,1H), 7.63 – 7.54 (m, 1H),8.14 (d, *J* = 7.5 Hz, 1H) ($HOBNC_6H_5NCHC_6H_4F$), 8.14 (s, 1H, $HOBNC_6H_5NCHC_6H_4F$),8.62 (s, 1H, $HOBNC_6H_5NCHC_6H_4F$),

^{13}C NMR (100 MHz, DMSO, 25 °C): δ = 117.23, 117.45($HOBNC_6H_5NCHC_6F$),128.30, 131.29 ($HOBNC_6H_5NCHC_6F$), 131.42 ($HOBNC_6H_5NCHC_6F$), 160, 146.43 ($HOBNC_6H_5NCHC_6F$),

^{11}B NMR (300 MHz, DMSO, 25°C): δ = 27.2

Compound 45 procedure A

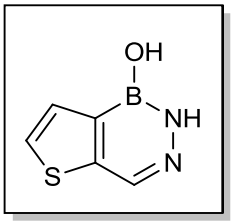

Isolated yield = 83%

^{1}H NMR (400 MHz, DMSO, 25 °C, TMS): δ = 7.59 (d, *J* = 4.7 Hz, 1H) 7.50 (d, *J* = 4.8 Hz, 1H) (HOBNC$_6$H$_5$NCHC$_4$S*H*$_2$), 8.13(s, 1H, *H*OBNHNCHC$_4$SH$_2$), 8.32 (s, 1H, HOBNHNC*H*C$_4$SH$_2$), 10.18 (s, 1H, HOBN*H*NCHC$_4$SH$_2$)

^{13}C NMR (100 MHz, DMSO, 25 °C): δ = 145.85 (HOBNHNC*H*C$_4$SH$_2$), 125.74, 134.25 (1H, HOBNC$_6$H$_5$NCHC$_4$SH$_2$)

^{11}B NMR (300 MHz, DMSO, 25°C): δ = 27.1

Compound 46 procedure A

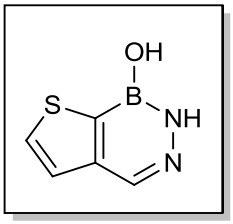

Isolated yield = 28%

^{1}H NMR (400 MHz, DMSO, 25 °C, TMS): δ = 7.51 (d, *J* = 4.8 Hz, 1H) 8.02 (d, *J* = 4.8 Hz, 1H) (HOBNC$_6$H$_5$NCHC$_4$S*H*$_2$),8.12 (s, 1H, *H*OBNHNCHC$_4$SH$_2$),8.32 (s, 1H, HOBNHNC*H*C$_4$SH$_2$),10.18 (s, 1H, HOBN*H*NCHC$_4$SH$_2$)

^{13}C NMR (100 MHz, DMSO, 25 °C): δ = 144.87 (HOBNHNC*H*C$_4$SH$_2$), 125.72, 134.28 (HOBNC$_6$H$_5$NCH*C*$_4$SH$_2$)

^{11}B NMR (300 MHz, DMSO, 25°C): δ = 27.26

Compound 47 procedure B

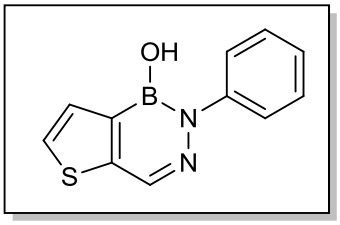

Isolated yield = 80%

^{1}H NMR (400 MHz, DMSO, 25 °C, TMS):δ = 7.24 (t, *J* = 7.3 Hz, 1H) 7.41 (t, *J* = 7.8 Hz, 2H) 7.53 (d, *J* = 7.7 Hz, 2H) (HOBNC$_6$*H*$_5$NCHC$_4$SH$_2$), 7.80 (d, *J* = 4.9 Hz, 1H) 7.89 (d, *J* = 4.9 Hz, 1H) (HOBNC$_6$H$_5$NCHC$_4$S*H*$_2$), 8.38 (s, 1H, *H*OBNC$_6$H$_5$NCHC$_4$SH$_2$), 8.95 (s, 1H, HOBNC$_6$H$_5$NC*H*C$_4$SH$_2$).

^{13}C NMR (100 MHz, DMSO, 25 °C): δ =125.36 (s, HOBN*C*$_6$H$_5$NCHC$_4$SH$_2$), 125.38, 128.58 (s, HOBN*C*$_6$H$_5$NCHC$_4$SH$_2$), 130.32, 130.05, 133.05 (HOBNC$_6$H$_5$NCH*C*$_4$SH$_2$),

^{11}B NMR (300 MHz, DMSO, 25°C):δ = 30.3

Compound 48 procedure B

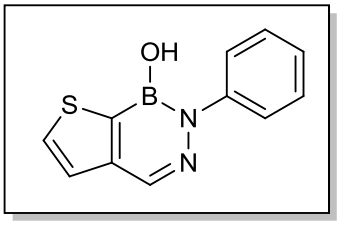

Isolated yield = 81%

^{1}H NMR (400 MHz, DMSO, 25 °C, TMS): δ = 7.24 (t, *J* = 7.3 Hz, 1H) 7.41 (t, *J* = 7.8 Hz, 2H)7.54 (d, *J* = 7.7 Hz, 2H)(HOBNC$_6$*H*$_5$NCHC$_4$SH$_2$), 7.81 (d, *J* = 5.0 Hz, 1H)7.89 (d, *J* = 4.9 Hz, 1H) (HOBNC$_6$H$_5$NCHC$_4$S*H*$_2$), 8.39 (s, 1H, *H*OBNC$_6$H$_5$NCHC$_4$SH$_2$), 8.93 (s, 1H, HOBNC$_6$H$_5$NC*H*C$_4$SH$_2$),

^{13}C NMR (100 MHz, DMSO, 25 °C): δ = 125.38, 125.66, 128.61 (HOBNC$_6$H$_5$NCHC$_4$SH$_2$), 130.05, 130.34, 133.06 (HOBNC$_6$H$_5$NCHC$_4$SH$_2$) 145.3 (HOBNC$_6$H$_5$NCHC$_4$SH$_2$),

^{11}B NMR (300 MHz, DMSO, 25°C): δ = 26.6

Compound 49 procedure A

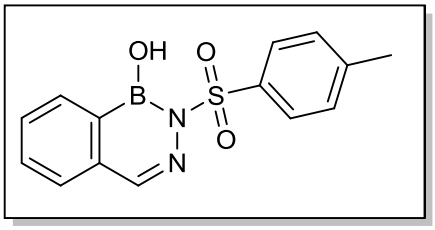

Isolated yield = 53%

^{1}H NMR (400 MHz, DMSO, 25 °C, TMS): δ = 3.39 (s, 3H, HOBNSO$_2$C$_6$H$_4$C*H*$_3$NCHC$_6$H$_4$), 7.41 (dd, *J* = 16.0, 8.2 Hz, 2H, HOBNSO$_2$C$_6$*H*$_4$CH$_3$NCHC$_6$H$_4$), 7.63–7.85 (m, 3H, HOBNSO$_2$C$_6$H$_4$CH$_3$NCHC$_6$*H*$_4$), 7.90 (d, J = 8.1 Hz, 2H, HOBNSO$_2$C$_6$*H*$_4$CH$_3$NCHC$_6$H$_4$), 8.13 (s, 1H, *H*OBNSO$_2$C$_6$H$_4$CH$_3$NCHC$_6$H$_4$), 8.21 (d, *J* = 6.2 Hz, 1H, HOBNSO$_2$C$_6$H$_4$CH$_3$NCHC$_6$*H*$_4$), 9.02 (s, 1H, HOBNSO$_2$C$_6$H$_4$C$_6$H$_3$NC*H*C$_6$H$_4$).

^{13}C NMR (100 MHz, DMSO, 25 °C): δ = 21.53 (HOBNSO$_2$C$_6$H$_4$*C*H$_3$NCHC$_6$H$_4$), 128.21 (HOBNSO$_2$*C*$_6$H$_4$CH$_3$NCHC$_6$H$_4$), 128.35 (HOBNSO$_2$C$_6$H$_4$CH$_3$NCH*C*$_6$H$_4$), 130.20 (HOBNSO2*C*6H4CH3NCHC6H4), 131.07, 132.26, 133.13 (HOBNSO$_2$C$_6$H$_4$CH$_3$NCH*C*$_6$H$_4$), 134.41, 136.34 (HOBNSO$_2$*C*$_6$H$_4$CH$_3$NCHC$_6$H$_4$), 142.81(HOBNSO$_2$C$_6$H$_4$CH$_3$NC*H*C$_6$H$_4$), 144.90 (HOBNSO$_2$C$_6$H$_4$CH$_3$NCH*C*$_6$H$_4$),

^{11}B NMR (300 MHz, DMSO, 25°C): δ = 31.36

Compound 50 procedure A

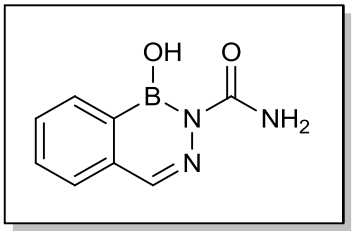

Isolated yield = 60%

^{1}H NMR (400 MHz, DMSO, 25 °C, TMS): δ = 7.43 (t, *J* = 6.8 Hz, 2H), 7.49 (d, *J* = 7.5 Hz, 1H) 7.62 (d, *J* = 6.7 Hz, 1H) (HOBNCONH$_2$NCHC$_6$*H*$_4$), 7.79 (s, 1H, *H*OBNCONH$_2$NCHC$_6$H$_4$), 7.83 (s, 1H, HOBNCONH$_2$NC*H*C$_6$H$_4$)

^{13}C NMR (100 MHz, DMSO, 25 °C): δ = 127.7, 128.11, 130.46, 130,72 (HOBNCONH$_2$NCH*C*$_6$H$_4$), 131.60 (HOBNCONH$_2$N*C*HC$_6$H$_4$), 145.94 (HOBN*C*ONH$_2$N*C*HC$_6$H$_4$)

^{11}B NMR (300 MHz, DMSO, 25°C): δ = 30.37

Compound 51 procedure A

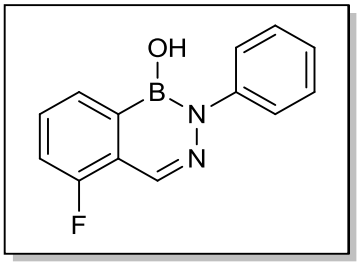

Isolated yield = 68%

^{1}H NMR (400 MHz, DMSO, 25 °C, TMS): δ =7.25 (t, *J* = 7.3 Hz, 1H)7.43 (t, *J* = 7.7 Hz, 2H)7.63 – 7.53 (m, 3H) ($HOBNC_6\mathit{H}_5NCHC_6F$), 7.61(s,1H), 7.77 – 7.64 (m, 1H),8.23 (d, *J* = 7.5 Hz, 1H) ($HOBNC_6H_5NCHC_6H_4F$), 8.34 (s, 1H, $\mathit{H}OBNC_6H_5NCHC_6H_4F$),9.19 (s, 1H, $HOBNC_6H_5NC\mathit{H}C_6H_4F$),

^{13}C NMR (100 MHz, DMSO, 25 °C): δ =117.34, 117.54 ($HOBNC_6H_5NCHC_6F$), 125.16, 125.7, 128.68 ($HOBNC_6H_5NCHC_6F$), 128.30, 131.29 ($HOBNC_6H_5NCHC_6F$), 131.42 ($HOBNC_6H_5NCHC_6F$), 160, 146.43 ($HOBNC_6H_5NCHC_6F$),

^{11}B NMR (300 MHz, DMSO, 25°C): δ = 27.9

Compound 52 procedure A

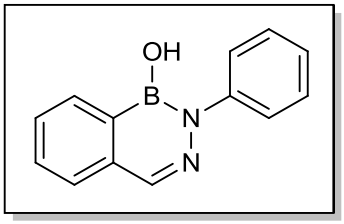

Isolated yield = 60%

^{1}H NMR (400 MHz, DMSO, 25 °C, TMS):, δ = 7.23 (t, *J* = 7.3 Hz, 1H) 7.41 (t, *J* = 7.9 Hz, 2H) 7.58 (d, *J* = 7.5 Hz, 2H) (HOBNC$_6$*H*$_5$NCHC$_6$H$_4$), 7.63 – 7.72 (m, 1H) 7.74–7.87 (m, 2H) (HOBNC$_6$H$_5$NCHC$_6$*H*$_4$), 8.21 (s, 1H, *H*OBNC$_6$H$_5$NCHC$_6$H$_4$), 8.40 (d, *J* = 7.6 Hz, 1H, HOBNHNCHC$_6$*H*$_4$), 8.99 (s, 1H, HOBNHNC*H*C$_6$H$_4$).

^{13}C NMR (100 MHz, DMSO, 25 °C): δ = 125.2, 125.33 (HOBNC$_6$H$_5$NCHC$_6$H$_4$), 127.45 (HOBNC$_6$H$_5$NCHC$_6$H$_4$), 128.61 (HOBNC$_6$H$_5$NCHC$_6$H$_4$), 129.48 131.91, 132.10 (HOBNC$_6$H$_5$NCHC$_6$H$_4$), 135.43 (HOBNC$_6$H$_5$NCHC$_6$H$_4$), 139.61 (HOBNC$_6$H$_5$NCHC$_6$H$_4$)

^{11}B NMR (300 MHz, DMSO, 25°C): δ = 26.96

Compound 53 procedure A

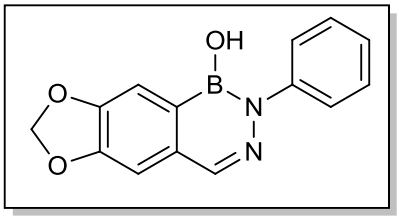

Isolated yield = 68%

^{1}H NMR (400 MHz, DMSO, 25 °C, TMS): δ =6.17 (s, 2H, HOBNC$_6$H$_5$NCHC$_6$H$_2$OC*H$_2$*O), 7.21 (t, *J* = 7.3 Hz, 1H)(HOBNC$_6$*H*$_5$NCHC$_6$H$_2$OCH$_2$O), 7.33 (s, 1H, HOBNC$_6$H$_5$NCHC$_6$*H*$_2$OCH$_2$O), 7.40 (t, *J* = 7.9 Hz, 2H)7.54 (d, *J* = 8.1 Hz, 2H) (HOBNC$_6$*H*$_5$NCHC$_6$H$_2$OCH$_2$O), 7.81 (s, 1H, HOBNC$_6$H$_5$NCHC$_6$*H*$_2$OCH$_2$O), 8.04 (s, 1H, *H*OBNC$_6$H$_5$NCHC$_6$H$_2$OCH$_2$O), 8.69 (s, 1H, HOBNC$_6$H$_5$NC*H*C$_6$H$_2$OCH$_2$O)

^{13}C NMR (100 MHz, DMSO, 25 °C): δ =101.95(HOBNC$_6$H$_5$NCHC$_6$H$_2$O*C*H$_2$O), 106.26 109.43 (HOBNC$_6$H$_5$NCH*C*$_6$H$_2$OCH$_2$O), 124.98, 125.27, 128.57 (HOBN*C*$_6$H$_5$NCHC$_6$H$_2$OCH$_2$O), 132.12 (HOBNC$_6$H$_5$NCH*C*$_6$H$_2$OCH$_2$O), 138.74(HOBNC$_6$H$_5$N*C*HC$_6$H$_2$OCH$_2$O), 149.24, 150.96 (HOBNC$_6$H$_5$NCH*C*$_6$H$_2$OCH$_2$O)

^{11}B NMR (300 MHz, DMSO, 25°C): δ = 33.5

Compound 54 procedure B

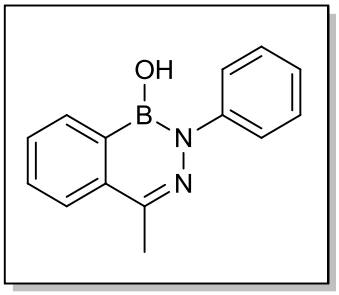

Isolated yield = 77%

^{1}H NMR (400 MHz, DMSO, 25 °C, TMS): δ =2.51 (s, 3H, HOBNC$_6$H$_5$NCHC*H*$_3$C$_6$H$_4$), 7.27 – 7.16 (m, 1H)7.40 (t, *J* = 7.6 Hz, 2H)7.57 (t, *J* = 9.0 Hz, 2H)(HOBNC$_6$*H*$_5$NCHCH$_3$C$_6$H$_4$), 7.62–7.75 (m, 1H)7.72–7.87 (m, 1H)7.89 (d, *J* = 8.0 Hz, 1H)8.42 (d, *J* = 7.5 Hz, 1H) (HOBNC$_6$H$_5$NCHCH$_3$C$_6$*H*$_4$), 8.81(s, 1H, *H*OBNC$_6$H$_5$NCHCH$_3$C$_6$H$_4$),

^{13}C NMR (100 MHz, DMSO, 25 °C): δ = 20.48 (HOBNC$_6$H$_5$NCH*C*H$_3$C$_6$H$_4$), 124.99, 125.81, 128.56 (HOBN*C*$_6$H$_5$NCHCH$_3$C$_6$H$_4$), 129.17 131.87, 132.32, 135.24, 143.23 (HOBN*C*$_6$H$_5$N*C*HCH$_3$*C*$_6$H$_4$)

^{11}B NMR (300 MHz, DMSO, 25°C): δ = 30.9

Compound 55 procedure B

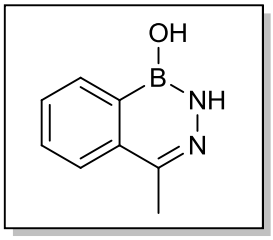

Isolated yield = 65%

IR (film): ν_{max} (cm^{-1}):

^{1}H NMR (400 MHz, DMSO, 25 °C, TMS): δ = 2.53 (s, 3H, HOBNHNCHC*H*$_3$C$_6$H$_4$), (s, 1H, HOBNHNC*H*CH$_3$C$_6$H$_4$), (s, 1H, HOBNHNCHCH$_3$C$_6$*H*$_4$)

^{13}C NMR (100 MHz, DMSO, 25 °C): δ = (s, 1H, HOBNHNCH*C*H$_3$C$_6$H$_4$), (s,1H, HOBNHN*C*HCH$_3$C$_6$H$_4$), (s,1H, HOBNHN*C*HCH$_3$*C*$_6$H$_4$)

^{11}B NMR (300 MHz, DMSO, 25°C): δ = 29.2

7.3 Mass confirmation and X-ray Crystallography analysis of compound 1

Mass Spectrum By Direct Infusion; Full Scan m/z 60-800; ESI+, Positive and negative electrospray ionization mode was tested for sample ionization.

Positive ionization mode (ESI+) analysis presents higher ion signals intensity.

m/z 298 is attributed to sodium adducts of the molecular ion of the original compound ([M+Na]+).

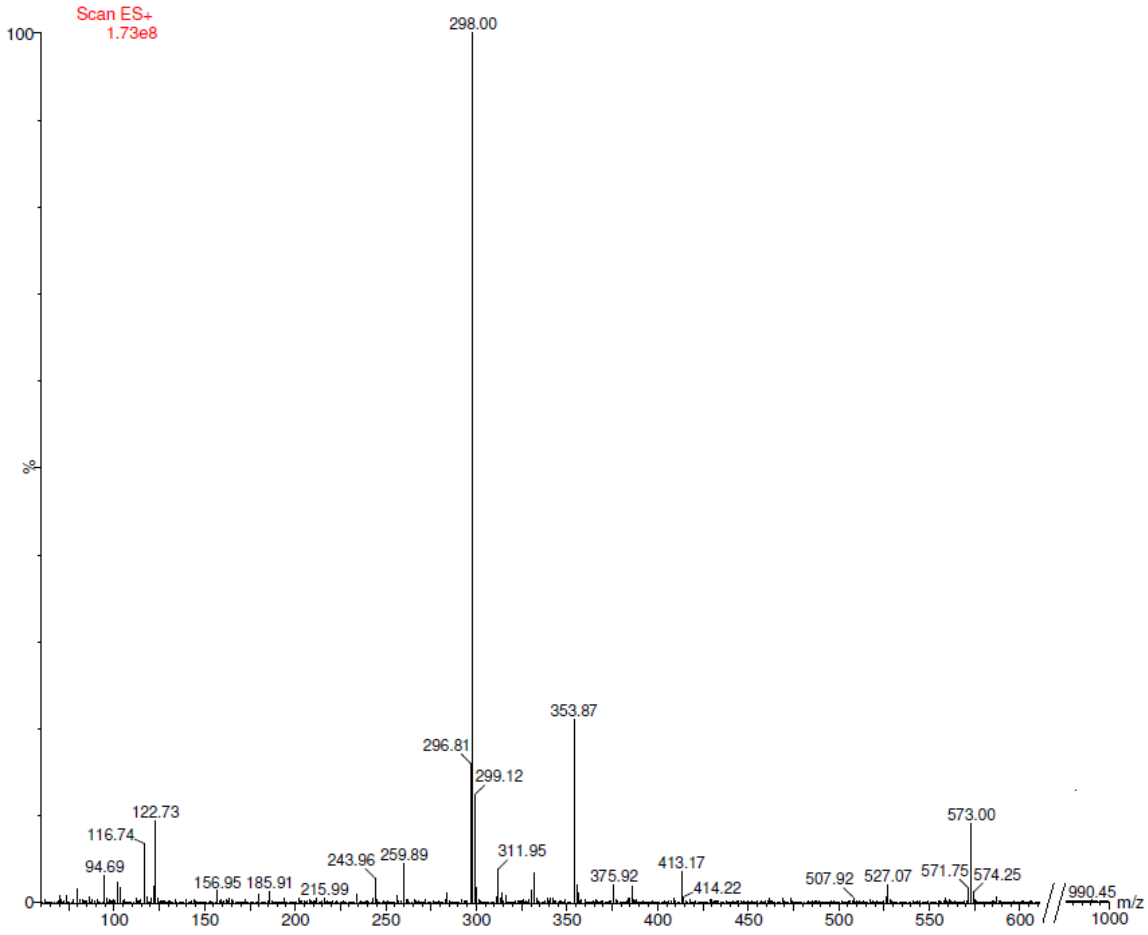

Figure 92 - Mass Spectrum of sample nr 226/10 (Full Scan m/z 60-800; ESI+; Capillary Potential 3,0kV; Source Potential 40V).

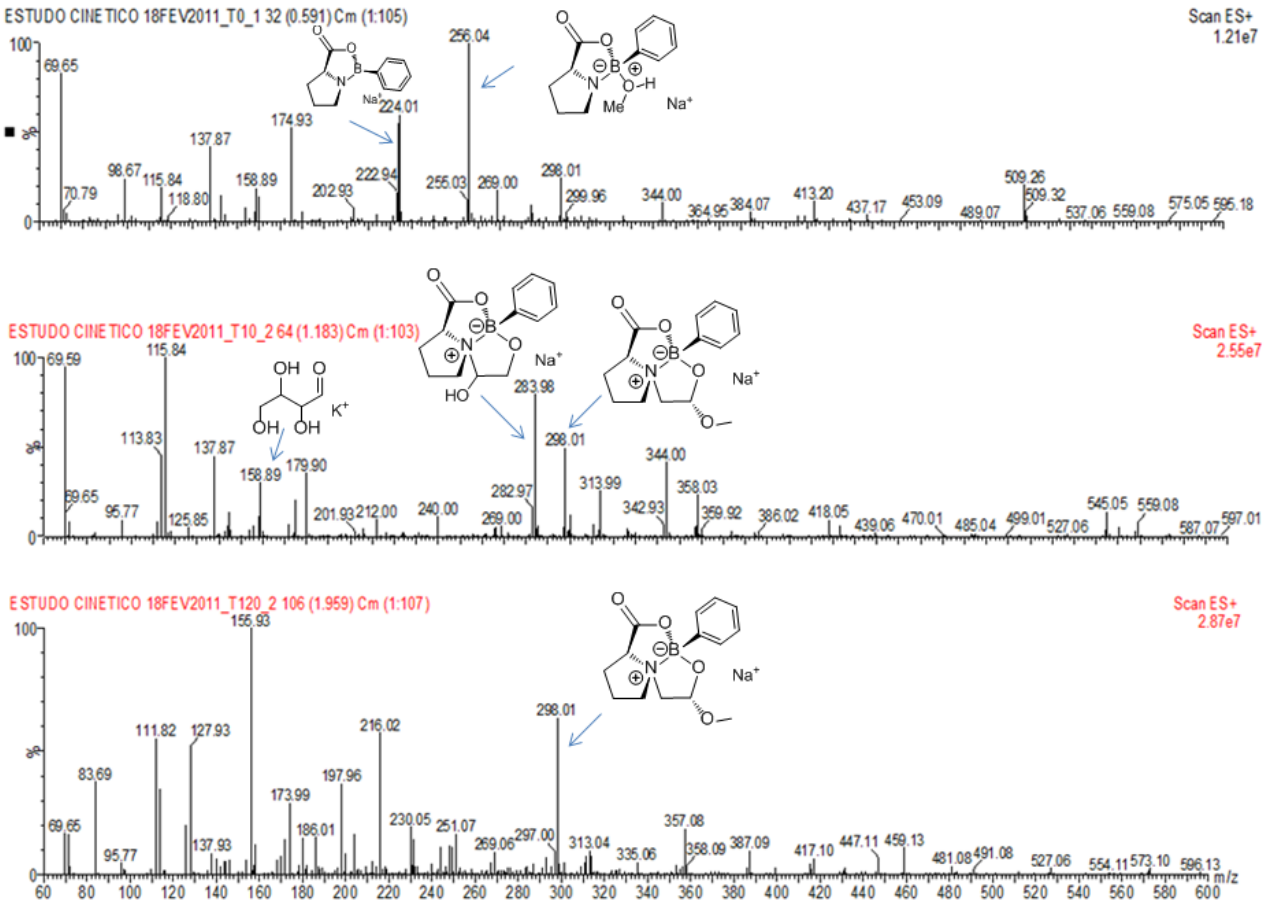

Figure 93 -Mass Spectrum of reaction products at T0, T10 and T120 (Full Scan m/z 60-600; ESI+; Capillary Potential 3,0kV; Source Potential 40V).

ESTUDO CINETICO 18FEV2011_T0_1 1 (0.018)

No	Mass	Inten	%BPI	%TIC	No	Mass	Inten	%BPI	%TIC
1:	69.65	2.40e7	90.71	5.50					
2:	70.85	3.34e6	12.63	0.77					
3:	72.49	3.90e6	14.75	0.89					
4:	98.67	7.46e6	28.24	1.71					
5:	113.77	2.75e6	10.40	0.63					
6:	115.78	3.31e6	12.52	0.76					
7:	137.87	4.42e6	16.74	1.02					
8:	142.84	4.39e6	16.61	1.01					
9:	158.95	4.70e6	17.81	1.08					
10:	174.93	7.63e6	28.89	1.75					
11:	222.94	4.83e6	18.30	1.11					
12:	224.01	2.11e7	80.05	4.86					
13:	255.03	3.91e6	14.78	0.90					
14:	256.04	1.82e7	68.73	4.17					
15:	298.01	5.34e6	20.21	1.23					
16:	413.20	4.45e6	16.85	1.02					
17:	509.26	2.64e7	100.00	6.07					
18:	510.33	5.89e6	22.29	1.35					

Figure 94 - List of signal intensities of m/z ions on full scan at T0 (m/z 60-600) mass spectrum.

ESTUDO CINETICO 18FEV2011_T10_2 1 (0.018)

No	Mass	Inten	%BPI	%TIC	No	Mass	Inten	%BPI	%TIC
1:	69.65	2.31e7	97.63	5.51					
2:	71.61	3.28e6	13.86	0.78					
3:	95.77	2.90e6	12.24	0.69					
4:	113.83	9.77e6	41.27	2.33					
5:	115.84	2.37e7	100.00	5.64					
6:	137.87	1.06e7	44.59	2.52					
7:	144.92	3.89e6	16.45	0.93					
8:	157.94	3.04e6	12.85	0.72					
9:	158.89	8.14e6	34.39	1.94					
10:	174.93	5.13e6	21.67	1.22					
11:	179.90	1.13e7	47.54	2.68					
12:	212.00	3.16e6	13.35	0.75					
13:	240.00	2.63e6	11.12	0.63					
14:	265.92	2.45e6	10.35	0.58					
15:	282.97	4.44e6	18.76	1.06					
16:	283.98	2.09e7	88.25	4.98					
17:	285.05	3.00e6	12.69	0.72					
18:	297.00	2.56e6	10.83	0.61					
19:	298.01	1.29e7	54.47	3.07					
20:	299.96	3.57e6	15.10	0.85					
21:	313.99	7.73e6	32.65	1.84					
22:	344.00	1.02e7	43.22	2.44					
23:	358.03	6.59e6	27.84	1.57					
24:	418.05	2.94e6	12.40	0.70					
25:	423.02	2.84e6	12.00	0.68					
26:	545.05	4.84e6	20.46	1.15					
27:	550.59	2.51e6	10.59	0.60					
28:	559.08	3.19e6	13.48	0.76					

Figure 95 - List of signal intensities of m/z ions on full scan at T10 (m/z 60-600) mass spectrum.

ESTUDO CINETICO 18FEV2011_T120_2 1 (0.018)

No	Mass	Inten	%BPI	%TIC	No	Mass	Inten	%BPI	%TIC
1:	69.65	5.76e6	20.79	1.00					
2:	71.61	4.81e6	17.35	0.84					
3:	83.69	1.08e7	38.99	1.88					
4:	111.82	1.48e7	53.34	2.57					
5:	113.83	9.16e6	33.05	1.59					
6:	125.85	1.07e7	38.78	1.87					
7:	127.93	1.64e7	59.27	2.85					
8:	145.99	3.20e6	11.54	0.56					
9:	153.92	2.86e6	10.32	0.50					
10:	155.93	2.77e7	100.00	4.81					
11:	157.94	3.54e6	12.78	0.62					
12:	171.91	4.92e6	17.75	0.85					
13:	173.99	8.72e6	31.46	1.51					
14:	179.97	4.32e6	15.59	0.75					
15:	185.94	6.53e6	23.55	1.13					
16:	197.96	1.13e7	40.74	1.96					
17:	204.00	4.49e6	16.19	0.78					
18:	216.02	1.52e7	54.85	2.64					
19:	230.05	5.18e6	18.69	0.90					
20:	231.00	5.41e6	19.51	0.94					
21:	244.02	2.96e6	10.68	0.51					
22:	248.05	3.59e6	12.94	0.62					
23:	249.06	3.56e6	12.83	0.62					
24:	251.07	4.21e6	15.18	0.73					
25:	269.06	3.00e6	10.84	0.52					
26:	293.10	3.69e6	13.32	0.64					
27:	296.94	3.86e6	13.92	0.67					
28:	298.01	1.93e7	69.61	3.35					
29:	311.03	3.56e6	12.84	0.62					
30:	312.98	2.83e6	10.19	0.49					
31:	313.99	3.76e6	13.58	0.65					
32:	357.15	9.82e6	35.41	1.70					
33:	387.09	3.96e6	14.27	0.69					
34:	417.10	2.99e6	10.78	0.52					
35:	447.11	2.87e6	10.35	0.50					
36:	459.13	3.68e6	13.27	0.64					

Figure 96 - List of signal intensities of m/z ions on full scan at T120 (m/z 60-600) mass spectrum-ray Crystallography.

Crystals of compound 1suitable for X-ray diffraction study were mounted on a loop with protective oil. X-ray data were collected at 150K on a Bruker AXS-KAPPA APEX II diffractometer using graphite monochromated Mo-Kα radiation (λ=0.71069 Å) and operating at 50kV and 30 mA. Cell parameters were retrieved using Bruker SMART1 software and refined using Bruker SAINT2 on all observed reflections. Absorption corrections were applied using SADABS3. Structure solution and refinement were performed using direct methods with program SIR974 and SHELXL975, both included in the package of programs WINGX-Version 1.70.016. Non-hydrogen atoms were refined anisotropically. A full-matrix least-squares refinement was used for the non-hydrogen atoms with anisotropic thermal parameters. All hydrogen atoms were inserted in idealized positions and allowed to refine riding in the parent carbon atom.

Crystallographic data for the compound 1: C42H54B3N3O12, fw=825.31, orthorhombic, space group P212121, a=9.9490(6) Å, b=19.6140(12) Å, c=21.5700(12) Å, V = 4209.2(4) Å3, Z=4, T=150K, ρ calc = 1.302 mg.m-3, μ= 0.094 mm-1, F(000) = 1752, colorless crystal (0.18 x 0.12 x 0.10 mm). Of 18706 reflections collected, 7938 were independent (Rint= 0.0587); 543 variables refined with 7938 reflections to final R indices R1(I > 2σ(I))= 0.0598, wR2(I > 2σ(I))= 0.1077, R1(all data)= 0.1414, wR2(all data)= 0.1261, GOF=0.931.

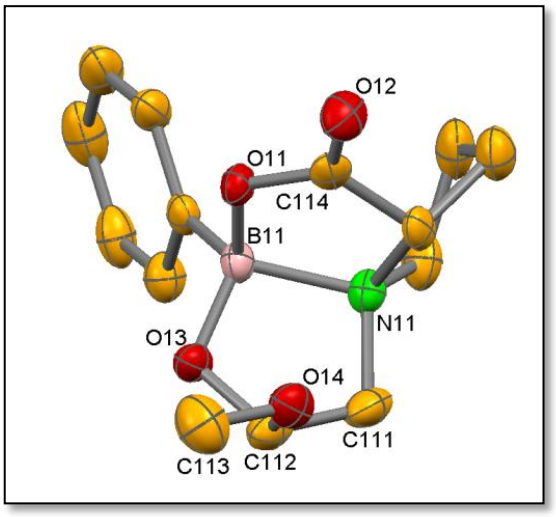

Figure 97 – Molecular diagram for compound 1. Ellipsoids are set at 50% probability.

Bond	Bond distances / Å				
	Mol 1	Mol 2	Mol 3	CSD[8] range	CSD[8] average
B1-O1	1.487(5)	1.480(5)	1.494(4)	1.381 - 1.678	1.477
B1-O3	1.451(5)	1.421(5)	1.464(4)	1.289 - 1.548	1.460
B1-N1	1.683(5)	1.686(5)	1.679(5)	1.559 - 1.898	1.644
O4-C12	1.417(4)	1.435(9)	1.406(5)	1.404 - 1.503	1.439
O4-C13	1.427(4)	1.402(10)	1.416(5)	1.360 - 1.511	1.432

Figure 98 – Selected bond distances for compound 1.

7.4 DFT calculations

Compound 1

All calculations were performed using the Gaussian 03 software package,[126] and the PBE1PBE functional, without symmetry constraints. That functional uses a hybrid generalized gradient approximation (GGA), including 25 % mixture of Hartree-Fock [127] exchange with DFT [128] exchange-correlation, given by Perdew, Burke and Ernzerhof functional (PBE). [129] The optimized geometries were obtained with a standard 6-31G(d,p) basis set. Transition state optimizations were performed with the Synchronous Transit-Guided Quasi-Newton Method (STQN) developed by Schlegel et al, [130] after a thorough search of the Potential Energy Surfaces (PES). Frequency calculations were performed to confirm the nature of the stationary points, yielding one imaginary frequency for the transition states and none for the minima. Each transition state was further confirmed by following its vibrational mode downhill on both sides, and obtaining the minima presented on the energy profiles. The energy values reported result from single point calculations using a standard 6-311++G(d,p)[131] basis set and the geometries optimized at the PBE1PBE/6-31G(d,p) level.

Energy profile for the entire mechanism for the formation of compound 1

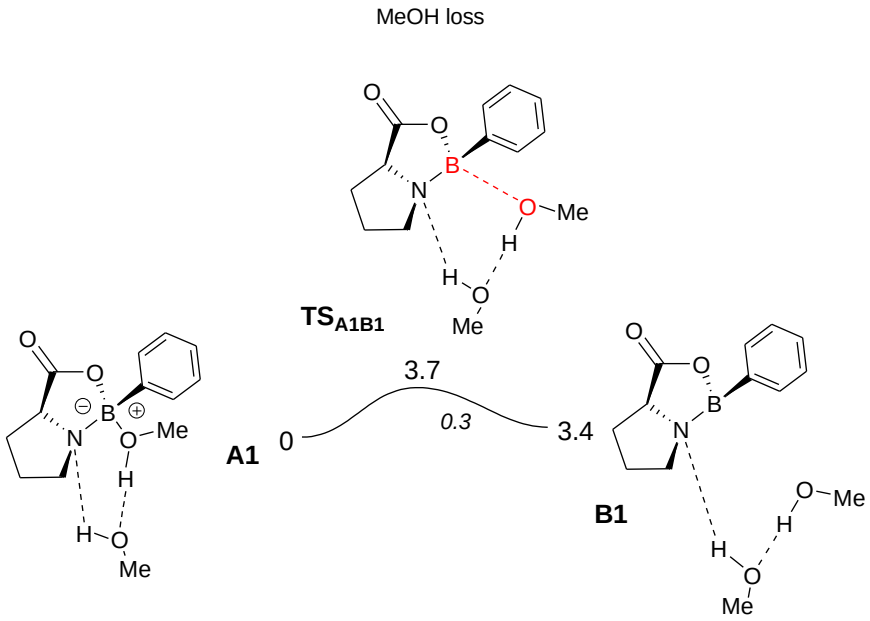

Figure 99 - Energy profile for MeOH decoordination, from A to B. The energy values (kcal/mol) are referred to A1 and the value in italics correspond to the energy barrier. The main transformation is highlighted in red, in the transition state.

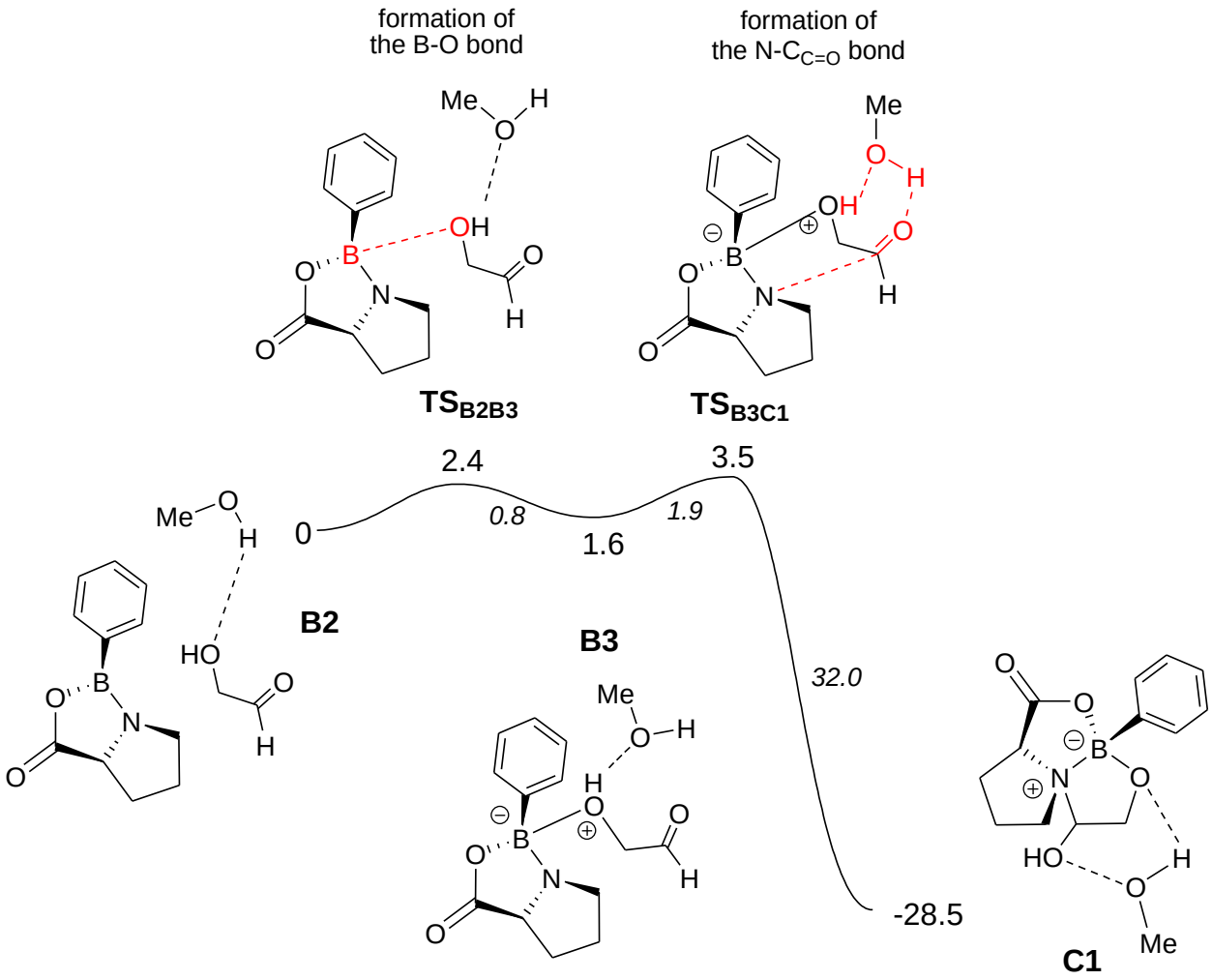

Figure 100 – Energy profile for the formation of intermediate C: the complex between proline, boronic acid and glycolaldehyde. The energy values (kcal/mol) are referred to B2 and values in italics correspond to energy barriers. The main transformations in each step are highlighted in red in the corresponding transition state.

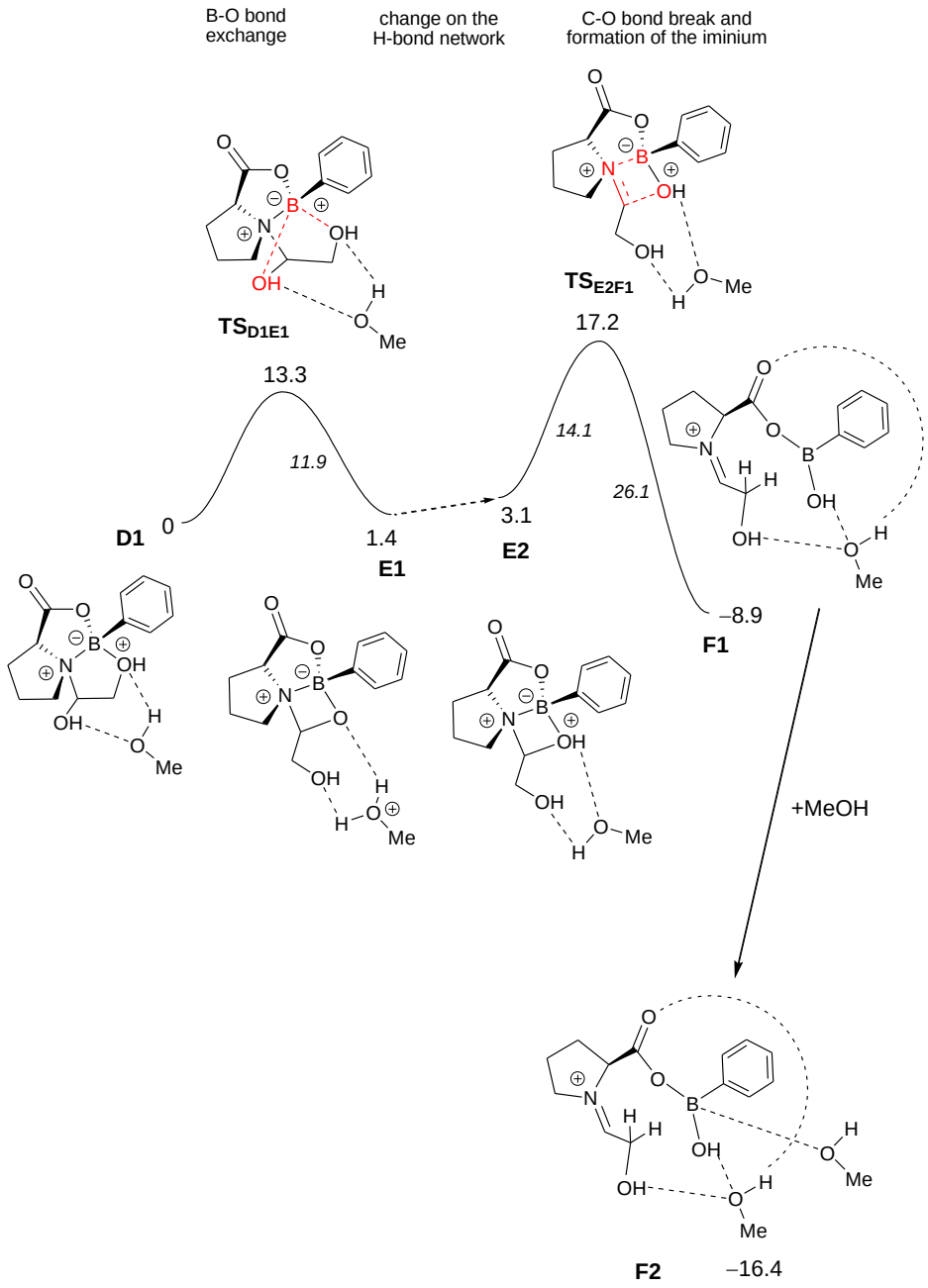

Figure 101 - Energy profile for the formation of the iminium ion F. The energy values (kcal/mol) are referred to D1 and values in italics correspond to energy barriers. The main transformations in each step are highlighted in red in the corresponding transition state.

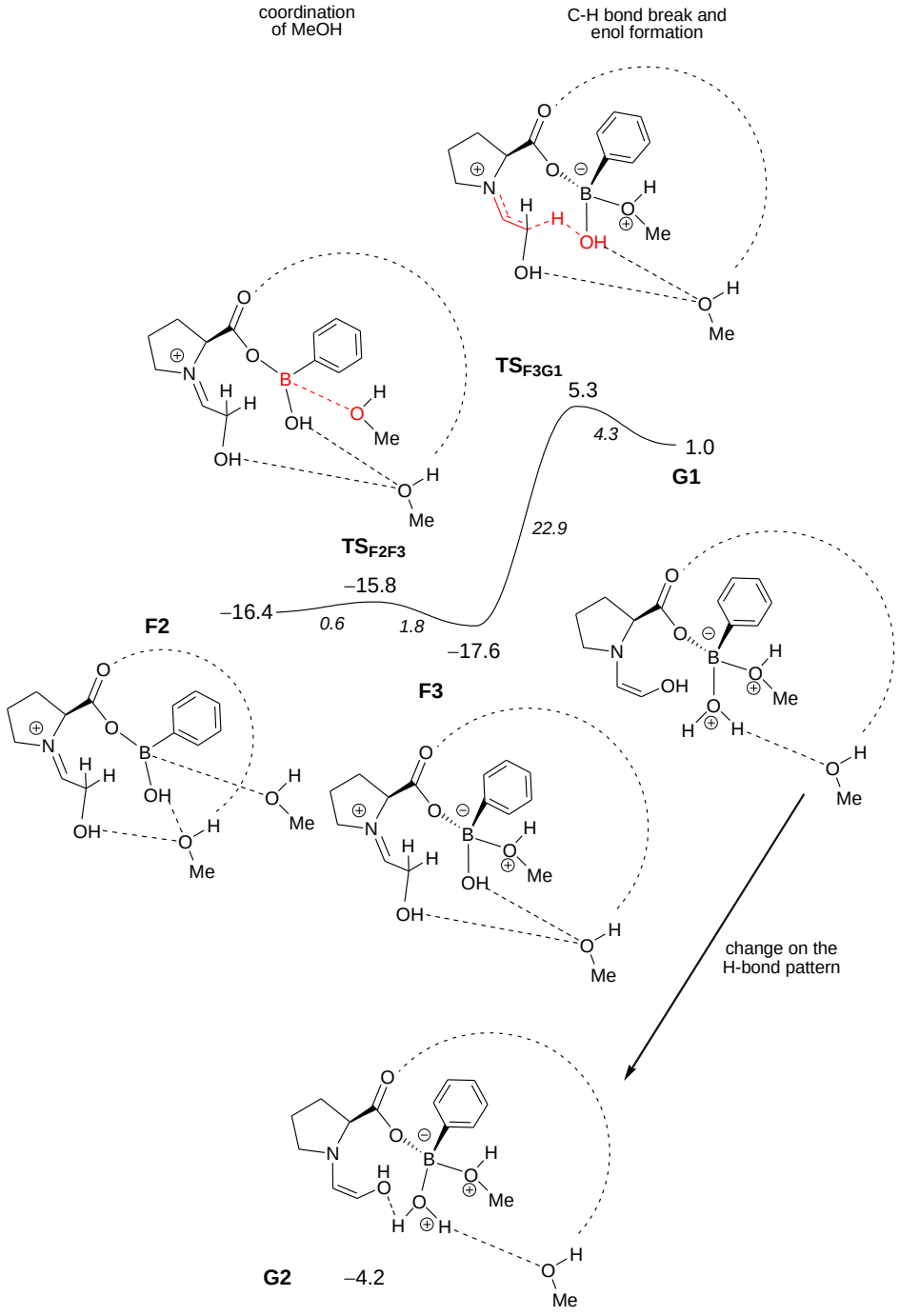

Figure 102 - Energy profile for the formation of the enol G. The energy values (kcal/mol) are referred to D1 and values in italics correspond to energy barriers. The main transformations in each step are highlighted in red in the corresponding transition state.

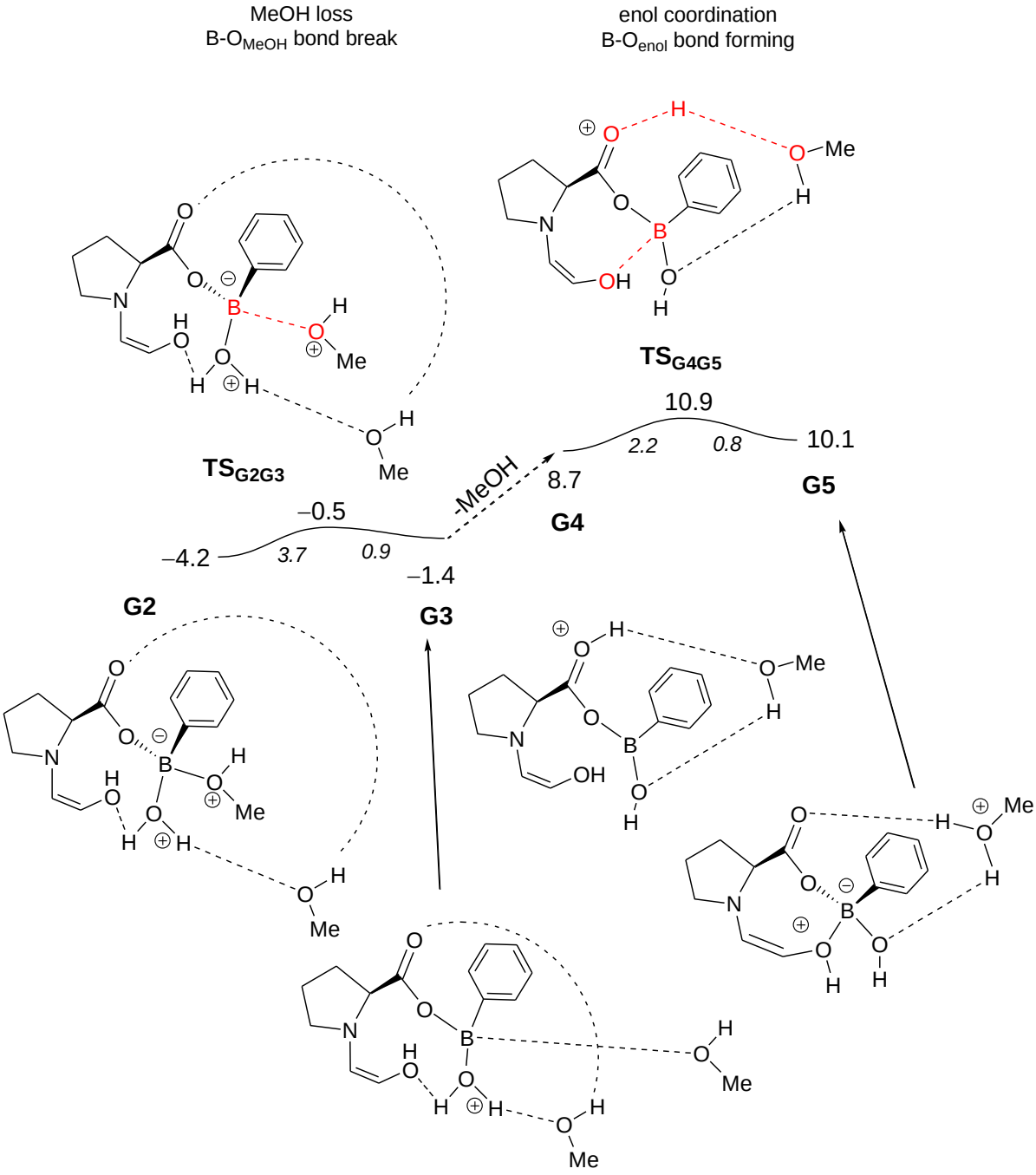

Figure 103 – Energy profile for the coordination of enol G. The energy values (kcal/mol) are referred to D1 and values in italics correspond to energy barriers. The main transformations in each step are highlighted in red in the corresponding transition state.

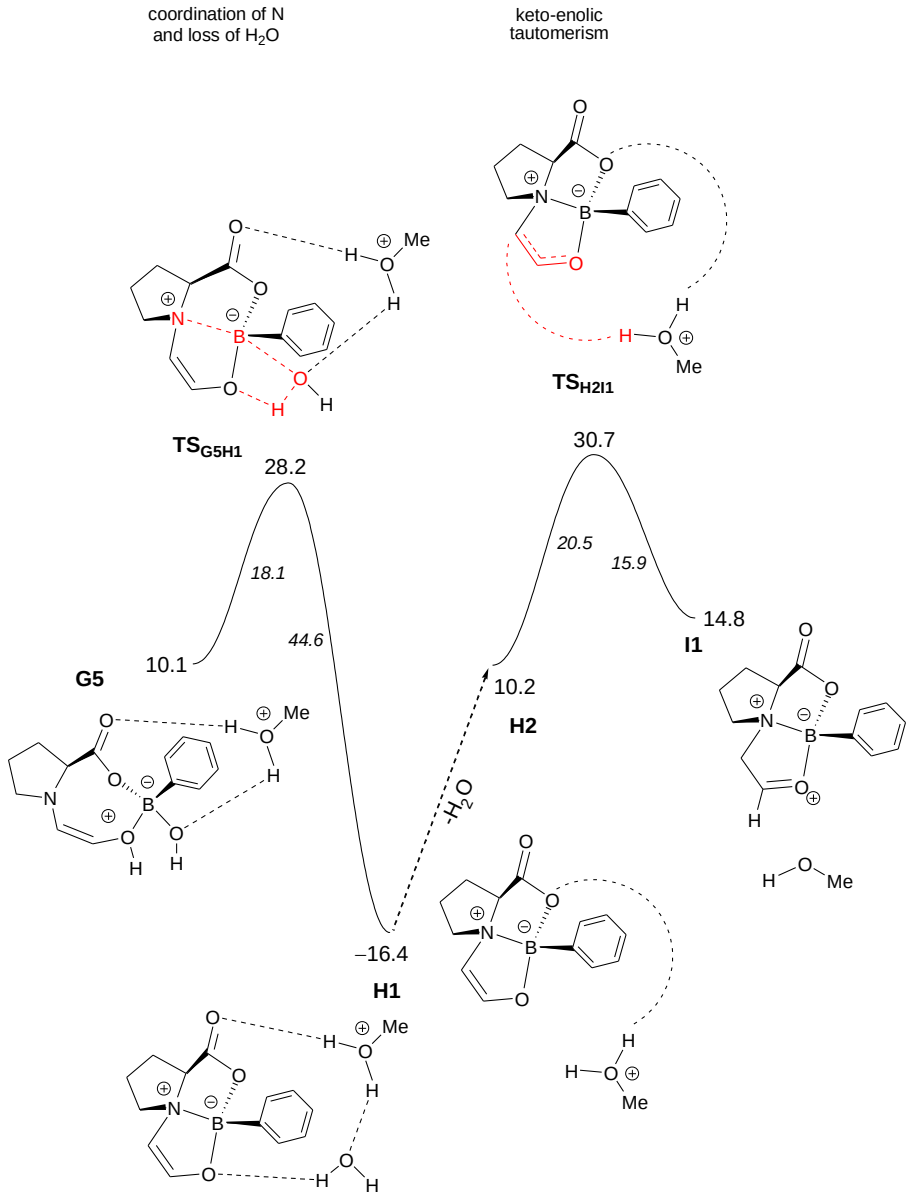

Figure 104 - Energy profile for the formation of coordinated adehylde, I, with elimination of one water molecule. The energy values (kcal/mol) are referred to D1 and values in italics correspond to energy barriers. The main transformations in each step are highlighted in red in the corresponding transition state.

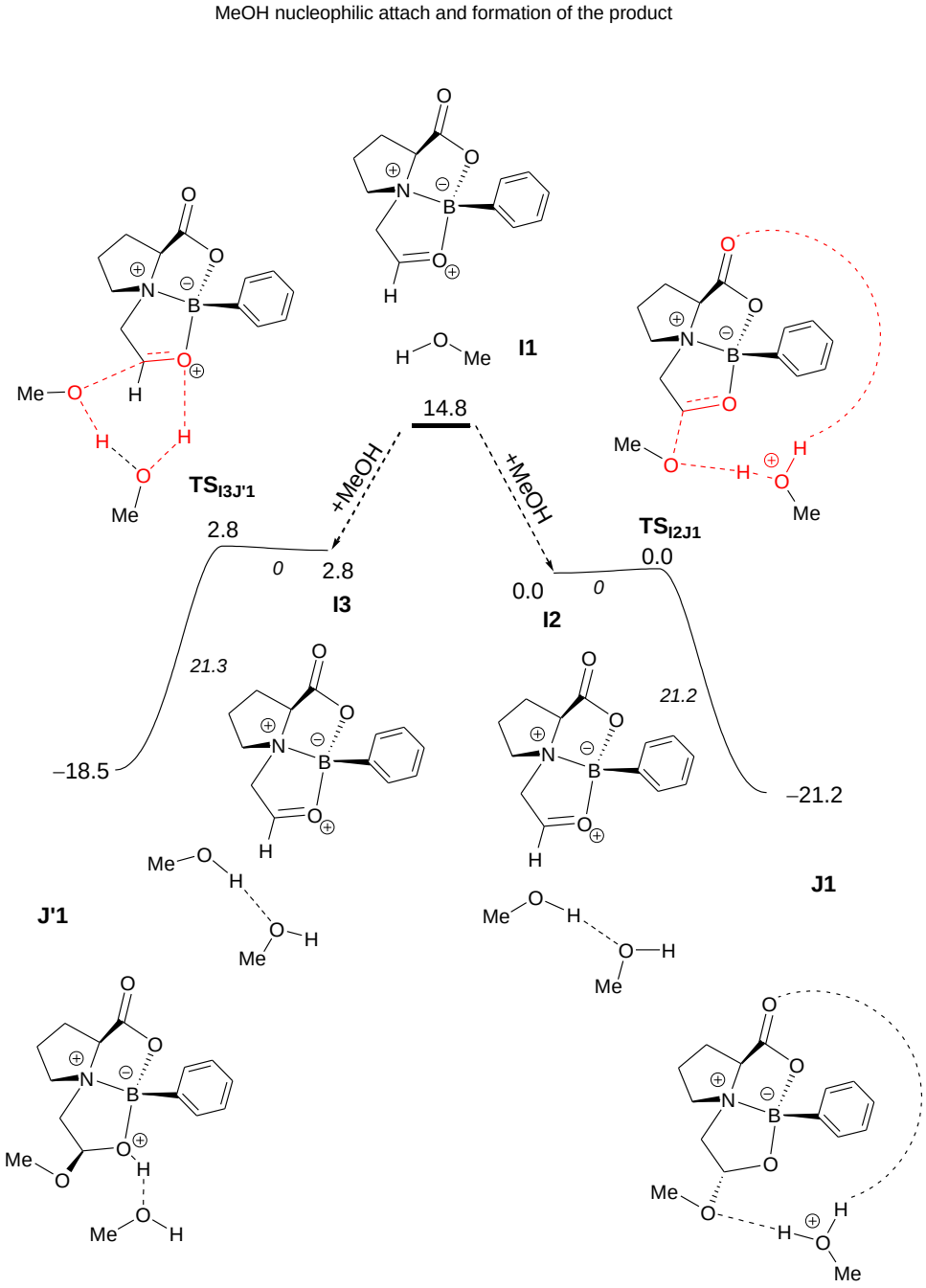

Figure 105– Energy profile for the formation of the two epimers of the product, J and J', by means of nucleophilic attack from methanol. The energy values (kcal/mol) are referred to D1 and values in italics correspond to energy barriers. The main transformations in each step are highlighted in red in the corresponding transition state.

Atomic coordinates for the optimized species

H_2O

H	*-0.543970*	*-0.163342*	*-0.198984*
O	*0.140786*	*0.430544*	*0.119861*
H	*0.868184*	*-0.155002*	*0.346423*

MeOH

C	*-0.476279*	*-0.051405*	*0.070908*
O	*0.555682*	*0.779749*	*0.545500*
H	*1.299299*	*0.217987*	*0.780535*
H	*-1.314871*	*0.597757*	*-0.193321*
H	*-0.831645*	*-0.767510*	*0.827108*
H	*-0.191986*	*-0.615678*	*-0.830031*

B

O	*1.603782*	*-0.028904*	*1.970849*
N	*1.718195*	*0.060532*	*-0.332843*
O	*3.511208*	*1.053340*	*2.520039*
C	*2.953430*	*0.639603*	*0.174958*
H	*3.826503*	*0.011264*	*-0.050954*
C	*2.770863*	*0.616020*	*1.686588*
C	*-2.623207*	*-1.169594*	*2.011230*
H	*-3.203753*	*-1.068831*	*2.923838*
C	*1.369063*	*0.706248*	*-1.583887*
H	*0.299244*	*0.612954*	*-1.784194*
H	*1.916111*	*0.252553*	*-2.422117*
C	*-0.543652*	*-0.827719*	*0.797351*
C	*-1.132608*	*-1.434923*	*-0.322430*
H	*-0.549919*	*-1.564792*	*-1.231140*
C	*-1.310794*	*-0.712891*	*1.966984*
H	*-0.864811*	*-0.259812*	*2.848272*
C	*-3.191409*	*-1.761051*	*0.885108*
H	*-4.215936*	*-2.121286*	*0.918665*
B	*0.907991*	*-0.288994*	*0.771035*
C	*-2.443080*	*-1.898551*	*-0.281739*
H	*-2.880924*	*-2.371299*	*-1.156357*
C	*3.096439*	*2.020663*	*-0.507210*
H	*3.990154*	*2.031503*	*-1.136702*
H	*3.207751*	*2.821688*	*0.227821*
C	*1.820423*	*2.156296*	*-1.357307*
H	*1.043717*	*2.686282*	*-0.795818*
H	*1.991119*	*2.702701*	*-2.288939*

J

O	*1.257013*	*-1.905747*	*0.300396*
O	*1.291281*	*0.033174*	*1.805769*
N	*1.417530*	*0.349918*	*-0.633080*
O	*3.552423*	*-1.460020*	*0.207878*
O	*2.692185*	*1.670666*	*2.438458*
C	*2.386920*	*-1.812264*	*-0.491533*
H	*2.536290*	*-2.776837*	*-1.002565*
C	*2.352386*	*1.271044*	*0.096601*
H	*3.387953*	*1.012878*	*-0.131784*
C	*2.142132*	*1.016290*	*1.587726*
C	*-2.997261*	*0.333431*	*1.435292*
H	*-3.531408*	*1.021117*	*2.085717*
C	*0.490252*	*1.213684*	*-1.425322*
H	*-0.485698*	*0.728915*	*-1.488121*
H	*0.906409*	*1.328879*	*-2.433546*
C	*-0.886145*	*-0.586271*	*0.636244*
C	*-1.622005*	*-1.444398*	*-0.193437*
H	*-1.087181*	*-2.163668*	*-0.809905*
C	*2.094602*	*-0.674763*	*-1.459576*
H	*2.983734*	*-0.269367*	*-1.949775*
H	*1.383174*	*-1.021945*	*-2.213084*
C	*-1.605038*	*0.295021*	*1.455139*
H	*-1.060783*	*0.942022*	*2.139522*
C	*-3.704952*	*-0.517759*	*0.590660*
H	*-4.791188*	*-0.491946*	*0.574122*
B	*0.706243*	*-0.612591*	*0.621875*
C	*-3.013492*	*-1.412741*	*-0.222684*
H	*-3.560734*	*-2.091662*	*-0.871613*
C	*1.965082*	*2.691870*	*-0.309350*
H	*2.555411*	*3.018420*	*-1.172502*
H	*2.150165*	*3.385326*	*0.513761*
C	*3.863985*	*-2.361939*	*1.253251*
H	*4.795571*	*-2.013469*	*1.701822*
H	*4.009865*	*-3.379992*	*0.863697*
H	*3.073786*	*-2.377891*	*2.009791*
C	*0.494872*	*2.544669*	*-0.696389*
H	*-0.142595*	*2.486533*	*0.192573*
H	*0.125314*	*3.357512*	*-1.325930*

J'

O	*1.086307*	*0.605002*	*0.313207*
O	*-0.420424*	*-0.436913*	*1.939790*
N	*-1.120615*	*1.592154*	*0.724585*
O	*2.253732*	*2.582216*	*0.126233*
H	*1.442642*	*1.898059*	*1.874992*

O	-1.503603	-0.064132	3.872927
C	1.243354	1.904462	0.784172
C	-1.609988	1.591432	2.138620
H	-1.134775	2.395820	2.708062
C	-1.173739	0.264188	2.759937
C	-2.180866	-2.742994	-1.262583
H	-2.876288	-3.539817	-1.012270
C	-2.320946	1.740269	-0.151319
H	-2.147748	1.206771	-1.087844
H	-2.465991	2.807070	-0.360401
C	-0.774479	-0.884900	-0.549777
C	-0.374428	-0.727387	-1.884674
H	0.355232	0.042865	-2.124771
C	-0.073005	2.595260	0.447435
H	-0.254427	3.527365	0.990278
H	-0.056047	2.797142	-0.626768
C	-1.679417	-1.915263	-0.260773
H	-1.973317	-2.085777	0.772588
C	-1.781381	-2.556621	-2.583353
H	-2.169213	-3.201629	-3.367208
B	-0.219735	0.091950	0.575984
C	-0.871361	-1.548262	-2.893251
H	-0.543698	-1.409004	-3.920221
C	-3.130685	1.738678	2.075185
H	-3.414981	2.793431	2.154198
H	-3.599336	1.195432	2.898494
C	3.536986	2.049289	0.389030
H	3.771268	2.088869	1.462756
H	4.252905	2.667649	-0.155003
H	3.611291	1.011852	0.047312
C	-3.466287	1.200715	0.685483
H	-3.454690	0.105651	0.672592
H	-4.438146	1.534207	0.314252

A1

O	1.798860	0.324042	2.231839
N	1.786530	0.662895	-0.151347
C	3.414697	-1.629447	-2.323282
C	1.632375	-2.707810	1.617142
O	3.513691	1.666611	2.802335
O	2.173123	-1.433355	-1.676226
C	2.938737	1.364966	0.454925
O	1.976612	-1.601551	0.783398
H	2.108328	-0.486811	-1.295495
H	3.901323	0.941572	0.141695
H	3.467084	-2.668965	-2.657111
C	2.814040	1.154383	1.966839
C	-2.483490	-0.244818	2.227909
H	4.267875	-1.435056	-1.658835
H	-3.047752	0.089869	3.094412
C	0.926702	1.689550	-0.781912
H	-0.127519	1.430184	-0.665047
H	3.504313	-0.983143	-3.204214
H	2.353014	-3.509686	1.444589
H	1.140592	1.736532	-1.859181
C	-0.354028	-0.441551	1.062005
C	-1.030580	-1.098751	0.021253
H	0.614906	-3.050261	1.411509
H	-0.474793	-1.435493	-0.853615
H	1.704650	-2.364122	2.649298
C	-1.109390	-0.023389	2.164498
H	-0.603970	0.480714	2.984379
C	-3.133344	-0.896825	1.183956
H	-4.204783	-1.071613	1.231045
B	1.213298	-0.176554	0.996256
C	-2.402824	-1.324931	0.077323
H	-2.904160	-1.834239	-0.741581
C	2.816656	2.843539	0.073300
H	3.345442	3.035326	-0.866993
H	2.055157	-1.804967	-0.218459
H	3.249501	3.482991	0.846502
C	1.310928	3.009552	-0.119767
H	0.810719	3.102415	0.851666
H	1.044078	3.882794	-0.721408

TSA1B1

O	1.480137	0.559898	2.327123
N	1.605510	0.835776	0.007583
C	2.895996	-1.489839	-2.498699
C	2.270325	-2.825984	1.979318
O	3.439499	1.491860	2.955039
O	1.851591	-1.535374	-1.552302
C	2.868098	1.316858	0.586719
O	2.685701	-1.861278	1.042389
H	1.820031	-0.682050	-1.068761
H	3.713287	0.676088	0.310304
H	2.913815	-2.449970	-3.020772
C	2.682038	1.159417	2.090306
C	-2.740635	-0.611371	2.213717
H	3.879984	-1.338390	-2.032705
H	-3.345776	-0.572309	3.115004
C	1.125440	1.817015	-0.972571
H	0.035720	1.781839	-1.044804
H	2.741897	-0.701519	-3.249051

H	2.759178	-3.798873	1.822660
H	1.537179	1.599358	-1.967919
C	-0.635782	-0.178327	1.076318
C	-1.187059	-0.720007	-0.096244
H	1.181981	-2.980729	1.971470
H	-0.575371	-0.802606	-0.991636
H	2.549729	-2.462124	2.971355
C	-1.432086	-0.143047	2.231928
H	-1.011875	0.257422	3.150673
C	-3.272713	-1.136734	1.037878
H	-4.294104	-1.507209	1.022466
B	0.810971	0.367600	1.117238
C	-2.493265	-1.197378	-0.115065
H	-2.902931	-1.622790	-1.026775
C	3.052371	2.763763	0.092415
H	3.794546	2.786265	-0.711572
H	2.382980	-2.118339	0.155141
H	3.411962	3.416304	0.891851
C	1.669487	3.146984	-0.447020
H	1.026945	3.508831	0.364174
H	1.711803	3.925568	-1.213571

B1

O	1.335467	0.324655	2.301337
N	1.496732	0.782473	0.025764
C	2.698630	-1.657274	-2.455684
C	3.170434	-2.687295	2.014760
O	3.324573	1.117792	3.023710
O	1.797721	-1.721721	-1.370489
C	2.766743	1.188938	0.645775
O	3.354878	-1.823606	0.918804
H	1.713284	-0.829722	-0.976889
H	3.598527	0.552594	0.326368
H	2.756529	-2.655412	-2.896906
C	2.567214	0.899271	2.124919
C	-3.003514	-0.385133	2.057079
H	3.710541	-1.363965	-2.143198
H	-3.633129	-0.307479	2.938843
C	1.105775	1.793544	-0.958485
H	0.022825	1.787544	-1.103029
H	2.357439	-0.962754	-3.235904
H	3.502363	-3.714019	1.800735
H	1.581288	1.590181	-1.927803
C	-0.833961	-0.113872	0.995263
C	-1.388530	-0.593365	-0.202089
H	2.124996	-2.724932	2.352504
H	-0.753741	-0.717730	-1.076184
H	3.772333	-2.301491	2.841691
C	-1.661920	-0.028265	2.125441
H	-1.241553	0.322345	3.064299
C	-3.537679	-0.849870	0.856943
H	-4.584976	-1.134276	0.803143
B	0.649428	0.314105	1.087396
C	-2.727781	-0.961630	-0.270873
H	-3.139858	-1.342181	-1.201090
C	2.980412	2.668300	0.263350
H	3.785992	2.742786	-0.473072
H	2.782414	-2.106684	0.185408
H	3.272019	3.268647	1.128703
C	1.643683	3.094957	-0.358111
H	0.953156	3.446741	0.417055
H	1.753850	3.894402	-1.095882

B2

O	0.394292	1.252945	-2.024581
C	-4.922287	1.777676	1.094416
H	-0.937872	0.269830	3.316543
O	-4.019892	2.276183	0.123149
N	0.113139	-0.560183	-0.615362
H	-4.046068	1.678368	-0.637137
C	-1.406145	0.522625	2.336438
H	-4.893210	2.465356	1.943018
O	2.645627	1.442950	-2.003800
H	-4.640567	0.778015	1.444854
C	-0.844643	1.764834	1.698072
H	-5.950446	1.754476	0.711975
C	1.534033	-0.248164	-0.632856
O	-1.306019	2.055317	0.428878
H	1.893225	0.133252	0.334380
O	-2.300843	-0.153013	1.884756
C	1.644322	0.901880	-1.627126
H	-2.283496	2.145545	0.435950
C	-3.526566	0.839137	-3.872333
H	0.246958	1.637986	1.655937
H	-3.712958	1.314685	-4.831073
H	-1.008578	2.583057	2.428629
C	-0.061333	-1.992957	-0.473680
H	-1.030521	-2.306637	-0.867699
H	-0.015166	-2.290056	0.583454
C	-1.986191	0.283665	-2.069772
C	-3.042678	-0.362954	-1.406742
H	-2.873129	-0.795174	-0.424375
C	-2.255444	0.886957	-3.306872
H	-1.453103	1.405430	-3.824651

C	-4.560336	0.187262	-3.205175
H	-5.553646	0.148066	-3.643740
B	-0.543558	0.343354	-1.488646
C	-4.317688	-0.412795	-1.968990
H	-5.122576	-0.920162	-1.443294
C	2.264215	-1.565088	-0.988016
H	2.876372	-1.889118	-0.141711
H	2.934355	-1.433864	-1.841294
C	1.127007	-2.565038	-1.258737
H	0.876531	-2.576349	-2.325078
H	1.385182	-3.586500	-0.965411

TSB2B3

O	0.296533	1.422741	-1.726736
C	-4.813659	1.935342	1.104527
H	-0.848292	0.225112	3.285053
O	-3.895637	2.271475	0.075256
N	0.079953	-0.460032	-0.351661
H	-4.039951	1.664808	-0.666223
C	-1.378350	0.467670	2.337004
H	-4.638430	2.628884	1.929893
O	2.539558	1.520458	-1.931274
H	-4.666142	0.912465	1.467463
C	-0.778360	1.618799	1.574724
H	-5.848242	2.061988	0.765629
C	1.503595	-0.194089	-0.536734
O	-1.289174	1.795711	0.288518
H	2.014629	0.106141	0.391022
O	-2.371861	-0.133907	2.005678
C	1.552760	1.005046	-1.478019
H	-2.270327	1.957867	0.302568
C	-3.332475	0.603563	-3.898774
H	0.302034	1.454918	1.501700
H	-3.415125	0.986797	-4.912154
H	-0.912999	2.527535	2.186155
C	-0.141016	-1.895716	-0.453490
H	-1.160049	-2.109406	-0.782988
H	0.003511	-2.383761	0.521813
C	-2.015039	0.315254	-1.868027
C	-3.109586	-0.361684	-1.301094
H	-3.041150	-0.720850	-0.276767
C	-2.155417	0.793813	-3.177972
H	-1.325704	1.330202	-3.630226
C	-4.404114	-0.070471	-3.320590
H	-5.323237	-0.219959	-3.880365
B	-0.651976	0.546902	-1.103844
C	-4.291283	-0.553389	-2.016921
H	-5.122356	-1.084272	-1.559349
C	2.134693	-1.493848	-1.086110
H	2.729539	-1.974867	-0.303378
H	2.802439	-1.287725	-1.926486
C	0.925174	-2.361608	-1.449124
H	0.585642	-2.140134	-2.467495
H	1.138190	-3.432975	-1.389904

B3

O	0.241259	1.454496	-1.741408
C	-4.443191	1.813058	1.409639
H	0.019810	-0.302782	2.196162
O	-3.842727	2.228088	0.178114
N	-0.135734	-0.304326	-0.173529
H	-4.117680	1.613397	-0.520904
C	-0.877421	0.125735	1.699198
H	-4.264379	2.613191	2.130862
O	2.482229	1.335461	-1.917788
H	-3.990898	0.884571	1.773482
C	-0.764949	1.610939	1.369942
H	-5.524038	1.696747	1.286235
C	1.311423	-0.083739	-0.328427
O	-1.332533	1.842451	0.074969
H	1.762962	0.328484	0.586078
O	-1.985041	-0.403861	1.810029
C	1.446660	0.976535	-1.420544
H	-2.342449	1.996730	0.127699
C	-3.248918	0.514074	-4.063220
H	0.270469	1.960464	1.345183
H	-3.256399	0.819189	-5.106126
H	-1.322613	2.208874	2.096712
C	-0.398967	-1.736346	-0.394678
H	-1.370307	-1.884211	-0.865772
H	-0.422014	-2.250856	0.575197
C	-2.095796	0.412441	-1.920291
C	-3.215738	-0.260592	-1.395827
H	-3.200869	-0.583080	-0.353796
C	-2.137711	0.788804	-3.267457
H	-1.283562	1.310169	-3.690934
C	-4.350163	-0.143838	-3.524475
H	-5.216959	-0.357944	-4.143458
B	-0.829419	0.777843	-1.019787
C	-4.331934	-0.534687	-2.186018
H	-5.180907	-1.065276	-1.762115
C	1.945292	-1.432626	-0.689643
H	2.331954	-1.917601	0.212748
H	2.777115	-1.298106	-1.385425

C	0.765241	-2.220996	-1.253593
H	0.590781	-1.951900	-2.302113
H	0.906421	-3.304174	-1.203627

TSB3C1

O	0.211383	1.433611	-1.779191
C	-4.199298	1.991936	1.854353
H	-0.106564	-0.296650	2.055806
O	-3.893861	1.847802	0.465359
N	-0.253559	-0.270268	-0.146069
H	-4.021311	0.915634	0.237963
C	-0.917790	0.118976	1.407334
H	-3.913310	3.005725	2.142485
O	2.455545	1.290594	-1.844495
H	-3.645378	1.252286	2.440239
C	-0.796285	1.638842	1.226644
H	-5.276148	1.877819	2.015910
C	1.211918	-0.050452	-0.256047
O	-1.418942	1.896439	-0.050676
H	1.607610	0.390742	0.667058
O	-2.096336	-0.336192	1.504109
C	1.393821	0.964565	-1.382247
H	-2.439452	1.906460	0.100055
C	-3.170766	0.531375	-4.243432
H	0.222783	2.031440	1.176681
H	-3.149152	0.880911	-5.272101
H	-1.349238	2.176384	1.998413
C	-0.494154	-1.714871	-0.412235
H	-1.435167	-1.857081	-0.937401
H	-0.569016	-2.223655	0.554819
C	-2.118580	0.410348	-2.051061
C	-3.212501	-0.357942	-1.614585
H	-3.214843	-0.732665	-0.588313
C	-2.120478	0.842928	-3.382935
H	-1.282957	1.433086	-3.744710
C	-4.246340	-0.225843	-3.789004
H	-5.064768	-0.470797	-4.460260
B	-0.915661	0.819701	-1.092867
C	-4.264938	-0.673357	-2.470078
H	-5.095820	-1.274993	-2.110908
C	1.858782	-1.403940	-0.551473
H	2.160988	-1.887210	0.383352
H	2.745483	-1.278417	-1.177210
C	0.718766	-2.176995	-1.206300
H	0.613481	-1.890042	-2.259318
H	0.850354	-3.261435	-1.166367

C1

O	0.173438	1.653747	-1.616384
C	-4.508908	2.015879	2.208331
H	0.295176	0.002032	1.979453
O	-3.818546	1.157038	1.325313
N	-0.277605	-0.188206	-0.061796
H	-2.494405	0.103853	1.715449
C	-0.580078	0.254781	1.367871
H	-5.187784	2.686033	1.667564
O	2.370039	1.308853	-1.945769
H	-3.828637	2.625937	2.818509
C	-0.784626	1.755694	1.182756
H	-5.103887	1.391524	2.878595
C	1.178278	-0.085813	-0.392751
O	-1.593574	1.866719	0.034371
H	1.752814	0.207360	0.492328
O	-1.665529	-0.404077	1.880383
C	1.321287	1.037423	-1.416096
H	-3.265402	1.671664	0.703666
C	-2.551574	0.059890	-4.455142
H	0.175434	2.275004	1.048095
H	-2.239091	0.069473	-5.496004
H	-1.290696	2.190876	2.049924
C	-0.685238	-1.600121	-0.338134
H	-1.730219	-1.626033	-0.644167
H	-0.575642	-2.176962	0.584827
C	-2.052351	0.523513	-2.111578
C	-3.341259	0.067032	-1.792947
H	-3.682662	0.073982	-0.760306
C	-1.683494	0.513528	-3.465002
H	-0.703097	0.889543	-3.745783
C	-3.820644	-0.396863	-4.112283
H	-4.501706	-0.750947	-4.881470
B	-1.021784	1.036539	-1.007957
C	-4.214851	-0.388819	-2.776896
H	-5.207393	-0.734778	-2.500478
C	1.608414	-1.452891	-0.928324
H	2.037315	-2.057769	-0.122625
H	2.366063	-1.334818	-1.706127
C	0.291819	-2.059629	-1.405560
H	0.001137	-1.651654	-2.379867
H	0.321769	-3.148741	-1.488690

D1

O	1.516107	1.327275	-1.921637
C	1.365368	-1.529982	4.154185
H	2.918271	-2.339259	-0.680462

O	1.346128	-0.784139	2.932398
N	1.387175	-1.024747	-1.344386
C	2.250344	-1.603143	-0.215780
H	0.402228	-2.012383	4.347222
O	2.723061	1.193003	-3.819657
H	1.630904	-0.885143	4.996700
C	3.017330	-0.393651	0.296082
H	2.129982	-2.299353	4.042009
C	2.177871	-0.828181	-2.620740
O	1.961043	0.596490	0.379036
H	3.210724	-1.164645	-2.486754
O	1.470516	-2.206910	0.719639
C	2.193780	0.672219	-2.885390
H	0.655142	-0.114180	2.982441
C	-2.458808	2.260078	-0.668640
H	3.797263	-0.056880	-0.392769
H	-2.962857	3.085044	-1.162699
H	3.422083	-0.557909	1.295297
C	0.241988	-1.947109	-1.698702
H	-0.611349	-1.726135	-1.061547
H	0.572685	-2.971416	-1.506467
C	-0.502129	0.829689	-0.448362
C	-1.160077	0.150200	0.592049
H	-0.677172	-0.692473	1.083340
C	-1.177312	1.890584	-1.069219
H	-0.689041	2.436674	-1.871623
C	-3.091172	1.573541	0.362632
H	-4.091336	1.858918	0.674346
B	0.952959	0.484660	-0.922169
C	-2.440198	0.514177	0.993434
H	-2.936564	-0.029797	1.791778
C	1.448410	-1.616192	-3.713284
H	1.883865	-2.615269	-3.808469
H	1.544881	-1.111310	-4.676746
C	0.022518	-1.700213	-3.178512
H	-0.519124	-0.760547	-3.336839
H	-0.560606	-2.502095	-3.635940
H	1.364077	-1.653023	1.537086
H	2.285741	1.501235	0.508016

TSD1E1

O	1.346334	1.138780	-0.832214
C	1.049098	0.788757	3.334745
H	1.626670	-3.101193	-0.440935
O	1.970174	0.023452	2.558919
N	1.275520	-1.190258	-1.301122
C	1.820301	-2.071950	-0.118375
H	0.404460	1.411344	2.704862
O	3.203106	1.709220	-1.991709
H	1.581330	1.417943	4.053882
C	3.314127	-1.911185	0.100037
H	0.431217	0.076733	3.882702
C	2.280649	-0.525160	-2.216662
O	3.595408	-0.546547	0.313936
H	3.254385	-1.005104	-2.160024
O	1.059521	-1.793003	0.974761
C	2.399221	0.890455	-1.687751
H	2.562669	0.604889	2.070217
C	-2.787760	1.718392	0.096863
H	3.874798	-2.323540	-0.750354
H	-3.205314	2.716728	0.012825
H	3.551061	-2.526801	0.978355
C	0.351308	-1.961333	-2.208106
H	-0.587144	-2.159276	-1.690219
H	0.842162	-2.909098	-2.452693
C	-0.906728	0.193184	-0.169253
C	-1.715829	-0.849812	0.323485
H	-1.291600	-1.837576	0.470399
C	-1.467834	1.484542	-0.266005
H	-0.859821	2.306300	-0.633721
C	-3.571454	0.668544	0.569826
H	-4.603548	0.849448	0.855258
B	0.535109	0.052152	-0.654658
C	-3.033133	-0.613268	0.687512
H	-3.642323	-1.424250	1.074089
C	1.684592	-0.608884	-3.639327
H	2.243411	-1.349421	-4.217377
H	1.768277	0.345288	-4.163941
C	0.241088	-1.069984	-3.428802
H	-0.427928	-0.225585	-3.225205
H	-0.161640	-1.606756	-4.290093
H	1.467997	-1.108616	1.591271
H	4.542769	-0.429853	0.445504

E1

O	1.210949	1.031491	-0.150982
C	2.113244	1.174248	3.028095
H	1.052295	-2.938920	-0.097349
O	2.466546	-0.162110	2.579638
N	1.163559	-1.150695	-1.205518
C	1.584647	-1.982288	-0.041218
H	1.946018	1.828196	2.170797
O	2.944291	1.925410	-1.273669
H	2.922096	1.539531	3.659734

C	3.057282	-2.277309	0.162913
H	1.204167	1.067078	3.617485
C	2.154646	-0.269302	-1.894785
O	3.767036	-1.080465	0.437367
H	3.158446	-0.692508	-1.868186
O	1.003918	-1.164778	0.965280
C	2.176605	1.027069	-1.088977
H	3.277160	-0.167490	2.032640
C	-3.124410	1.276263	-0.574258
H	3.438134	-2.779214	-0.736030
H	-3.578116	2.182125	-0.964945
H	3.137060	-2.985749	0.998612
C	0.326932	-1.804506	-2.248204
H	-0.631041	-2.093752	-1.810293
H	0.851942	-2.693720	-2.616843
C	-1.131717	-0.015691	-0.048415
C	-1.959971	-1.031928	0.453074
H	-1.514935	-1.926366	0.884865
C	-1.739834	1.143134	-0.555763
H	-1.118492	1.957195	-0.921427
C	-3.927703	0.250523	-0.081327
H	-5.008585	0.354477	-0.092458
B	0.422905	-0.165647	-0.070828
C	-3.345011	-0.903918	0.436818
H	-3.970622	-1.697386	0.834507
C	1.636878	-0.127462	-3.339941
H	2.283106	-0.698101	-4.012210
H	1.662408	0.913554	-3.668259
C	0.226812	-0.724404	-3.310033
H	-0.514784	0.019732	-3.002829
H	-0.080866	-1.128149	-4.276409
H	1.716520	-0.649790	1.851995
H	4.710191	-1.229686	0.305238

E2

O	1.096370	1.103774	-0.097132
C	2.607813	0.136025	3.641897
H	1.323621	-2.829791	-0.540219
O	2.679405	0.151713	2.201205
N	1.156824	-0.918759	-1.416854
C	1.776813	-1.841011	-0.424123
H	1.603978	0.400198	3.982934
O	2.557203	2.350159	-1.272000
H	3.343250	0.830308	4.052188
C	3.289018	-1.958662	-0.366342
H	2.850485	-0.877823	3.958429
C	1.993003	0.141779	-2.078433
O	3.932271	-0.735930	-0.161289
H	3.035878	-0.160695	-2.162418
O	1.196794	-1.226574	0.746851
C	1.945826	1.335884	-1.134043
H	2.473958	1.039799	1.869773
C	-3.276793	0.942873	-0.101043
H	3.629437	-2.376190	-1.321659
H	-3.852215	1.841419	-0.301725
H	3.528250	-2.705881	0.402926
C	0.296807	-1.536139	-2.468674
H	-0.585826	-1.974288	-1.997788
H	0.875013	-2.315807	-2.977656
C	-1.128166	-0.187145	0.034848
C	-1.799448	-1.352710	0.438120
H	-1.232855	-2.250098	0.680005
C	-1.891521	0.961492	-0.226352
H	-1.391918	1.883586	-0.513162
C	-3.923388	-0.226446	0.291899
H	-5.004398	-0.241033	0.393332
B	0.417392	-0.147469	-0.151051
C	-3.183852	-1.375174	0.565743
H	-3.686913	-2.282725	0.885394
C	1.343540	0.371313	-3.455777
H	1.980716	-0.064690	-4.229581
H	1.247540	1.436961	-3.673681
C	0.002002	-0.362591	-3.384398
H	-0.775049	0.265250	-2.936263
H	-0.353355	-0.689695	-4.363326
H	1.849166	-0.733622	1.398130
H	4.005028	-0.549887	0.784218

TSE2F1

O	0.771004	1.155222	-0.285584
C	2.817954	0.463507	3.368551
H	0.932409	-2.696414	-0.587710
O	2.903336	0.242522	1.948840
N	1.387353	-1.040626	-1.686182
C	1.617375	-1.846787	-0.589643
H	1.987860	1.132442	3.609532
O	2.874545	1.901694	-0.451361
H	3.756910	0.883642	3.734319
C	3.025735	-2.293950	-0.229709
H	2.653100	-0.508937	3.832152
C	2.183398	0.149199	-1.982334
O	3.956333	-1.254610	-0.167275
H	3.252318	-0.057666	-2.051349
O	1.090725	-1.015895	0.695582

C	2.024064	1.156343	-0.848875
H	3.056289	1.084190	1.484933
C	-3.579035	0.574689	-0.259906
H	3.325259	-2.976381	-1.035200
H	-4.247239	1.327100	-0.666625
H	2.979077	-2.886872	0.693415
C	0.399374	-1.341721	-2.736661
H	-0.521756	-1.732584	-2.294565
H	0.799155	-2.086436	-3.436403
C	-1.329657	-0.211136	0.212539
C	-1.876862	-1.362559	0.809298
H	-1.217533	-2.110011	1.243269
C	-2.204950	0.756485	-0.317904
H	-1.796988	1.659459	-0.764455
C	-4.100217	-0.577501	0.329260
H	-5.175970	-0.719087	0.375815
B	0.175970	-0.002520	0.136497
C	-3.251687	-1.545674	0.865516
H	-3.666519	-2.434838	1.329601
C	1.598718	0.651983	-3.321126
H	2.242330	0.290108	-4.127909
H	1.578939	1.742342	-3.384757
C	0.211241	0.011399	-3.407414
H	-0.526924	0.601210	-2.855217
H	-0.136536	-0.082559	-4.438138
H	1.844186	-0.552178	1.236390
H	4.024618	-0.931895	0.740696

F1

O	0.511643	-0.187255	-0.448949
C	3.498537	0.568708	3.443622
H	1.660010	-3.515699	-1.562454
O	2.925389	0.344955	2.148041
N	1.969056	-1.605325	-2.124163
C	2.101701	-2.560040	-1.278548
H	3.034354	1.432661	3.926264
O	2.066066	1.437564	-0.221063
H	4.578936	0.719426	3.369254
C	2.787257	-2.519510	0.043437
H	3.298230	-0.322709	4.038027
C	2.383063	-0.189636	-1.927941
O	3.604135	-1.420447	0.224388
H	3.442694	-0.152714	-1.682683
O	0.187192	0.289701	1.907216
C	1.636875	0.439460	-0.750818
H	3.040451	1.129784	1.589944
C	-3.795525	-0.194046	-0.999220
H	3.356707	-3.463505	0.106618
H	-4.215419	-0.406331	-1.977952
H	1.981822	-2.620943	0.793118
C	1.250886	-1.767678	-3.416825
H	0.414363	-2.456344	-3.285787
H	1.961645	-2.192995	-4.133252
C	-1.858599	0.085832	0.444522
C	-2.727739	0.353083	1.515129
H	-2.308829	0.566921	2.494213
C	-2.418970	-0.187357	-0.812450
H	-1.766396	-0.401837	-1.655616
C	-4.639095	0.076258	0.076667
H	-5.715750	0.074251	-0.066343
B	-0.335580	0.108353	0.692942
C	-4.105036	0.350029	1.334300
H	-4.764760	0.561271	2.170304
C	2.034383	0.476851	-3.266373
H	2.894128	0.406028	-3.939741
H	1.803750	1.535384	-3.132842
C	0.861943	-0.347146	-3.794274
H	-0.070650	-0.061231	-3.299628
H	0.722206	-0.243839	-4.871769
H	1.158891	0.309366	1.999663
H	3.393739	-0.934601	1.050928

F2

O	-0.200433	0.592466	0.268083
C	-1.102597	4.505923	-0.360952
C	2.991498	0.758042	3.939594
H	0.798072	-2.423596	-1.568854
O	-1.259174	3.171733	-0.812967
O	2.256634	0.731477	2.709748
N	1.088370	-0.441512	-1.777603
C	1.261370	-1.536801	-1.134956
H	2.630165	1.559990	4.588940
H	-1.243838	4.594381	0.723050
O	1.332444	2.217495	0.626509
H	4.061065	0.886940	3.751425
H	-1.790469	5.195410	-0.866076
C	2.021238	-1.749522	0.129718
H	-0.079147	4.809388	-0.592468
H	2.825329	-0.200627	4.431234
C	1.529431	0.913017	-1.348190
O	2.851178	-0.704509	0.486896
H	2.601055	0.895308	-1.158171
O	-0.496514	0.875223	2.657577
C	0.866826	1.316238	-0.031379
H	2.338982	1.581825	2.247824

H	-2.126975	2.858529	-0.533142
C	-4.525923	0.686732	-0.215266
H	2.595474	-2.678861	-0.029982
H	-4.967253	0.499312	-1.189722
H	1.260736	-2.010505	0.886830
C	0.302491	-0.361524	-3.039100
H	-0.540669	-1.052935	-2.985631
H	0.967493	-0.666071	-3.854232
C	-2.557043	0.861120	1.207488
C	-3.400810	1.151204	2.291659
H	-2.961011	1.327904	3.268988
C	-3.146621	0.627109	-0.046288
H	-2.513727	0.382297	-0.896446
C	-5.342720	0.983659	0.874306
H	-6.420041	1.032359	0.745951
B	-1.024412	0.811802	1.434121
C	-4.779642	1.214487	2.127833
H	-5.418293	1.443180	2.975612
C	1.129946	1.816582	-2.522137
H	1.963278	1.879181	-3.228576
H	0.885935	2.821379	-2.176835
C	-0.070910	1.108103	-3.141272
H	-0.968826	1.334397	-2.560973
H	-0.247313	1.402232	-4.177516
H	0.475912	0.817317	2.729976
H	2.647237	-0.360082	1.382571

TSF2F3

O	-0.151464	0.722699	0.179527
C	-0.876650	4.543425	0.299569
C	2.949180	0.880395	3.877472
H	0.558557	-2.449097	-1.462701
O	-1.191087	3.286751	-0.282273
O	2.250536	0.904987	2.628128
N	1.011608	-0.516978	-1.809480
C	1.094897	-1.575323	-1.091229
H	2.751857	1.789994	4.451453
H	-1.263989	4.629421	1.321832
O	1.501408	2.259675	0.414027
H	4.026506	0.767773	3.723690
H	-1.261864	5.376906	-0.300154
C	1.828565	-1.759172	0.192631
H	0.211688	4.608909	0.338309
H	2.573992	0.021852	4.434869
C	1.561386	0.822810	-1.469011
O	2.708930	-0.742675	0.509021
H	2.636243	0.745045	-1.315748
O	-0.505855	1.482655	2.460316
C	0.961244	1.347019	-0.166648
H	2.514544	1.681426	2.111381
H	-2.148034	3.175780	-0.263392
C	-4.466730	0.384858	-0.309760
H	2.352170	-2.726326	0.094132
H	-4.881543	0.070342	-1.263058
H	1.042589	-1.934969	0.948003
C	0.206042	-0.447549	-3.057516
H	-0.666902	-1.096171	-2.964397
H	0.838524	-0.807134	-3.876285
C	-2.535963	0.945687	1.064219
C	-3.407529	1.186307	2.138233
H	-2.992668	1.494856	3.093657
C	-3.093089	0.540479	-0.158823
H	-2.437156	0.338186	-1.002692
C	-5.312637	0.632903	0.769493
H	-6.386013	0.512505	0.655897
B	-1.007649	1.139110	1.269198
C	-4.781860	1.032799	1.994057
H	-5.441648	1.223308	2.835183
C	1.168467	1.695764	-2.669481
H	1.968251	1.672423	-3.415937
H	1.015076	2.731923	-2.363686
C	-0.100072	1.034687	-3.201625
H	-0.959215	1.317743	-2.586785
H	-0.315152	1.298908	-4.238567
H	0.460906	1.418087	2.549471
H	2.507401	-0.332804	1.377681

F3

O	-0.285501	1.210406	-0.290841
C	-0.531252	4.201348	1.587876
C	3.098813	1.630740	3.529607
H	-0.054938	-2.310501	-0.973114
O	-1.234742	3.305169	0.702415
O	2.307469	1.391553	2.364580
N	0.832720	-0.659553	-1.711940
C	0.629359	-1.490504	-0.755919
H	2.930107	2.640046	3.916579
H	-0.701274	3.915486	2.627654
O	1.605319	2.425048	-0.053093
H	4.163522	1.491760	3.319103
H	-0.877744	5.217440	1.395670
C	1.210545	-1.450659	0.614076
H	0.521339	4.111295	1.328103
H	2.785654	0.906935	4.282372

C	1.585726	0.620831	-1.614223
O	2.380083	-0.714005	0.691778
H	2.606738	0.416772	-1.297561
O	-0.499304	1.346265	2.145692
C	0.952139	1.522299	-0.546153
H	2.519722	2.028191	1.664030
H	-2.189807	3.453074	0.765017
C	-4.614062	0.888300	-0.589267
H	1.369129	-2.502247	0.906502
H	-5.135436	1.022225	-1.532963
H	0.398221	-1.075017	1.264652
C	0.171734	-0.778792	-3.035918
H	-0.813513	-1.231902	-2.913697
H	0.796179	-1.428769	-3.658237
C	-2.589805	1.124053	0.748692
C	-3.277995	0.555938	1.829291
H	-2.755883	0.429695	2.774080
C	-3.284500	1.281464	-0.461118
H	-2.777074	1.719017	-1.320343
C	-5.275401	0.321221	0.497506
H	-6.312249	0.012243	0.402024
B	-1.085263	1.600771	0.921145
C	-4.605107	0.154187	1.707143
H	-5.120320	-0.286238	2.555996
C	1.476405	1.212021	-3.025655
H	2.319329	0.867022	-3.632523
H	1.510142	2.302848	-3.000406
C	0.159501	0.648801	-3.557782
H	-0.693847	1.192341	-3.142207
H	0.091758	0.679139	-4.646675
H	0.455340	1.494282	2.238022
H	2.353825	-0.081837	1.442230

TSF3G1

O	-0.219548	1.728819	-0.537888
C	-0.159738	4.016603	1.751692
C	2.815711	1.981947	3.666811
H	-0.465308	-1.964337	-0.630594
O	-1.159219	3.065985	1.305911
O	2.225421	1.478353	2.466486
N	0.618752	-0.561512	-1.651716
C	0.395780	-1.303231	-0.562651
H	2.591231	3.044399	3.806926
H	0.094736	3.827896	2.796660
O	1.892982	2.336392	-0.084974
H	3.899201	1.838565	3.650758
H	-0.568673	5.018549	1.624014
C	1.056939	-1.277734	0.651624
H	0.700983	3.865180	1.101001
H	2.394326	1.412820	4.495838
C	1.529470	0.581111	-1.700955
O	2.330661	-0.731864	0.708405
H	2.546523	0.295549	-1.432856
O	-0.172603	0.835642	1.726749
C	1.099463	1.639983	-0.689216
H	2.568299	1.940652	1.682992
H	-2.009085	3.134579	1.763358
C	-4.426031	0.762023	-0.812115
H	0.855259	-2.118741	1.318641
H	-4.960871	0.923396	-1.743458
H	0.140497	-0.144153	1.272760
C	-0.252108	-0.632218	-2.835560
H	-1.293138	-0.778377	-2.532480
H	0.052172	-1.480363	-3.460049
C	-2.412612	1.028219	0.527429
C	-3.058252	0.354705	1.575575
H	-2.528239	0.178383	2.509098
C	-3.123209	1.225974	-0.666669
H	-2.647154	1.751922	-1.490801
C	-5.047073	0.091381	0.240242
H	-6.064114	-0.272209	0.127620
B	-0.948674	1.596730	0.701588
C	-4.362877	-0.112004	1.435161
H	-4.844155	-0.636485	2.255261
C	1.408368	1.068841	-3.153886
H	2.134226	0.519547	-3.761232
H	1.629488	2.133747	-3.257216
C	-0.021445	0.696788	-3.546908
H	-0.725001	1.448602	-3.179182
H	-0.149052	0.612113	-4.627999
H	0.681381	1.225599	2.086909
H	2.472107	-0.317566	1.571094

G1

O	-0.132779	1.419724	-0.352234
C	-0.588604	3.960438	0.923942
C	2.136560	2.208483	3.711455
H	-0.175608	-2.237604	-1.216640
O	-0.663371	2.743089	1.723130
O	2.107539	1.229242	2.666096
N	0.829876	-0.569497	-1.884960
C	0.616879	-1.541317	-0.955148
H	1.560579	3.097917	3.440894
H	-0.685516	4.805043	1.605522

O	1.932365	2.147999	0.140821
H	3.172136	2.482677	3.919902
H	-1.385607	3.961726	0.178428
C	1.218186	-1.756237	0.237403
H	0.394045	3.949308	0.459088
H	1.705625	1.742151	4.597426
C	1.675627	0.588126	-1.685864
O	2.225536	-0.938983	0.737032
H	2.701331	0.314229	-1.429786
O	-0.034566	0.442555	1.878319
C	1.189138	1.461678	-0.537748
H	2.464633	1.600131	1.836008
H	-1.473454	2.771949	2.258763
C	-4.426909	0.977532	-0.390170
H	0.957046	-2.634568	0.822406
H	-4.974421	1.136859	-1.314416
H	0.084367	-0.448199	1.474334
C	-0.014771	-0.454262	-3.076874
H	-1.062700	-0.658734	-2.832085
H	0.303801	-1.176968	-3.839254
C	-2.324654	0.984311	0.832226
C	-3.023362	0.555912	1.972965
H	-2.480503	0.357186	2.895977
C	-3.052667	1.190050	-0.348418
H	-2.531445	1.509210	-1.247752
C	-5.101410	0.556730	0.754015
H	-6.173699	0.388725	0.721661
B	-0.782879	1.305576	0.918805
C	-4.398778	0.344016	1.937132
H	-4.920857	0.004496	2.826705
C	1.602512	1.317294	-3.038814
H	2.365087	0.890781	-3.697386
H	1.800027	2.388513	-2.952396
C	0.200657	0.982539	-3.546617
H	-0.538171	1.645783	-3.086354
H	0.112333	1.082652	-4.630445
H	0.958651	0.803509	2.280511
H	3.009988	-1.472574	0.906594

G2

O	-0.151015	1.207258	-0.262520
C	-0.619002	3.887609	0.688387
C	2.124421	2.693684	3.835321
H	-0.341083	-2.304316	-2.055952
O	-0.693038	2.785273	1.637483
O	2.100891	1.703477	2.806454
N	0.694638	-0.528638	-2.141072
C	0.293932	-1.645886	-1.469305
H	1.439433	3.519257	3.615671
H	-0.743918	4.813013	1.250112
O	1.915278	1.992068	0.144544
H	3.139285	3.078602	3.957730
H	-1.397806	3.778624	-0.068384
C	0.525046	-2.062269	-0.214417
H	0.373478	3.836307	0.247576
H	1.818448	2.203890	4.760081
C	1.648635	0.441278	-1.663876
O	1.241287	-1.299274	0.726095
H	2.562997	-0.031869	-1.286078
O	0.076854	0.542097	2.065731
C	1.154924	1.289872	-0.500809
H	2.372016	2.077384	1.948598
H	-1.525546	2.857467	2.134018
C	-4.424174	0.638554	-0.067650
H	0.094652	-2.983005	0.159063
H	-5.010339	0.664486	-0.981530
H	0.449283	-0.310204	1.664501
C	0.243227	-0.254045	-3.504184
H	-0.839212	-0.392717	-3.591015
H	0.731495	-0.926675	-4.224066
C	-2.280339	0.851339	1.057729
C	-2.921528	0.552621	2.271043
H	-2.337257	0.483594	3.187316
C	-3.056391	0.887907	-0.109502
H	-2.575012	1.098062	-1.061302
C	-5.042820	0.350342	1.147168
H	-6.110272	0.153792	1.179813
B	-0.753289	1.236009	1.039357
C	-4.290629	0.304937	2.318045
H	-4.768924	0.066785	3.263406
C	1.955588	1.296198	-2.909391
H	2.790248	0.839630	-3.449519
H	2.244868	2.317369	-2.651775
C	0.669613	1.191806	-3.726982
H	-0.092096	1.873055	-3.332044
H	0.818108	1.427015	-4.782901
H	0.914050	1.086255	2.449728
H	1.958788	-1.828815	1.093505

TSG2G3

O	-0.093731	0.902255	-0.193780
C	-0.698456	3.864402	0.815536
C	1.920908	2.805845	3.636702
H	0.068296	-2.557274	-2.093971

O	-0.600062	2.847763	1.816474
O	1.886576	1.665701	2.745876
N	0.864141	-0.655936	-2.165822
C	0.632623	-1.833876	-1.512335
H	1.081735	3.466928	3.422922
H	-0.893494	4.838757	1.273102
O	1.952540	1.730707	0.281696
H	2.875283	3.305009	3.476471
H	-1.490959	3.632945	0.096391
C	0.965031	-2.227875	-0.272930
H	0.262607	3.896983	0.301684
H	1.872728	2.418411	4.653379
C	1.713964	0.401541	-1.685667
O	1.601232	-1.383094	0.649494
H	2.713387	0.042345	-1.413221
O	-0.007814	0.179859	2.098497
C	1.195325	1.066651	-0.424149
H	1.959351	1.879798	1.731912
H	-1.456742	2.794149	2.261184
C	-4.430854	1.204211	-0.025492
H	0.685030	-3.207056	0.096339
H	-4.992576	1.505967	-0.904429
H	0.588287	-0.519500	1.723480
C	0.294001	-0.374477	-3.481540
H	-0.759601	-0.668363	-3.518538
H	0.829408	-0.923525	-4.269519
C	-2.299995	0.770632	1.061888
C	-2.997839	0.403405	2.224786
H	-2.440367	0.067456	3.095756
C	-3.041859	1.167393	-0.062987
H	-2.521787	1.430561	-0.980947
C	-5.103498	0.845541	1.141532
H	-6.188764	0.872025	1.170802
B	-0.750702	0.744469	1.053681
C	-4.387324	0.443176	2.266926
H	-4.913806	0.151989	3.170806
C	1.793681	1.381873	-2.874626
H	2.653009	1.104100	-3.491825
H	1.935649	2.417712	-2.557745
C	0.488466	1.129671	-3.628214
H	-0.339727	1.664178	-3.150753
H	0.538050	1.446728	-4.672014
H	1.012068	1.127614	2.735655
H	2.404376	-1.808581	0.971733

G3

O	-0.147465	0.701167	-0.223225
C	-0.685224	3.986751	0.874811
C	1.869730	2.786740	3.589967
H	0.501584	-2.730678	-2.178350
O	-0.646470	2.989039	1.887308
O	1.718857	1.601035	2.767139
N	1.005425	-0.728891	-2.204404
C	0.939390	-1.941393	-1.573918
H	1.016220	3.445594	3.435605
H	-1.064642	4.939116	1.261086
O	1.829849	1.631023	0.346802
H	2.803004	3.256183	3.283499
H	-1.304547	3.674138	0.025839
C	1.303275	-2.298497	-0.332434
H	0.339337	4.133450	0.527385
H	1.944982	2.454210	4.624493
C	1.710580	0.422118	-1.705303
O	1.779408	-1.377147	0.611014
H	2.757031	0.200400	-1.464818
O	-0.121708	-0.098763	2.029671
C	1.126689	0.961316	-0.415206
H	1.732882	1.746521	1.696761
H	-1.556094	2.805635	2.152774
C	-4.421494	1.487496	0.045829
H	1.172094	-3.314522	0.019803
H	-4.954372	1.907073	-0.802037
H	0.618675	-0.651515	1.678414
C	0.389095	-0.498310	-3.509058
H	-0.609226	-0.944410	-3.549460
H	0.993431	-0.938664	-4.315248
C	-2.348489	0.717548	1.056417
C	-3.066677	0.386389	2.218645
H	-2.541778	-0.062143	3.058049
C	-3.051278	1.268398	-0.028918
H	-2.517561	1.511378	-0.944432
C	-5.112976	1.161557	1.211667
H	-6.183979	1.331545	1.270576
B	-0.826716	0.471694	1.000280
C	-4.436474	0.610264	2.298349
H	-4.980147	0.347640	3.200682
C	1.618759	1.443289	-2.861021
H	2.501642	1.321712	-3.495218
H	1.605321	2.478320	-2.510858
C	0.355789	1.021267	-3.610119
H	-0.536332	1.409991	-3.108216
H	0.344299	1.373878	-4.643605
H	0.863388	1.120462	2.893246
H	2.635710	-1.670211	0.943937

G4

O	1.519880	0.538547	0.243104
C	4.279173	2.970239	2.274275
H	0.356381	-3.213584	-1.822483
O	3.905827	1.594325	2.455836
N	1.396001	-1.384316	-1.700710
C	0.919262	-2.570099	-1.153347
H	3.541668	3.508165	1.671710
O	3.725298	0.165518	0.542907
H	5.244614	2.970803	1.769634
C	1.073330	-2.959975	0.116101
H	4.384667	3.442018	3.252129
C	2.689703	-0.884446	-1.302965
O	1.664272	-2.132589	1.052821
H	3.406339	-1.686279	-1.077067
O	1.435823	0.620303	2.617076
C	2.647675	-0.040211	-0.054297
H	3.795251	0.875735	1.436451
C	-2.778053	0.578839	-0.058296
H	0.687695	-3.908994	0.470666
H	-3.262055	0.309112	-0.991860
H	0.832539	0.537052	3.364546
C	1.112394	-1.066095	-3.097231
H	0.036602	-0.935715	-3.248507
H	1.457514	-1.863133	-3.775297
C	-0.764423	0.791945	1.281459
C	-1.552362	1.265550	2.344819
H	-1.091802	1.563605	3.286291
C	-1.401184	0.454163	0.075410
H	-0.801602	0.078768	-0.749137
C	-3.539952	1.050427	1.008866
H	-4.616077	1.150782	0.902986
B	0.755331	0.629729	1.426984
C	-2.927717	1.397427	2.212334
H	-3.523275	1.772515	3.038564
C	3.179583	-0.047003	-2.516869
H	3.874121	-0.664896	-3.092574
H	3.715956	0.859822	-2.226369
C	1.902948	0.213956	-3.314487
H	1.355636	1.068318	-2.903385
H	2.105061	0.412419	-4.369096
H	3.030252	1.499631	2.875887
H	2.088811	-2.670174	1.729021

TSG4G5

O	1.678514	0.642470	0.267004
C	3.682188	3.233788	2.056477
H	-0.183854	-2.572430	-1.826713
O	3.834373	1.805658	2.211705
N	1.380834	-1.191065	-1.765649
C	0.524228	-2.086674	-1.161639
H	2.807865	3.466712	1.443994
O	3.903490	0.477084	0.212049
H	4.590749	3.598374	1.579787
C	0.436472	-2.397045	0.137097
H	3.587660	3.675087	3.048212
C	2.712954	-0.952126	-1.263002
O	1.206551	-1.736168	1.092943
H	3.138010	-1.846527	-0.781665
O	1.687536	0.396199	2.621848
C	2.788139	0.110359	-0.183482
H	3.923492	1.243387	1.236323
C	-2.635969	0.874030	0.116542
H	-0.296932	-3.099659	0.510106
H	-3.129813	0.995331	-0.842792
H	1.138890	0.359442	3.412466
C	1.301819	-0.970504	-3.210496
H	0.340833	-0.521346	-3.478586
H	1.403734	-1.917315	-3.762523
C	-0.600524	0.539595	1.403557
C	-1.374545	0.573489	2.574235
H	-0.913098	0.461210	3.556124
C	-1.259188	0.690951	0.173480
H	-0.677059	0.668051	-0.743230
C	-3.382613	0.902720	1.291640
H	-4.458230	1.045528	1.248859
B	0.933487	0.343367	1.444268
C	-2.751199	0.751485	2.524665
H	-3.331904	0.776285	3.441462
C	3.539511	-0.575734	-2.512038
H	4.001905	-1.484761	-2.906730
H	4.338060	0.132722	-2.284994
C	2.483599	-0.052528	-3.483282
H	2.219527	0.984673	-3.249262
H	2.811847	-0.090982	-4.523788
H	3.022828	1.385259	2.607501
H	1.289934	-2.280188	1.883428

G5

O	1.703351	0.616599	0.207243
C	3.140385	3.269363	1.982349
H	-0.235294	-2.442364	-1.834427
O	3.602724	1.899806	2.046690

N	1.488269	-1.300073	-1.828079
C	0.521112	-2.008262	-1.185523
H	2.239215	3.339393	1.369420
O	3.895229	0.745851	-0.089561
H	3.947648	3.859869	1.552100
C	0.342501	-2.230709	0.124124
H	2.945806	3.601856	3.001203
C	2.792184	-1.009744	-1.268465
O	1.169063	-1.569443	1.073242
H	3.151516	-1.846275	-0.649179
O	1.755826	0.224795	2.563717
C	2.820002	0.189836	-0.331665
H	3.812214	1.500375	1.074126
C	-2.508521	1.520183	0.474410
H	-0.510576	-2.745534	0.539076
H	-2.973958	2.082049	-0.330002
H	1.171025	0.431067	3.302209
C	1.473333	-1.162280	-3.288778
H	0.553880	-0.669721	-3.618037
H	1.530381	-2.148337	-3.771075
C	-0.542059	0.444753	1.415111
C	-1.315435	0.087292	2.530562
H	-0.876547	-0.489444	3.346960
C	-1.166384	1.162914	0.388043
H	-0.590006	1.446782	-0.488553
C	-3.255996	1.157843	1.591987
H	-4.303454	1.435695	1.659977
B	0.980378	0.057034	1.347531
C	-2.658776	0.436655	2.622911
H	-3.239219	0.147929	3.493970
C	3.695919	-0.824004	-2.498618
H	4.116264	-1.795133	-2.775181
H	4.522063	-0.140605	-2.298297
C	2.722768	-0.340309	-3.571687
H	2.511573	0.727494	-3.447048
H	3.099350	-0.492127	-4.584911
H	2.871160	1.273497	2.391407
H	1.315186	-2.086363	1.876613

TSG5H1

O	1.999795	0.907238	0.137131
C	4.360355	2.981134	2.927049
H	1.019966	-3.478462	-0.793599
O	3.689439	1.921119	2.255776
N	1.383450	-1.349281	-1.054200
C	1.232990	-2.529296	-0.305676
H	4.063103	3.961729	2.538792
O	4.123122	0.935762	-0.500055
H	5.445228	2.870281	2.839067
C	1.320636	-2.433193	1.013365
H	4.089970	2.920398	3.982494
C	2.751752	-0.872586	-1.330508
O	1.553892	-1.127448	1.490175
H	3.505973	-1.614857	-1.050353
O	1.365080	0.913416	2.613422
C	3.052519	0.388378	-0.527738
H	3.947535	1.896299	1.320108
C	-2.333284	1.633186	-0.383231
H	1.282900	-3.200384	1.772535
H	-2.676055	2.426509	-1.040394
H	0.667970	1.530705	2.860910
C	0.556207	-1.240220	-2.272894
H	-0.453236	-0.916764	-2.005451
H	0.489424	-2.220438	-2.766484
C	-0.506670	0.371803	0.610661
C	-1.452999	-0.392142	1.311721
H	-1.132867	-1.188669	1.980191
C	-0.971847	1.390742	-0.237367
H	-0.256458	2.003267	-0.780366
C	-3.255531	0.860710	0.318983
H	-4.318899	1.049666	0.207493
B	1.016063	0.147738	0.739399
C	-2.814627	-0.152494	1.167792
H	-3.533184	-0.753070	1.716931
C	2.771989	-0.572629	-2.839703
H	3.081648	-1.474307	-3.376830
H	3.475070	0.225252	-3.087188
C	1.311406	-0.243325	-3.140199
H	1.073171	0.782118	-2.837732
H	1.061235	-0.345575	-4.197992
H	2.244792	1.415809	2.535347
H	1.471078	-0.940915	2.448517

H1

O	1.984689	0.572022	0.559275
C	3.346035	3.137290	2.278128
H	1.945159	-3.545677	-0.547833
O	3.998971	1.848926	2.219423
N	1.428235	-1.410419	-0.747760
C	1.616413	-2.658660	-0.024235
H	2.346179	3.076084	1.843807
O	4.076930	0.888083	-0.105635
H	3.967040	3.843120	1.728604
C	1.342596	-2.507341	1.271284

H	3.297282	3.431205	3.325705
C	2.726355	-0.793054	-1.209034
O	0.924540	-1.285789	1.656656
H	3.534234	-1.525291	-1.144622
O	2.702398	0.072475	3.369880
C	3.002423	0.303956	-0.208908
H	4.105586	1.531021	1.236772
C	-1.912549	2.181876	-0.440901
H	1.410175	-3.270596	2.038096
H	-1.981583	3.192523	-0.832449
H	2.476570	0.092074	4.304325
C	0.557404	-1.525213	-1.965589
H	-0.487581	-1.515018	-1.653635
H	0.784296	-2.479833	-2.451649
C	-0.548303	0.291051	0.264015
C	-1.728319	-0.395567	0.587635
H	-1.668318	-1.394500	1.013775
C	-0.666925	1.591813	-0.247253
H	0.230200	2.160883	-0.483761
C	-3.070378	1.475613	-0.125613
H	-4.043984	1.932689	-0.275082
B	0.853608	-0.393852	0.477090
C	-2.977246	0.185690	0.391696
H	-3.878363	-0.362610	0.649810
C	2.495808	-0.304865	-2.651934
H	2.985175	-0.997150	-3.341826
H	2.928218	0.684014	-2.821002
C	0.975361	-0.347523	-2.825128
H	0.504359	0.568648	-2.456418
H	0.678930	-0.480285	-3.867680
H	3.447864	1.120544	2.733502
H	1.980615	-0.372153	2.882367

H2

O	1.595875	-0.966552	0.567599
C	1.041506	0.468371	3.549273
H	2.875014	-2.911146	-2.841601
O	0.331938	-0.287274	2.522188
N	1.839384	-1.248462	-1.823665
C	2.129563	-2.651600	-2.103301
H	1.707955	-0.241680	4.034430
O	3.240247	0.508084	0.959679
H	0.298930	0.832384	4.256832
C	1.347049	-3.445178	-1.369888
H	1.609445	1.279774	3.093632
C	3.012802	-0.491134	-1.247167
O	0.473741	-2.828276	-0.559164
H	3.898377	-1.133541	-1.256601
C	2.672950	-0.229561	0.204577
H	-0.388970	0.221503	2.103395
C	-1.824131	1.547269	-0.150534
H	1.333847	-4.528872	-1.376088
H	-1.816217	2.583656	0.175300
C	1.393571	-0.480874	-3.042524
H	0.317286	-0.610814	-3.165152
H	1.906887	-0.911526	-3.907436
C	-0.610616	-0.525035	-0.623715
C	-1.827799	-1.100471	-1.011587
H	-1.843079	-2.140965	-1.323669
C	-0.637096	0.816229	-0.191069
H	0.287679	1.320663	0.094502
C	-3.018790	0.947902	-0.545421
H	-3.946000	1.511844	-0.515862
B	0.708895	-1.411550	-0.603020
C	-3.016575	-0.374418	-0.979242
H	-3.945994	-0.846077	-1.283909
C	3.195292	0.768999	-2.097012
H	3.983873	0.598886	-2.834898
H	3.496397	1.617352	-1.478284
C	1.841972	0.947093	-2.787095
H	1.127005	1.461754	-2.138495
H	1.916219	1.517294	-3.715457
H	0.967065	-0.625643	1.698352

TSH2I1

O	0.861119	0.380392	0.954296
C	2.604055	-2.367319	3.319719
H	2.121928	-3.075055	-0.653414
O	2.400521	-1.512174	2.163959
N	1.373912	-1.018134	-0.915879
C	1.486398	-2.306768	-0.219678
H	3.029024	-1.753674	4.113165
O	2.693715	1.699176	0.960708
H	3.320062	-3.129671	3.017567
C	0.260878	-2.573466	0.374757
H	1.661791	-2.817402	3.637646
C	2.505798	-0.057668	-0.689263
O	-0.536066	-1.579341	0.518223
H	3.394934	-0.599891	-0.353685
C	2.054126	0.814660	0.475021
H	2.031046	-1.992782	1.163584
C	-1.787953	2.708656	-1.589851
H	-0.027727	-3.528062	0.815440
H	-1.722746	3.792055	-1.559083

C	1.211599	-1.148465	-2.402186
H	0.183549	-1.439782	-2.626050
H	1.895599	-1.931050	-2.748282
C	-0.956798	0.535917	-0.876622
C	-1.976298	-0.065053	-1.631472
H	-2.087623	-1.147896	-1.630054
C	-0.888643	1.937528	-0.859538
H	-0.138078	2.436577	-0.251129
C	-2.779524	2.090369	-2.347110
H	-3.484513	2.690996	-2.913936
B	0.078404	-0.323548	-0.070978
C	-2.877555	0.700825	-2.363039
H	-3.662885	0.217323	-2.936191
C	2.762964	0.651660	-2.028493
H	3.721642	0.319836	-2.434012
H	2.821439	1.733675	-1.893632
C	1.603609	0.219004	-2.934212
H	0.760490	0.907993	-2.848784
H	1.895286	0.166637	-3.985185
H	1.790022	-0.764674	2.331575

I1

O	0.304904	1.615757	0.577052
C	4.088542	-3.240782	1.847301
H	0.268178	-2.592376	-0.425112
O	2.938718	-2.455435	2.155169
N	0.936571	-0.559124	-0.344103
C	0.540954	-1.827321	0.314185
H	5.012637	-2.739185	2.153003
O	2.286005	2.234987	1.450807
H	4.107232	-3.373625	0.763882
C	-0.647818	-1.496174	1.126482
H	4.039735	-4.228937	2.317059
C	2.129280	0.127301	0.304541
O	-1.085116	-0.346389	1.035826
H	2.525367	-0.490704	1.116106
C	1.608485	1.445404	0.865347
H	1.344193	-2.246542	0.949482
C	-2.189842	2.434071	-2.846900
H	-1.145842	-2.209579	1.789413
H	-2.213616	3.444491	-3.243265
C	1.294614	-0.745031	-1.801156
H	0.380808	-0.717891	-2.396513
H	1.778757	-1.722164	-1.901673
C	-1.299923	0.827570	-1.254560
C	-2.145846	-0.145206	-1.811798
H	-2.165023	-1.158855	-1.410714
C	-1.343223	2.124513	-1.786754
H	-0.717813	2.899666	-1.352367
C	-3.012234	1.451739	-3.390959
H	-3.676794	1.693774	-4.214758
B	-0.310346	0.528803	-0.078769
C	-2.992558	0.158621	-2.871114
H	-3.643702	-0.604899	-3.285503
C	3.146787	0.351880	-0.818519
H	3.858761	-0.478764	-0.850537
H	3.708633	1.272085	-0.645895
C	2.282931	0.368321	-2.077672
H	1.759800	1.323938	-2.194113
H	2.850631	0.183871	-2.991937
H	2.916673	-2.323408	3.108938

I2

O	-1.050858	-2.102362	0.767539
O	-1.040377	-0.034801	2.035611
N	-0.329582	-0.016414	-0.302158
O	3.158283	-0.998369	-0.118492
O	2.034787	-1.818766	2.211697
O	0.832379	0.785300	2.970905
C	-0.192314	-2.352368	-0.084548
H	0.150319	-3.382111	-0.212598
C	0.618588	0.784816	0.572341
H	1.645778	0.435394	0.431308
C	0.177186	0.517931	1.999637
C	-5.162525	0.564168	0.873360
H	-5.784223	1.219979	1.475119
C	-0.867960	0.941919	-1.332482
H	-1.839903	0.585719	-1.677783
H	-0.158583	0.968386	-2.166487
C	-2.992068	-0.432124	0.419393
C	-3.573607	-1.134889	-0.648140
H	-2.977298	-1.824513	-1.245628
C	0.300924	-1.223575	-0.892912
H	1.410138	-1.187335	-0.865075
H	-0.007322	-1.365080	-1.937650
C	-3.812976	0.414312	1.178486
H	-3.391089	0.946821	2.026780
C	-5.715982	-0.133999	-0.196056
H	-6.769673	-0.020880	-0.432304
B	-1.476916	-0.560963	0.790234
C	-4.920673	-0.988001	-0.957874
H	-5.354140	-1.543660	-1.783745
C	0.434518	2.254985	0.155766
H	1.256152	2.547741	-0.504068

H	0.454545	2.918365	1.023083
C	4.532874	-0.909518	-0.458628
C	2.232856	-2.973357	3.025751
H	5.086273	-0.284826	0.251807
H	1.363421	-3.161847	3.664005
H	4.600368	-0.449634	-1.446444
H	3.125499	-2.876188	3.652238
H	5.004415	-1.898240	-0.505190
H	2.371562	-3.824347	2.356096
C	-0.893371	2.267501	-0.600866
H	-1.748379	2.305449	0.082308
H	-0.979630	3.108069	-1.292462
H	3.048901	-1.379067	0.774135
H	1.938083	-1.050217	2.792589

H	0.709346	2.958808	1.007669
C	4.365756	-1.343290	-0.401772
C	2.234554	-2.804235	3.267800
H	4.919331	-0.595536	0.178622
H	1.369724	-2.914836	3.930080
H	4.488142	-1.113354	-1.462427
H	3.146210	-2.738447	3.871156
H	4.804565	-2.330413	-0.212999
H	2.303795	-3.687446	2.630022
C	-0.853446	2.454510	-0.474084
H	-1.626064	2.483352	0.302089
H	-0.973870	3.342035	-1.098577
H	2.844557	-1.501477	0.844948
H	2.019658	-0.877188	2.953662

TSI2J1

O	-0.876561	-2.060176	0.563794
O	-0.971783	-0.061628	1.957100
N	-0.352710	0.126940	-0.398030
O	2.977944	-1.321746	-0.109150
O	2.087156	-1.675373	2.412540
O	0.829419	0.906639	2.890126
C	-0.104434	-2.208703	-0.388035
H	0.282306	-3.203991	-0.619417
C	0.648033	0.845675	0.492449
H	1.648670	0.427859	0.342126
C	0.204739	0.571537	1.920665
C	-5.158037	0.305149	0.959449
H	-5.802309	0.877878	1.619437
C	-0.966927	1.181608	-1.287570
H	-1.983918	0.880805	-1.543767
H	-0.356543	1.247172	-2.194238
C	-2.942529	-0.512675	0.384160
C	-3.509170	-1.180346	-0.713509
H	-2.888533	-1.787133	-1.373002
C	0.243578	-0.997704	-1.158383
H	1.342180	-0.933643	-1.222949
H	-0.179262	-1.068173	-2.168733
C	-3.793106	0.226111	1.219196
H	-3.381107	0.730170	2.089294
C	-5.697244	-0.357158	-0.139566
H	-6.762770	-0.299753	-0.340108
B	-1.410456	-0.552492	0.700577
C	-4.871407	-1.103794	-0.978031
H	-5.292463	-1.631386	-1.828336
C	0.544441	2.331827	0.128941
H	1.307943	2.585424	-0.612622

J1

O	-0.192580	-1.966513	-0.156039
O	-0.152355	-0.350689	1.632479
N	-0.015105	0.414095	-0.688646
O	2.055856	-1.646889	0.125467
O	2.055033	-1.778631	2.730432
O	1.683171	0.625030	2.404493
C	0.974871	-1.760649	-0.827700
H	1.200943	-2.605809	-1.490815
C	0.823278	1.256089	0.231065
H	1.856103	1.304513	-0.120170
C	0.814217	0.505410	1.537668
C	-4.470792	-0.052271	1.368715
H	-5.007820	0.470208	2.154900
C	-0.930069	1.355124	-1.410224
H	-1.821206	0.808964	-1.725478
H	-0.401319	1.740211	-2.289536
C	-2.360847	-0.732344	0.361260
C	-3.090809	-1.418493	-0.621033
H	-2.559761	-1.983336	-1.384073
C	0.778373	-0.453382	-1.597265
H	1.698617	0.041582	-1.918574
H	0.166500	-0.664550	-2.477894
C	-3.078933	-0.057330	1.359222
H	-2.541425	0.454875	2.154674
C	-5.173909	-0.726608	0.373698
H	-6.259827	-0.725211	0.379172
B	-0.788081	-0.742027	0.322915
C	-4.482261	-1.414088	-0.620817
H	-5.028518	-1.954257	-1.388429
C	0.166642	2.651604	0.272603
H	0.784570	3.348670	-0.299168

H	0.095792	3.040186	1.291079
C	3.350438	-1.893305	-0.421496
C	1.155989	-2.578092	3.547858
H	4.064209	-1.824022	0.400156
H	0.121360	-2.348054	3.293550
H	3.611735	-1.146328	-1.178971
H	1.375501	-2.328403	4.584240
H	3.399929	-2.893926	-0.865353
H	1.391419	-3.623679	3.357091
C	-1.194829	2.451497	-0.397850
H	-1.949933	2.119666	0.320300
H	-1.560966	3.363380	-0.874017
H	1.938718	-1.946089	1.744162
H	1.894477	-0.732727	2.818944

I3

O	-0.932913	-1.157731	-2.036645
O	-1.496633	1.117921	-2.717021
N	-2.015715	0.345579	-0.462593
O	0.756091	-2.785458	-0.111572
O	-0.181589	-1.602619	2.181044
H	-1.544947	-2.914724	-1.259404
O	-3.523767	1.895512	-3.318521
C	-1.487922	-1.831469	-1.158013
C	-3.269755	0.819437	-1.179237
H	-3.951178	-0.019861	-1.344104
C	-2.807201	1.342594	-2.539869
C	2.661784	1.847347	-2.127563
H	3.180731	2.423574	-2.887465
C	-1.810201	1.300708	0.699391
H	-0.743317	1.475388	0.830732
H	-2.209720	0.817092	1.595072
C	0.617953	0.788361	-1.334285
C	1.318071	0.379897	-0.183272
H	0.816574	-0.159567	0.620651
C	-2.082127	-1.074467	-0.037152
H	-3.103666	-1.398439	0.190174
H	-1.469059	-1.254446	0.876068
C	1.317117	1.529963	-2.298280
H	0.798206	1.861557	-3.192913
C	3.338491	1.428980	-0.986184
H	4.386534	1.678506	-0.850990
B	-0.874408	0.410153	-1.658649
C	2.663002	0.698334	-0.010657
H	3.180845	0.389456	0.892960
C	-3.863347	1.927907	-0.317740
H	-4.540159	1.510771	0.434698
H	-4.427591	2.625518	-0.940196
C	-0.080257	-1.887652	3.567710
C	1.286136	-4.050471	-0.512197
H	-0.641298	-1.119184	4.102773
H	0.610237	-4.818272	-0.131967
H	0.960044	-1.853907	3.910329
H	2.280208	-4.218170	-0.085914
H	-0.506412	-2.866499	3.817818
H	1.343475	-4.131811	-1.602741
C	-2.623542	2.529731	0.337684
H	-2.076690	3.166616	-0.366293
H	-2.851173	3.129931	1.220953
H	1.350647	-2.088400	-0.424023
H	0.320444	-2.251880	1.660498

TSI3J'1

O	-1.056725	-1.257067	-1.624251
O	-1.576074	0.856795	-2.742478
N	-2.134686	0.548031	-0.386065
O	1.064641	-3.024351	-0.227680
O	-0.301031	-2.138806	1.952030
H	-1.691967	-2.820243	-0.523915
O	-3.571843	1.571905	-3.504392
C	-1.667432	-1.738850	-0.663959
C	-3.357907	0.964183	-1.184329
H	-4.109521	0.170007	-1.173129
C	-2.877899	1.164900	-2.622816
C	2.486049	1.985074	-1.973654
H	2.976401	2.635337	-2.691589
C	-1.868973	1.670004	0.597061
H	-0.792164	1.765447	0.739414
H	-2.342142	1.395037	1.544641
C	0.505179	0.765531	-1.263622
C	1.223768	0.313717	-0.141241
H	0.753792	-0.331655	0.601856
C	-2.263079	-0.767870	0.277324
H	-3.290536	-1.013473	0.564547
H	-1.630206	-0.844200	1.181834
C	1.161410	1.605570	-2.174070
H	0.627820	1.957457	-3.052366
C	3.180464	1.529418	-0.857562
H	4.213234	1.825451	-0.700266
B	-0.979212	0.350435	-1.564749
C	2.547309	0.693398	0.061367
H	3.084601	0.344956	0.938774
C	-3.844318	2.272516	-0.565920
H	-4.557385	2.073266	0.240256

H	-4.342172	2.884565	-1.320804
C	0.048866	-2.484655	3.281675
C	1.724211	-4.271243	-0.437600
H	-0.666404	-2.002355	3.951395
H	1.099363	-5.043870	0.013242
H	1.054583	-2.136291	3.546509
H	2.709698	-4.294442	0.039889
H	-0.004370	-3.567348	3.448073
H	1.833736	-4.486965	-1.505327
C	-2.555884	2.876536	-0.012652
H	-1.944674	3.308839	-0.812661
H	-2.731046	3.655915	0.731611
H	1.600822	-2.319539	-0.610550
H	0.330705	-2.550261	1.330246

J'1

O	-0.894265	-1.431764	-0.118092
O	-1.151130	-0.103274	-2.132693
N	-1.878342	0.735708	0.018543
O	1.120151	-2.764368	-0.379033
O	-0.968302	-1.863814	2.190717
H	-2.549548	-2.067332	0.912306
O	-3.106108	-0.009060	-3.250357
C	-1.676543	-1.432021	1.111232
C	-3.061086	0.573911	-0.910125
H	-3.742075	-0.194099	-0.532333
C	-2.469558	0.108566	-2.244986
C	2.737988	1.634266	-1.506485
H	3.206153	2.172434	-2.325258
C	-1.685980	2.227421	0.201922
H	-0.617453	2.446856	0.203860
H	-2.110090	2.493083	1.174858
C	0.802319	0.467967	-0.599487
C	1.537529	0.242159	0.579784
H	1.086109	-0.300324	1.411138
C	-2.007385	0.042404	1.317948
H	-2.998043	0.195863	1.753061
H	-1.254489	0.450874	1.997446
C	1.431406	1.169780	-1.637973
H	0.891693	1.340096	-2.565889
C	3.446611	1.401495	-0.331064
H	4.465968	1.761184	-0.228798
B	-0.681870	-0.048183	-0.779087
C	2.845392	0.703123	0.714686
H	3.393947	0.522555	1.634639
C	-3.694650	1.953818	-1.037801
H	-4.403851	2.130769	-0.222562
H	-4.230474	2.038113	-1.985516
C	-0.914776	-3.279685	2.382888
C	1.279720	-3.300412	-1.709000
H	-1.919982	-3.714070	2.347694
H	2.228864	-3.834841	-1.770841
H	-0.489574	-3.434635	3.373747
H	1.236776	-2.504939	-2.457521
H	-0.273116	-3.755048	1.634501
H	0.459794	-4.000681	-1.864330
C	-2.482371	2.874174	-0.918267
H	-1.908812	2.888054	-1.851333
H	-2.745965	3.905473	-0.675206
H	-0.024981	-2.078984	-0.187556
H	1.836400	-2.136804	-0.194280

compound 26

Fran_OM

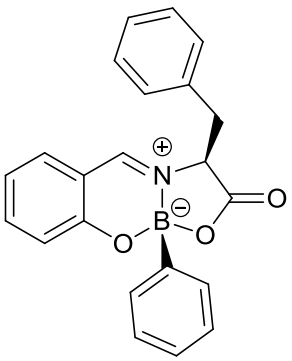

Fran_Am_WI

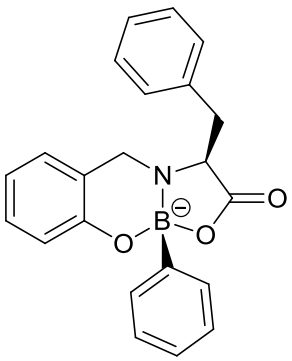

Fran_WE

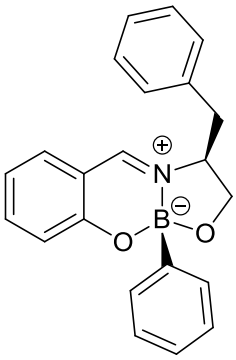

Fran_Am_WoutI

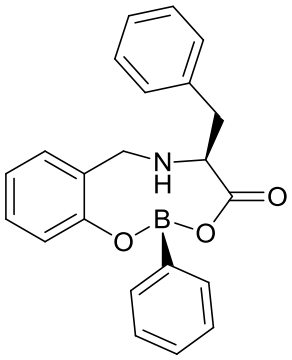

Fran_OM1

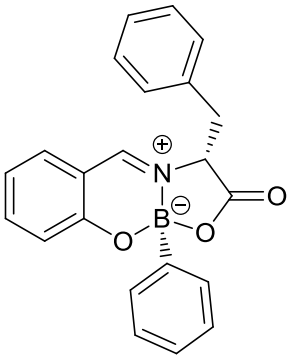

Fran_OM2

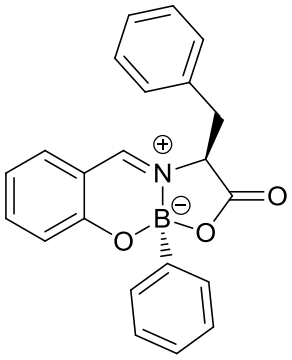

Fran_OM3

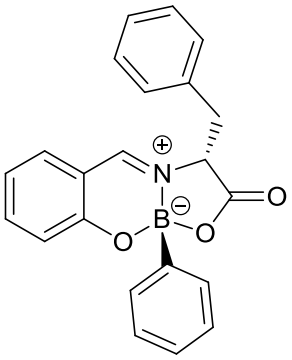

Water

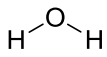

Hydronium Ion

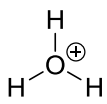

Fran_OM

C	-5.604574000	-0.013974000	1.963233000
C	-5.514288000	-1.40407 000	2.139029000
C	-4.533631000	-2.152672000	1.513721000
C	-3.579445000	-1.524324000	0.698582000
C	-3.678613000	-0.117603000	0.503600000
C	-4.699108000	0.615875000	1.135315000
O	-2.655943000	-2.256234000	0.103315000
B	-1.427758000	-1.640418000	-0.425402000
N	-1.816966000	-0.195647000	-0.934691000
C	-2.821374000	0.472032000	-0.477577000
O	-1.020408000	-2.247137000	-1.710757000
C	-0.724437000	-1.340023000	-2.631561000
C	-1.065267000	0.080455000	-2.139160000
C	0.212104000	0.903695000	-1.892791000
C	-0.104172000	2.286712000	-1.392302000
C	-0.222608000	-1.611871000	0.637025000
C	0.981334000	-2.280870000	0.379768000
C	2.035769000	-2.259923000	1.290646000
C	1.909502000	-1.561149000	2.487231000
C	0.721640000	-0.889092000	2.768668000
C	-0.326817000	-0.918590000	1.853560000
C	-0.085119000	2.569754000	-0.023283000
C	-0.424199000	3.837622000	0.443475000
C	-0.790259000	4.838544000	-0.451642000
C	-0.813544000	4.566911000	-1.817949000
C	-0.473514000	3.300514000	-2.282675000
O	-0.231762000	-1.560281000	-3.707766000
H	-6.383735000	0.551947000	2.462064000
H	-6.231643000	-1.907780000	2.781025000
H	-4.464530000	-3.226946000	1.645733000
H	-4.759251000	1.687443000	0.960894000
H	-3.048255000	1.452914000	-0.897064000
H	-1.688594000	0.586149000	-2.883706000
H	0.744198000	0.935666000	-2.849171000
H	0.845335000	0.369100000	-1.177986000
H	1.087642000	-2.831762000	-0.551411000
H	2.957078000	-2.790678000	1.065546000
H	2.730461000	-1.540364000	3.198755000
H	0.612848000	-0.345348000	3.703594000
H	-1.247202000	-0.391023000	2.098584000
H	0.202188000	1.788459000	0.676818000
H	-0.397192000	4.043788000	1.509733000
H	-1.050266000	5.828446000	-0.088119000
H	-1.089371000	5.345389000	-2.523609000
H	-0.483360000	3.096619000	-3.351488000

Fran_AM_WI

C	-4.373399000	-0.239318000	0.541012000
C	-3.200058000	-2.343879000	0.337274000
C	-1.963324000	-1.685996000	0.412138000
C	-1.943092000	-0.282090000	0.564297000
C	-3.143935000	0.416358000	0.612578000
O	-0.841922000	-2.399196000	0.367517000
B	0.479584000	-1.774083000	0.010557000
N	0.392461000	-0.261453000	-0.197990000
C	-0.584638000	0.366440000	0.672229000
O	0.846444000	-2.274261000	-1.363617000
C	0.694183000	-1.333056000	-2.268118000
C	0.229665000	-0.028025000	-1.611981000
C	1.052816000	1.139149000	-2.188454000
C	0.596397000	2.500778000	-1.749559000
C	1.572357000	-2.251045000	1.105499000
C	1.429063000	-3.436022000	1.839803000
C	2.388214000	-3.850093000	2.761502000
C	3.525909000	-3.075806000	2.980692000
C	3.688356000	-1.887712000	2.271358000
C	2.721586000	-1.489152000	1.350295000
C	1.226121000	3.170328000	-0.695203000
C	0.785042000	4.420539000	-0.270722000
C	-0.298851000	5.031184000	-0.895932000
C	-0.936363000	4.377520000	-1.948052000
C	-0.490831000	3.128528000	-2.368492000
O	0.904245000	-1.463703000	-3.458877000
C	-4.388855000	-1.626130000	0.408027000
H	-5.302085000	0.323727000	0.583100000
H	-3.196131000	-3.424155000	0.222877000
H	-3.110252000	1.500785000	0.713485000
H	-0.216542000	0.259427000	1.704297000
H	-0.661780000	1.443593000	0.481085000
H	-0.827357000	0.119156000	-1.908782000
H	1.002874000	1.050594000	-3.279980000
H	2.096252000	0.983667000	-1.893002000
H	0.534793000	-4.035061000	1.684501000
H	2.248182000	-4.776586000	3.315848000
H	4.276341000	-3.392786000	3.702211000
H	4.569411000	-1.270862000	2.440686000
H	2.836407000	-0.554179000	0.804905000
H	2.062262000	2.688472000	-0.195147000
H	1.289114000	4.918523000	0.553919000
H	-0.644443000	6.007628000	-0.566630000
H	-1.783945000	4.843400000	-2.444783000
H	-0.993934000	2.622840000	-3.189774000

H	-5.336966000	-2.156791000	0.348030000

Fran_WE

C	-4.459186000	-0.444114000	1.838294000
C	-3.251061000	-2.518561000	1.444731000
C	-2.307191000	-1.837383000	0.661340000
C	-2.480178000	-0.442794000	0.446341000
C	-3.563327000	0.233093000	1.038085000
O	-1.310204000	-2.515762000	0.120209000
B	-0.138193000	-1.841992000	-0.438727000
N	-0.576145000	-0.425728000	-0.952428000
C	-1.627296000	0.185312000	-0.513131000
O	0.251719000	-2.429869000	-1.775178000
C	0.428423000	-1.602856000	-2.750731000
C	0.102167000	-0.181716000	-2.210033000
C	1.423038000	0.595638000	-2.054774000
C	1.189849000	1.996154000	-1.556107000
C	1.109374000	-1.814917000	0.566706000
C	2.343196000	-2.392638000	0.240681000
C	3.420304000	-2.353823000	1.123839000
C	3.286829000	-1.727854000	2.359425000
C	2.069150000	-1.147268000	2.708254000
C	0.997420000	-1.196231000	1.821589000
C	1.257221000	2.287274000	-0.190116000
C	0.998718000	3.574582000	0.274289000
C	0.666711000	4.588763000	-0.619354000
C	0.595895000	4.309442000	-1.982278000
C	0.854888000	3.023172000	-2.444608000
C	-4.295525000	-1.825728000	2.029322000
H	-5.287769000	0.078441000	2.303884000
H	-3.122165000	-3.585825000	1.588736000
H	-3.681351000	1.297759000	0.851527000
H	-1.894819000	1.153314000	-0.939040000
H	-0.552404000	0.351854000	-2.908807000
H	1.902420000	0.597437000	-3.039264000
H	2.080556000	0.048304000	-1.372046000
H	2.458993000	-2.885086000	-0.721634000
H	4.365137000	-2.813829000	0.846689000
H	4.125715000	-1.693308000	3.049138000
H	1.955192000	-0.660677000	3.673492000
H	0.052440000	-0.743430000	2.117580000
H	1.519433000	1.497169000	0.509877000
H	1.062328000	3.785691000	1.338112000
H	0.469723000	5.593670000	-0.257265000
H	0.345912000	5.097021000	-2.687602000
H	0.807129000	2.812623000	-3.511084000

H	-5.004250000	-2.366356000	2.650436000

Fran_Am_WoutI

C	-4.242741000	-0.562512000	1.855195000
C	-2.854891000	-2.541574000	1.681464000
C	-2.207311000	-1.988912000	0.575344000
C	-2.591981000	-0.724020000	0.102595000
C	-3.597801000	-0.013477000	0.751135000
O	-1.242231000	-2.667455000	-0.066316000
B	-0.045175000	-1.998070000	-0.528497000
N	-0.424284000	-0.431945000	-0.960853000
C	-1.893530000	-0.253705000	-1.130595000
O	0.352916000	-2.538783000	-1.837797000
C	0.626843000	-1.620289000	-2.747457000
C	0.345234000	-0.214325000	-2.208592000
C	1.658123000	0.542154000	-1.962485000
C	1.426850000	1.896733000	-1.346103000
C	1.154422000	-1.950531000	0.537471000
C	2.411201000	-2.498239000	0.250162000
C	3.455980000	-2.443740000	1.170885000
C	3.265073000	-1.834046000	2.407437000
C	2.021437000	-1.289261000	2.720921000
C	0.982598000	-1.351898000	1.795518000
C	1.621257000	2.094935000	0.024925000
C	1.358158000	3.333947000	0.607405000
C	0.901443000	4.389803000	-0.173701000
C	0.709234000	4.204052000	-1.541795000
C	0.967122000	2.967071000	-2.121465000
O	1.072152000	-1.821580000	-3.848632000
C	-3.870409000	-1.828000000	2.307959000
H	-5.030507000	-0.010149000	2.357232000
H	-2.548288000	-3.522821000	2.028230000
H	-3.884337000	0.968239000	0.380287000
H	-0.107060000	0.218806000	-0.239021000
H	-2.107285000	0.794196000	-1.363934000
H	-2.176513000	-0.867899000	-1.994499000
H	-0.265710000	0.339064000	-2.928745000
H	2.152605000	0.622887000	-2.935575000
H	2.305632000	-0.061963000	-1.318319000
H	2.567091000	-2.983547000	-0.710448000
H	4.420169000	-2.879826000	0.923341000
H	4.078257000	-1.788262000	3.126566000
H	1.860013000	-0.822835000	3.689355000
H	0.012553000	-0.937129000	2.068768000
H	1.995440000	1.276321000	0.637452000
H	1.518844000	3.472501000	1.672575000

H	0.701479000	5.356902000	0.277975000
H	0.362586000	5.027842000	-2.159132000
H	0.823475000	2.830826000	-3.191312000
H	-4.372726000	-2.262251000	3.167788000

Water

O	-0.484569000	0.162495000	0.000000000
H	-0.438146000	1.122212000	0.000000000
H	0.435715000	-0.113707000	0.000000000

HydroniumIon

O	0.022975000	0.036527000	-0.053275000
H	-0.161136000	0.991580000	0.052168000
H	0.570910000	-0.168924000	-0.837340000
H	-0.778869000	-0.519357000	0.013612000

Fran_OM1

C	-4.108728000	0.359383000	1.864953000
C	-4.225344000	-0.973081000	2.293688000
C	-3.172857000	-1.863950000	2.190582000
C	-1.955662000	-1.454465000	1.623396000
C	-1.828703000	-0.100481000	1.202241000
C	-2.909246000	0.790278000	1.339394000
O	-0.958171000	-2.312937000	1.544232000
B	0.184698000	-2.081841000	0.642053000
N	0.400194000	-0.516982000	0.556842000
C	-0.529447000	0.341711000	0.805405000
O	1.460423000	-2.458500000	1.282665000
C	2.389599000	-1.515303000	1.189011000
C	1.825411000	-0.256031000	0.494862000
C	-0.004485000	-2.763412000	-0.797117000
O	3.528035000	-1.620905000	1.565319000
C	3.717567000	0.473874000	-1.051546000
C	0.861917000	-3.772745000	-1.237350000
C	0.699922000	-4.379685000	-2.480958000
C	-0.338642000	-3.984353000	-3.318786000
C	-1.213560000	-2.982598000	-2.904199000
C	-1.044326000	-2.384532000	-1.659501000
C	3.885472000	1.851396000	-1.215223000
C	4.853438000	-0.335273000	-0.971417000
C	6.125041000	0.222174000	-1.053789000
C	6.280897000	1.595970000	-1.217216000
C	2.330757000	-0.108232000	-0.960203000
C	5.156320000	2.411832000	-1.297598000
H	-4.947412000	1.040480000	1.958860000
H	-5.164676000	-1.315197000	2.719204000
H	-3.259886000	-2.891724000	2.525646000
H	-2.782792000	1.822610000	1.021957000
H	-0.295238000	1.407784000	0.780587000
H	2.090187000	0.636317000	1.070557000
H	1.672835000	-4.089323000	-0.585834000
H	1.384458000	-5.163011000	-2.795683000
H	-0.466995000	-4.453846000	-4.290314000
H	-2.027630000	-2.669153000	-3.552611000
H	-1.743208000	-1.606388000	-1.356436000
H	3.008948000	2.492140000	-1.290471000
H	4.740027000	-1.405003000	-0.827670000
H	6.997913000	-0.420700000	-0.988222000
H	7.274926000	2.028599000	-1.283867000
H	1.624204000	0.550462000	-1.478151000
H	2.272904000	-1.080990000	-1.458960000
H	5.267425000	3.484171000	-1.431009000

Fran_OM2

C	-5.917158000	0.394394000	1.889835000
C	-5.927267000	-0.971400000	2.214987000
C	-4.823759000	-1.777107000	1.999438000
C	-3.662874000	-1.240732000	1.421511000
C	-3.642417000	0.145607000	1.106104000
C	-4.772400000	0.945882000	1.353453000
O	-2.615831000	-2.021236000	1.231359000
B	-1.528244000	-1.636393000	0.319853000
N	-1.422808000	-0.058303000	0.344003000
C	-2.399061000	0.713382000	0.684101000
O	-0.205984000	-1.976665000	0.897233000
C	0.653328000	-0.976745000	0.812655000
C	-0.018958000	0.278324000	0.206316000
C	-1.704035000	-2.206018000	-1.168954000
C	0.468694000	1.565002000	0.854373000
O	1.812375000	-1.006204000	1.139764000
C	0.065787000	2.844336000	0.160531000
C	-0.787754000	-3.117533000	-1.708828000
C	-0.941553000	-3.627719000	-2.996041000
C	-2.021364000	-3.229876000	-3.778462000
C	-2.945450000	-2.322178000	-3.265290000
C	-2.783904000	-1.820882000	-1.977638000
C	-0.559202000	3.870134000	0.875647000
C	-0.919957000	5.062819000	0.253099000
C	-0.659699000	5.248458000	-1.100476000
C	-0.031415000	4.236912000	-1.823252000
C	0.328642000	3.048049000	-1.198114000
H	-6.793924000	1.006944000	2.069475000
H	-6.822427000	-1.409589000	2.647651000

H	-4.828523000	-2.831621000	2.252880000
H	-4.727193000	2.005365000	1.112868000
H	-2.251860000	1.793434000	0.698735000
H	0.227520000	0.263126000	-0.865136000
H	1.561014000	1.471353000	0.886361000
H	0.138296000	1.582900000	1.899681000
H	0.056857000	-3.436098000	-1.102875000
H	-0.217636000	-4.337147000	-3.388443000
H	-2.143742000	-3.624127000	-4.783698000
H	-3.791557000	-2.006518000	-3.870207000
H	-3.519918000	-1.114276000	-1.597068000
H	-0.756379000	3.735313000	1.937223000
H	-1.402231000	5.847259000	0.829282000
H	-0.940248000	6.176324000	-1.589797000
H	0.182926000	4.375312000	-2.878990000
H	0.829290000	2.274163000	-1.775157000

Fran_OM3

C	-4.148091000	-1.287526000	2.542322000
C	-4.246911000	0.032025000	2.072926000
C	-3.230321000	-2.178534000	2.015846000
C	-2.352428000	-1.766961000	1.001471000
C	-2.459648000	-0.436467000	0.512398000
C	-3.414397000	0.443301000	1.053178000
O	-1.489079000	-2.630939000	0.502666000
B	-0.325884000	-2.190491000	-0.279469000
N	-0.732159000	-0.858179000	-1.035922000
C	-1.679212000	-0.083994000	-0.633429000
O	-0.111338000	-3.069760000	-1.450957000
C	0.064632000	-2.389201000	-2.568648000
C	-0.015447000	-0.865076000	-2.304064000
C	0.452096000	0.545373000	-4.368947000
C	1.004364000	-1.995907000	0.594347000
C	2.162988000	-2.736059000	0.326834000
C	3.320747000	-2.574264000	1.084592000
C	3.345130000	-1.658370000	2.131765000
C	2.205429000	-0.909718000	2.418123000
C	1.053744000	-1.081022000	1.657041000
C	1.235782000	-0.264200000	-5.197401000
C	0.660858000	1.926156000	-4.384077000
C	1.629659000	2.492911000	-5.207521000
C	2.204892000	0.302356000	-6.019227000
C	2.405445000	1.680525000	-6.028190000
O	0.263121000	-2.871781000	-3.655806000
C	-0.600696000	-0.051626000	-3.462977000
H	-4.808181000	-1.620656000	3.338380000
H	-4.975791000	0.712347000	2.499543000
H	-3.154542000	-3.199143000	2.374708000
H	-3.484632000	1.452580000	0.654416000
H	-1.927443000	0.815930000	-1.196392000
H	1.012967000	-0.537247000	-2.093415000
H	2.151347000	-3.458265000	-0.485720000
H	4.204611000	-3.164491000	0.857495000
H	4.246966000	-1.527695000	2.723712000
H	2.216222000	-0.193562000	3.235642000
H	0.173993000	-0.487833000	1.901823000
H	1.080568000	-1.339172000	-5.181202000
H	0.055652000	2.568418000	-3.747419000
H	1.775994000	3.569301000	-5.207730000
H	2.806023000	-0.338504000	-6.658010000
H	3.161903000	2.119073000	-6.672536000
H	-1.206666000	0.770278000	-3.068267000
H	-1.273859000	-0.697861000	-4.036326000

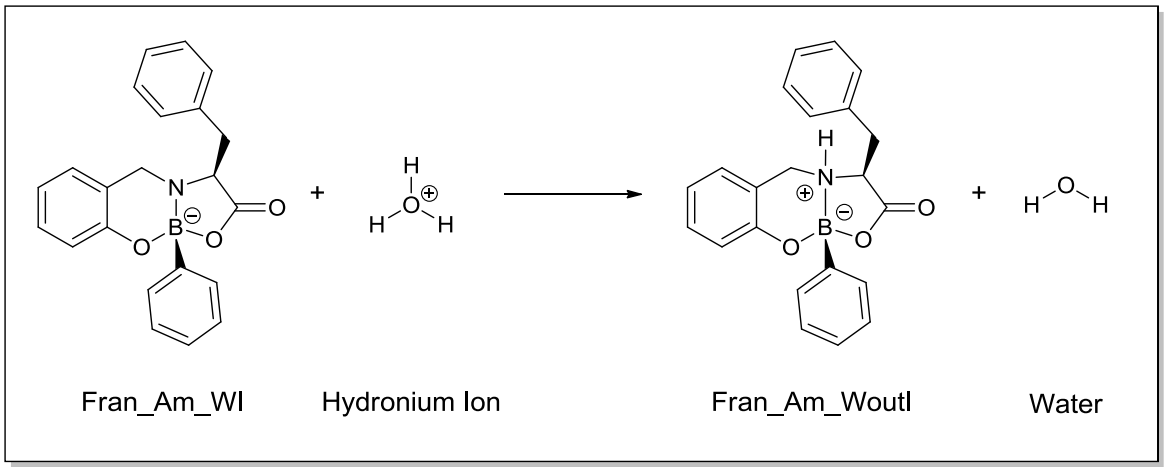

	Reagents (kcal/mol)		Products (kcal/mol)	
(kcal/mol)	UnprotonatedAmine	Hydronium Ion	ProtonatedAmine	Water
ElectronicEnergy	- 724.122,76	- 48.082,31	- 724.460,38	- 47.902,17
ThermalEnthalpies	- 723.878,02	- 48.057,99	- 724.205,66	- 47.886,17
SUM	-771.936,02		- 772.091,83	
Thermal Free Energies	- 723.925,95	- 48.072,42	- 724.252,29	- 47.900,02
SUM	- 771.998,37		- 772.152,31	

7.5 Biological assays

Human neutrophil elastase activity assay of bicycle-boronate heterocycle collection with fluorogenic peptide substrate

Fluorometric assays for the Human neutrophil elastase (HNE) (Merck, Germany) inhibition activity were carried out in 200 µL assay buffer (0.1 M HEPES pH 7.5 at 25 °C) containing 20 µL of 0.17 µM HNE in assay buffer (stock solution 1.7 µM in 0.05 M acetate buffer, pH 5.5), and 5 µL of each concentration of tested inhibitors. Reaction was initiated by the addition of 175 µL of fluorogenic substrate to final concentration of 200 µM (MeO-Suc-Ala-Ala-Pro-Val-AMC, Merck, Germany), and activity was monitored (excitation 380 nm; emission 460 nm) for 30 min, at 25ºC on a Fluorescence Microplate Reader Tecan infinite M200 (Tecan, Switzerland). The Km of this substrate of HNE was previously determined to be 185 µM (data not shown). For all assays, saturated substrate concentration was used, throughout, in order to obtain linear fluorescence curves. Inhibitors stock solutions were prepared in DMSO, and serial dilutions were made in DMSO. Controls were performed using enzyme alone, substrate alone, enzyme with DMSO and a positive control (MeOSuc-Ala-Ala-Pro-Ala-CMK, Calbiochem, Germany). By computing the log of inhibitors concentrations versus the percentage of activity and using the GrafPad program the IC_{50} values were determined by non-linear regression analysis. Assays were performed in triplicate and data presented as the mean and the standard deviation.

Human neutrophil elastase activity assay of diazaborine collection with fluorogenic peptide substrate

Fluorometric assays for the Human neutrophil elastase (HNE) (Merck, Germany) inhibition activity were carried out in 200 µL assay buffer (0.1 M HEPES pH 7.5 at 25 °C) containing 20 µL of 0.17 µM HNE in assay buffer (stock solution 1.7 µM in 0.05 M acetate buffer, pH 5.5), and 5 µL of each concentration of tested inhibitors. The diazaborines were preincubated for 30' minute with the enzyme before the substrate was added. Reaction was initiated by the addition of 175 µL of fluorogenic substrate to final concentration of 200 µM (MeO-Suc-Ala-Ala-Pro-Val-AMC, Merck, Germany), and activity was monitored (excitation 380 nm; emission 460 nm) for 30 min, at 25ºC on a Fluorescence Microplate Reader Tecan infinite M200 (Tecan, Switzerland). The Km of this substrate of HNE was previously determined to be 185 µM (data not shown). For all assays, saturated substrate concentration was used, throughout, in order to obtain linear fluorescence curves. Inhibitors stock solutions were prepared in DMSO, and serial dilutions were made in DMSO. Controls were performed using enzyme alone, substrate alone, enzyme with DMSO and a positive control (MeOSuc-Ala-Ala-Pro-Ala-CMK, Calbiochem, Germany). By computing the log of inhibitors concentrations versus the percentage of activity and using the GrafPad program the IC_{50} values were determined by non-linear regression analysis. Assays were performed in triplicate and data presented as the mean and the standard deviation.

Phenylalanine hydroxylase activity

Escherichia coli TOP 10 and the prokaryotic expression vector pTrcHis were obtained from Invitrogen (Carlsbad, CA). The cofactor (6R)-L-*erythro*-5,6,7,8-tetrahydrobiopterin (BH_4), L-Phe, Hepes, were from Sigma (St. Louis, MO, USA). Ascorbic acid was obtained from Merck (Darmstadt, Germany). Unless stated otherwise, all reagents were of analytical grade. The hPAH protein was expressed in *E. coli* as a fusion protein with the hexa-histidyl tag (6xHis-(pep)EK-hPAH) as described [132]. Cells were grown at 37 °C, and the induction of protein expression by 1 mM isopropyl-β-D-thiogalactoside (IPTG) was performed during 3 h, at 37 °C. The recombinant tetramers were isolated by size exclusion chromatography (SEC), using a HiLoad Superdex 200 HR column (1.6 cm × 60 cm, GE-Healthcare) and a mobile phase containing 20 mM Na-Hepes, 200 mM NaCl, pH 7 pumped at a flow rate of 0.7 $mL \cdot min^{-1}$. The hPAH activity was measured essentially as previously described [132] in a 200 μL final volume reaction mixture, containing 100 μM L-Phe, 0.1 M Na-Hepes, pH 7, 0.1 mg·mL catalase, 5 μg of recombinant hPAH tetramers, 100 μM of each compound or 1% DMSO (vehicle control). After 4 minutes preincubation, 100 μM $(NH_4)_2Fe(II)SO_4$ was added and unless otherwise stated the reaction was started by addition of 75 μM BH_4 (together with 5 mM ascorbic acid) after 1 minute incubation with the iron. To study the specific activity of the non-activated hPAH, 100 μM L-Phe and 100 μM of each compound were added together with 75 μM BH_4 at the start of the hydroxylation reaction. To evaluate activation of the enzyme by the compound, hPAH was incubated 4 minutes with each compound and the L-Phe substrate was added together with 75 μM BH_4 at the start of the reaction. Blank reactions where the substrate L-Phe was omitted, were also made for each compound. The amount of L-Tyr produced after 1 min was quantified by a HPLC method [133] using a LiChroCART® 250-4 LiChrospher® 60 RP-select B (5 μm) column (Merck

KGaA, Darmstadt, Germany), a 5% ethanol mobile phase pumped at 0.7 mL·min and fluorimetric detection (λ_{exc}= 274 nm and λ_{em}= 304 nm). Specific activities are presented as mean ± SEM obtained from three independent experiments. Differential scanning fluorimetry (DSF) was performed in a C1000 Touch thermal cycler equipped with a CFX96 optical reaction module (Bio Rad). For all fluorescence measurements, samples containing purified recombinant hPAH tetramers at 100 μg/mL in 20 mM NaHepes, 200 mM NaCl, pH 7, 2.5-fold Sypro Orange (Invitrogen; 5000-fold stock solution), 1% DMSO (unless otherwise stated) and 100 μM of each compound were incubated at 20 ºC for 10 minutes. The PCR plate was sealed with Optical-Quality Sealing Tape (Bio-Rad) and centrifuged at 500x*g* for 5 min. The DSF was carried out by increasing the temperature from 20 to 90 °C, with a 1 s hold time every 0.2 °C and fluorescence acquisition using the FRET channel. Control experiments in the absence of DMSO and/or compounds were routinely performed in each microplate. Data were processed using CFX Manager Software V3.0 (Bio-Rad) and the GraphPad Prism 6. Temperature scan curves were fitted to a biphasic dose-response function and the T_m values were obtained from the midpoint of the first and second transitions. To monitor the binding properties of the regulatory and catalytic domain towards each compound, DSF assays were run in the presence of increased compound concentrations (0–2.56 mM) or 1% DMSO (vehicle control).

8. References

1. Copi J. C., Schramm D.N., Turner M.S., Science, 1995267: 192–99.
2. Hinshaw G., NASA/WMAP, 2005.
3. Knauth D.C.,Lambert D.L., Crane P., Nature 2000,405: 656–658.
4. Miyaura N., Suzuki A., J.Chem.Soc. 1979, 866–867.
5. Sakai M., Ueda M., Miyaura N., Angew. Chem. Int. Ed. Engl. 1998, 37: 3279---3281.
6. G. Springsteen, B. H. Wang, Tetrahedron 2002, 58, 5291-5300.
7. Petasis N.A., Akritopoulou I., Tetrahedron Lett. 1993, 34: 583---586
8. Gillis P., Burke M.D., J. Am. Chem. Soc., 2007, 129: 6716–6717
9. Abreu A., Alas S.J., Beltra H.I, Santillan R., Farfan N., J. Org. Chem. 2006, 691: 337–348
10. Braun M.B., Schlecht S., Engelmann M., Grimme S, Eur. J. Org. Chem. 2008, 5221–5225;
11. Kaiser, White, Hutton J. Am. Chem. Soc. 2008, 130, 16450–16451
12. Christinat N., Scopelliti R., Severin K., J. Org. Chem. 2007, 72: 2192-2200
13. Dunitz J.D, Hawley D.M., Miklol D., White D.N.J., Berlin Y., Maru R, Prelog V., Helv.Chim.Acta. 1971,54 (6) 183
14. Prelog V., Zaehner H., Bickel H., 1973. Antibiotic A 28829. US Patent 3,769,418.
15. Kohno J., Kawahata T., Otake T., Morimoto M., Mori H, Ueba N, Nishio M., Kinumaki A., Komatsubara S, Kawashima K., antibiotic. Biosci. Biotech. Biochem. 1996, 60: 1036–1037.
16. Davies D.H., Norris G.L.F., 1980. Growth promotion. US Patent 4,225,593.

17. Schummer D., Irschik H., Reichenbach H., Hofle G., Liebigs Annalen der Chemie 1994, 57: 283– 289.
18. Schummer D., Schomburg D., Irschik H., Reichenbach H., Hofle G., Liebigs. 1996, 965–969.
19. Arai M., Koizumi Y, Sato H, Kawabe T, Suganuma M, Kobayashi H, Tomoda H, Omura S., J. Antib. 2004, 57, 662–668.
20. Nakamura H., Haga T. et al. ChemMedChem, 2006, 1: 729.
21. Trippier P.C., McGuigan C., Med. Chem. Commun. 2010, 1: 183–198
22. Kumar S.K, Khan S.R. et al, J. Med. Chem. 2003, 46: 2813.
23. Nakamura H., Asai A. et al., Bioorg. Med. Chem. Lett. 2009, 19: 3220.
24. Powers R.A., Caselli E., Focia P.J., Prati F., Shoichet B.K., Biochem. 2001, 40: 9014. (b) Caselli E., Powers R.A:, Blasczcak L.C:, Wu C.Y., Prati F., Shoichet B.K., Chem. Biol., 2001, 8, 17; (c) . Morandi, Caselli E., Morandi S., Focia P.J., Blasquez J., Shoichet B.K., Prati F., J. Am. Chem. Soc., 2003, 125: 685.
25. Adams J., Stein R.L., Bioorg. Med. Chem. Lett. 1998, 8: 333.
26. The Nobel Prize in Chemistry 2004; http//nobelprize.org/nobel_prizes/chemistry/laureates/2001/chemdv04.pdf
27. Ciechanover A., EMBO J. 1998, 17: 7151–7160.
28. Kisselev A.F, Goldberg A.L:, Chem. Biol. 2001, 8: 739–758.
29. Voges D., Zwickl P., Baumeister W., Annu. Rev. Biochem. 1999, 68: 1015–1068.
30. Chatterjee M.S., Kauer J.C., Das M., Messina P., Freed B., Biazzo W, Siman R., J.Med. Chem. 1995, 38: 2276-2277
31. Adams J. et al. Bioorg. Med. Chem. Lett. 1998, 8: 333–338

32. Dick L.R, Fleming P.E., Drug Disc. Today 2010, 54: 4365-4377

33. Bachovchin W.W., J. Med. Chem. 2011, 54: 4365–4377

34. Csizmadia V., Raczynski A., Csizmadia E.; Fedyk E.R., Rottman J, Alden C.L., Neurotoxicology 2008, 29: 232–243.

35. Silver D.A., Pellicer I., Fair W.R., Heston W.D., Cordon-Cardo, Clin. Cancer Res. 1997, 3: 81–85; Kidwai N., Gong Y, Sun X, Deshpande C.G, Yeldandi A.V., Rao M.S., Breast Cancer Res. 2004, 6: R18–R23; Bodor, Med. Res. Rev. 1984, 4: 449–469; Bodor, Chem. Tech. 1984, 14: 28–38; Bodor N., Buchwald P., Med. Res. Rev. 2000, 20: 58–101; Bodor N., Buchwald P., Mol. Biotech- nol. 2004, 26: 123–132.

36. Kochanek K.D., Murphy S.L., Anderson R.N., Scott C., Natl. Vital. Stat. Rep. 2004, 53

37. Merkel M., Eckel R.H:, Goldberg I.J., J. Lipid Res. 2002, 43: 1997.

38. Ishida T., Choi S., Kundu R.K., Hirata K., Rubin E.M., Cooper A.D:, Quertermous T., Clin. Invest. 2003, 111: 347.

39. Sato R., Arch. Biochem. Biophys. 2010, 501: 177.

40. Das B:C. et al. Bioorg. Med. Chem. Lett. 2011, 21: 5638–5641

41. Connolly B.A., Sanford D.G., Chiluwal A.K., Healey S.E, Peters D.E:, Dimare M.T., Wu W., Liu Y., Zhou Y, Li Y, Jin Z., Sudmeier J.L., Lai J.H., Bachovchin W.W., J. Med. Chem. 2008, 51: 6005–6013.;

42. CouttsS.J., Kelly T.A:, Snow R.J., Kennedy C.A:, Barton R.W., Adams J., Krolikowski D.A., Freeman D.M., Campbell S.J., Ksiazek J.F., Bachovchin W.W, J. Med. Chem. 1996, 39: 2087–2094.

43. Cheng J.D., Valianou M., Canutescu A.A., Lee H.O., Wang H., Lai J.H., Bachovchin W.W., Weiner L.M., Mol. Cancer Ther. 2005, 4: 351–360.

44. Kubota T., Flentke G.R., Bachovchin W.W:, Stollar B.D., Clin. Exp. Immunol. 1992, 89: 192–197;

45. Kelly T.A., Adams J., Bachovchin W.W:, Barton R.W., Campbell S.J., Coutts S.J., Kennedy C.A., Snow R.J., J. Am. Chem. Soc. 1993, 115: 12637–12638.

46. Mentlein R., Gallwitz B., Schmidt W.E.D., Eur. J. Biochem. 1993, 214: 829–835.;

47. Drucker D.J., Nauck M.A., Lancet 2006, 368: 1696–705.

48. Bachovchin W.W. et al, J. Med. Chem. 2011, 54(7): 2022-2028

49. Balzarini J., Nat. Rev. Microbiol. 2007, 5: 583.

50. Jay J.L., Lai B.E., Myszka D.G:, Mahalingam A., Langheinrich K., Katz D.F., Kiser P.F., Mol. Pharmaceutics 2010, 7: 116.

51. Berube M., Dowlut M., Hall D.G., J. Org. Chem., 2008, 73: 6471.

52. Zervosen A. et al., Bioorg. Med. Chem. 2012, 20: 3915–3924

53. Matteï P.J., Neves D., Dessen A., Curr. Opin. Struct. Biol. 2010, 20: 749.

54. Sauvage E., Kerff F., Terrak M., Ayala J.A., Charlier P., FEMS Microbiol. Rev. 2008, 32: 234.

55. Sauvage E. et al., Am. Chem. Soc. 2009, 131: 15262.

56. Trivedi R.et al., Bioorg. Med. Chem. Lett. 2011, 21: 3890–3893

57. Almond M.R., Wilson J.D., Rideout, J. L., U.S. Pat. 4,916,218, 1990.

58. Gosselin G., Bergogne M.C., Imbach J.L., Nucleic Acid Chem. 1991, 4: 41.

59. Matsuda F., Terashima S., Tetrahedron 1988, 44: 4721

60. ZalkinH. et al. Proc.Nat.Acad.Sci.Ares Mol.Biol. 1993, 66: 203

61. DeciccoC.P. et al., Bioorg. Med. Chem. Lett. 2001, 11: 2561–2564

62. Edwards P.D, Bernstein P.R., Med. Res. Rev. 1994, 14: 127

63. PrattR.F. et al., Biochemistry 2010, 49: 6411–6419.

64. Dewar M.J.S., Dietz R., J. Chem. Soc. 1959, 2728–2730

65. Chissick S.S:, Dewar M.J.S., Maitlis P.M., Tetrahedron Lett. 1960, 1: 8 – 10

66. Dewar M.J.S., Kubba V.P., Pettit R., J. Chem. Soc. 1958, 3073 – 3076;

67. Davies K.M., Dewar M.J.S., Rona P., J. Am. Chem. Soc. 1967, 89: 6294 – 6297

68. Liu Z., Marder T.B., Angew. Chem. Int. Ed. 2008, 47: 242 – 244

69. Burdett J.K., Chemical bonding in solids, Oxford University Press, New York, 1995, 71 – 72.

70. Fritsch A.J., In Special topics in heterocyclic chemistry.1987, 30: 381

71. Dewar M.J.S., Prog. Boron Chem. 1964, 1: 235

72. Niedenzu K., Angew. Chem., Int. Ed. 1964, 3: 86.

73. Glogowski M.E., Grisdale P.J., Williams J.L..R, Regan T.H., J. Organomet. Chem. 1973, 54: 51–60.; Brown H.C., Dodson V.H., J. Am. Chem. Soc. 1957, 79: 2302–2306.

74. Katzenellenbogen J.A:, J. Med. Chem. 2011, 54: 5271–5282.

75. Woon E.C.Y., Schofield C.J.,Angew. Chem. Int. Ed. 2012, 51: 6672 – 6675

76. Chowdhury R., McDonough M.A., Mecinovic J., Loenarz C., Flashman E., Hewitson K.S., Domene C., Schofield C.J, Structure 2009, 17: 981.

77. González M.A., Current Bioactive Compounds 2007

78. Connolly J.D., Hill R.A., London Chapman e Hall 199,1 2: 895-899

79. Schmitz F.J., Chang J.S., Hossain M.B., Van der Helm D., J. Org. Chem.1985, 50: 2862-2865.

80. Potts B.C.M., Faulkner D.J., Jacobs R.S., J. Nat. Prod. 1992, 55: 1701-1717.

81. Betancur-Galvis L., Zuluaga C., Arnó M., González M.A., Zaragozá R.J., J. Nat. Prod. 2002, 65: 189-192.

82. Dumdei E.J., De Silva E.D., Choudhary M.I., Clardy, J., J. Am. Chem. Soc. 1989, 111: 2712-2713.

83. Weisser R., Yue W., Reiser O., 2005 Org.Lett., 7 : 5353-5356

84. Macdonald S.J.F., Belton D.J., Buckley D.M., Spooner J.E., Anson M.S., Harrison L.A., Mills K., Upton R.J., Dowle M.D., Smith R.A., Molloy C.R., Risley C., J. Med. Chem.1998, 41:3919-3922.

85. Lucas S.D., Gonçalves L.M., Cardote T.A.F., Correia H.F., Moreira R., Guedes R.C., Med. Chem. Commun.2012, 3: 1299-1304;

86. Mulchande J., Oliveira R., Carrasco M., Gouveia L., Guedes R.C., Iley J., Moreira R., J. Med. Chem. 2010, 53:241-253.

87. Smoum R., Srebnik M., Chem. Rev. 2007

88. Ohbayashi H., Expert Opin Investig Drugs 2002, 11:965–980.

89. OhmotoK. et all. J Med Chem 2001, 44: 1268–1285.

90. Sjo, Future Med Chem 2012, 4: 651-660

91. Groutas, Dou, Alliston, Esp. Opin. Ther. Pat. 2011, 21: 339-354

92. Ohmoto K et al. J Med Chem 2000;43:4927–4929.

93. Ohbayashi H., Expert Opin Ther Pat 2005, 15:759–771.

94. Nakayama Y. et al. Bioorg Med Chem Lett 2002,12: 2349–2353.

95. Kobayashi *et al,* 1996, Bio.Org Med Chem. 4: 2115-2134

96. Power J.C., Asgian J.L., Ekici O.D., Chem.Rev 2002, 102: 4639-4750

97. Macdonald S.J. et al j.Med.Chem. 1998, 41: 3919-3922

98. Candeis N.R., Gois P.M.P., Tetrahedron 2010, 66:2736-2745

99. Montalbano F., Gois P.M.P., Org. Let 2012, 14: 988-991

100. Groziak M.P., Am.J.Ther 2011, 8: 321-328

101. Wiberg K.B., Tetrahedron 1968, 24: 1083–1096;

102. Carpenter J.E., Weinhold F.J., J. Mol. Struct. 1988, 169: 41–62;

103. Carpenter J.E., PhD Thesis, University of Wisconsin (Madison WI), 1987.

104. Foster J.P., Weinhold F.J., J. Am. Chem. Soc. 1980, 102: 7211–7118

105. Reed A.E., Weinhold F.J., J. Chem. Phys. 1983, 78: 4066–4073;

106. Reed A.E., Weinhold, J. Chem. Phys. 1985, 78: 1736–1740;

107. Reed A.E., Weinstock R.B., Weinhold F., J. Chem. Phys. 1985, 83: 735–746;

108. Reed A.E., Curtiss L.A., Weinhold F., Chem. Rev. 1988, 88: 899–926;

109. WeinholdF., Carpenter J.E., Plenum: New York, 1988; p. 227.

110. Parr R.G, Yang W.,*Dens. Func. The. At. Mol.*; Oxford University Press: New York, 1989.

111. Santana A.B., Lucas S.D., Moreira R., Biorg. Med.Chem.Lett 2012, 22: 3993-3997

112. GOLD 5.1, CCDCSoftware Ltd; Cambridge, UK. (www.ccdc.cam.ac.uk/products/gold_suite)

113. Hedstrom L., *Chem. Rev.,* 2002**, 102***:*4501-4523.

114. Pey A.L., Ying M., Cremades N., Velazquez-Campoy A., Scherer T, Thçny B., Sancho J., Martinez A.,J. Clin. Invest. 2008, 118: 2858–2867.

115. Cary O., Bio. Targ. Ther. 2010, 4: 231–236 e.

116. Torreblanca R., Sancho J., Hurtado-Guerrero R., Chem. Biochem 2012, 13: 1266-1269
117. Pey A.L., Serano L, Martinez A , Am.J.Hum.Genet. 2011, 811: 1006-1024
118. Blau N., Spronsen F.J., Levy H.L. Lancet 2010, 376: 1417-1427
119. Scriver C.R., Human Mutation 2010, 28: 831-845
120. Donlon J., Levy H., Scriver C.R., 2008, The metabolic and molecular bases of inherited diseases.
121. Baldock C., de Boer G.D., Rafferty J.B., Stuitje A.R., Rice D.W., Biochemical Pharmacology 1998, 55: 1541–1549.
122. Groziak M.P., Canguly A.D., Robinsons P.D., J. Am. Chem. SOC.1994,116: 1591-1605
123. Turnowsky F., Fuchs K., Jeschek C., Hogenauer G., J. Bacteriol. 1989, 171: 6555– 6565.
124. Kater M.M., Koningstein G.M., Nijkamp H.J.J., Stuitje A.R., Plant Mol Biol 1994, 25: 771–790.
125. Dewar M.J.S., Dougherty R.C.; J. Am. Chem. Soc. 1964, 86: 433–436,
126. Gaussian 03, Revision C.02, Frisch M. J., Trucks G. W., Schlegel H. B., Scuseria G. E., Robb M. A., Cheeseman J. R., Montgomery J. A., Vreven T., Kudin K. N., Burant J. C., Millam J. M., Iyengar S. S., Tomasi J., Barone V., Mennucci B., Cossi M., Scalmani G., Rega N., Petersson G. A., Nakatsuji H., Hada M., Ehara M., Toyota K., Fukuda R., Hasegawa J., Ishida M., Nakajima T., Honda Y., Kitao O., Nakai H., Klene M., Li X., Knox J. E., Hratchian H. P., Cross J. B., Adamo C., Jaramillo J., Gomperts R., Stratmann R. E., Yazyev O., Austin A. J., Cammi R., Pomelli C., Ochterski J. W., Ayala P. Y., Morokuma K., Voth G. A., Salvador P.,

Dannenberg J. J., Zakrzewski V. G., Dapprich S., Daniels A. D., Strain M. C., Farkas O., Malick D. K., Rabuck A. D., Raghavachari K., Foresman J. B., Ortiz J. V., Cui Q., Baboul A. G., Clifford S., Cioslowski J., Stefanov B. B., Liu G., Liashenko A., Piskorz P., Komaromi I., Martin R. L., Fox D. J., Keith T., Al-Laham M. A., Peng, C. Y., Nanayakkara, A., Challacombe M.,GillP. M. W., Johnson B., Chen W., Wong M. W., Gonzalez C., Pople J. A. Gaussian, Inc., Wallingford CT, 2004.

127. Hehre W. J., RadomL., Schleyer P. v.R., Pople, J. A. Ab Initio Molecular Orbital Theory, John Wiley & Sons, NY, 1986.
128. Parr R. G., Yang, W., Oxford University Press: New York, 1989.
129. Perdew J. P., Burke K., Ernzerhof M., Phys. Rev. Lett. 1997, 78, 1396.
130. Ditchfield R., Hehre W. J., Pople J., A. J. Chem. Phys. 1971, 54, 724.; Hehre W. J., Ditchfield R., Pople, J.; A. J. Chem. Phys. 1972, 56, 2257.; Hariharan P. C., J. A. Mol. Phys. 1974, 27, 209.; Gordon M. S.; Chem. Phys. Lett. 1980, 76, 163.; Hariharan, P. C., J. A. Theor. Chim. Acta 1973, 28, 213.
131. Peng C., Ayala P. Y., Schlegel H. B., Frisch M. J., J. Comp. Chem., 1996, 17, 49.; Peng C., Schlegel H. B., Israel J. Chem., 1994, 33, 449.
132. Leandro, P., Rivera, I., Lechner, M. C., de Almeida, I. T., and Konecki, D. (2000) The V388M mutation results in a kinetic variant form of phenylalanine hydroxylase. Mol. Genet. Metab. 69, 204-212.
133. Kand'ar, R., and Zakova, P. (2009) Determination of phenylalanine and tyrosine in plasma and dried blood samples using HPLC with fluorescence detection. *Journal of chromatography. B, Analytical technologies in the biomedical and life sciences 877*, 3926-3929.